FUNCTIONAL TESTING OF VESTIBULAR FUNCTION

EDITED BY: Stefano Ramat, Michael C. Schubert and Herman Kingma
PUBLISHED IN: Frontiers in Neurology

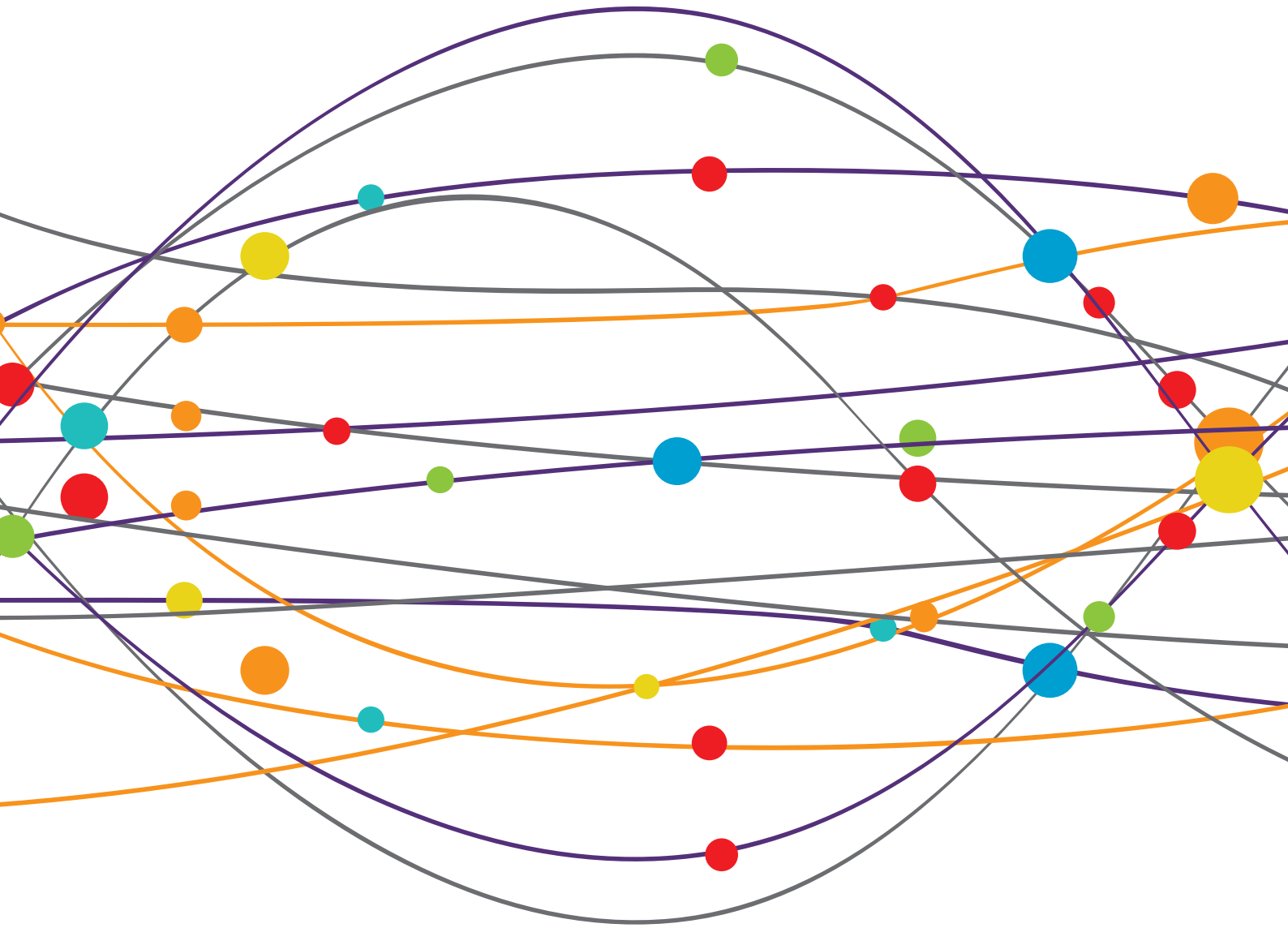

frontiers Research Topics

frontiers

ISSN 1664-8714
ISBN 978-2-88963-959-5
DOI 10.3389/978-2-88963-959-5

About Frontiers

Frontiers is more than just an open-access publisher of scholarly articles: it is a pioneering approach to the world of academia, radically improving the way scholarly research is managed. The grand vision of Frontiers is a world where all people have an equal opportunity to seek, share and generate knowledge. Frontiers provides immediate and permanent online open access to all its publications, but this alone is not enough to realize our grand goals.

Frontiers Journal Series

The Frontiers Journal Series is a multi-tier and interdisciplinary set of open-access, online journals, promising a paradigm shift from the current review, selection and dissemination processes in academic publishing. All Frontiers journals are driven by researchers for researchers; therefore, they constitute a service to the scholarly community. At the same time, the Frontiers Journal Series operates on a revolutionary invention, the tiered publishing system, initially addressing specific communities of scholars, and gradually climbing up to broader public understanding, thus serving the interests of the lay society, too.

Dedication to Quality

Each Frontiers article is a landmark of the highest quality, thanks to genuinely collaborative interactions between authors and review editors, who include some of the world's best academicians. Research must be certified by peers before entering a stream of knowledge that may eventually reach the public - and shape society; therefore, Frontiers only applies the most rigorous and unbiased reviews.
Frontiers revolutionizes research publishing by freely delivering the most outstanding research, evaluated with no bias from both the academic and social point of view. By applying the most advanced information technologies, Frontiers is catapulting scholarly publishing into a new generation.

What are Frontiers Research Topics?

Frontiers Research Topics are very popular trademarks of the Frontiers Journals Series: they are collections of at least ten articles, all centered on a particular subject. With their unique mix of varied contributions from Original Research to Review Articles, Frontiers Research Topics unify the most influential researchers, the latest key findings and historical advances in a hot research area! Find out more on how to host your own Frontiers Research Topic or contribute to one as an author by contacting the Frontiers Editorial Office: researchtopics@frontiersin.org

FUNCTIONAL TESTING OF VESTIBULAR FUNCTION

Topic Editors:
Stefano Ramat, University of Pavia, Italy
Michael C. Schubert, Johns Hopkins University, United States
Herman Kingma, Maastricht University, Netherlands

Citation: Ramat, S., Schubert, M. C., Kingma, H., eds. (2020). Functional Testing of Vestibular Function. Lausanne: Frontiers Media SA. doi: 10.3389/978-2-88963-959-5

Table of Contents

frontiers in Neurology

EDITORIAL
published: 30 June 2020
doi: 10.3389/fneur.2020.00654

Editorial: Functional Testing of Vestibular Function

Michael C. Schubert[1]*, *Stefano Ramat*[2] and *Herman Kingma*[3,4]

[1] Laboratory of Vestibular NeuroAdaptation, Otolaryngology Head and Neck Surgery, Johns Hopkins University, Baltimore, MD, United States, [2] Department of Electrical, Computer and Biomedical Engineering, University of Pavia, Pavia, Italy, [3] Department of Otolaryngology, Maastricht, Netherlands, [4] Department of Medical Physics, Tomsk Research State University, Tomsk, Russia

Keywords: vestibular function, vestibulo-ocluar reflex, gaze stability, balance, head impulse

Editorial on the Research Topic

Functional Testing of Vestibular Function

The vestibular ocular reflex is responsible for stabilizing the eyes in space (known as gaze stability) and the body in space (postural and gait stability) during head motion. This is achieved initially by generating exceptionally short latency vestibular oculomotor reflexes (∼10 ms) of the same magnitude and velocity, but in the opposite direction of the sensed head motion. The head motion signal also descends via the vestibulo-spinal system for postural and gait stability. Knowledge of this reflexive function has spawned the development of tests and measures that assay the behavioral relevance of vestibular sensation, without measuring the physiologic performance (i.e., measure gaze stability without recording the movement of the eyes). The focus of this special topic is on the diagnostic accuracy and rehabilitative efforts using novel tests and measures of vestibular behavior.

Millar et al. illustrate that vestibular rehabilitation improves gaze stability and other functional outcome measures, but that such recovery correlates with residual otolith function not change in semicircular canal function. Similarly, Allum et al. report that balance rehabilitation can restore normal balance 3 months after acute bilateral semicircular canal loss as long as otolith function is spared.

Using the novel functional head impulse test (fHIT), Romano et al. report that athletes of different sports have different gaze stabilization performances when tested at the highest head angular accelerations. van Dooren et al. compared the fHIT with dynamic visual acuity during gait on a treadmill and quantify the oscillopsia in patients with bilateral vestibular hypofunction to report that the fHIT correlates with experienced oscillopsia as measured by the Oscillopsia Severity Questionnaire. Sjögren et al. investigated nine patients with total unilateral vestibular loss using passive and active head impulses and the fHIT. They report normal VOR performance toward the affected side during active head impulses and that visual acuity as measured by the fHIT correlated with the latency of covert saccades.

Ramaioli et al. compared dynamic visual acuity during translational and angular head motion in a group of normal subjects and report that the well-known under-compensatory translational VOR gains are correlated with worse DVA scores during translational head motion.

Figtree and Migliaccio propose an interesting low-cost motion tracking system for posturography based on a stereo vision system that tracks a body-fixed pattern of markers. Coupled to a force plate it represents an affordable alternative for functional assessment of balance abilities.

Dasgupta and Ratnayake conducted a retrospective review of superior canal dehiscence (SCD) in children and correlated functional (audiometry), behavioral (eye movements), and anatomical (computed tomography scan) findings to reveal that children with SCD show phenotypes different from those reported in adults.

Fu et al. studied the high acceleration VOR in a set of 47 patients with acute vestibular neuritis using the video head impulse test and the dizziness handicap inventory (DHI). At 6 months

OPEN ACCESS

Edited and reviewed by:
Michael Strupp,
Ludwig Maximilian University of Munich, Germany

***Correspondence:**
Michael C. Schubert
mschube1@jhmi.edu

Specialty section:
This article was submitted to Neuro-Otology, a section of the journal Frontiers in Neurology

Received: *13 May 2020*
Accepted: *02 June 2020*
Published: *30 June 2020*

Citation:
Schubert MC, Ramat S and Kingma H (2020) Editorial: Functional Testing of Vestibular Function. Front. Neurol. 11:654. doi: 10.3389/fneur.2020.00654

follow-up, the patients had significant reduction in compensatory saccades (overt and covert), but also that the patients with normal to mild DHI scores (DHI $\leq$ 30) had higher VOR gain and lower number of covert saccades.

Taken together, this collection of papers underlines the importance of functional testing for quantifying the ecological ability of patients with vestibular hypofunction, and reveals the importance of how errant vestibular information impacts quality of life. Functional testing appears especially useful for assessing the effectiveness of rehabilitation programs, where the functional ability of the patient is more concerning and may be more informative than the objective measurement *per se* (e.g., VOR gain). The plasticity of our nervous system indeed is challenged by vestibular failure. The brain expends a fascinating repertoire of mechanisms to ensure functional navigation of everyday life, be it via recalibration or substitution.

AUTHOR CONTRIBUTIONS

All authors listed have made a substantial, direct and intellectual contribution to the work, and approved it for publication.

Conflict of Interest: The authors declare that the research was conducted in the absence of any commercial or financial relationships that could be construed as a potential conflict of interest.

frontiers in Neurology

METHODS
published: 29 June 2018
doi: 10.3389/fneur.2018.00507

An Inexpensive 6D Motion Tracking System for Posturography

William V. C. Figtree[1] *and Americo A. Migliaccio*[1,2,3]*

[1] Balance and Vision Laboratory, Neuroscience Research Australia, Sydney, NSW, Australia, [2] Graduate School of Biomedical Engineering, University of New South Wales, Sydney, NSW, Australia, [3] Department of Otolaryngology-Head and Neck Surgery, Johns Hopkins University, Baltimore, MD, United States

Computerized posturography is most often performed with a force plate measuring center-of-pressure (COP). COP is related to postural control actions but does not monitor the outcome of those actions, i.e., center-of-mass (COM) stability. For a more complete analysis of postural control COM should also be measured; however, existing motion tracking technology is prohibitively expensive and overcomplicated for routine use. The objective of this work was to create and validate an inexpensive and convenient stereo vision system which measured a trunk-fixed target's 3D position and orientation relating to COM. The stereo vision system would be complementary to typical force plate methods providing precise 6D position measurements under laboratory conditions. The developed system's measurement accuracy was worst in the inferior-superior axis (depth) and pitch coordinates with accuracy measures 1.1 mm and 0.8°, respectively. The system's precision was worst in the depth and roll coordinates with values 0.1 mm and 0.15°, respectively. Computer modeling successfully predicted this precision with 11.3% mean error. Correlation between *in vivo* target position (TP) and COP was above 0.73 with COP generally demonstrating larger excursions oscillating around TP. Power spectral analysis of TP revealed 99% of the signal was bound below 1.1 Hz matching expectations for COM. The new complementary measurement method enables identification of postural control strategies and as a result more complete analysis. Stereo vision is a useful complement to typical force plate equipment. The system presented here is inexpensive and convenient demonstrating potential for routine use in clinic and research. In order to use this system in clinic, future work is required in interpretation of this system's data and normal reference values must be established across gender and age in a healthy population followed by values from patients with different pathologies.

Keywords: posturography, sway, stereo vision, center-of-pressure, center-of-mass

OPEN ACCESS

Edited by:
Stefano Ramat,
University of Pavia, Italy

Reviewed by:
Marcos Rossi-Izquierdo,
Hospital Universitario Lucus Augusti, Spain
Hamlet Suarez,
Hospital Británico, Uruguay

***Correspondence:**
Americo A. Migliaccio
a.migliaccio@neura.edu.au

Specialty section:
This article was submitted to Neuro-Otology, a section of the journal Frontiers in Neurology

Received: *19 April 2018*
Accepted: *11 June 2018*
Published: *29 June 2018*

Citation:
Figtree WVC and Migliaccio AA (2018) An Inexpensive 6D Motion Tracking System for Posturography. Front. Neurol. 9:507. doi: 10.3389/fneur.2018.00507

INTRODUCTION

The assessment of human postural control is an important outcome in clinic and research for evaluation of falls risk and identification of specific balance disorders (1). During quiet standing tasks, maintenance of a stable center-of-mass (COM) within a limit of stability is achieved by shifting the body's center-of-pressure (COP) based on multisensory input from visual, vestibular, and proprioceptive systems among others (2, 3). While there are mechanisms within the central nervous system to compensate for irregular sensory function, well-established methodology,

such as the Romberg test, can identify abnormal systems by stressing the postural control systems (4). Thus, posturography can be used to differentiate the contribution of the visual, vestibular, and proprioceptive systems to a patient's balance. Posturography when coupled with a platform with apliable (e.g., foam) surface or a moveable platform can provide a functional test of vestibular function alone. For example, when the platform has a foam surface or sways to take away proprioception and the subject has their eyes closed, or when the platform sways and the visual surround moves with it so that proprioception and visual cues should be ignored. Although posturography cannot be used to localize a vestibular lesion there is a correlation between COP/sway and gaze velocity (a measure of visual stability mediated by the vestibulo-ocular reflex), i.e., COP/sway and gaze velocity is greater in patients with vestibular hypofunction compared to control subjects (5–7). Also, studies measuring gaze stability during balance perturbations delivered directly to the body show an inverse correlation between gaze fixation (larger is better) and latency to step (shorter is better, implying better postural stability) (8).

Computerization of these posturographic tests became prominent in the 1980s and employed a variety of technologies including: EMG, force plates, potentiometers, computer vision, wearable inertial sensors (accelerometers and gyroscopes), and electromagnetic trackers (1, 4, 9). To date postural control is most often evaluated using force plate measured COP as this methodology is sensitive to small changes in the subject's ability to balance, produces real-time results, and is both inexpensive and convenient (4, 10, 11). COP is a 2D variable, related to ankle torque, which provides insight into the subject's postural control mechanisms; however, it does not directly measure COM stability, the actual outcome of those mechanisms (12). While there are many successful methods for estimation of COM based on COP they are not widely adopted as they can be prone to error (10). It would instead be preferable to have a direct measure of sway trajectory complementary to COP which is convenient for measurement in routine practice.

The goal of this work is to create a system which captures the complete 6D motion of a body for posturographic testing. This system should be both inexpensive and convenient to implement and use. Stereo vision systems offer an appropriate solution; in fact, they are already well established in the study of gait and posture (13–16). However, their implementation often suffers from a lack of specialization, instead making use of expensive, one-size-fits-all commercial systems which need to be customized. They also frequently require the placement of many markers on the body which is time consuming and not ideal for routine use (4). There is a huge variety of affordable camera technology and code libraries specifically for calibration and implementation of computer stereo vision (17). In this work we take advantage of these resources to implement and validate a stereo vision system specifically for static posturography which is easy to use and, when used in complement to force plate measures, provides a more complete analysis of postural control. We present this implementation step-by-step from theoretical foundations to equipment validation. To date we are unaware of any other publication which covers these topics in such detail for static posturography.

MATERIALS AND METHODS

Theory

We developed a stereo vision system able to track a rigid body's 6D motion. The rigid body (or target) comprises three markers. Two cameras whose relative position and orientation are known, observe the same marker. By locating the marker's centroid in each 2D image plane the marker's 3D position centroid may be calculated relative to a predefined coordinate system. By tracking the three markers attached to the rigid body, the body's 6D position and orientation may be calculated by determining the linear transform which aligns the paired marker centroids from one frame to the next.

Marker Centroid Calculation

We begin with a classic camera model which maps a 3D point onto a 2D image plane using homogeneous coordinates. Homogenous coordinates allow operations such as rotation, translation, and perspective projection to be combined into a single matrix multiply operation (18); their use here greatly simplifies the mathematics involved. The mapping between $\mathbb{R}^3$ Cartesian coordinates and $\mathbb{R}^4$ homogenous coordinates is $[x\,y\,z] \leftrightarrow [x \cdot wy \cdot wz \cdot ww]$ where w is a scaling factor. The classic pinhole camera model follows:

$$\begin{bmatrix} u \\ v \\ 1 \end{bmatrix} = C \cdot E \cdot w \cdot \begin{bmatrix} x \\ y \\ z \\ 1 \end{bmatrix} \tag{1}$$

Where:

$$E = [R \mid T] \tag{2}$$

$$C = \begin{bmatrix} f_u & s_k & p_u \\ 0 & f_v & p_v \\ 0 & 0 & 1 \end{bmatrix} \tag{3}$$

Cartesian coordinates: x, y, and z are mapped to image plane coordinates: u and v by first transforming them to homogeneous coordinates with scaling factor w. Next the camera's extrinsic matrix E brings the coordinate frame to that of the camera's point of view, requiring the augmentation of a rotation (matrix R) and a translation (vector T) (19). Finally the camera's intrinsic matrix C projects the marker's homogeneous coordinates onto the camera's image plane. C's elements are: horizontal and vertical focal length f_u and f_v, respectively; horizontal and vertical principal point (focal center) coordinates p_u and p_v, respectively; and camera skewness s_k (19).

A stereo vision system uses two such camera models observing the same 3D point, for instance, a marker centroid. Assuming the system is calibrated each camera's intrinsic and extrinsic matrix is known leaving a system of six equations with five unknowns, solvable for the observed centroid's coordinates.

A typical solution applies image rectification, a process which reprojects captured images onto a common image plane. As

part of this process virtual camera models are defined such that: intrinsic skewness is zero; both horizontal and vertical focal lengths are equal and the same across cameras (f); the cameras' principle axes are aligned; and, assuming a horizontal stereo configuration, their optical center is offset only horizontally, i.e., along the baseline (T_x). Operating in this new, virtual image plane, the camera models may be written as follows. Numeric subscripts 1 and 2 designate the left and right camera, respectively; the left camera is used as reference.

$$\begin{bmatrix} u_1 \\ v_1 \\ 1 \end{bmatrix} = \begin{bmatrix} f & 0 & p_{u1} & 0 \\ 0 & f & p_v & 0 \\ 0 & 0 & 1 & 0 \end{bmatrix} \cdot \begin{bmatrix} x \\ y \\ z \\ 1 \end{bmatrix} \tag{4}$$

$$\begin{bmatrix} u_2 \\ v_2 \\ 1 \end{bmatrix} = \begin{bmatrix} f & 0 & p_{u2} & T_x \cdot f \\ 0 & f & p_v & 0 \\ 0 & 0 & 1 & 0 \end{bmatrix} \cdot \begin{bmatrix} x \\ y \\ z \\ 1 \end{bmatrix} \tag{5}$$

The solution to Equations (4) and (5) for centroid position (x, y, z) is Equation (6) below where horizontal disparity ($u_2 - u_1$) is mapped to the homogeneous coordinates of the viewed 3D position by reprojection matrix (or Q-matrix) Q (20).

$$w \begin{bmatrix} x \\ y \\ z \\ 1 \end{bmatrix} = Q \cdot \begin{bmatrix} u_1 \\ v_1 \\ u_2 - u_1 \\ 1 \end{bmatrix} \tag{6}$$

Where:

$$Q = \begin{bmatrix} 1 & 0 & 0 & -p_{u1} \\ 0 & 1 & 0 & -p_v \\ 0 & 0 & 0 & f \\ 0 & 0 & -\frac{1}{T_x} & \frac{p_{u1} - p_{u2}}{T_x} \end{bmatrix} \tag{7}$$

Application of Equation (6) requires a calibrated system whose image rectification transforms and Q-matrix are known. In practice this information is gathered in a single calibration process where the stereo vision system is presented with multiple views of a known calibration pattern, typically a checkerboard or grid of dots. Since the pattern geometry (planar pattern, grid interval, size, etc.) is known a robust solution for each camera's intrinsic and extrinsic matrices as well as any non-linear image distortion can be estimated from the captured images. There are multiple algorithms available which perform this estimation, a good summary of which is provided by Dubrofsky (21). From this individual camera information, rectification transforms, and their corresponding Q-matrix can be calculated (20).

Target Position and Orientation Estimation

A minimum of three non-collinear points are required to determine the orientation of a 3D rigid body. The change in position of these three points from one frame to the next is used to calculate the change in both position and orientation of the rigid body. We use a rigid body consisting of an L shaped marker pattern where a marker is placed in the bend (M2) and at each end point (M1 and M3) of the L (see **Figure 1B**).

We define target position (TP) as the translation of marker 2 from an initial reference frame to the current frame:

$$P = M_2 - M_{2ref} \tag{8}$$

In order to calculate the orientation of the target a minimum of three non-planar vectors are required to form a basis. As the rigid body rotates, so does the basis. We defined the basis vectors:

X_A, Marker 1's position vector subtracted by Marker 2's position vector;

X_B, Marker 3's position vector subtracted by Marker 2's position vector; and

$X_C = X_A \times X_B$.

By defining marker 2 as the origin we isolate the rotational component of the motion.

The orientation of the object can then simply be defined as the rotation matrix which rotates the initial basis to the current basis (22):

$$R = \begin{bmatrix} X_A & X_B & X_C \end{bmatrix} \cdot \begin{bmatrix} X_A & X_B & X_C \end{bmatrix}_{ref}^{-1} \tag{9}$$

We decompose this rotation into a set of Fick Euler angles (rotation sequence: roll—ψ, pitch—ϕ, and yaw—θ) using the following conversion formula where numeric subscripts designate individual elements of rotation matrix R (23).

$$\begin{bmatrix} \psi \\ \phi \\ \theta \end{bmatrix} = \begin{bmatrix} \text{atan2}\left(\frac{R_{32}}{\cos(-\sin(R_{31}))}, \frac{R_{33}}{\cos(-\sin(R_{31}))}\right) \\ -\sin(R_{31}) \\ \text{atan2}\left(\frac{R_{21}}{\cos(-\sin(R_{31}))}, \frac{R_{11}}{\cos(-\sin(R_{31}))}\right) \end{bmatrix} \tag{10}$$

Implementation

Our stereo vision system consists of two monochrome cameras (BFLY-PGE-13E4M-CS, PointGrey, Canada) externally triggered with a microcontroller (MK20DX256, NXP Semiconductors, Netherlands) to capture simultaneous 640 × 512 pixel resolution frames at 100 Hz. Each camera has a lens (12VM412ASIR, Tamron, Japan) adjusted to a focal length of 6.9 mm with an IR low pass filter (R5000212478-15188, Edmund Optics, USA) mounted externally. These cameras are ceiling mounted at a height of 2,275 mm with a baseline of 870 mm and a vergence angle of 54°. This configuration views the specified measurement volume, see **Table 1** and **Figure 1C**.

The target consists of a 3D printed, ABS plastic body which has a compartment for some minor electronics and a 55 mm L shaped pattern on top with recesses for each marker. A spherical marker is fixed at the bend and each endpoint of the L pattern (**Figure 1B**). These markers are white, semi-opaque, 12 mm diameter, Acetal plastic ball bearings (BL-01200-AC, Miniature Bearings Australia, Australia). Markers are backlit with IR LEDs (TSHF6410, 890 nm, Vishay Semiconductors, USA). This choice of spherical marker and backlighting produces bright circular disks in the image plane which are easily tracked and whose COM corresponds to the same 3D marker centroid in both image planes. The target is mounted on a stiff pivot joint and

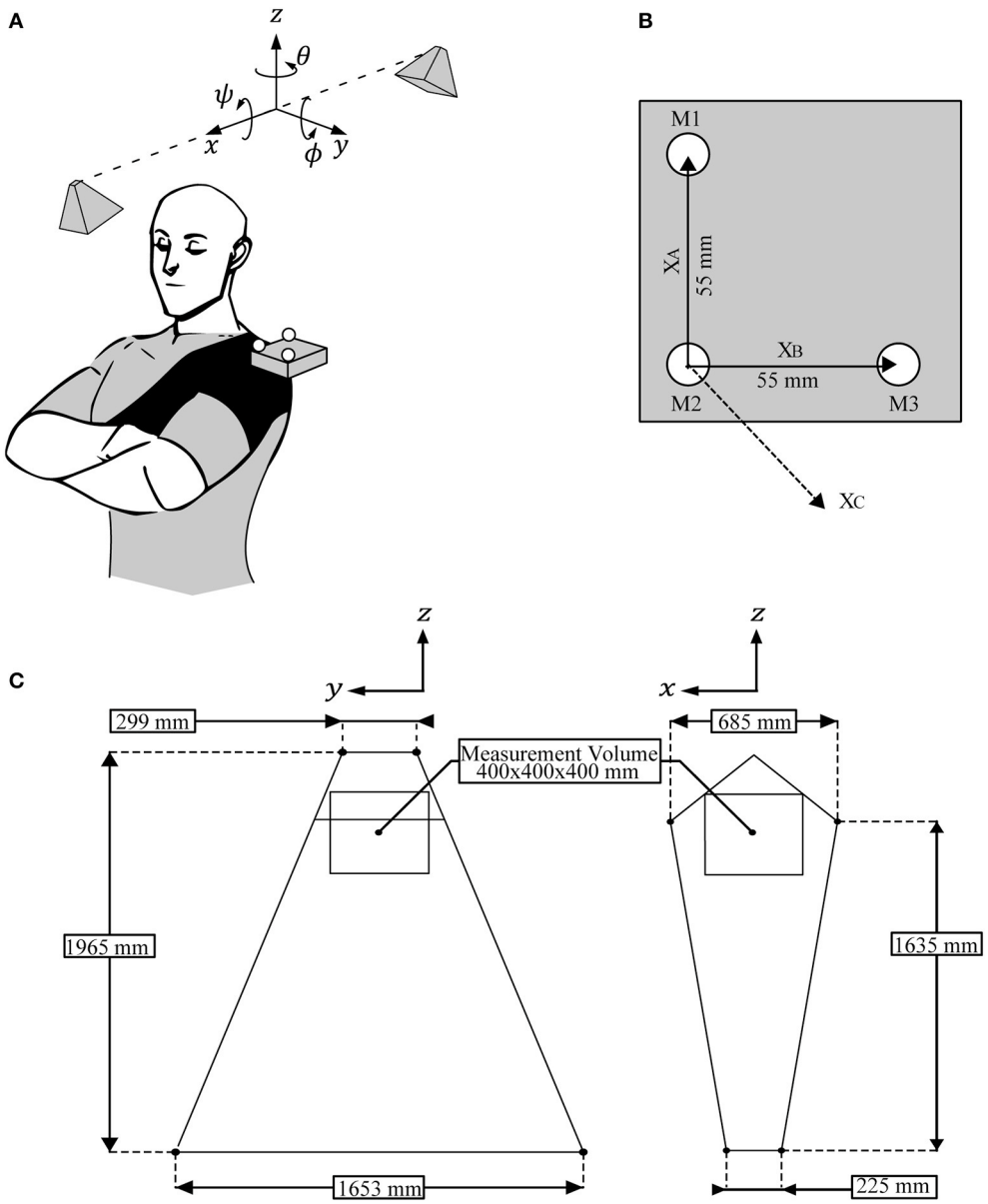

FIGURE 1 | System implementation. **(A)** A subject wearing a shoulder brace with incorporated stereo vision target attached by a stiff pivot joint. The system's two cameras are mounted above the subject's left shoulder. The coordinate frame is aligned such that: the *z* axis is vertical, the *x* axis is horizontal and aligned with the stereo vision baseline, and the *y* axis is perpendicular to *x* and *z*. The subject is positioned with their anterior, left lateral, and superior directions aligned with the *x*, *y*, and *z* axes, respectively. **(B)** Top view of the stereo vision target. Markers M1, M2, and M3 are affixed in an L pattern on the target's top surface with 55 mm spacing. Vector X_A is the difference between the position of M2 and M1. Similarly vector X_B is the difference between the position of M2 and M3. Vector X_C is the cross product of X_A and X_B. **(C)** The volume viewable by both of the system's cameras in the *yz* plane (left diagram) and the *xz* plane (right diagram). Posturographic measurements are taken from the labeled measurement volume which is a cube with 400 mm sides aligned with the system's axes and centered at a height of 1,370 mm. It is a sub-volume of the viewable volume.

incorporated into a shoulder brace (538CP Shoulder Support, LP Support, USA). The brace is strapped firmly around the subject's upper arm and torso so that it moves rigidly with the subject, see **Figure 1A**. The pivot joint allows an operator to adjust the target to approximately face the stereo vision system.

Our stereo vision system is controlled through a custom user interface written using NI LabVIEW 2014 SP1 f3 and NI Vision Development Module 2014 SP1. Calibration was performed using LabVIEW's stereo calibration example program. The calibration pattern used was a flat grid of 15 × 12 black dots on a white background with 26.4 mm dot spacing and 13.5 mm dot diameter. This provided: intrinsic, C, and extrinsic, E, camera matrices as well as the reprojection matrix, Q, and image rectification transforms. Captured images were rectified as

TABLE 1 | System specifications.

Parameter	Specification	Source
Bandwidth	0.01–10 Hz	Expected bandwidth of posturographic motion (24)
Sampling frequency	100 Hz	Recommended rate based on the degradation of typical posturographic parameters when subsampling signals (24)
Measurement volume	400 mm cube at 1,370 mm height	This cube encompasses the 95th male percentile and 5th female percentile shoulder height, 1,525 and 1,215 mm, respectively, and is centered between the two (25). The cube is wide enough to encompass the typical limit of stability (LOS), 196 mm, observed in young healthy male subjects [LOS = 1525 mm* tan(7.34°) = 196 mm] (26)
Position resolution	4.2 mm	This position resolution is equal to the standard deviation of the absolute values of the test-retest difference of COP range over 10 sessions and 10 subjects. Data is collected from healthy subjects standing on a solid surface (27). Such resolution should minimally impact measurement noise
Orientation Resolution	0.2°	This orientation resolution is calculated from the position resolution by assuming an inverted pendulum sway model and worst case (minimum) subject height equal to 1,215 mm (5th female percentile shoulder height). [Orientation Resolution = (180°* 4.2 mm)/(π* 1,215 mm) = 0.2°]

per calibration; such that Equation (6) could be used to calculate the position of marker centroids. Captured images were then low pass filtered (each pixel's intensity was set to the average of the surrounding eight pixels) to reduce the random noise arising from the image sensor electronics.

Markers were identified in each image by searching for their key defining features, specifically markers are: bright, of a certain size, round, and slow moving. After low pass filtering, images were intensity thresholded to keep only the brightest image segments; this separated the markers from their background and reduced the complexity of further image processing. The resulting, bright image segments were then filtered by their: area (number of pixels) keeping only those segments which were the expected size of a marker; and their Heywood circularity (28), keeping only those segments which were sufficiently round to be a marker. The remaining segments' centroids were then calculated using a COM algorithm (28). Finally, segments were identified as markers in one of two ways. First-time execution identified markers by looking for the target's known L-shaped pattern; an operator could repeat this first-time execution whenever they deemed the images to be suitable for such identification (i.e., when there were few artifacts or cluttering segments). Subsequent execution identified markers by finding the segments which would result in the smallest marker movement; each permutation of paired segments and last known marker centroids were compared and the permutation with the lowest cost (defined as the summed straight-line distances between current potential marker centroids and the known prior marker centroids) was selected.

Having identified the marker centroids in each image plane the 3D marker positions were calculated using Equation (6) and stored as the current basis. The reference basis was manually selected from some prior time. Given the reference basis and the current basis the target's position (Equation 8) and orientation (Equation 10) were calculated for each frame and saved to disk. Prior to analysis the target's position and orientation signals were low pass filtered with a 10 Hz, 10th order, zero-phase, Butterworth filter keeping the signal's bandwidth as per **Table 1** and reducing high frequency noise.

System Modeling

The stereo vision system was developed and tested in a temporary environment. A key aspect of its development was modeling the expected measurement precision. Such modeling gave confidence in system performance prior to installation and in-place validation. All modeling was performed using MATLAB R2016b.

The law of error propagation maps the uncertainty of independent variables to the uncertainty of dependent variables (29). It forms the foundation of our modeling approach and can be written as follows for a linear system approximation (30).

$$\Lambda_F = J(\bar{x}) \cdot \Lambda_x \cdot J(\bar{x})^T \tag{11}$$

Here: Λ_x and Λ_F are the covariance matrices of independent variables and dependent variables, respectively; $\bar{x}$ is the system model defining the relationship between independent and dependent variables; and $J(\bar{x})$ is the Jacobian of $\bar{x}$ with partial derivatives taken with respect to the independent variables.

Application of the model requires quantification of the uncertainty on the model's inputs, and repeated calculation of the expected uncertainty of the system's outputs given the variety of situations we reasonably expect. We performed modeling as a two-step process first simulating the precision of the measurement of a single marker's position (equivalent to the target's position) and then secondly simulating the precision of the measurement of the target's orientation.

When simulating position measurement the model ($\bar{x}$) is Equation (6). This has independent variables: u_1, u_2, and v comprising the centroids of a marker in rectified image space; and dependent variables: x, y, and z. The uncertainty in marker centroids is typically dominated by quantization uncertainty and in the absence of further details is often estimated as a standard deviation equal to 0.5 pixels (30). Other application specific estimates can be found in literature, for instance for fiducial localization (31, 32) or edge detection (33, 34). We bypassed such estimates and measured input uncertainty directly in order to produce a more accurate system model. We measured the centroid of one marker over 10 s at the closest, central, and furthest distances expected for our application (700, 900, and 1,100 mm, respectively). The average centroid variance was 0.001819 pixels^2. Assuming no covariance between centroid coordinates we substituted this variance into Λ_x and

determined an expression for Λ_F using MATLAB's symbolic expressions. This expression is dependent upon marker centroid coordinates which can be determined for any marker position using Equations (4) and (5). The estimated uncertainty of x, y, and z was then calculated for each marker position in a 3D grid matching the measurement volume (**Table 1**) with 100 mm spacing.

When simulating orientation measurement the model ($\overline{x}$) is Equation (10). This has nine independent variables: the x, y, and z coordinates of the three target markers; and dependent variables: ψ, ϕ, and θ. The expected uncertainty of the marker position coordinates can be substituted directly from the prior position measurement simulation. Assuming no covariance between these coordinates we substituted into Λ_x and determined an expression for Λ_F using MATLAB's symbolic expressions. The expression is dependent upon the 3D marker positions which can be determined by rotating a horizontal reference model matching the target's dimensions. The estimated uncertainty of ψ, ϕ, and θ was then calculated for each target orientation in a polar grid with range $\pm 20^\circ$ in each axis and 10° spacing.

System Validation

The goal of system validation is to provide accuracy and precision statistics regarding the measurement of TP and orientation. Although precision is easily quantified through repeated measures, accuracy can only be obtained by comparing measurements to a reference. We used equipment that manually controlled the position and orientation of the target to provide this reference. Horizontal TP was controlled using a grid with 1 mm increments. This grid was mounted on a vertical sliding axis for depth control. Target orientation was controlled using a manual 3D gimbal with 1° increments.

The accuracy, trueness, and precision of the system's measurement of TP were evaluated by translating the target using the sliding grid. The target was sequentially fixed at points in the grid pattern matching the system's measurement volume, a 400 mm cube centered along the baseline at a depth of 900 mm. Using 100 mm grid spacing 125 fixation points were defined. Each position was held for 1 s providing 100 observations per position. Prior to evaluation a reference target was measured at the center of the cube to define the coordinate frame from which relative translations were measured. This was orthogonalized using the Gram-Schmidt process and aligned to the coordinate frame with a slight rotation. Errors for each xyz component of position were defined for each observation as the difference between the grid location and measured marker position. The xyz accuracy of each observation was defined as the absolute value of the errors. The accuracy, trueness, and precision of each fixation point were then defined as the mean accuracy, mean error, and error standard deviation, respectively, of all observations corresponding to that fixation point. Finally the typical accuracy, trueness, and precision of any subset of the measurement volume were defined as the median accuracy, trueness, and precision of the fixation points within that subset. Subsets taken included: all fixations, to provide a measure of typical performance; and horizontal grid levels, to provide a performance trend with increasing depth.

The accuracy, trueness, and precision of the system's measurement of target orientation were evaluated by manually rotating the target using a gimbal. The target was fixed in a 3D polar grid pattern which spanned $\pm 20^\circ$ about each axis and used a spacing interval of 10°. The gimbal was translated vertically to the closest, central, and furthest depths in the measurement volume (700, 900, and 1,100 mm, respectively). Evaluating the polar grid pattern at each of these depths defined a total of 375 orientations. Each orientation was held for 1 s providing 100 observations per orientation. Prior to evaluation of each polar grid pattern a reference target orientation was defined from which relative orientations could be determined. This reference target was centered along the baseline and oriented such that its markers lay in a horizontal plane facing the system's cameras. For each observation the 3D rotation (difference rotation) between the measured orientation and the polar grid orientation was determined. Errors for each observation were defined as the Euler Fick angles of this difference rotation. The $\psi\varphi\theta$ accuracy of each observation was calculated as the absolute value of the errors. The accuracy, trueness, and precision of each orientation were calculated as the mean accuracy, mean error, and error standard deviation, respectively, of the 100 observations corresponding to each orientation. Finally the typical accuracy, trueness, and precision of any subset of these orientations were defined as the median accuracy, trueness, and precision of that subset. Subsets taken included: all orientations, to provide a measure of typical performance; all orientations at each depth, to provide a performance trend with increasing depth; and orientations pooled by rotation purely about each axis, to provide a performance trend with changing target orientation.

In Vivo Validation

Participation in this study was voluntary and informed written consent was obtained as approved by the University of New South Wales Human Ethics Committee.

To provide insight into the benefits of a complementary stereo vision—force plate system an *in vivo* validation was performed. A custom z-axis force plate was used to capture vertical ground reaction forces at 100 Hz. The force plate consisted of a 450 × 450 mm steel plate supported by load cells in each corner (Xtran S1W 750N, Applied Measurement Australia, Australia). From these ground reaction forces the subject's instantaneous COP was calculated (35). COP was then filtered to match the stereo vision system with a low pass 10 Hz, 10th order, zero-phase, Butterworth filter.

One subject (male, age 69) with left sided superior vestibular neuritis (onset 8 months prior to assessment in this study), as confirmed by a Neurologist (clinical assessment upon referral included: Romberg test positive on foam, video head impulse test on horizontal canals [right canal gain = 0.76, left canal gain = 0.5 with a volley of overt refixation saccades 120–150 ms after head impulse onset], no observed spontaneous or positional nystagmus, no observed gait difficulty), was simultaneously recorded with the force plate and the stereo vision system. Recordings included capture of a shared external trigger which was used to synchronize each data time series. The subject stood on a foam surface (to limit proprioceptive input and increase the

balance challenge) with their feet together and arms crossed for a period of 20 s under two conditions. The first condition required the subject's eyes to be open (predominantly visual and vestibular input) and the second required them to be closed (predominantly vestibular input).

Stereo vision was compared to COP by extracting the stereo vision target's x and y position data. System correlation was assessed using Spearman's correlation coefficient. In the time domain, data was assessed using traditional posturographic parameters: path length, the total distance traveled by a point; and the range of x and y position. Frequency content was assessed by computation of the power spectral density (PSD) of each signal by Welch's method followed by calculation of the frequency below which 99% of the power spectrum is contained (referred to as f99) (36).

RESULTS

System Performance

Typical performance was estimated by summary statistics of trueness, accuracy, and precision of position and orientation measures calculated from the complete 375 validated positions and orientations. Performance mean and standard deviation is presented in **Table 2**. Performance five number summaries (median, 1st, and 3rd quartiles, maxima, and minima) are presented as box plots in **Figure 2**. These box plots provide a detailed view of typical performance and the spread of that performance across the measurement volume. We use the median as a measure of performance rather than mean because it is more robust to outliers.

Median measurement trueness is within 0.4 mm and 0.23° for each coordinate; however, a wide interquartile range demonstrates a large spread of measurement trueness across possible target positions and orientations. Measurement accuracy thus better demonstrates the typical error expected on a given datum with median accuracy <1.1 mm and <0.8° for each coordinate. Accuracy positive skew is due to its calculation as the absolute value of errors. Measurement precision is a good estimate of noise and possible measurement resolution, median precision is <0.10 mm and <0.14° for each coordinate.

System modeling gave an estimate of system performance prior to installation and validation. modeling was performed across 375 TP s and orientations matching the validation procedure and the measurement volume. Modeling results were summarized by: mean and standard deviation presented in **Table 2**; and median presented in **Figure 2**. The mean difference between modeled and validated precision was 11.3% with modeling always underestimating the validated result. The minimum 1.7%, and maximum 18.5%, differences occurred in the y and z coordinates, respectively.

Effect of Target Depth

The effect of target depth on measurement precision was investigated by calculating the mean and 95% confidence interval of precision data pooled by test depth. At each depth there were a total 75 positions and 125 orientations. Precision trends plotted against depth are presented in **Figure 3**. Measurement precision of z, ψ, ϕ, and θ demonstrated the strongest linear trends ($R^2 > 0.97$) with precision worsening with increasing depth. The z coordinate had the most pronounced depth trend of the position coordinates with slope equal to 0.00014 mm/mm. Trends for x and y also had a strong linear fit ($R^2 = 0.82$ and $R^2 = 0.735$, respectively) but had near zero slope i.e., <0.00004 mm/mm. The ψ and ϕ coordinates have the most pronounced depth trend of the orientation coordinates with equal slope 0.00026°/mm. The θ coordinate is affected by depth approximately half as much as ψ and ϕ with slope equal to 0.00011°/mm.

Effect of Target Orientation

The effect of target orientation on orientation measurement trueness was investigated by calculating the mean and 95% confidence interval of trueness data pooled by orientation displacement. Only target orientations due purely to rotation about a single axis were considered, other data was discarded. At each orientation a total of three measures contributed from each of the three tested depths. Orientation trueness trends are presented in **Figure 4**. For clarity, only the data regarding measurement of the changing coordinate is shown.

Changing ψ most affected the measurement trueness of ψ ($R^2 = 0.90$, Trueness $= 0.055 + 0.043\psi$), ϕ and θ were comparatively unaffected ($R^2 < 0.52$, slope $< 0.010°/°$). Changing ϕ most affected the measurement trueness of ϕ ($R^2 = 0.95$, Trueness $= 0.244–0.046\phi$); although, both ψ and θ were also affected ($R^2 = 0.79$, and $R^2 = 0.58$, respectively; slope $< 0.03°/°$). Changing θ did not significantly affect trueness in any coordinate, most affected was ϕ ($R^2 = 0.76$, Trueness $= -0.070–0.012\theta$), other coordinates exhibited almost no effect ($R^2 < 0.42$, slope $< 0.009°/°$).

Orientation error measured as a percentage of actual target orientation can be extracted from the slopes of these linear regression fits. Regarding the data belonging to the changing coordinate, orientation error was: 4.3% in ψ, 4.6% in ϕ, and 0.9% in θ; although, the fit for θ is poor ($R^2 = 0.417$).

In Vivo Methods Comparison

A single subject's force plate measured COP and stereo vision measured x and y (TP) were collected over 20 s while standing on a foam surface under two conditions: eyes open, and eyes closed (**Figure 5**). The two system's time series data were well correlated under both conditions (Spearman's, $p_1 = 0.87$ and $p_2 = 0.73$). COP contained a broader power spectrum ($f99_1 = 3.42$ Hz, $f99_2 = 3.52$ Hz) compared to TP ($f99_1 = 1.07$ Hz, $f99_2 = 0.97$ Hz). The broader power spectrum contributed to a longer path length in COP ($path_1 = 832$ mm, $path_2 = 3{,}176$ mm) compared to TP ($path_1 = 350$ mm, $path_2 = 1{,}778$ mm). Each system's position range was similar during the eyes open condition ($range_{COP} = [43\text{ mm}, 47\text{ mm}]$, $range_{TP} = [44\text{ mm}, 43\text{ mm}]$) but differed significantly during the eyes closed condition ($range_{COP} = [128\text{ mm}, 189\text{ mm}]$, $range_{TP} = [303\text{ mm}, 327\text{ mm}]$). There is a clear change in behavior during the 6.5 to 10 s interval in the eyes closed condition. Removing this interval, the eyes closed condition no longer shows such a significant difference between system's position range ($range_{COP} = [109\text{ mm}, 149\text{ mm}]$, $range_{TP} = [144\text{ mm}, 122\text{ mm}]$). Both systems demonstrated an increase

TABLE 2 | Typical performance results of target position and orientation measurement from validation and modeling.

Performance measure	Position (mm)			Orientation (°)		
	x	*y*	*z*	ψ	ϕ	θ
Trueness	−0.3710 ± 0.3494	0.0682 ± 0.7404	−0.3483 ± 1.3883	0.1623 ± 1.2318	0.1412 ± 0.7750	−0.2342 ± 0.8711
Accuracy	0.4244 ± 0.2821	0.6017 ± 0.4361	1.1778 ± 0.8114	0.7418 ± 0.7657	0.9747 ± 0.5111	0.6277 ± 0.8711
Precision	0.0449 ± 0.0141	0.0567 ± 0.0206	0.0955 ± 0.0338	0.1492 ± 0.0559	0.1412 ± 0.0306	0.0918 ± 0.0566
Modeled precision	0.0384 ± 0.0062	0.0530 ± 0.0084	0.0779 ± 0.0239	0.1182 ± 0.0048	0.1155 ± 0.0030	0.0783 ± 0.0023

Typical performance measures are presented as mean ± standard deviation data across all tested positions and orientations.

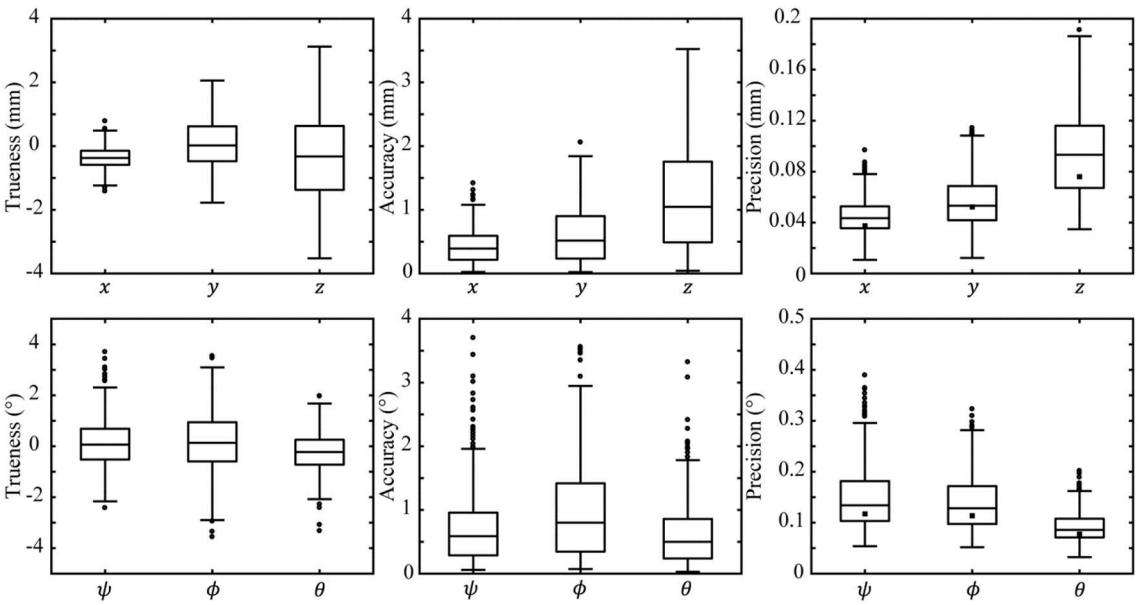

FIGURE 2 | Results of validation and modeling evaluated over the whole measurement volume. The top and bottom rows plot measurement trueness (left column), accuracy (middle column), and precision (right column) for position and orientation, respectively. Validation data of each coordinate are represented as a box plot. The central line of each box plot indicates the median of its data, the top and bottom edges indicate the 1st and 3rd quartiles, respectively, and the whiskers represent the minimum and maximum datum excluding outliers. Outliers (datum further than 1.5 times the inter quartile range from the 1st and 3rd quartiles) are drawn as open circles. Median modeled precision is overlayed on each box plot as a filled square.

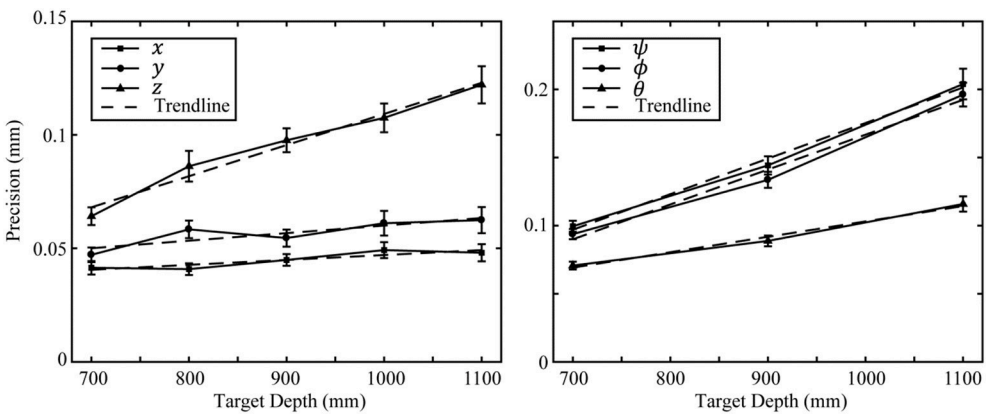

FIGURE 3 | Precision depth trends. The left figure plots position measurement precision against target depth. The right figure plots orientation measurement precision against target depth. Error bars represent the 95% confidence interval of each datum. Linear trend lines are plotted for each data series.

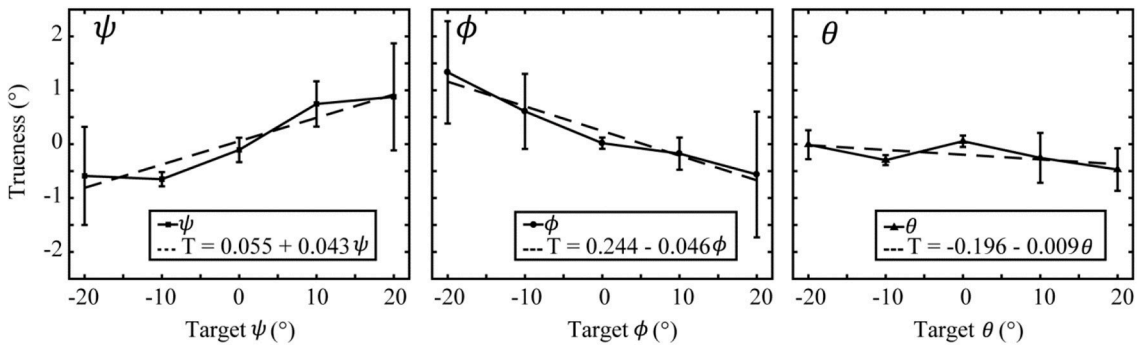

FIGURE 4 | Orientation trueness plotted against target orientation. Pure rotations about the roll axis (left figure), pitch axis (middle figure), and yaw axis (right figure) are shown. Error bars represent the 95% confidence interval of each datum. Trend lines are plotted for the measurement trueness corresponding to each figure's primary axis.

in task difficulty from the eyes open to the eyes closed condition with an order of magnitude increase in the path length and position range parameters.

The change in behavior during the 6.5–10 s interval reflects a change in balance strategy due to sudden imbalance. In the *x* (anterior-posterior) direction at 6.5 s the subject pressed hard with the front of their foot as shown by the COP data. This shifted their COM back such that COP was directed through the subject's heel, shown by the flat oscillation between 7.5 and 9 s in COP data. While the subject's COP was directed through their heel the subject's trunk continued backwards until they were able to regain postural control by pivoting forwards at their hips during the 8–9 s period as shown by the TP data. This backward and then forward trunk motion and inferred hip pivot response was captured by the complementary stereo vision—force plate system. It would have been missed had either of these systems not been present.

In the same period of instability a change in balance strategy is also observed in the *y* (mediolateral) direction. Ordinarily the subject's body acts approximately as an inverted pendulum since their feet are together. However, at 8 s the subject loads their left foot heavily, unloading their right foot (as seen in the leftwards COP data) and simultaneously shifts their shoulder rightwards (as seen in the TP data). As a result the subject acts as a double inverted pendulum and they are able to control their COM by applying torque both with their ankles and hips. Again this change in posture and control strategy would not have been captured without the complementary system.

DISCUSSION

The developed stereo vision system is able to measure target position and orientation within the specifications required for posturography. Position measures are, at worst, precise to 0.1 ± 0.04 mm and orientation measures are, at worst, precise to 0.15 ± 0.06°. However, there is systematic inaccuracy which, depending on the coordinate, typically contributes 0.4–1.1 mm position error and 0.5–0.8° orientation error. Modeling closely predicted system precision (mean error = 11.3%) but did not model systematic error. *In vivo* comparison between force plate measured COP and stereo vision measured *xy* TP demonstrates good correlation (Spearman's, $\rho \geq 0.73$) in the time series data. Comparable *in vivo* parameters show similar changes between conditions for both systems. During periods of instability the complementary stereo vision—force plate system provided additional insight to the subject's posture and control.

We followed an affordable approach to stereo vision and in keeping with this methodology we used manual equipment for validation rather than expensive, highly accurate robotic (37), or vision systems (38). As such we expect that a significant portion of the quoted positional inaccuracy is contributed by the validation equipment and is not actually inherent to the stereo vision system. Equipment gradation creates an imperfect reference contributing an unpredictable bias to each measured error. The sliding grid's 1 mm position gradation and the gimbal's 1° orientation gradation are expected to have contributed up to 0.5 mm position error and 0.5° orientation error in each coordinate. Had a more accurate reference been used in validation remaining systematic error could have been corrected by a model. Nevertheless the reported inaccuracy is small as compared to force plate errors which have been reported up to ±30 mm (35). Therefore, we consider the affordable approach taken here to be suitable for this application.

The trend of position measurement precision worsening with increasing depth is a well-known phenomenon of stereo vision systems as is the fast rate of precision decline in the depth measurement itself (39). It follows that any orientation measure based on such position measurements would also have worsening precision due to error propagation and it is unsurprising that the orientation coordinates most dependent on a depth measure (ψ) and ϕ would be the most affected.

It is surprising that there is a strong relationship between target orientation error and target orientation. This effect is not significantly observed in pure θ rotations but contributes up to 5% error in the ψ and ϕ coordinates. This is due to the target

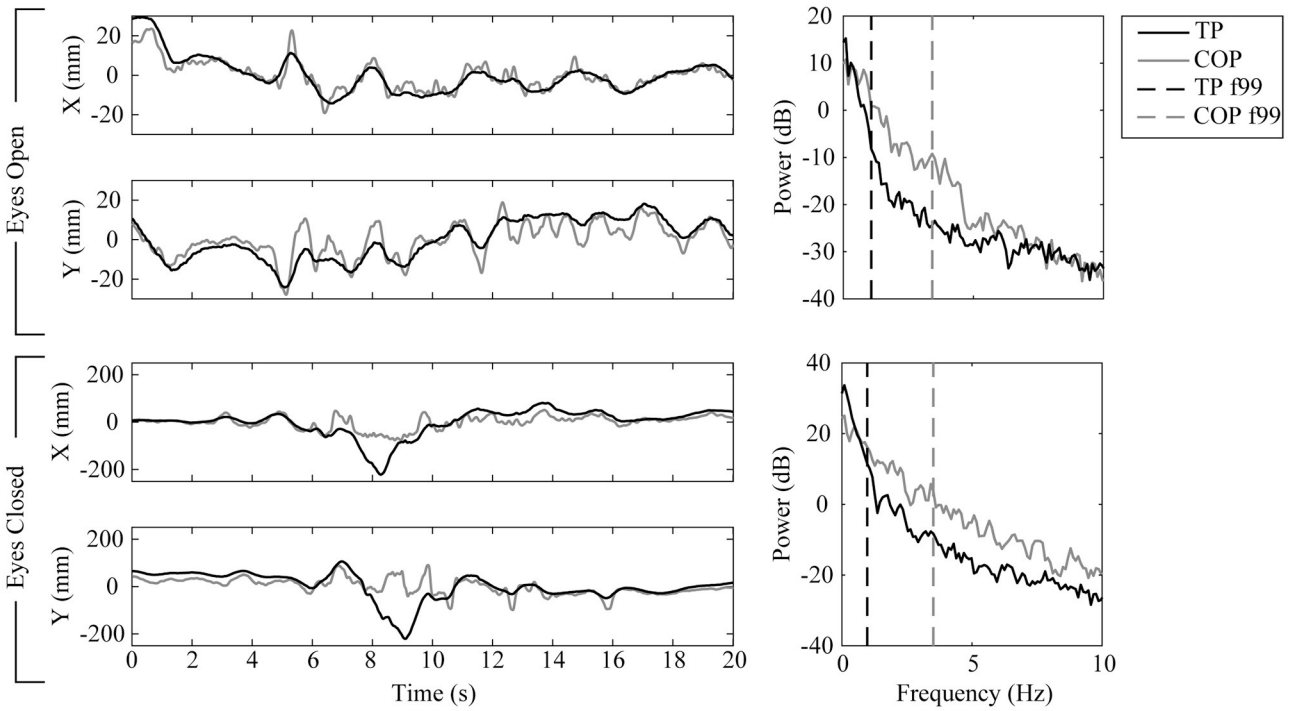

FIGURE 5 | *In vivo* method results for one subject tested while standing on a foam surface under two conditions: eyes open (top half), and eyes closed (bottom half). Force plate recorded COP results and stereo vision recorded target position (TP) results are rendered in gray and black, respectively. Time series (left column) for each condition are split into *x* (top graph) and *y* (bottom graph) coordinates. Power spectrums (right column) estimate the distribution of power among the time series' frequency components; each time series' f99 parameter (the frequency below which 99% of the signal's power is contained) is overlayed as a vertical dashed line.

design. The intention of the target's spherical markers was to produce circular image segments whose centroids corresponded to the markers' exact 3D centers. However, due to the beam pattern of the infra-red backlighting, it was observed that instead elliptical image segments were produced when the target was tilted away from each camera's optical axis. These elliptical segments became increasingly eccentric the further the target was tilted. This contributed error in two ways: first, given each camera had a separate point of view, their image segment centroids no longer corresponded to the same 3D location which produced a mismatch and violated the assumptions made for accurate position estimation; second, since this elliptical pattern changed with tilt, the same 3D point is not necessarily tracked between frames which resulted in under or overestimation of target movement. This suggests the more common passive target design utilizing reflective markers and global lighting would be more accurate at large target angles. However, external lighting can create complicated scenes in the presence of unanticipated reflective objects which increases measurement setup complexity and time. Our approach prioritizes easy setup and the observed backlighting effect could be minimized with an improved target design. Such a design would reduce the directionality of the LEDs and position them at the center of the spherical markers.

While considering system design it is worth exploring the possibility of including redundant markers on the target and also the trade-offs between the simple solution presented here and other more complex solutions for target position and orientation estimation. The approach presented here is by far the simplest, three markers is the minimum required for 3D orientation calculation, and a minimum of one marker (M2) is used to define 3D TP. However, this minimal approach does cause problems when markers are occluded; when any marker is obscured orientation information is lost, similarly if M2 is obscured position information is lost. Without altering hardware design a marginally more robust solution for TP may be defined as the mean marker position. Then given any combination of visible markers a TP is defined. Unfortunately the mean position changes depending on the set of visible markers creating discontinuities and confusing data. Another method of position estimation is the calculation of the instantaneous center of rotation (COR) of the target using all three markers (40). In a rigid body the COR is unambiguous avoiding the confusion created by the mean position option. It also removes the influence of rotation on the position estimate, i.e., markers can translate during pure target rotations (41). With only three markers COR is a less robust solution; however, with additional redundant markers COR can be calculated from any set of three markers protecting from data loss as a result of occlusion. In fact with more than three available markers the most representative COR can be selected or solved by least squares giving the system an inherent robustness to noise and

outlying estimates (42). Target orientation estimation would similarly benefit from the addition of redundant markers as a best fit solution could be chosen from multiple three marker estimates. However, in this application COR does have some important flaws: in the presence of small rotations, as is the case in static posturography, COR is extremely susceptible to noise (43); in this case we also expect COR to simply correspond the position of the subject's ankles and not their COM since, assuming they have adopted an ankle strategy, this is the position they are rotating about. For these reasons COR was not used for this application. Multiple markers were also determined to be unnecessary as they were rarely occluded, nevertheless in more challenging environments they would be a good addition.

It has been shown that during quiet standing tasks, points affixed to a subject's body have proportional movement (16). Considering a subject's COM as such a point it is expected that stereo vision measured TP would be proportional to COM when the target is affixed to the subject's shoulder. Our *in vivo* results indicate that this is the case. In the quiet standing task COP must oscillate about COM to maintain balance (3); our data demonstrated COP oscillation about TP. In gross movements COP must shift in the direction of COM movement to counteract the body's momentum; our data demonstrated this with a good positive correlation between COP and TP in both the x and y coordinates (Spearman's, $\rho \geq 0.73$). Finally COM is composed of frequencies below 1 Hz since the human body acts as a mechanical low pass filter (44); we measured the TP's power spectrum which matched this frequency range (f99 $<$ 1.1 Hz). Stereo vision measured TP can therefore be used as a reasonable estimate of scaled COM in quiet standing tasks when stability is maintained.

Both stereo vision and force plate systems were able to detect the increased task difficulty between the eyes open and the eyes closed conditions. This challenge was demonstrated by the order of magnitude increase in traditional posturographic parameters: path length, and position range. However, a more complete analysis of the subject's postural control could be determined by considering the data captured by both systems in complement. During the easier eyes open condition, COP (captured by the force plate) simply oscillated about TP (captured by the stereo vision system) which indicated that the subject was able to maintain balance by using an ankle strategy. In contrast the harder eyes closed condition necessitated a combined hip-ankle strategy after the subject became unstable. Having reached their limit of stability (as identified by the force plate) the subject pivoted at their hips (as identified by the stereo vision system) to maintain stability. This insight into employed strategy could not be identified without the data from both the force plate and the stereo vision system. Further parametric analysis could therefore be based on adopted strategy rather than some assumed strategy.

This study presents preliminary results for the developed stereo vision system and its use in complement with a force plate. In order to validate the use of this system in a clinical setting further work is required to standardize the interpretation of the measured sway including identification of postural strategies, and parameterization of COM control for balance assessment. Future work must also establish normal reference values across gender and age in a healthy population followed by an analysis of deviation from these reference values given populations which different pathologies. Correlation was shown between the developed stereo vision system and a force plate in static posturography. This stereo vision system can be used to measure sway while subjects stand on a platform with a foam surface or a moving platform. With this configuration the contribution of proprioception and vision to the vestibulospinal response can be minimized to isolate the vestibular contribution. COP/sway and latency to step during a balance perturbation, via the platform or directly to the body, also provide functional test measures of vestibular function. For further clinical validation future work should correlate these measures with other established optical systems followed by other technologies including dynamic force platforms, inertial sensors, and electromagnetic trackers.

CONCLUSIONS

A stereo vision system was developed to directly measure 6D human sway for static posturography. This approach was inexpensive and made accessible by the abundant resources available for stereo vision development. Preliminary results show 3D position and orientation measures were precise to, at worst, 0.1 ± 0.04 mm and $0.15 \pm 0.06^{\circ}$, respectively. Computer modeling was able to predict this precision with 11.3% mean error. 3D position and orientation measures were typically accurate to 1.1 mm and 0.8° in the worst case coordinates: depth and pitch. *In vivo* comparison between stereo vision measured position and force plate measured COP demonstrated good correlation and both systems were able to discern task difficulty. However, when used in complement, balance strategy could be identified which could inform further parametric analysis. Balance strategy could not be identified with the data from only one system. This stereo vision system coupled to a foam platform or a balance perturbation system can be used to provide a functional test of vestibular function. For clinical use, future work must standardize balance assessment parameters, establish normal reference values across gender and age in healthy and pathologic populations, and investigate correlation with existing systems.

ETHICS STATEMENT

This study was carried out in accordance with the recommendations of the National Statement on Ethical Conduct in Human Research and processes outlined in the UNSW Human Research Ethics Operations Manual, UNSW Human Ethics Committee. The protocol was approved by the UNSW Human Ethics Committee. All subjects gave written informed consent in accordance with the Declaration of Helsinki.

AUTHOR CONTRIBUTIONS

AM conceived and supervised this work. WF carried out the research, modeling, implementation, validation, and analysis with input from AM. WF wrote the manuscript with critical feedback from AM.

FUNDING

This work was supported by the NHMRC Development Grant (APP105550); and a Garnett Passe and Rodney Williams Memorial Foundation Senior Principle Research Fellowship to AM.

ACKNOWLEDGMENTS

We thank Dr. Phillip Cremer, Associate Professor at the University of Sydney and neurologist at North Shore Vertigo and Neurology Clinic, for his diagnosis of vestibular neuritis in our subject. We also thank Dr. Richard Fitzpatrick, Associate Professor at the University of New South Wales, for his advice and assistance in configuring the force plate equipment used in our study.

REFERENCES

1. Mancini M, Horak FB. The relevance of clinical balance assessment tools to differentiate balance deficits. *Eur J Phys Rehabil Med.* (2010) 46:239–48.
2. Massion J. Postural control system. *Curr Opin Neurobiol.* (1994) 4:877–87. doi: 10.1016/0959-4388(94)90137-6
3. Winter DA. Human balance and posture control during standing and walking. *Gait Posture* (1995) 3:193–214.
4. Browne JE, O'Hare NJ. Review of the different methods for assessing standing balance. *Physiotherapy* (2001) 87:489–95. doi: 10.1016/S0031-9406(05)60696-7
5. Lafond D, Corriveau H, Hebert R, Prince F. Intrasession reliability of center of pressure measures of postural steadiness in healthy elderly people. *Arch Phys Med Rehabil.* (2004) 85:896–901. doi: 10.1016/j.apmr.2003.08.089
6. Sevilla-Garcia MA, Boleas-Aguirre MS, Perez-Fernandez N. The limits of stability in patients with Ménière's disease. *Acta Otolaryngol.* (2009) 129:281–8. doi: 10.1080/00016480802226171
7. Krebs DE, Gill-Body KM, Riley PO, Parker SW. Double-blind, placebo-controlled trial of rehabilitation for bilateral vestibular hypofunction: preliminary report. *Otolaryngol Head Neck Surg.* (1993) 109:735–41. doi: 10.1177/019459989310900417
8. Diehl MD, Pidcoe PE. The influence of gaze stabilization and fixation on stepping reactions in younger and older adults. *J Geriatr Phys Ther.* (2010) 33:19–25. doi: 10.1097/JPT.0b013e3181d073d3
9. Visser JE, Carpenter MG, van der Kooij H, Bloem BR. The clinical utility of posturography. *Clin. Neurophysiol.* (2008) 119:2424–36. doi: 10.1016/j.clinph.2008.07.220
10. Crétual A. Which biomechanical models are currently used in standing posture analysis? *Clin Neurophysiol.* (2015) 45:285–95. doi: 10.1016/j.neucli.2015.07.004
11. Palmieri RM, Ingersoll CD, Stone MB, Krause BA. Center-of-pressure parameters used in the assessment of postural control. *J Sport Rehabil.* (2002) 11:51–66. doi: 10.1123/jsr.11.1.51
12. Winter DA, Patla AE, Frank JS. Assessment of balance control in humans. *Med. Prog. Technol.* (1990) 16:31–51.
13. Harris GF, Wertsch JJ. Procedures for gait analysis. *Arch Phys Med Rehabil.* (1994) 75:216–25.
14. Newton RU, Neal RJ. Three-dimensional quantification of human standing posture. *Gait Posture* (1994) 2:205–12. doi: 10.1016/0966-6362(94)90105-8
15. Sturnieks DL, Menant J, Delbaere K, Vanrenterghem J, Rogers MW, Fitzpatrick RC, et al. Force-controlled balance perturbations associated with falls in older people: A prospective cohort study. *PLoS ONE* (2013) 8:70981. doi: 10.1371/journal.pone.0070981
16. Tax CMW, Bom AP, Taylor RL, Todd N, Cho, KKJ, Fitzpatrick RC, et al. The galvanic whole-body sway response in health and disease. *Clin. Neurophysiol.* (2013) 124:2036–45. doi: 10.1016/j.clinph.2012.12.041
17. Culjak I, Abram D, Pribanic T, Dzapo H, Cifrek M. (2012). A brief introduction to OpenCV. In *2012 Proceedings of the 35th International Convention MIPRO*, Opatija (2012). p. 1725–30.
18. Riesenfeld RF. Homogeneous coordinates and projective planes in computer graphics. *IEEE Comput. Graph. Appl.* (1981) 1:50–5. doi: 10.1109/MCG.1981.1673814
19. Hartley R, Zisserman A. "Camera models," In: *Multiple View Geometry in Computer Vision*, Cambridge: Cambridge University Press (2003). p. 153–177. Available online at: http://www.cambridge.org/au/academic/subjects/computer-science/computer-graphics-image-processing-and-robotics/multiple-view-geometry-computer-vision-2nd-edition?format=PB&isbn=9780521540513#yDMCED32uG1Zqr3G.97
20. Kaehler A, Bradski G. *Learning OpenCV 3: Computer Vision in C++ with the OpenCV Library. 1st Edn*. Beijing; Boston, MA; Farnham; Tokyo; Sebastopol, CA: O'Reilly Media (2017).
21. Dubrofsky E. *Homography Estimation.* Master's thesis, Vancouver BC: The University of British Columbia, (2009).
22. Black HD. A passive system for determining the attitude of a satellite. *AIAA J.* (1964) 2:1350–1. doi: 10.2514/3.2555
23. Gregory G. *Slabaugh Computing Euler Angles From a Rotation Matrix*. Technical report. London: City, University of London (1999). Available online at: http://citeseerx.ist.psu.edu/viewdoc/summary?doi=10.1.1.371.6578 (Accessed June 19, 2018).
24. Scoppa F, Capra R, Gallamini M, Shiffer R. Clinical stabilometry standardization: basic definitions–acquisition interval–sampling frequency. *Gait Posture* (2013) 37:290–92. doi: 10.1016/j.gaitpost.2012.07.009
25. Standards Association of Australia. *Ergonomics - The Human Factor: A Practical Approach To Work Systems Design*. Homebush, NSW: Standards Australia (1994).
26. Huo F. *Limits of Stability and Postural Sway in Young and Older People*. Master's thesis Kingston, ON: Queen's University (1999).
27. Pinsault N, and Vuillerme N. Test–retest reliability of centre of foot pressure measures to assess postural control during unperturbed stance. *Med Eng Phys.* (2009) 31:276–86. doi: 10.1016/j.medengphy.2008.08.003
28. National Instruments *NI Vision Concepts Help*. Technical report Austin, TX: National Instruments (2016). Available online at: https://zone.ni.com/reference/en-XX/help/370281AC-01/ (Accessed April 7, 2017).
29. ISO/IEC. Guide 98-3:2008. *Uncertainty of Measurement - Part 3: Guide to the Expression of Uncertainty in Measurement (GUM:1995)*. Geneva: International Organization for Standardization (2008-10).
30. Schreve K. How accurate can a stereovision measurement be? In:*2014 15th International Workshop on Research and Education in Mechatronics (REM)*, El Gouna (2014). p. 1–7.
31. Bose CB, Amir J. Design of fiducials for accurate registration using machine vision. *IEEE Trans Pattern Anal Mach Intell.* (1990) 12:1196–200. doi: 10.1109/34.62609
32. Sklair C, Hoff W, Gatrell L. Accuracy of locating circular features using machine vision. In: *Proceedings of SPIE Conference on Intelligent Robotic Systems – Cooperative Intelligent Robotics in Space II*, Boston, MA (1992).
33. Hyde PD, Davis LS. Subpixel edge estimation. *Pattern Recognit.* (1983) 16:413–20. doi: 10.1016/0031-3203(83)90063-8
34. Lopez-Molina C, De Baets B, Bustince H. Quantitative error measures for edge detection. *Pattern Recognit.* (2013) 46:1125–39. doi: 10.1016/j.patcog.2012.10.027
35. Schmiedmayer H, Kastner J. Parameters influencing the accuracy of the point of force application determined with piezoelectric force plates. *J Biomech.* (1999) 32:1237–42. doi: 10.1016/S0021-9290(99)00109-8

36. Kirchner M, Schubert P, Schmidtbleicher D, Haas CT. Evaluation of the temporal structure of postural sway fluctuations based on a comprehensive set of analysis tools. *Phys Stat Mech Its Appl.* (2012) 391:4692–703. doi: 10.1016/j.physa.2012.05.034
37. Liu J, Zhang Y, Li Z. Selection of cameras setup geometry parameters in binocular stereovision. In: *2006 IEEE Conference on Robotics, Automation and Mechatronics,* Bangkok (2006), 1–6.
38. Faria C, Sadowsky O, Bicho E, Ferrigno G, Joskowicz L, Shoham M, et al. Validation of a stereo camera system to quantify brain deformation due to breathing and pulsatility. *Med Phys.* (2014) 41:113502. doi: 10.1118/1.4897569
39. Chang C, Chatterjee S. Quantization error analysis in stereo vision. In: *Conference Record of the Twenty-Sixth Asilomar Conference on Signals, Systems and Computers* (1992), 1037–41.
40. Spiegelman JJ, Woo, S. L.-Y. A rigid-body method for finding centers of rotation and angular displacements of planar joint motion. *J Biomech.* (1987) 20:715–21. doi: 10.1016/0021-9290(87)90037-6
41. Migliaccio AA, Della Santina CC, Carey JP, Minor LB, Zee DS. The effect of binocular eye position and head rotation plane on the human torsional vestibuloocular reflex. *Vision Res.* (2006) 46:2475–86. doi: 10.1016/j.visres.2006.02.008
42. Chang LY, Pollard NS. Constrained least-squares optimization for robust estimation of center of rotation. *J Biomech.* (2007) 40:1392–400. doi: 10.1016/j.jbiomech.2006.05.010
43. Panjabi MM. Centers and angles of rotation of body joints: a study of errors and optimization. *J Biomech.* (1979) 12:911–20. doi: 10.1016/0021-9290(79)90059-9
44. Baratto L, Morasso PG, Re C, Spada G. A new look at posturographic analysis in the clinical context: sway-density versus other parameterization techniques. *Motor Control* (2002) 6:246–70. doi: 10.1123/mcj.6.3.246

Conflict of Interest Statement: The authors declare that the research was conducted in the absence of any commercial or financial relationships that could be construed as a potential conflict of interest.

frontiers in Neurology

ORIGINAL RESEARCH
published: 19 November 2018
doi: 10.3389/fneur.2018.00979

Functional Head Impulse Testing Might Be Useful for Assessing Vestibular Compensation After Unilateral Vestibular Loss

Julia Sjögren, Per-Anders Fransson, Mikael Karlberg, Måns Magnusson and Fredrik Tjernström*

Department of Clinical Sciences Lund, Faculty of Medicine, Skåne University Hospital, Lund University, Lund, Sweden

OPEN ACCESS

Edited by:
Stefano Ramat,
University of Pavia, Italy

Reviewed by:
Michael Fetter,
Stiftung Rehabilitation Heidelberg, Germany
Americo Migliaccio,
Neuroscience Research Australia (NeuRA), Australia

****Correspondence:***
Julia Sjögren
julia.sjogren@med.lu.se

Specialty section:
This article was submitted to Neuro-Otology, a section of the journal Frontiers in Neurology

Received: *14 September 2018*
Accepted: *30 October 2018*
Published: *19 November 2018*

Citation:
Sjögren J, Fransson P-A, Karlberg M, Magnusson M and Tjernström F (2018) Functional Head Impulse Testing Might Be Useful for Assessing Vestibular Compensation After Unilateral Vestibular Loss. Front. Neurol. 9:979. doi: 10.3389/fneur.2018.00979

Background: Loss of the vestibulo-ocular reflex (VOR) affects visual acuity during head movements. Previous studies have shown that compensatory eye-saccades improve visual acuity and that the timing of the saccade is important. Most of the tests involved in testing VOR are made with passive head movement, that do not necessarily reflect the activities of daily living and thus not being proportionate to symptoms and distresses of the patients.

Objective: To examine differences between active (self-generated) or passive (imposed by the examiner) head rotations while trying to maintain visual focus on a target.

Method: Nine subjects with unilateral total vestibular loss were recruited (4 men and 5 women, mean age 47) and tested with video Head Impulse Test (vHIT) and Head Impulse Testing Device-Functional Test (HITD-FT) during passive and active movements while looking at a target. VOR gain, latencies of covert saccades, frequency of covert saccades and visual acuity were measured and analyzed.

Results: Active head-impulses toward the lesioned side resulted in better visual acuity ($p = 0.002$) compared to conventional passive head-impulses and generated eye-saccades with significantly shorter latencies ($p = 0.004$). Active movements to the lesioned side generated dynamic visual acuities that were as good as when testing the intact side.

Conclusion: Actively generated head impulses resulted in normal dynamic visual acuity, even when performed toward the side of total vestibular loss. This might be attributed to the appearance of short-latency covert saccades. The results show a strong relationship between self-generated movements, latencies of covert saccades and outcome in HITD-FT, i.e., a better dynamic visual function with less retinal slip which is the main function of the VOR. The method of active HITD-FT might be valuable in assessing vestibular compensation and monitoring ongoing vestibular rehabilitation.

Keywords: vHIT, DVA, vestibulo-ocular reflex, vestibular loss, vestibular rehabilitation

INTRODUCTION

The vestibulo-ocular reflex (VOR) has an important function in stabilizing gaze, i.e., keeping the visual target on the fovea during movements of the head to maintain visual acuity (1). After a chronic unilateral vestibular loss (uVL), the reflex is impaired and can clinically be tested with the head-impulse test (HIT). This bedside test is quick and easy to perform and consists of a quick low amplitude rotation of the patient's head, stimulating the semi-circular canals in the plane of the movement. When performed toward the side of the vestibular lesion, the eyes will lag due to reduced vestibular input. This will cause the gaze to follow the direction of the head, instead of being locked on the target. When perceived, a corrective saccade is generated, disclosing the impairment (2). Due to central vestibular compensation however, the corrective eye-saccade does not always follow after the head movement but can start while the head is still moving. Such a saccade is impossible to detect by the observer (3) but can be recorded with search coils or video-oculography (1, 4). A saccade that occurs while the head is still moving is defined as a covert saccade and a saccade that occurs after the head has stopped moving as an overt saccade (1, 5). Although the mechanism of covert saccades is unknown, there are studies that suggest that the low latency of covert saccades is triggered either by retinal slip (i.e., when the image on the retina moves away from the fovea and is thus not in focus (6), by somatosensory cues from the cervical segment (7), by possible residual labyrinthine function, by other cues that the head is about to or has just begun to rotate (8) or by generated internal models (i.e., preformed saccades that are triggered by certain movements with little or no feedback information) (9).

Peripheral vestibular semi-circular canal function is conventionally tested, by measuring the gain of the angular VOR (aVOR). A reduced gain together with a corrective eye-saccade is universally accepted as a sign of VOR hypofunction (10). Vestibular function can also be evaluated with so called "functional testing," i.e., how well the aVOR performs with respect to its goal of stabilizing gaze in space (11). Those tests measure how well a subject acquire visual information during a head movement and reflects the combined effects of VOR and catch-up saccades on dynamic reading ability (12, 13). Due to their short-latencies, covert saccades may in particular reduce blurred vision (oscillopsia) and improve visual performance (14). The test however is generally performed with passive head movements, i.e., an examiner rotates the subject's head. Most movements in everyday life consist of active voluntary self-movements which are also encouraged by the general concept of vestibular rehabilitation, that invariably consists of training the brain to an absent VOR. Thus, the main aim of this study is to assess how well patients manage to maintain visual fixation during active head movements.

METHODS

Subjects

Nine subjects (4 men and 5 women) with a mean age of 47 years (range 40–50 years), were recruited for the study: eight with unilateral vestibular loss after translabyrinthine surgery for vestibular schwannoma, with a mean time since surgery of 8 years (range 1–16 years) and one with congenital unilateral vestibular loss, probably due to an intrauterine cytomegalovirus infection. The total unilateral vestibular loss was confirmed by bi-thermal caloric tests, video head-impulse test of all six semi-circular canals and cervical vestibular evoked myogenic potentials.

Ethical Approval

The experiments were performed in accordance with the Helsinki declaration and approved by the local ethical board (Dnr 2016/32, EPN, Lund University, Sweden). All subjects gave their written and informed consent prior to participation.

Experimental Protocol

The ability to maintain focus on a visual reference point while performing fast rotational accelerations and decelerations of the head in the horizontal plane were assessed in all subjects using two methods. (1) The ability to control the eye movements so the focus did not deviate from a fixed visual reference point during fast accelerations and decelerations of the head, was assessed using an Interacoustics video-head impulse test (vHIT) system (EyeSeeCam version 1.2) (9). (2) The reading performance during fast rotational accelerations of the head was assessed with the Head Impulse Testing Device-Functional Test (HITD-FT) (15). All procedures were performed by the same examiner.

vHIT Testing

The subject sat in an arm-less chair 1.5 m in front of a white wall facing an attached 3 × 3 cm blue marker placed at eye level, which served as visual focusing point during the head movement tests. The subject was instructed to keep focusing on the visual target on the wall at all times during the investigations. In all tests the same examiner stood behind the subject, then started to impose manual fast rotational horizontal head movements with peak velocities exceeding 150°/s, accelerations/decelerations chiefly within 3,000–8,000°/s^2 and a movement amplitude of about 10–20°. The head movement testing continued until the Interacoustics software had accepted the performance of at least 10 passive head movement recordings in each direction. After the conventional passive head movement testing, the subject was asked to perform active horizontal head movements of similar velocity, acceleration, and amplitude as used when assessing the performance during passive head movements. The subjects were allowed to train a few times before the actual test. The head movement testing continued during active head movements until the Interacoustics software had accepted the performance of at least 10 head movement recordings in each direction (i.e., the head movement performance criteria imposed by the software were identical during active and passive head movements). The Interacoustics system record eye and head movements at a sample frequency of 220 Hz, whilst the analyses of the recorded data were based on signal-processed data elevated to the sampling frequency of 1,000 Hz by the software.

HITD-FT Testing

The subjects were placed 1.5 m from the HITD-FT computer monitor. The patient was wearing a head mounted accelerometer.

Static visual acuity was first evaluated using an eye chart displayed on the monitor with letter sizes scaled according to the subject's viewing distance. The size of the visual stimuli used during the test was then determined based on the assessed visual acuity by increasing that of the smallest line seen by 0.8 log-MAR. This stimulus size, which is eight lines bigger than the best static visual acuity, would then remain constant during the test. The examiner manually imposed horizontal head-impulses, a minimum of 10 valid impulses in each direction. The HITD-FT software had the same criteria for a valid head-impulse during active and passive head movements, the impulses had to reach an acceleration between 3,000 and 6,000°/s^2. When the imposed head angular acceleration exceeded a user-defined threshold, a Landolt's C optotype in one of eight possible orientations was briefly displayed on the screen. The HITD-FT monitor was full HD (1,920 × 1,080 resolution) with a maximum response time of 5 ms and a refresh rate of 60 Hz. The duration of the letter display was set to two frames, this resulted in the optotype being visual during about 33 ms with no delay (16) which results in the visual display being visible around the time of maximum head acceleration.

Data Analysis

The vHIT performance during passive and active head movements were assessed by both the Interacoustics software and a customized software. The Interacoustics software determined

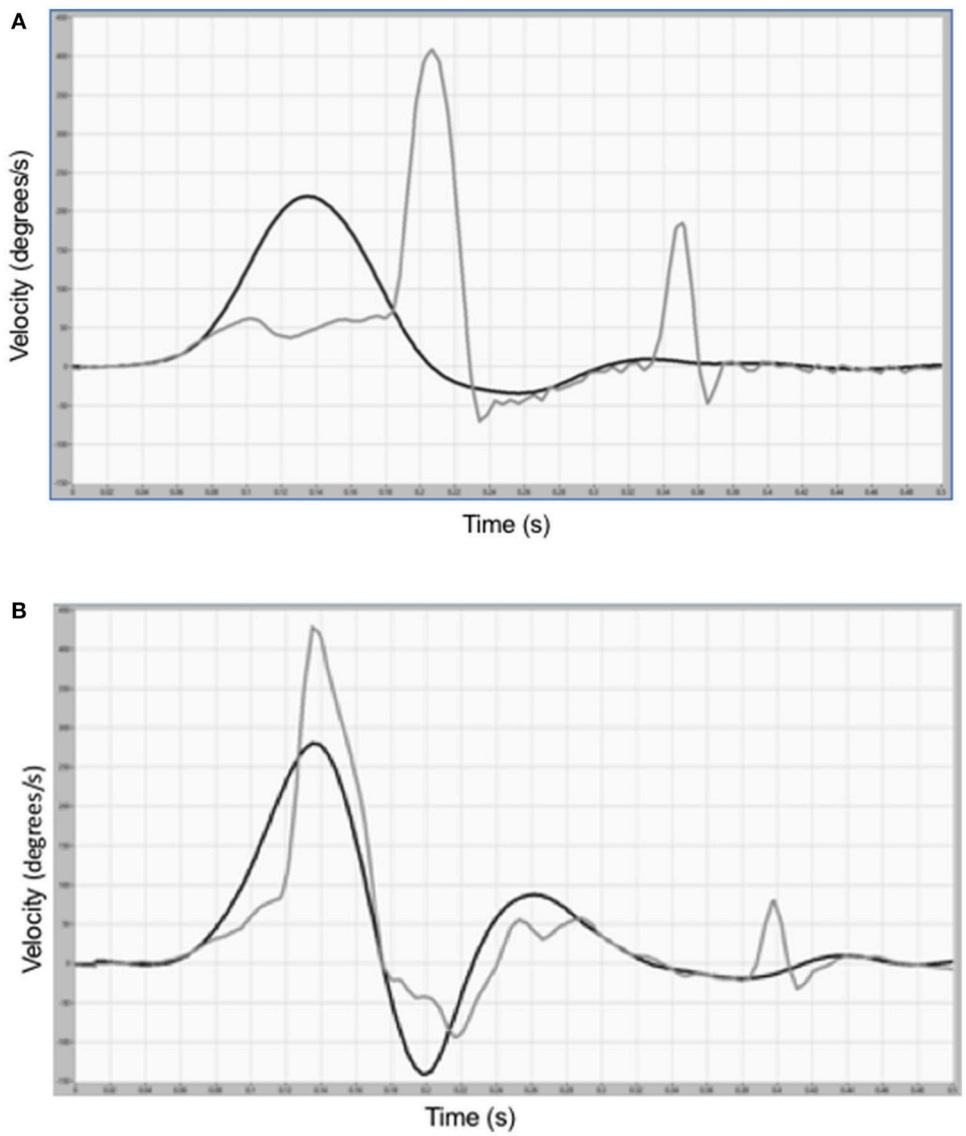

FIGURE 1 | (A) Eye and head velocity traces during a conventional, passive head-impulse test toward the ipsilesional side in one representative subject show low eye velocity during the head movement and late covert saccade (after 135 ms) and an overt compensatory saccade. **(B)** Eye and head velocity traces in the same subject during an active head rotation toward the ipsilesional side show a large early (after 60 ms) covert saccade that occurs during the head movement.

TABLE 1 | Recorded performance during head-impulses in ipsilesional and contralesional directions.

		HITD-FT		VOR gain		Saccade latency		% Covert saccades	
		Mean (%)	SEM	Mean	SEM	Mean(s)	SEM	Mean (%)	SEM
Ipsilesional	Passive	64.4	8	0.34	0.02	0.134	0.015	77	12
	Active	91.2	3.1	0.54	0.06	0.085	0.009	99	1
Contralesional	Passive	93.7	3.5	0.92	0.03	0.233	0.031	27	13
	Active	91.1	4.2	0.89	0.05	0.208	0.025	35	12

TABLE 2 | Repeated measures GLM-ANOVA analyses of HITD-FT scores, gain, saccade latency and frequency of covert saccades, determining if the performance depended on active/passive head impulses and on ipsilesional/contralesional head movement directions.

		Active/ Passive	Ipsi/ Contralesional	Active/Passive + Ipsi/Contralesional
HITD-FT	*p*-value	**0.021**	**0.008**	**0.005**
	F-value	8.1	12.1	15.2
VOR gain	*p*-value	**0.006**	**<0.001**	**0.015**
	F-value	13.7	90.2	9.5
Saccade latency	*p*-value	**0.048**	**0.001**	0.372
	F-value	5.4	23.5	0.9
% Covert saccades	*p*-value	0.104	**0.001**	0.725
	F-value	3.4	23.5	0.1

Bold statistics denote p-values < 0.05.

TABLE 3 | Repeated measures GLM-ANOVA analyses of the performance during active vs. passive head-impulses when the head movements were performed in ipsilesional and contralesional directions.

Active vs. Passive	Contralesional		Ipsilesional	
	p-value	*F*-value	*p*-value	*F*-value
HITD-FT	0.638	0.2	**0.002**	19.6
VOR gain	0.370	0.9	**0.005**	14.4
Saccade latency	0.387	0.8	**0.004**	16.4
% Covert saccades	0.303	1.2	0.084	3.9

Bold statistics denote p-values < 0.05.

the average gain (i.e., the quotient between average eye velocity and head velocity) during the head acceleration phase (0–100 ms). The customized software determined whether the eye movement recordings included saccades, and if so, the time from when head movement started until the first saccade reached peak velocity (denotes peak latency). The software also determined if the saccade started while the head still moved in the initial movement direction (Covert) or after the head movement had stopped or had started to move in the reverse direction (Overt). The start of the head movement was defined to be when the head movement velocity exceeded 30°/s. An eye movement was defined as a saccade if the eye peak velocity exceeded 80°/s, if both the acceleration and deceleration flanks exceed 3,000°/s^2 and if the saccade duration was within 10–80 ms. The HITD-FT data was calculated by the fHIT 1.0 system (16). The proportion of head impulses that generated covert saccades was measures in percentage.

Statistical Analysis

The parameters HITD-FT score, vHIT gain, saccade peak latency, and the proportion of covert/overt saccades made, were analyzed using repeated measures GLM ANOVA (General Linear Model Analysis of Variance) (17). The main factors and factor interactions analyzed were: "Active/Passive" (Active vs. Passive head movements; d.f. 1); "Ipsi/contralesional" (Ipsilesional vs. Contralesional head movement direction; d.f. 1). When analyses of some parameters revealed significant main factor interactions, repeated measures GLM ANOVA analyses were performed on all parameters with only one main factor "Active/Passive" (Active vs. Passive head movements; d.f. 1) individually on ipsilesional and contralesional data.

The Wilcoxon matched-pairs signed-rank test (Exact sig. 2-tailed) was used for within-group *post-hoc* comparisons, i.e., analyzing the difference between ipsilesional and contralesional head movement responses during active and passive head movements (17).

In all analyses, p-values < 0.05 were considered significant. Non-parametric statistical tests were used in all statistical evaluations since the Shapiro-Wilk test revealed that some data sets were not normally distributed and normal distribution could not be obtained by log-transformation. The repeated measures GLM ANOVA analysis was used after ensuring that all model residuals had normal or approximate normal distribution (17).

Sample size analyses, using the statistical package G-power™, were performed on the parameters used that were unaffected by boundaries (i.e., the HITD-FT and the % Covert saccades parameters could only assume values within the range of 0–100). The sample size analysis of the vHIT gain parameter revealed an effect size of 1.8, which shows that with the p-value set to 0.05 (2-tailed), our study would require $n = 5$ subjects to reach a power value of 0.8 for this parameter. The sample size analysis of the saccade peak latency parameter revealed an effect size of 2.2, which shows that with the p-value set to 0.05 (2-tailed), our study would require $n = 4$ subjects to reach a power value of 0.8 for this parameter.

The statistical analyses were performed with SPSS version 24 and the power analysis was performed with GPower 3.1.

RESULTS

Passive and active eye and head velocity traces from a subject during conventional HIT toward the ipsilesional side are shown in **Figure 1**. During passive HIT there are one late covert and one overt saccade after the head movement (**Figure 1A**), but during active HIT there is a large early covert saccade during the head movement (**Figure 1B**).

Table 1 shows the mean HITD-FT-score, mean gain, mean peak saccade latency, and the mean frequency of impulses that generated a covert saccade for impulses toward the lesioned side and toward the contralesional side.

The outcome in HITD-FT was influenced by whether the test was active or passive ($p = 0.021$) and toward which side the test was performed ($p = 0.008$; **Table 2**). The greatest increase of HITD-FT score during active movements was toward the lesioned side ($p = 0.002$, **Table 3**) as is demonstrated in **Figure 2**. **Figure 2** also shows that during active head movements, no difference can be seen in performance regardless of whether the head movement was executed toward the ipsilesional or contralesional side.

The gain values increased significantly when the head movements were active ($p = 0.006$; **Table 2**) and separated GLM ANOVA analyses show that for head movements toward the ipsilesional side there was significant change ($p = 0.005$, **Table 3**). Saccade latency was significantly shorter ($p = 0.048$, **Table 2**) when performing active head movements, especially toward the ipsilesional side ($p = 0.004$, **Table 3**).

The percentage of generated coverts during head movements are shown in **Table 1**. Although the frequency of coverts increased during active movements, it was not statistically significant (**Tables 2**, **3**). **Table 4** shows post-hoc Wilcoxon analyses of HITD-FT scores, gain, saccade latency, and frequency of covert saccades.

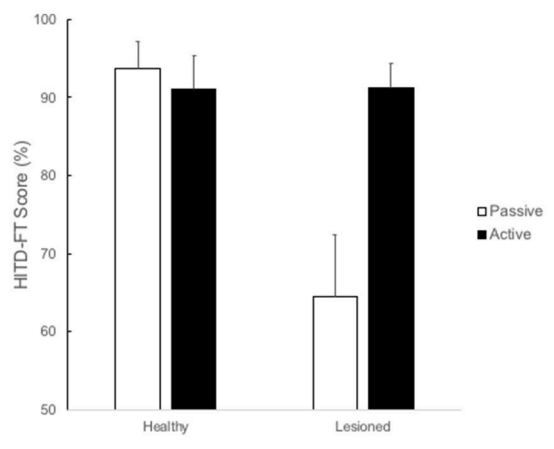

FIGURE 2 | HITD-FT (%) rate of correct answers (%) in correlation to passive (white) or active (black) head-impulses toward the ipsi and contralesional side. Active head-impulses resulted in a better HITD-FT score (91.2%) compared to passive head-impulses (64.4%) $p = 0.002$.

DISCUSSION

The dynamic visual acuity was found to be better during active head impulses as compared to passive ones, and the main reason seems to be a shorter latency of the first covert saccade. Actively generated head movements in our subjects with long-standing uVLs, yield similar HITD-FT scores toward the contralesional and the ipsilesional side. This is consistent with previous findings of less difference in dynamic visual acuity during self-generated movements than passively imposed movements in patients with uVL (18). It has been shown that covert saccades are triggered earlier during active head turns (19, 20), and that the latency correlates to dynamic visual acuity (21), but the combination of active head movements and covert saccade with regard to dynamic visual acuity has not been examined before. **Figure 3** shows the saccade latencies plotted against HITD-FT values during active and passive head movements. Since most of the scores during active head movements are close to 100%, statistical correlation analyses become problematic.

Vestibular rehabilitation has been shown to increase dynamic visual acuity during active movement (22), an effect attributed to increased VOR gain. This is consistent with the results of the present study but, depending on how the VOR gain is calculated, the gain increase might be an artifact generated by the covert saccades. Simplified, in the EyeSeeCam-device the gain is derived from head and eye velocity during the acceleration phase calculated with a regression model including saccades (23). If the covert saccade in the case of an active head movement is generated during the acceleration phase, it would mean by itself a higher gain value (**Figures 1A,B**). In the present study, however, we have not focused on gain calculations and other studies have found higher gain values during active than during passive movements (9, 19).

It has also been shown that a higher percentage of generated covert saccades are correlated with better visual acuity (13), though that has not been examined with regards to saccade latency. In the present study the percentage of covert saccades did increase when performing active movements, but not significantly so.

TABLE 4 | *Post-hoc* Wilcoxon analyses of HITD-FT scores, gain, saccade latency, and frequency of covert saccades.

		Ipsilesional/Contralesional
HITD-FT	Passive	**0.008**
	Active	1.0
VOR gain	Passive	**0.004**
	Active	**0.012**
Saccade latency	Passive	**0.004**
	Active	**0.004**
% Covert Saccades	Passive	**0.008**
	Active	**0.016**

Bold statistics denote p-values < 0.05.

The main shortcoming of the present study is the relatively small sample size, with a relatively small age-span. This makes it difficult to do analyzes of subjective parameters as well as to generalize the results to other populations, e.g., the age-dependent presby-vestibulopathy that are also affected by other factors relevant to vestibular compensation. However, the results show a strong relationship between self-generated movements, latencies of covert saccades and outcome in HITD-FT, i.e., a better dynamic visual function with less retinal slip, which is the main function of the VOR. Most of vestibular rehabilitation exercises are designed to challenge a deficient VOR, in order to induce compensation (24). All patients in the present study (except the one with congenital uVL) performed our VOR exercises albeit some years previously. The group comprised only well-compensated patients. We considered the homogeneity of the group of importance in order to elucidate whether active and passive head impulses differ, both in ocular responses as well as in dynamic visual acuity. Future studies will have to compare the full range from acute onset of vestibular loss as well as fully compensated patients to establish whether active head impulses generate a satisfactory measure of compensation as well as could be used to monitor vestibular rehabilitation.

The generation of covert saccades seems to be part of central vestibular rehabilitation, and they are possibly related to better compensation after suffering vestibular loss, though subjective parameters seem to be difficult to correlate to HITD-FT results (12). Our material is too small to estimate subjective outcome. However, it could be argued that the active movements are physiologically more similar to everyday head movements (25), especially when moving actively as in walking. Our results suggest that HITD-FT with actively imposed impulses may be a better tool for assessing the effect of vestibular adaptation than conventional passive head-impulses. To our knowledge this has not been shown prior to this study. In addition to perhaps being a tool for assessing compensation it is also instructive for patients in the mechanism of gaze stabilization, further motivating them to continue with vestibular rehabilitation exercises. More prospective research is needed with larger cohorts in assessing the course of active HITD-FT over time after uVL preferably together with subjective estimates of vestibular function, such as self-reports, e.g., the Dizziness Handicap Inventory and Vertigo Symptom Scale.

The nature of the saccades generated in active vs. passive movements is intriguing and raise still more questions. Obviously in some cases both active and passive impulses triggered feed-back reflexes since they have relative constant latencies. However, some patients have saccades with active movements with close to no latency at all, which could be interpreted as having cortical origin (feed-forward mechanism). If the actively generated saccades are of cortical origin, why do some impulses yield saccades that have latencies at all? If they are triggered by the same reflex action, a possible relay station would be the vestibular nuclei. Another hypothetical explanation could be that when performing an active head movement to one side the inhibitory neurons of the saccadic system are in turn inhibited, thus making the system as such "trigger-happy" for releasing any saccade. Indeed, an elaborate mathematical model has been put forward (9) and further studies are needed to further study the nature and origin of saccades, as from a rehabilitation point of view they seem to be a desirable trait to acquire.

CONCLUSION

Actively generated head impulses result in almost normal HITD-FT values even when performed toward the side of total

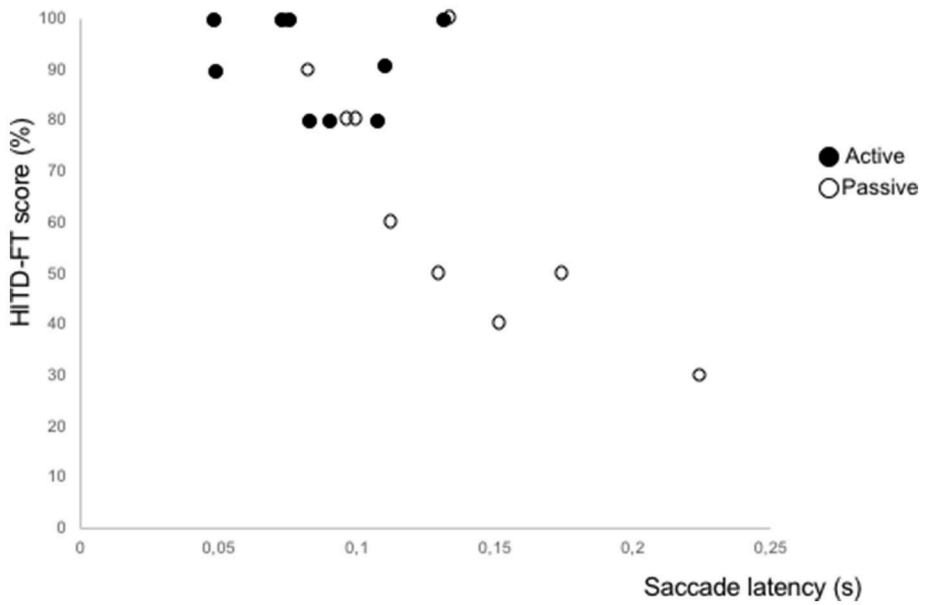

FIGURE 3 | Graphical illustration of HITD-FT scores vs. latencies of corrective saccades, triggered during passive and active ipsilesional head-impulses.

vestibular loss in patients with chronic unilateral vestibular loss. This might be attributed to the appearance of short-latency covert saccades. The method of active HITD-FT might be valuable in assessing vestibular compensation and monitoring ongoing vestibular rehabilitation.

DATA AVAILABILITY STATEMENT

The raw data supporting the conclusions of this manuscript will be made available by the authors, without undue reservation, to any qualified researcher.

AUTHOR CONTRIBUTIONS

FT and P-AF conceived the study, interpreted results and contributed to the manuscript. JS executed the study, interpreted results and contributed to the manuscript. MK and MM interpreted results and contributed to the manuscript.

FUNDING

The research was supported by grants from Agnes Ljunggrens foundation.

REFERENCES

1. Weber KP, Aw ST, Todd MJ, McGarvie LA, Curthoys IS, Halmagyi GM. Head impulse test in unilateral vestibular loss: vestibulo-ocular reflex and catch-up saccades. *Neurology* (2008) 70:454–63. doi: 10.1212/01.wnl.0000299117.48935.2e
2. Halmagyi GM, Curthoys IS. A clinical sign of canal paresis. *Arch Neurol.* (1988) 45:737–9. doi: 10.1001/archneur.1988.00520310043015
3. Tjernstrom F, Nystrom A, Magnusson M. How to uncover the covert saccade during the head impulse test. *Otol Neurotol.* (2012) 33:1583–5. doi: 10.1097/MAO.0b013e318268d32f
4. MacDougall HG, Weber KP, McGarvie LA, Halmagyi GM, Curthoys IS. The video head impulse test: diagnostic accuracy in peripheral vestibulopathy. *Neurology* (2009) 73:1134–41. doi: 10.1212/WNL.0b013e3181bacf85
5. Bloomberg J, Melvill Jones G, Segal B. Adaptive modification of vestibularly perceived rotation. *Exp Brain Res.* (1991) 84:47–56. doi: 10.1007/BF00231761
6. Scherer M, Schubert MC. High-velocity angular vestibulo-ocular reflex adaptation to position error signals. *J Neurol Phys Ther.* (2010) 34:82–6. doi: 10.1097/NPT.0b013e3181dde7bc
7. Macdougall HG, Curthoys IS. Plasticity during vestibular compensation: the role of saccades. *Front Neurol.* (2012) 3:21. doi: 10.3389/fneur.2012.00021
8. Schubert MC, Zee DS. Saccade and vestibular ocular motor adaptation. *Restor Neurol Neurosci.* (2010) 28:9–18. doi: 10.3233/RNN-2010-0523
9. Colagiorgio P, Versino M, Colnaghi S, Quaglieri S, Manfrin M, Zamaro E, et al. New insights into vestibular-saccade interaction based on covert corrective saccades in patients with unilateral vestibular deficits. *J Neurophysiol.* (2017) 117:2324–38. doi: 10.1152/jn.00864.2016
10. Non publ. *Barany Society*, Seoul, South Korea (2016).
11. Herdman SJ, Tusa RJ, Blatt P, Suzuki A, Venuto PJ, Roberts D. Computerized dynamic visual acuity test in the assessment of vestibular deficits. *Am J Otol.* (1998) 19:790–6.
12. Corallo G, Versino M, Mandala M, Colnaghi S, Ramat S. The functional head impulse test: preliminary data. *J Neurol.* (2018) 265(Suppl. 1):35–9. doi: 10.1007/s00415-018-8910-z
13. Ramaioli C, Colagiorgio P, Saglam M, Heuser F, Schneider E, Ramat S, et al. The effect of vestibulo-ocular reflex deficits and covert saccades on dynamic vision in opioid-induced vestibular dysfunction. *PLoS ONE* (2014) 9:e110322. doi: 10.1371/journal.pone.0110322
14. Wettstein VG, Weber KP, Bockisch CJ, Hegemann SC. Compensatory saccades in head impulse testing influence the dynamic visual acuity of patients with unilateral peripheral vestibulopathy1. *J Vestib Res.* (2016) 26:395–402. doi: 10.3233/VES-160591
15. Versino M, Colagiorgio P, Sacco S, Colnaghi S, Quaglieri S, Manfrin M, et al. Reading while moving: the functional assessment of VOR. *J Vestib Res.* (2014) 24:459–64. doi: 10.3233/VES-140531
16. Ramat S, Colnaghi S, Boehler A, Astore S, Falco P, Mandala M, et al. A device for the functional evaluation of the VOR in clinical settings. *Front Neurol.* (2012) 3:39. doi: 10.3389/fneur.2012.00039
17. Altman D. Practical statistics for medical research. New York: Chapman & Hall NY (1991).
18. Tian JR, Shubayev I, Demer JL. Dynamic visual acuity during passive and self-generated transient head rotation in normal and unilaterally vestibulopathic humans. *Exp Brain Res.* (2002) 142:486–95. doi: 10.1007/s00221-001-0959-7
19. Black RA, Halmagyi GM, Thurtell MJ, Todd MJ, Curthoys IS. The active head-impulse test in unilateral peripheral vestibulopathy. *Arch Neurol.* (2005) 62:290–3. doi: 10.1001/archneur.62.2.290
20. Peng GC, Minor LB, Zee DS. Gaze position corrective eye movements in normal subjects and in patients with vestibular deficits. *Ann N Y Acad Sci.* (2005) 1039:337–48. doi: 10.1196/annals.1325.032
21. Hermann R, Pelisson D, Dumas O, Urquizar C, Truy E, Tilikete C. Are covert saccade functionally relevant in vestibular hypofunction? *Cerebellum* (2018) 17:300–7. doi: 10.1007/s12311-017-0907-0
22. Schubert MC, Migliaccio AA, Clendaniel RA, Allak A, Carey JP. Mechanism of dynamic visual acuity recovery with vestibular rehabilitation. *Arch Phys Med Rehabil.* (2008) 89:500–7. doi: 10.1016/j.apmr.2007.11.010
23. Lee SH, Yoo MH, Park JW, Kang BC, Yang CJ, Kang WS, et al. Comparison of video head impulse test (vHIT) gains between two commercially available devices and by different gain analytical methods. *Otol Neurotol.* (2018) 39:e297–300. doi: 10.1097/MAO.0000000000001799
24. Tjernstrom F, Zur O, Jahn K. Current concepts and future approaches to vestibular rehabilitation. *J Neurol.* (2016) 263(Suppl. 1):S65–70. doi: 10.1007/s00415-015-7914-1
25. Carriot J, Jamali M, Brooks JX, Cullen KE. Integration of canal and otolith inputs by central vestibular neurons is subadditive for both active and passive self-motion: implication for perception. *J Neurosci.* (2015) 35:3555–65. doi: 10.1523/JNEUROSCI.3540-14.2015

Conflict of Interest Statement: The authors declare that the research was conducted in the absence of any commercial or financial relationships that could be construed as a potential conflict of interest.

frontiers in Neurology

ORIGINAL RESEARCH
published: 07 March 2019
doi: 10.3389/fneur.2019.00085

Recovery Pattern of High-Frequency Acceleration Vestibulo-Ocular Reflex in Unilateral Vestibular Neuritis: A Preliminary Study

Wei Fu[1†], Feng He[2†], Dong Wei[2], Ya Bai[2], Ying Shi[2], Xiaoming Wang[1] and Junliang Han[2*]*

[1] Department of Geriatrics, Xijing Hospital, Fourth Military Medical University, Xi'an, China, [2] Department of Neurology, Xijing Hospital, Fourth Military Medical University, Xi'an, China

Objective: To explore the recovery pattern of the high-frequency acceleration vestibulo-ocular reflex (VOR) function in unilateral vestibular neuritis (UVN).

Methods: Forty-seven consecutive patients with UVN were recruited within 10 days of symptom onset for this study. The high-frequency acceleration horizontal VOR function was assessed using the video head impulse test (vHIT). Patients returned for follow-up evaluation at ∼6 months after the onset of symptoms. According to the dizziness handicap inventory questionnaire (DHI), the patients were classified into the normal to mild dizziness group (DHI score ≤30) and moderate to severe dizziness group (DHI score >30) at the follow-up. All the obtained horizontal vHIT gains and corrective saccades parameters were analyzed.

Results: vHIT results showed a significantly horizontal VOR gain recovery in UVN patients at the follow-up on the lesion side ($p < 0.01$). A significantly reduction in the occurrence of corrective saccades (overt and covert) and velocity of corrective saccades (overt and covert) were observed at the follow-up ($p < 0.05$). At the follow-up, the normal to mild dizziness group (DHI score ≤30) had a significantly higher normal rate of VOR gain, the mean vHIT gains and occurrence of isolated covert saccades ($P < 0.05$). Furthermore, the occurrence of mixed saccades and the mean velocity of covert saccades were significantly lower in normal to mild dizziness group ($P < 0.05$).

Conclusion: Apart from the recovery of the VOR gain, recovery pattern of corrective saccades can play a key role in vestibular compensate.

Keywords: video head impulse test, saccades, covert saccades, vestibulo-ocular reflex, vestibular compensate, vestibular function, horizontal semicircular canal

OPEN ACCESS

Edited by:
Michael C. Schubert, Johns Hopkins University, United States

Reviewed by:
Jorge Kattah, University of Illinois at Chicago, United States
Hong Ju Park, Asan Medical Center, South Korea

***Correspondence:**
Xiaoming Wang
xmwang@fmmu.edu.cn
Junliang Han
hanjlfmmu@163.com

[†]These authors have contributed equally to this work

Specialty section:
This article was submitted to Neuro-Otology, a section of the journal Frontiers in Neurology

Received: *05 September 2018*
Accepted: *22 January 2019*
Published: *07 March 2019*

Citation:
Fu W, He F, Wei D, Bai Y, Shi Y, Wang X and Han J (2019) Recovery Pattern of High-Frequency Acceleration Vestibulo-Ocular Reflex in Unilateral Vestibular Neuritis: A Preliminary Study. Front. Neurol. 10:85. doi: 10.3389/fneur.2019.00085

INTRODUCTION

Vestibular neuritis (VN) is a common disease causing acute attacks of vertigo. It is characterized by sudden onset of prolonged vertigo with unidirectional spontaneous horizontal–torsional nystagmus, absence of other auditory, or neurologic findings (1). And the vestibulo-ocular reflex (VOR) hypofunction of VN can be identified by caloric irrigation test and head impulse test (HIT) (2). HIT is a simple and valid means of evaluating VOR function in the high-frequency range of 4–7 Hz (3). The subject maintains fixation on an static target while the operator applied unpredictable, sudden, passive, head turns in the horizontal plane, and examiner looks for

corrective saccades (4). If the VOR function is intact, the subject can stabilize their gaze on a target during head rotations. However, if the VOR function is deficient, the eyes fail to fix on the target and the patient makes a corrective saccades to refixate the target (4).There are two corrective saccades types: overt saccades and covert saccades. HIT can detect overt saccades, but covert saccades is invisible (5). Fortunately, the video head impulse test (vHIT) can recognize covert saccades and quantifying the VOR gain (eye velocity/head velocity) (6). Thus, vHIT provides a tool that allowing analysis of VOR gain and the corrective saccades, seems to offer new interesting perspectives.

In addition, vHIT is also a quantitative baseline to track recovery of VOR dysfunction. In this study, we measured the horizontal VOR gain and corrective saccades in unilateral vestibular neuritis (UVN) patients from the acute stage to the follow-up. And we also analyzed the correlation with parameters of vHIT and chronic symptoms (dizziness handicap inventory questionnaire) at the follow-up in order to determine which parameters of vHIT are better to predict symptom recovery.

METHODS

Participants

We identified 47 consecutive patients with acute UVN from the period between 2016 and 2018 (25 men, 22 women; mean age 56.8 years; ranging from 19 to 71 years). The diagnostic criteria for UVN included the following: a history of sudden vertigo (more than 24 h) with unidirectional spontaneous horizontal–torsional nystagmus, and caloric examine showing a lack of unilateral caloric response (canal paresis >25%) (1). Exclusion criteria: (1) History of neurologic disorders or auditory disorders; (2) patients with tumors, traumatic and infection; (3) magnetic resonance imaging (MRI) which revealed brain lesions. All acute UVN patients were treated immediately with corticosteroids (tapering over 2 weeks) and vitamin B12.

The 47 UVN patients were initially examined using vHIT at the acute phase (within 10 days) after onset of vertigo and then scheduled for follow-up examination ∼6 months later. In addition, all patients also were inquired the recovery condition of symptom and completed the chinese version of the dizziness handicap inventory (DHI) questionnaire at the follow-up (7). And the patients were classified into the normal to mild dizziness group (DHI score ≤30) and moderate to severe dizziness group (DHI score >30) at the follow-up.

All subjects provided written informed consents to participate in this study. The study was approved by the Institutional Review Board of Xijing Hospital, Fourth Military Medical University.

vHIT

The vHIT was recorded in all subjects using the ICS Impulse system (Otometrics, Denmark). The horizontal canals were evaluated. The subject was instructed to gaze at a target that was 1.2 m away. First, calibration is performed. In each trial, the examiner stood behind the patients and performed head impulses by a small angle (∼10–20°) and an appropriate velocity (150–200°/s). And 20 impulses were recorded for each direction. In our study, the horizontal vHIT were performed with jaw hand position (8). The mean horizontal vHIT gains and corrective saccades parameters (covert and overt) were measured. Abnormal criteria is the horizontal vHIT gain values <0.8 and corrective saccades peak velocity >100°/s (9, 10).

Statistical Analysis

Statistical comparisons of the horizontal vHIT gains, peak head velocities, and corrective saccades parameters (velocity of saccade and latency of saccade) at the acute stage and the follow-up of UVN were made using the Student's *t*-test, and occurrence of saccades (overt and covert) at the acute stage and the follow-up were compared with Chi-square test or Fisher exact test. A Student's *t*-test, Chi-square test, and Fisher exact test also were used to investigate the relationship between two DHI groups (DHI score ≤30 and DHI score >30) and vHIT results at the follow-up. Spearman's correlation test was used to analyze the correlation between the DHI score and vHIT gains or corrective saccades parameters. $p < 0.05$ was considered statistically significant. Statistical analysis were done by using SPSS software (version19, SPSS Inc., Chicago, IL, USA).

RESULTS

In 47 UVN patients, the mean peak head velocity on the lesion side was 174.44 ± 18.32°/s at the acute stage and 175.19 ± 17.49°/s at the follow-up, respectively. The mean peak head velocity on the healthy side was 175.14 ± 16.10°/s at the acute stage and 174.14 ± 15.85°/s at the follow-up, respectively. There was no significant difference in the mean peak head velocity (lesion side and healthy side) between the acute stage and the follow-up ($p > 0.05$, **Table 1**).

TABLE 1 | vHIT results in unilateral vestibular neuritis patients at the acute stage and the follow-up examination ($n = 47$).

	Acute stage	Follow-up	*p*-value
PEAK HEAD VELOCITIES			
Lesion-side mean head velocity (°/s)	174.44 ± 18.32	175.19 ± 17.49	>0.05[a]
Healthy-side mean head velocity (°/s)	175.14 ± 16.10	174.14 ± 15.85	>0.05[a]
vHIT Gain			
Lesion-side mean gain	0.47 ± 0.15	0.69 ± 0.23	<0.01[a]
Healthy-side mean gain	0.97 ± 0.12	1.00 ± 0.13	>0.05[a]
OVERT SACCADE PARAMETERS			
Occurrence of overt saccade (%)	100(47/47)	59.58(28/47)	<0.01[b]
Velocity of overt saccade (°/s)	203.00 ± 62.00	152.46 ± 29.70	<0.01[a]
Latency of overt saccade (ms)	310.02 ± 41.91	314.21 ± 38.84	>0.05[a]
COVERT SACCADE PARAMETERS			
Occurrence of covert saccade (%)	100(47/47)	87.23(41/47)	<0.05[c]
Velocity of covert saccade (°/s)	209.23 ± 48.17	186.14 ± 45.69	<0.05[a]
Latency of covert saccade (ms)	130.30 ± 24.91	123.41 ± 24.47	>0.05[a]

[a] *t-test.* [b] *Chi-square test.* [c] *Fisher exact test.*

vHIT Parameters at the Acute Stage and the Follow-Up

The mean horizontal vHIT gains on the lesion side were 0.47 ± 0.15 at the acute stage and 0.69 ± 0.23 at the follow-up, respectively, and the gains at the follow-up were significantly higher than the gains at the acute stage ($p < 0.01$, **Table 1**). The healthy side had the mean horizontal vHIT gains were 0.97 ± 0.12 and 1.00 ± 0.13 at the acute stage and the follow-up, respectively, and this was not significantly different ($p > 0.05$, **Table 1**). The occurrence of overt saccade were 100% at the acute stage and 59.58% at the follow-up, respectively, and the occurrence of overt saccade showed a significant decrease at the follow-up ($p < 0.01$, **Table 1**). The occurrence of covert saccade were 100% at the acute stage and 87.23% at the follow-up, respectively, and the occurrence of covert saccade showed a significant decrease at the follow-up ($p < 0.05$, **Table 1**). The mean velocity of overt saccades were 203.00 ± 62.00°/s at the acute stage and 152.46 ± 29.70°/s at the follow-up, respectively, and the mean velocity of overt saccades showed a significant decrease at the follow-up ($p < 0.01$, **Table 1**). The mean velocity of covert saccades were 209.23 ± 48.17°/s at the acute stage and 186.14 ± 45.69°/s at the follow-up, respectively, and the mean velocity of covert saccades also decreased significantly at the follow-up ($p < 0.05$, **Table 1**). The mean latency of overt saccades were 310.02 ± 41.91 ms at the acute stage and 314.21 ± 38.84 ms at the follow-up, respectively, and this was not significantly different ($p > 0.05$, **Table 1**). The mean latency of covert saccades were 130.30 ± 24.91 ms at the acute stage and 123.41 ± 24.47 ms at the follow-up, respectively, and this also was not significantly different ($p > 0.05$, **Table 1**).

vHIT Parameters and Symptoms in UVN Patients at the Follow-Up

At the follow-up, the DHI score was equal to or <30 (normal to mild dizziness group) in 28 UVN patients and >30 (moderate to severe dizziness group) in 19 UVN patients. 57.14% UVN patients in the normal to mild dizziness group and 21.05% UVN patients in the moderate to severe dizziness group had a normal vHIT gains at the follow-up. And the proportion of patients with normal vHIT gains were significantly higher in the normal to mild dizziness group ($p < 0.05$, **Table 2**, **Figure 1**). The mean horizontal vHIT gains on the lesion side were 0.77 ± 0.25 in the normal to mild dizziness group and 0.62 ± 0.19 in the moderate to severe dizziness group, respectively, and the mean gains in the normal to mild dizziness group were significantly higher than the moderate to severe dizziness group ($p < 0.05$, **Table 2**, **Figure 2**). The DHI score was negatively correlated with lesion side vHIT gains ($R = -0.372$, $p = 0.009$, **Figure 3**). 21.42% UVN patients in the normal to mild dizziness group and 0% UVN patients in the moderate to severe dizziness group had not a corrective saccades at the follow-up, and this was not significantly different ($p = 0.06$, **Table 2**). The proportion of patients with occurrence of isolated covert saccades in the normal to mild dizziness group (39.29%) were significantly higher than the moderate to severe dizziness group (10.53%) ($p < 0.05$, **Table 2**, **Figure 1**). However, the proportion of patients with occurrence of mixed saccades (overt and covert) in the normal to mild dizziness group (39.29%) were significantly lower than the moderate to severe dizziness group (89.47%) ($p < 0.01$, **Table 2**, **Figure 1**). Furthermore, the mean velocity of overt saccades were 155.10 ± 33.60°/s and 160.52 ± 30.94°/s in normal to mild dizziness group and moderate to severe dizziness group at the follow-up, respectively, and this was not significantly different ($p > 0.05$, **Table 2**). The mean velocity of covert saccades were 170.41 ± 45.15°/s and 201.10 ± 40.46°/s in normal to mild dizziness group and moderate to severe dizziness group at the follow-up, respectively, and the mean velocity of covert saccades in normal to mild dizziness group were significantly lower than the moderate to severe dizziness group ($p < 0.05$, **Table 2**, **Figure 4**). The DHI score was positively correlated with velocity of covert saccades ($R = 0.315$, $p = 0.044$; **Figure 5**). The mean latency of overt saccades were 308.93 ± 46.84 ms and 306.97 ± 30.96 ms in normal to mild dizziness group and moderate to severe dizziness group at the follow-up, respectively, and this was not significantly different ($p > 0.05$, **Table 2**). The mean latency of covert saccades were 124.85 ± 27.21 ms and 123.43 ± 22.45 ms in normal to mild dizziness group and moderate to severe dizziness group at the follow-up, respectively, and this also was not significantly different ($p > 0.05$, **Table 2**).

DISCUSSION

VN has long been known to affect the superior vestibular nerve, inferior vestibular nerve, or both (11, 12). The vHIT advent has provided clinicians with diagnostic tools to identify dysfunctions of the pathway of each single semicircular canals. It

TABLE 2 | vHIT results in unilateral vestibular neuritis patients with normal to mild dizziness and moderate to severe dizziness at the follow-up ($n = 47$).

	Normal to mild dizziness (DHI ≤ 30; $n = 28$)	Moderate to severe dizziness (DHI > 30; $n = 19$)	*p*-value
Normal vHIT gain (%)	57.14(16/28)	21.05(4/19)	<0.05[b]
Lesion-side mean gain	0.77 ± 0.25	0.62 ± 0.19	<0.05[a]
Without saccade (%)	21.42(6/28)	0(0/19)	0.06[c]
Occurrence of isolated covert saccade (%)	39.29(11/28)	10.53(2/19)	<0.05[b]
Occurrence of mixed saccade (%)	39.29(11/28)	89.47(17/19)	<0.01[b]
Velocity of overt saccade (°/s)	155.10 ± 33.60	160.52 ± 30.94	>0.05[a]
Latency of overt saccade (ms)	308.93 ± 46.84	306.97 ± 30.96	>0.05[a]
Velocity of covert saccade (°/s)	170.41 ± 45.15	201.10 ± 40.46	<0.05[a]
Latency of covert saccade (ms)	124.85 ± 27.21	123.43 ± 22.45	>0.05[a]

[a]*t-test.* [b]*Chi-square test.* [c]*Fisher exact test. DHI, dizziness handicap inventory.*

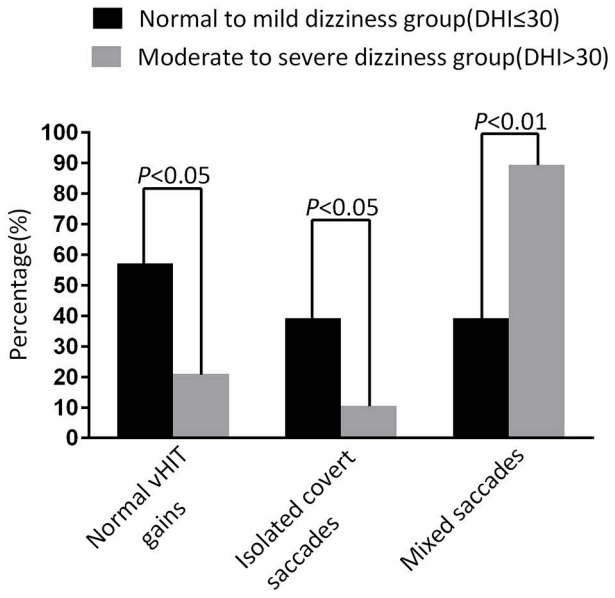

FIGURE 1 | Comparison of normal vHIT gains rate, occurrence of isolated covert saccades, and occurrence of mixed saccades measured from normal to mild dizziness group (DHI ≤30) and moderate to severe dizziness group (DHI >30) with UVN at the follow-up. The normal to mild dizziness group (DHI ≤30) were significantly more likely to have a normal vHIT gain, high occurrence of isolated covert saccades, and low occurrence of mixed saccades.

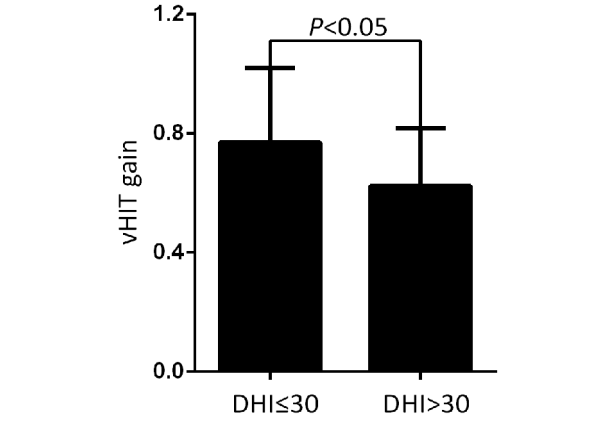

FIGURE 2 | Comparison of the mean horizontal vHIT gains on the lesion side from normal to mild dizziness group (DHI ≤30) and moderate to severe dizziness group (DHI >30) with UVN at the follow-up. The mean gains in the normal to mild dizziness group (DHI ≤30) were significantly higher than the moderate to severe dizziness group (DHI >30).

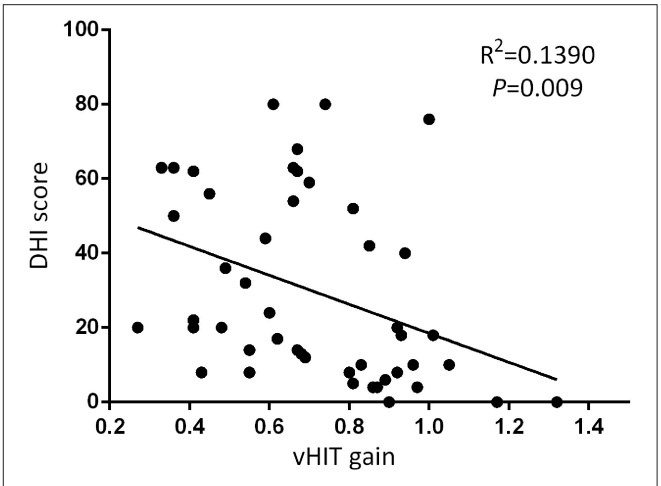

FIGURE 3 | The DHI score was negatively correlated with lesion side vHIT gains at the follow-up.

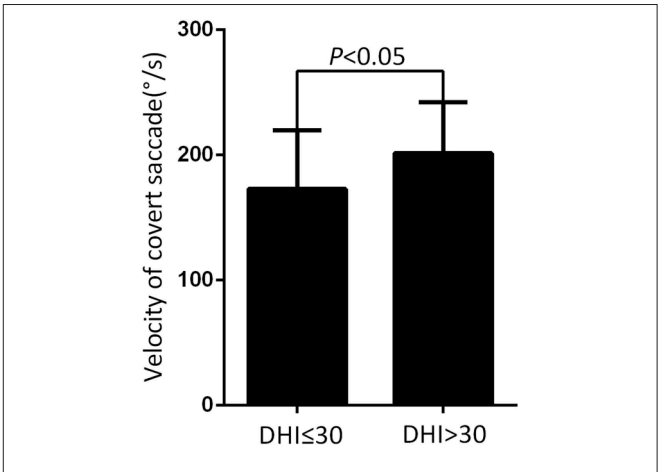

FIGURE 4 | Comparison of the mean velocity of covert saccade from normal to mild dizziness group (DHI ≤30) and moderate to severe dizziness group (DHI >30) with UVN at the follow-up. The mean velocity of covert saccades at the normal to mild dizziness group (DHI ≤30) were significantly lower than the moderate to severe dizziness group (DHI >30).

became evident that both nerve divisions could be affected, both together and independently or rare patterns of the ampullary afferents (13–15).

In recent years, there have been some studies of using vHIT in patients with UVN, but these studies have focused on diagnostic efficacy evaluation and gain is a common parameter to track deterioration or recovery of VOR function at the follow-up (9, 16). Few studies have evaluated quantitatively the corrective saccades in UVN. In our study, we investigated both gain and corrective saccades parameters of the horizontal semicircular canal changes in UVN patients from the acute stage to the follow-up. We found that lesion side vHIT gains always improved to a varying extent at the follow-up. On the healthy side, the vHIT gain was normal even in the acute stage and no worsening of gain could be found at the follow-up. Buki et al. reported that lesion side vHIT gains improved and healthy side vHIT gains were in the normal range at 2 months follow-up in 44 VN patients (16). After testing with search coils in 37 VN patients at different time periods (1–240 weeks), palla et al. revealed the similar result (17). This is consistent with the result obtained by us in VN patients. The gains recovery depended on restoration of the horizontal semicircular canals function. It has some reasons to explain such recovery. Firstly, regeneration of peripheral sensory hair cells.

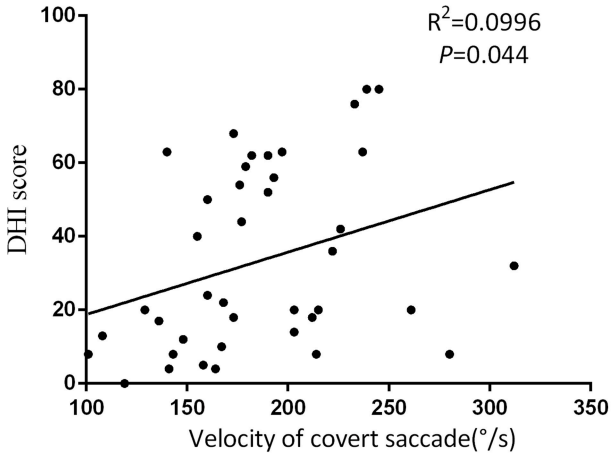

FIGURE 5 | The DHI score was positively correlated with velocity of covert saccades at the follow-up.

Secondly, sprouting of new afferent terminals from remaining fibers in the vestibular nerve. Thirdly, increased synaptic weight of remaining vestibular inputs (18). These mechanisms include cellular recovery, spontaneous re-establishment of the tonic firing rate centrally (19).

However, vHIT gain is not always recover quickly and abnormal vHIT gain could persists for a long time. Sometimes there is rarely recovery of high-frequency acceleration VOR function in our daily life (20). The major question remains that how compensate slow phase eye velocity in our daily life. Fortunately, there is a saccadic substitution of the slow phase eye movement, thereby preventing dynamic VOR deficit during natural head accelerations (20). However, previous studies focus on the recovery of vHIT gain without sufficient recognition of the fact that changes in corrective saccades parameters are a very effective way of overcoming the inadequate VOR function. Therefore, we evaluated the saccades parameters (overt and covert) of the horizontal semicircular canal in UVN by means of the vHIT at the acute stage and the follow-up. And the corrective saccades was analyzed quantitatively. We observed a significant gradual reduction in the occurrence of saccades (overt and covert) at the follow-up. Interestingly, the decrease of occurrence of overt saccades was significantly more evident at the follow-up (100% at the acute stage vs. 59.58% at the follow-up). However, covert saccade still was detected in most of UVN patients (100% at the acute stage vs. 87.23% at the follow-up). In addition, in our study, velocity of saccade (overt and covert) was also significantly decreased at the follow-up. However, latency of saccade (overt and covert) no significant differences at the acute stage and the follow-up. Martin-Sanz et al. found a significantly faster reduction in the velocity and organization of the compensatory saccades was observed in UVN patients recovery stage (21). Furthermore, a recent study by Yang et al. found that the incidence of corrective saccades and peak velocities of corrective saccades had decreased significantly at the 1-month follow-up (22). Our results were similar to these studies. These results show that saccades and vHIT gain play the same role in the vestibular compensation process.

Due to poor vestibular compensation, some UVN patients have difficulties recovering the VOR (18). They were troubled by chronic dizziness, disequilibrium, and limitations in daily activities (23). It is very important in identifying characteristics of vestibular function tests in good vestibular compensation patients and poor vestibular compensation patients. Kim et al. reported that patients have a positive bedside head impulse test (bHIT) result on follow-up, they are more likely to be dizzy (24). As we know, when performing a bHIT, overt saccades are detectable for the clinician but covert saccades cannot be detected. Due to the lack of quantitative analysis, Kim et al. study only reveal the occurrence of overt saccades can predict symptom recovery. Therefore, one great benefit of vHIT is that it allow the clinician to identify such recovery of peripheral vestibular function. To determine which parameters of HIT are better to predict symptom recovery. In our study, we chose DHI score to quantify symptom during the follow-up. The UVN patients were divided into two groups according to the final DHI score: the normal to mild handicap group (DHI $\leq$30) and the moderate to severe handicap group (DHI $>$30). And we found that most of patients have normal vHIT gain and/or isolated covert saccades in the normal to mild group (DHI $\leq$30). The mean gains at the normal to mild dizziness group were significantly higher than the moderate to severe dizziness group. However, patients with abnormal vHIT gain and/or mixed saccades continue to be troubled by some or all of chronic symptoms. Cerchiai et al. reported that lower values of VOR gain and a high occurrence of overt saccades could give rise to a worse prognosis after acute unilateral vestibulopathy (25). Besides, Wettstein et al. found that it has correlation between compensatory covert saccades and improved performance of dynamic visual acuity-testing in patients with unilateral peripheral vestibular loss (26). These studies results were similarly our research findings. And compare overt saccades with covert saccades, covert saccades can play a very key role in compensation of inadequate VOR response and return to a normal lifestyle (20). In addition, we further found that velocity of covert saccades decline probably related to symptom recovery. The diminution of covert saccades velocity is more obvious in the normal to mild group (DHI $\leq$30). It may act to minimize the effect of the unilateral vestibular loss on the patient dynamic VOR deficit and conceal their dysfunction (21).

Limitations of the Study

There are some limitations in this study. First, the number of subjects and follow-up time were insufficient. The future study with a large samples and longer follow-up time need to further confirm our results. Second, we only analyzed the horizontal semicircular canals without analyzing the vertical semicircular canals. This was due to most of VN affected the superior vestibular nerve (27). And horizontal VOR was damage and saccades were more easily observed. Last, we only recruit UVN

patients. Further studies are necessary to investigate the recovery pattern in different vestibular diseases, such as bilateral vestibular hypofunction (BVH), meniere's disease (MD), or vestibular migraine (VM).

CONCLUSION

Apart from the recovery of the VOR gain, recovery pattern of corrective saccades can play a key role in vestibular compensate.

AUTHOR CONTRIBUTIONS

WF designed the experiment, analyzed the data, and wrote the article. FH, DW, YB, and YS collected data and prepared figures. XW and JH guided the study.

ACKNOWLEDGMENTS

Thank you for support and help from Dr. Ning Chang.

REFERENCES

1. Baloh RW. Clinical practice. Vestibular neuritis. *N Engl J Med*. (2003) 348:1027–32. doi: 10.1056/NEJMcp021154
2. Brandt T, Strupp M. General vestibular testing. *Clin Neurophysiol*. (2005) 116:406–26. doi: 10.1016/j.clinph.2004.08.009
3. Weber KP, MacDougall HG, Halmagyi GM, Curthoys IS. Impulsive testing of semicircular-canal function using video-oculography. *Ann N Y Acad Sci*. (2009) 1164:486–91. doi: 10.1111/j.1749-6632.2008.03730.x
4. Halmagyi GM, Curthoys IS. A clinical sign of canal paresis. *Arch Neurol*. (1988) 45:737–9. doi: 10.1001/archneur.1988.00520310043015
5. Weber KP, Aw ST, Todd MJ, McGarvie LA, Curthoys IS, Halmagyi GM. Head impulse test in unilateral vestibular loss: vestibulo-ocular reflex and catch-up saccades. *Neurology*. (2008) 70:454–63. doi: 10.1212/01.wnl.0000299117.48935.2e
6. Alhabib SF, Saliba I. Video head impulse test: a review of the literature. *Eur Arch Otorhinolaryngol*. (2017) 274:1215–22. doi: 10.1007/s00405-016-4157-4
7. Zhang Y, Liu B, Wang Y, Zhou Y, Wang R, Gong J, et al. Analysis of reliability and validity of the Chinese Version of Dizziness Handicap Inventory (DHI). *Zhonghua Er Bi Yan Hou Tou Jing Wai Ke Za Zhi*. (2015) 50:738–43. doi: 10.3760/cma.j.issn.1673-0860.2015.09.008
8. Fu W, He F, Zhao R, Wei D, Bai Y, Wang X, et al. Effects of hand positions during video head-impulse test (vHIT) in patients with unilateral vestibular neuritis. *Front Neurol*. (2018) 9:531. doi: 10.3389/fneur.2018.00531
9. MacDougall HG, Weber KP, McGarvie LA, Halmagyi GM, Curthoys IS. The video head impulse test: diagnostic accuracy in peripheral vestibulopathy. *Neurology*. (2009) 73:1134–41. doi: 10.1212/WNL.0b013e3181bacf85
10. Yang CJ, Lee JY, Kang BC, Lee HS, Yoo MH, Park HJ. Quantitative analysis of gains and catch-up saccades of video-head-impulse testing by age in normal subjects. *Clin Otolaryngol*. (2016) 41:532–8. doi: 10.1111/coa.12558
11. Baloh RW, Ishyama A, Wackym PA, Honrubia V. Vestibular neuritis: clinical-pathologic correlation. *Otolaryngol Head Neck Surg*. (1996) 114:586–92. doi: 10.1016/S0194-5998(96)70251-6
12. Fetter M, Dichgans J. Vestibular neuritis spares the inferior division of the vestibular nerve. *Brain*. (1996) 119 (Pt 3):755–63. doi: 10.1093/brain/119.3.755
13. Halmagyi GM, Aw ST, Karlberg M, Curthoys IS, Todd MJ. Inferior vestibular neuritis. *Ann N Y Acad Sci*. (2002) 956:306–13. doi: 10.1111/j.1749-6632.2002.tb02829.x
14. Aw ST, Fetter M, Cremer PD, Karlberg M, Halmagyi GM. Individual semicircular canal function in superior and inferior vestibular neuritis. *Neurology*. (2001) 57:768–74. doi: 10.1212/WNL.57.5.768
15. Magliulo G, Gagliardi S, Ciniglio AM, Iannella G, Gagliardi M. Selective vestibular neurolabyrinthitis of the lateral and superior semicircular canal ampulla and ampullary nerves. *Ann Otol Rhinol Laryngol*. (2012) 121:640–4. doi: 10.1177/000348941212101003
16. Buki B, Hanschek M, Junger H. Vestibular neuritis: involvement and long-term recovery of individual semicircular canals. *Auris Nasus Larynx*. (2017) 44:288–93. doi: 10.1016/j.anl.2016.07.020
17. Palla A, Straumann D. Recovery of the high-acceleration vestibulo-ocular reflex after vestibular neuritis. *J Assoc Res Otolaryngol*. (2004) 5:427–35. doi: 10.1007/s10162-004-4035-4
18. Lacour M, Helmchen C, Vidal PP. Vestibular compensation: the neuro-otologist's best friend. *J Neurol*. (2016) 263 (Suppl. 1):S54–64. doi: 10.1007/s00415-015-7903-4
19. Fetter M. Acute unilateral loss of vestibular function. *Handb Clin Neurol*. (2016) 137:219–29. doi: 10.1016/B978-0-444-63437-5.00015-7
20. Macdougall HG, Curthoys IS. Plasticity during vestibular compensation: the role of saccades. *Front Neurol*. (2012) 3:21. doi: 10.3389/fneur.2012.00021
21. Martin-Sanz E, Rueda A, Esteban-Sanchez J, Yanes J, Rey-Martinez J, Sanz-Fernandez R. Vestibular restoration and adaptation in vestibular neuritis and ramsay hunt syndrome with vertigo. *Otol Neurotol*. (2017) 38:e203–8. doi: 10.1097/MAO.0000000000001468
22. Yang CJ, Cha EH, Park JW, Kang BC, Yoo MH, Kang WS, et al. Diagnostic value of gains and corrective saccades in video head impulse test in vestibular neuritis. *Otolaryngol Head Neck Surg*. (2018) 159:347–53. doi: 10.1177/0194599818768218
23. Kerber KA. Chronic unilateral vestibular loss. *Handb Clin Neurol*. (2016) 137:231–4. doi: 10.1016/B978-0-444-63437-5.00016-9
24. Kim HA, Hong JH, Lee H, Yi HA, Lee SR, Lee SY, et al. Otolith dysfunction in vestibular neuritis: recovery pattern and a predictor of symptom recovery. *Neurology*. (2008) 70:449–53. doi: 10.1212/01.wnl.0000297554.21221.a0
25. Cerchiai N, Navari E, Sellari-Franceschini S, Re C, Casani AP. Predicting the outcome after acute unilateral vestibulopathy: analysis of vestibulo-ocular reflex gain and catch-up saccades. *Otolaryngol Head Neck Surg*. (2018) 158:527–33. doi: 10.1177/0194599817740327
26. Wettstein VG, Weber KP, Bockisch CJ, Hegemann SC. Compensatory saccades in head impulse testing influence the dynamic visual acuity of patients with unilateral peripheral vestibulopathy1. *J Vestib Res*. (2016) 26:395–402. doi: 10.3233/VES-160591
27. Taylor RL, McGarvie LA, Reid N, Young AS, Halmagyi GM, Welgampola MS. Vestibular neuritis affects both superior and inferior vestibular nerves. *Neurology*. (2016) 87:1704–12. doi: 10.1212/WNL.0000000000003223

Conflict of Interest Statement: The authors declare that the research was conducted in the absence of any commercial or financial relationships that could be construed as a potential conflict of interest.

frontiers in Neurology

METHODS
published: 02 April 2019
doi: 10.3389/fneur.2019.00306

Functional and Objective Audiovestibular Evaluation of Children With Apparent Semicircular Canal Dehiscence–A Case Series in a Pediatric Vestibular Center

Soumit Dasgupta and Sudhira Asanka Bandara Ratnayake*

Department of Paediatric Audiology and Audiovestibular Medicine, Alder Hey Children's NHS Foundation Trust, Liverpool, United Kingdom

Semicircular canal dehiscence is a bony abnormality in the otic capsule especially involving the superior semicircular canal. Since its identification in 1998, there is significant research regarding the pathology in the adult population. This condition generates a third window effect that is well–described in the literature. However, the entity is rare in the pediatric population with limited research. Difficulties encountered in children are obtaining a direct history that is essential for the diagnosis followed by neurovestibular tests that may be difficult to perform. This study presents observations regarding different clinical and diagnostic aspects of semicircular canal dehiscences in children as a retrospective audit in a tertiary pediatric vestibular center. Of 580 children assessed in a 30 months period undergoing comprehensive functional and objective audiovestibular assessment, 13 children (2.2%) were detected to possess radiological semicircular canal dehiscences (high resolution computed tomography scans at 0.625 mm slices reformatted in the axial, coronal and sagittal planes). The right superior semicircular canal was most commonly affected (66.6%). There were 4 bilateral semicircular canal dehiscences. Clinical suspicion of the condition was raised with reliable surrogate history from carers or from older children (100%), a mixed or conductive hearing loss (80% of hearing losses) in the presence of normal impedance audiometry (92.3%), normal transient otoacoustic emissions (84.6%) on the side of the dehiscence and the presence of replicable pathological saccades in the video head impulse test (76.9%). Disequilibrium symptoms and typical third window symptoms were absent or difficult to elicit in children (46.15 and 30.76% respectively). Only 3 (0.5%) fulfilled the adult criteria of a superior semicircular canal dehiscence syndrome. The abnormal video head impulse test characterized by pathological saccades may affect other non-dehisced ipsilateral canals. Semicircular canal dehiscences are rare in children but may be considered as an etiology for hearing losses and imbalance. Children with semicircular canal dehiscence may present differently from the classical superior semicircular canal dehiscence syndrome found in adults.

Keywords: semicircular canal dehiscence, third window, audiovestibular, video head impulse, pediatric, high resolution CT

OPEN ACCESS

Edited by:
Stefano Ramat,
University of Pavia, Italy

Reviewed by:
Marco Mandalà,
Azienda Ospedaliera Universitaria Senese, Italy
Bryan Kevin Ward,
Johns Hopkins University, United States

****Correspondence:***
Soumit Dasgupta
soumit.dasgupta@alderhey.nhs.uk

Specialty section:
This article was submitted to Neuro-Otology, a section of the journal Frontiers in Neurology

Received: *29 October 2018*
Accepted: *11 March 2019*
Published: *02 April 2019*

Citation:
Dasgupta S and Ratnayake SAB (2019) Functional and Objective Audiovestibular Evaluation of Children With Apparent Semicircular Canal Dehiscence–A Case Series in a Pediatric Vestibular Center. Front. Neurol. 10:306. doi: 10.3389/fneur.2019.00306

INTRODUCTION

The pathological entity of superior semicircular canal dehiscence (SSCD) since its first description by Minor (1) has seen immense interest and research. Originally described in patients with sound or pressure induced vertigo and nystagmus (Tullio's and Hennebert's phenomenon) with symptoms of chronic disequilibrium, the clinical features that subsequently came into light included oscillopsia, auditory features including conductive hearing loss, autophony, conductive dysacusis including gaze evoked tinnitus, pulsatile tinnitus, low frequency hearing loss, phonophobia, and aural fullness (2). Vestibular symptoms may be absent (3).

The pathophysiology of the auditory features of SSCD can be attributed to the pathological presence of a third window in addition to the natural two windows for maintaining integrity of inner ear sound conduction. The pathological third window shunts away a proportion of the sound energy delivered at the stapes footplate-oval window interface and thus from the cochlea resulting in abnormally elevated air conduction thresholds in pure tone audiometry. The same mobile third window lowers the impedance or pressure difference of the cochlear traveling wave between the scala vestibuli and the scala tympani in the inner ear by allowing a new path for the sound to enter the inner ear thereby generating enhanced bone conduction thresholds in bone conducted pure tone audiometry (4). The vestibular features in SSCD are due to its enhanced vulnerability to pressure changes created by sound conduction. Other conditions in the otic capsule generating a similar third window effect are posterior and lateral semicircular canal dehiscences, enlarged vestibular aqueducts, the X linked gusher syndrome, facial nerve canal dehiscences, dilated bony internal auditory meatus, and dehiscent carotid canals.

The etiology of SSCD appears to be developmental and congenital (5) and it has been suggested that thinning or dehiscence of the bone in the otic capsule over the semicircular canal is more prevalent in children younger than 12 months and with age, the semicircular canals may develop more bony covering (6). Carey et al. suggested that there may be a malformation in neonatal bony development (7). Head trauma may also lead to a dehiscent semicircular canal (5). Congenital SSCD may be accompanied with deficient tegmens and dysplasia found in some syndromic conditions (5). Nadgir et al. (8) however, proposed a predominantly acquired etiology and suggested that frank dehiscences increased with age due to bony demineralization. The debate is unresolved.

The diagnosis of the condition in addition to the clinical features rested primarily on imaging with a high resolution CT scan. However, a CT scan is not sufficient on its own to confirm a diagnosis as many as 9% may have a dehiscence on a coronal temporal bone CT with a 1 mm slice, many of whom are asymptomatic (5, 9) and unless reformatted with slices <0.625 mm in the Poschl and Stenver's views, CT scan may still over diagnose the condition (5). Thus, it is crucial to consider physical symptoms and physiological evidence of a third window (5).

Whilst auditory symptoms suggest a third window phenomenon, subsequent research has shown that vestibular evoked myogenic potentials (VEMPs) are reliable, sensitive and specific indicators of a pathological third window due to lowering of impedance in the vestibular system as regards sound and pressure resulting in lower thresholds and higher amplitudes in the VEMPs (2). The cervical VEMP was the first VEMP identified and now it has been discovered that air conducted ocular VEMPs have a sensitivity and specificity of more than 90% to detect a pathological third window (10). The use of VEMPS in semicircular canal dehiscences in children has limited evidence.

SSCD is very well-described in the adult population, however, evidence of the condition in the pediatric population is evolving. Data regarding quantification of vestibular function in the condition in children is meager. Until 2007, only 3 children were described with the condition (3). Chen et al. (11) in a retrospective cohort analysis in the pediatric population analyzed 131 temporal bones in children presenting with hearing loss over the age of 3 years and observed that 18 (15%) showed CT evidence of semicircular canal dehiscence with 13 SSCD and 5 posterior semicircular canal dehiscences (PSCD). The series did not include vestibular function test data. Lee et al. (12) in a cohort of 7 children observed that hearing loss was the predominant presenting feature with disequilibrium as the next common presenting complaint in children. Third window features could only be elicited in the 3 oldest children. Of vestibular function tests, VEMPS were performed which were found to be abnormal in the majority. Meiklejohn et al. (13) studied live and cadaveric temporal bone specimens in children younger than 7 years and observed that the prevalence of radiographic semicircular canal dehiscence declined with increased age in children, reinforcing the idea that the otic capsule thickens with age. Normal, mixed and sensorineural hearing losses (SNHL) were reported in the live cohort of 19 children, however, there were no children with third window features or with disequilibrium. Sugihara et al. (14) identified an incidence of 6.2% of SCDS in the pediatric population in a large multicenter review. This study very interestingly did not suggest that other inner ear anomalies are significantly associated with SCDS in children. Hagiwara et al. (15) pointed out that radiographic evidence of semicircular canal dehiscence does not necessarily suggest a semicircular canal dehiscence syndrome i.e., clinical symptoms. There have been some isolated case reports also (3, 16, 17).

The present study was a retrospective study that looked into audiovestibular quantification of semicircular canal dehiscences in the pediatric population in detail for the first time in a tertiary pediatric balance center in the United Kingdom to analyse the patterns of clinical presentation, auditory and vestibular functions and the relationship between behavioral audiometry with objective vestibular function.

PATIENTS AND METHODS

Patients

A retrospective case note audit was performed in children who underwent vestibular quantification in the pediatric age group

as a service improvement exercise in Alder Hey Children's NHS Foundation Trust, a tertiary children's hospital in Liverpool, United Kingdom between the period of February, 2016 and July, 2018. These children attended the secondary and tertiary audiovestibular clinics in the hospital. The study was approved by the clinical audit department of the hospital. Being a retrospective audit, the study population did not require ethical committee approval. Only children above the age of 5 years up to 17 years were included in the case series. Dysplastic vestibular pathologies with hypoplasia/aplasia of canals with dehiscences as shown in imaging were excluded.

Methods

Anamnesis

History for audiovestibular manifestations in young children are often surrogate and obtained from carers. This was attempted to be as comprehensive as possible with accounts from both carers, from schools as well as children themselves wherever obtainable. A subjective narrative is extremely important in children with balance problems or hearing losses. A frank history of disequilibrium or disorientation that adults can generally narrate so well is frequently impossible from children including teenagers. Therefore, since balance in children can be observed by others and balance problems may lead to predictable behavior, an accurate description from carers were absolutely crucial which in turn can be fairly reliable indicators of the problems. Similarly with hearing loss, a deficit in communication and educational performance were deemed as a key indicator of a positive history. Some children narrated symptoms of conductive dysacusis. Key points in history are shown in **Table 1**.

TABLE 1 | Symptoms of pediatric vestibular disease.

- Obvious dizziness/vertigo/lightheadedness (usually describable by children above 8 years of age)
- Fright or pallor
- Clutching at objects to steady oneself
- Bumping into things
- Clumsiness
- Sudden very brief lasting falls with immediate complete recovery
- Periodic episodes of nausea or vomiting ± migrainous features
- Delayed motor functions
- Loss of postural control
- Difficulty with ambulating in the dark
- Difficulty with or avoidance to ride a bike or in amusement park rides due to imbalance
- Abnormal movements during walking, running
- Abnormal behavior observed up by significant others (care giver, school or peer group)
- Difficulties in challenging movements (swimming, dancing)
- Oscillopsia
- Difficulties in challenging visual environments for example in superstores and in crowded places
- Poor head eye or hand eye coordination
- Third window symptoms if described by older children—conductive dysacusis (for example hearing one's own footsteps), gaze evoked tinnitus (audible eye movements), autophony (altered perception or perverted self-monitoring of own voice), Tullio's phenomenon (dizziness on hearing loud sounds), Hennebert's phenomenon (pressure induced dizziness for example on coughing and sneezing), pulsatile tinnitus (tinnitus that is synchronous with pulse beat)

Audiovestibular Quantification

With full verbal informed consent, all children underwent otoscopy, tympanometry, stapedial reflex tests, pure tone audiometry; transient otoacoustic emissions (OAE) and a neurovestibular examination that included observation of the subjective visual vertical (measurement of head tilt with respect to earth's vertical to assess static gravitational sensor function); a full videonystagmography (VNG) examination with and without visual fixation to observe and measure smooth pursuits and saccades (to assess central vestibular function), eccentric eye movements (to assess nystagmus); the passive head shake (appearance of post headshake nystagmus) and the head heave test (translational counter part of the head thrust test for utricular function); the amplitude and symmetry of ocular counter rolling (ocular movements in response to head roll to assess gravitational sensor function). All these tests were video recorded. Further tests performed were the vHIT in all 6 semicircular planes; the VOR suppression test and office rotatory chair tests under VNG control and the vestibulo-spinal test battery including the Romberg, the Unterberger, the tandem gait and the one legged stance as well as sharpened Romberg's test with and without proprioception to eliminate as much proprioception as possible (i.e., in a foam cushion) removed. Some children also underwent the mastoid vibration test under VNG control to yield additional information on low frequency lateral semicircular canal responses and some older children were subjected to the Dix Hallpike, the supine roll test and the deep head hanging test to test for benign positional paroxysmal vertigo (BPPV) especially when they complained of positional dizziness. Caloric testing was not performed due to its logistic issues when performed in children especially taking into account the distress caused in children by caloric testing. At the time of the study, the center did not possess VEMPS that it now does. One of the reasons as to why the case review was undertaken was to assess whether the service provisions available at that time permitted the diagnosis of superior semicircular canal dehiscences in children that in turn would suggest areas for improvement.

In addition, a full neurological examination was performed in all children as well as a full oculomotor and musculoskeletal examination as part of the holistic test battery. The history and the neurotological investigations were performed by the authors who are experienced clinicians specializing in pediatric vestibular disorders who peer reviewed each other's observations to reach a consensus. The audiovestibular examination and tests are given in **Table 2** which also qualifies the tests.

Pure tone audiometry involved measurement with air conduction and bone conduction with the acoustic stimuli delivered through TDH39 head phones and thresholds up to 20 dBHL were considered as normal. Pure tone air conduction thresholds were performed from 500 Hz up to 6k Hz for every child to obtain as much information on hearing as possible especially because meaningful speech containing consonants are mainly between 4 and 6 kHz. For this paper, pure tone averages between 500 Hz and 4 kHz in every child was averaged for air and bone conduction thresholds. Bone conduction thresholds were performed wherever indicated especially with masking

TABLE 2 | The pediatric audiovestibular test battery.

Audiological tests	Vestibular tests
• Pure tone audiometry with masking • Tympanometry • Stapedial reflexes • Otoscopy • Transient otoacoustic emissions	• Full neurological examination • Musculoskeletal examination • Full oculomotor examination • Assessment of subjective visual vertical • Videonystagmography with and without visual fixation for head shake, head heave, ocular counter rolling and ectopic eye movements • Video head impulse test • Vestibulo-spinal test battery with and without foam cushion for Romberg, Unterberger, tandem gait; one legged stance and sharpened Romberg • Office rotatory chair tests and suppression of visual fixation • Mastoid vibration test • Dix Hallpike, supine roll and deep head hanging tests

VNG software was used to video record and play back for head shake, head heave, ocular counter rolling, mastoid vibration, positional tests and suppression of visual fixation tests; Unterberger test: child is asked to walk/jog in place with eyes closed; Sharpened Romberg's test: placing one heel in front of toe as in tandem gait but not moving with eyes open and closed with and without proprioception.

but occasionally were difficult to obtain in young children due to intolerance or the complexity of the task. Transient otoacoustic emissions were measured at stimulus intensity of 80–88 dBSPL on both ears by equipment from Otodynamics; VNG and vHIT were performed by the ICS Impulse software from Otometrics. For the vHIT, an abnormal result was denoted by lower than normal vestibulo-ocular reflex gain (VOR) in the semicircular canals with catch up overt and covert saccades and by normal VOR gain with replicable and repeatable overt and covert saccades. Normal VOR gain with catch up refixation saccades after vestibular pathology have been recently identified as an important observation in the evolving literature with the vHIT (18). A minimum of 10 thrusts in different semicircular canals (laterals and right anterior left posterior RALP and left anterior right posterior LARP) were achieved to draw meaningful conclusions. The normal gain in the lateral semicircular canal was considered to be 0.8 to 1 and that of the vertical canals to be 0.7 to 1. It is worth pointing out that in a new and emerging evidence in the pediatric population, the vertical canal gains involving RALP and LARP may be lower than in the adult population (19) that could be to contamination by a developing cervical neck musculature. All children presenting with hearing loss underwent the full set of aetiological investigations as recommended by the British Association of Audiovestibular Physicians (20) that included MRI and genetic testing, ophthalmological examination, drawing of family tree and blood investigations, looking into metabolic conditions that can cause hearing loss and autoimmune ear disorders. These were unremarkable in our case series diagnosed with canal dehiscence.

High Resolution CT

Based on anamnesis and audiovestibular information; children with third window symptoms, hearing losses and balance problems either alone or in combination with and without tinnitus were subjected to a high resolution CT scan to obtain a comprehensive idea about the bony otic capsule. The slices were 0.625 mm thick with a high spatial filter. Axial, coronal and sagittal reconstructions were performed. The investigation was performed by a senior radiology consultant colleague specializing in pediatric head and neck radiology.

Statistical Methods

Following the diagnostic algorithm, children with CT evidence of semicircular canal dehiscences were subjected to descriptive analysis performed by Quick Statistics Calculators, an online digital portal (https://www.socscistatistics.com/tests/).

RESULTS

The observations for the full case series are given in **Table 3**. **Figures 1–3** show representative cases.

Total number of children seen in the period of study were 580. Out of these, 13 children (2.2%) had radiological evidence of semicircular canal dehiscences. There were 6 boys and 7 girls in the case series. The average age in the female population was 11.28 (range 9 to 17 years) years whilst in the male population it was 9.83 years (range 6 to 14 years) in the case series presenting with semicircular canal dehiscences.

The 13 children with semicircular canal dehiscences involved either the superior semicircular canal (2.06% of the whole population) or the posterior semicircular canal (0.5% of the whole population). In 26 ears studied, SSCD was detected in 15 (57.69% of the semicircular dehiscence group) and PSCD was detected in 3. There were 4 children with bilateral semicircular canal dehiscence either both SSCD or with SSCD and PSCD (cases 2,6,7, and 12). One child presented with both superior and posterior canal dehiscence on one side (case 9). Ten (66.6%) out of the 15 SSCD were on the right as were all the 3 PSCD on the right.

Children presenting with symptoms of hearing loss, i.e., deficits in communication for example difficulties to hear or engage in conversation in the class room, difficulties to respond to orally delivered instructions were observed in 8; however, it must be noted that actual measured hearing losses (i.e., >20 dBHL in air conducted thresholds in any frequency) were detected in 10 as there was 1 child with unilateral sensorineural hearing loss who did not present with any symptoms of hearing loss (case 13) and 1 child with asymmetrical conductive hearing loss where the left ear showed better air conduction thresholds than the right did not complain of a hearing loss either (case 6). Measured hearing loss in terms of air conduction thresholds averaged between 500 Hz and 4 kHz therefore, was found in 76.9% of which 6 were bilateral and 4 were unilateral. Three children did not have a hearing loss. The hearing loss was mixed or conductive in 8 (80% of hearing losses and 61.5% of the whole case series) and was sensorineural in 2 children. These 2 children presented with SNHL on one ear (cases 4 and 13). The average air conduction hearing threshold between 500 Hz and 4kHz on the left ear was 29.4 dBHL and on the right was 32.5 dBHL (the mean of the summated averages of air conduction thresholds in each child) whilst the

TABLE 3 | Clinical features and audiovestibular assessment in children with semicircular canal dehiscence; $n = 13$.

Child	HS	BS	TWS	Tymp	SRT	OAE	VNG/VFT	VOR LLSC	VOR RLSC	VOR LASC	VOR RASC	VOR LPSC	VOR RPSC	AC/BC R	AC/BC L	Type HL	Saccade	Diagnosis
1	Yes	Yes	Nil	Norm	Norm	Abn	Norm	1.16	1.09	0.55	0.75	0.85	0.69	55/46	58/46	Mixed	Yes	R PSCD
2	Nil	Yes	GET	Norm	Norm	Norm	Norm	0.67	0.48	0.62			1.46	7/−5	4/3	Nil	No	L SSCD R PSCD
3	Yes	Nil	Nil	Norm	Norm	Norm	Norm	0.96	0.96	0.41	0.85	0.82	0.51	27/7	10/na	CHL	Yes	R SSCD
4	Yes	Nil	Nil	Flat	Reduced	Abn	Norm	1.1	0.88					100/nt	17/4	SNHL	No	R SSCD
5	Yes	Yes	Nil	Norm	Norm	Norm	Abn	1.14	1.17	1.13	1.08	0.90	1.1	45/9	45/10	CHL	Yes	RSSCD
6	Nil	Nil	Nil	Norm	Norm	Norm	Norm	0.79	0.94	0.67	0.75	1.07	0.78	42/2.5	23/10	CHL	Yes	Bilateral SSCD
7	Nil	Nil	CD	Norm	Norm	Norm	Norm	0.94	0.94	0.79	0.92	0.99	0.83	9/6	7/6	Nil	Yes	Bilateral SSCD
8	Yes	Nil	Nil	Norm	Norm	Norm	Norm	0.86	0.83	0.50	0.89	0.82	0.39	25/14	45/20	CHL	Yes	R SSCD
9	Yes	Yes	Nil	Norm	Norm	Norm	Abn	0.86	0.90	0.73	0.48	0.54	0.47	36/30	41/26	Mixed	Yes	R SSCD R PSCD
10	Yes	Nil	Nil	Norm	Norm	Norm	Abn	0.82	0.90	0.73	0.88	0.75	0.73	17/15	21/15	Mixed	Yes	L SSCD
11	Nil	Yes	Auto/ tinnitus	Norm	Norm	Norm	Norm	0.95	0.90	0.41	0.37	0.66	0.59	12/7	17/9	Nil	Yes	R SSCD
12	Yes	Yes	CD	Norm	Norm	Norm	Norm	1.07	1.01	0.07	0.07	1.06	1.03	44/35	39/36	Mixed	Yes	Bilateral SSCD
13	Nil	Nil	Nil	Norm	Norm	Norm	Norm	1.18	0.99	0.65			0.98	4/10	55/51	SNHL	No	R SSCD

Children in case group; Legends: HS, hearing symptoms; BS, balance symptoms; TWS, Third window symptoms; Tymp, tympanometry in dehisced ear/s; SRT, stapedial reflex test in dehisced ear/s; OAE, transient otoacoustic emission in dehisced ear/s; VNG/VFT, videonystagmography/other vestibular function tests; VOR, vestibulo-ocular reflex gain; LL/RL/LA/RA/LP/RP SC, left lateral, right lateral, left anterior, right anterior, left posterior, right posterior semi-circular canals; PTA AC R and L, pure tone audiometry air conduction thresholds averaged 500 Hz–4 kHz right and left; BC R and L, pure tone audiometry bone conduction thresholds averaged 500 Hz–4 kHz right and left; na, not performed; nt, no detectable threshold; HL, hearing loss; CHL, conductive hearing loss; SNHL, sensorineural hearing loss; GET, gaze evoked tinnitus; CD, conductive dysacusis; Auto, autophony; Tinn, tinnitus; Norm, normal; Abn, abnormal.

average bone conduction thresholds (the mean of the summated averages of bone conducted thresholds in each child) between 500 Hz and 4kHz was 20 dBHL on the left and 18 dBHL on the right.

As regards bone conduction thresholds, 5 children exhibited negative bone conduction thresholds in at least one frequency (cases 2,5,6,7, and 11) out of which 3 children (cases 2, 7, and 11) presented with third window symptoms as well and indeed fulfilled the criteria for an adult superior semicircular canal dehiscence syndrome (5). Two children (cases 5 and 6) had conductive hearing losses without any third window symptoms.

Tympanometry was normal in 12 children (92.3%) whilst stapedial reflexes were normal in 12 children as well. There was some otitis media with effusion in one child with unilateral profound sensorineural hearing loss (case 4) where tympanometry was flat with depressed stapedial reflexes on the dehisced side which was the side of the hearing loss. Transient otoacoustic emissions were normally recordable in 10 children on both ears (76.9%) and in 11 children on the dehisced sides (84.6%). They were absent in 2 children with sensorineural hearing loss on the ipsilateral ear of the hearing loss (cases 4 and 13) and in case 1 with a mixed hearing loss on both sides.

Three children were diagnosed with bilateral hearing losses but unilateral semicircular canal dehiscence (cases 1, 5 and 8), 2 children demonstrated bilateral semicircular canal dehiscences with bilateral hearing loss (cases 6 and 12). Four children (30.7%; cases 2,7,11 and 12) narrated classical third window symptoms. The hearing loss localized to the dehisced side in 11 ears but there were 5 ears where a hearing loss was detected with no radiographic evidence of dehiscence on the ipsilateral ear.

Six children presented with definite features of pediatric disequilibrium, i.e., symptoms as listed in **Table 2** (46.15% of the study group and) while the rest 53.85% were asymptomatic. Three children had abnormal balance function tests not including the vHIT (head shake test, mastoid vibration test, head heave test, ocular counter rolling and subjective visual vertical test). Ten children (76.9%) had abnormal vHITs with either low VOR gain and saccades or with normal VOR gain and replicable or repeatable saccades (i.e., saccades that were consistent and multiple), 3 children had normal vHITs. The average gain of the left lateral semicircular canal in the case series was 0.96; the right lateral semi-circular canal was 0.92; the left superior semi-circular canal was 0.6; the right superior semi-circular canal was 0.70; the left posterior semi-circular canal was 0.85 and the right posterior semicircular canal was 0.8. Out of 18 ears with semicircular canal dehiscences, abnormal vHIT with saccades were detected in 12 (66.6% of all ears with semicircular canal dehiscence) and in 7 children they localized to the same canal in the affected side. It was observed that in 5 children, abnormal canal function was detected in other canals on the same side rather than the canal affected, i.e., for SCDS, the abnormal vHIT was seen in either the lateral or the posterior canals. In 2 children, there was unilateral vHIT abnormality in bilateral SCDS. All children had normal neurological and oculomotor function.

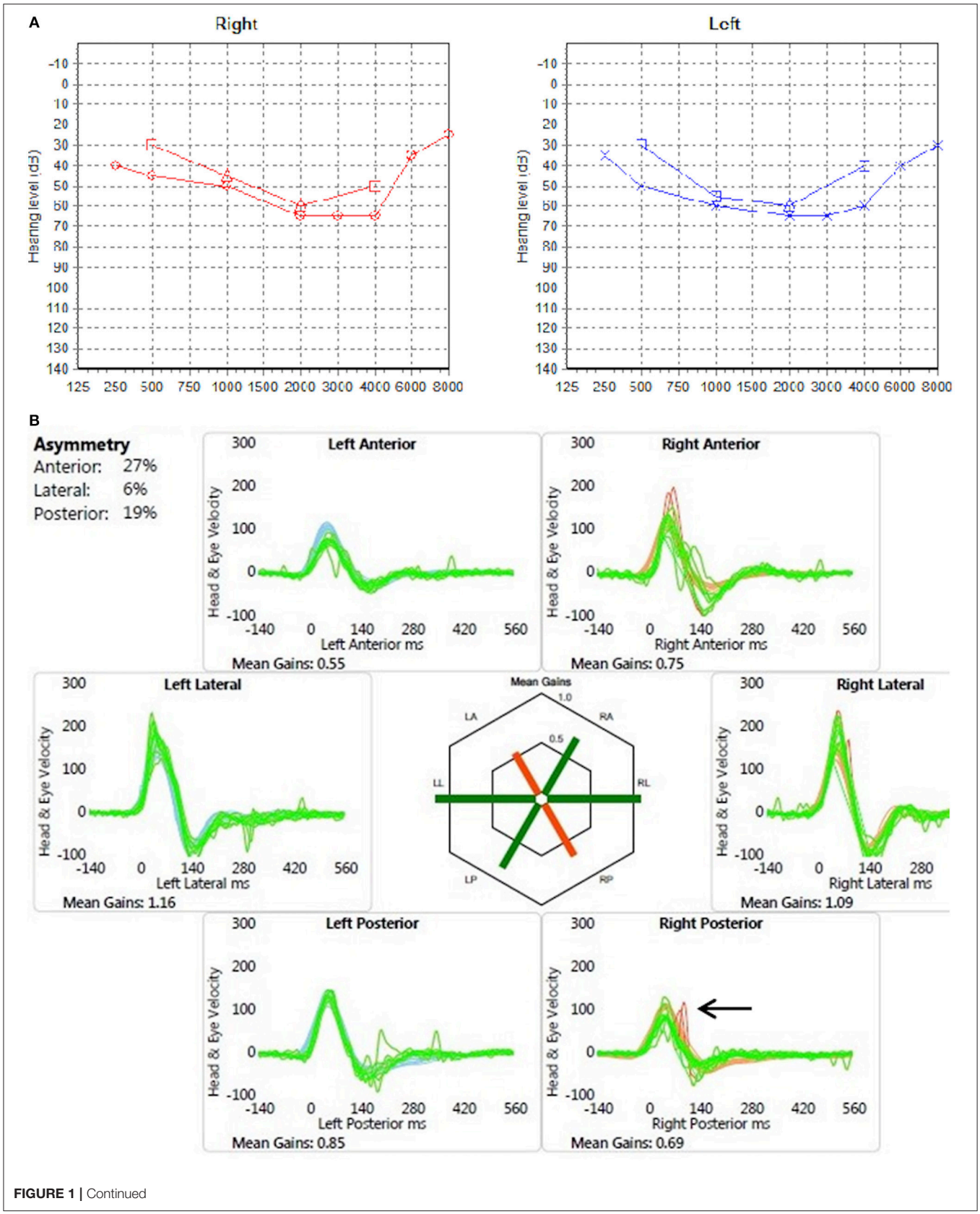

FIGURE 1 | Continued

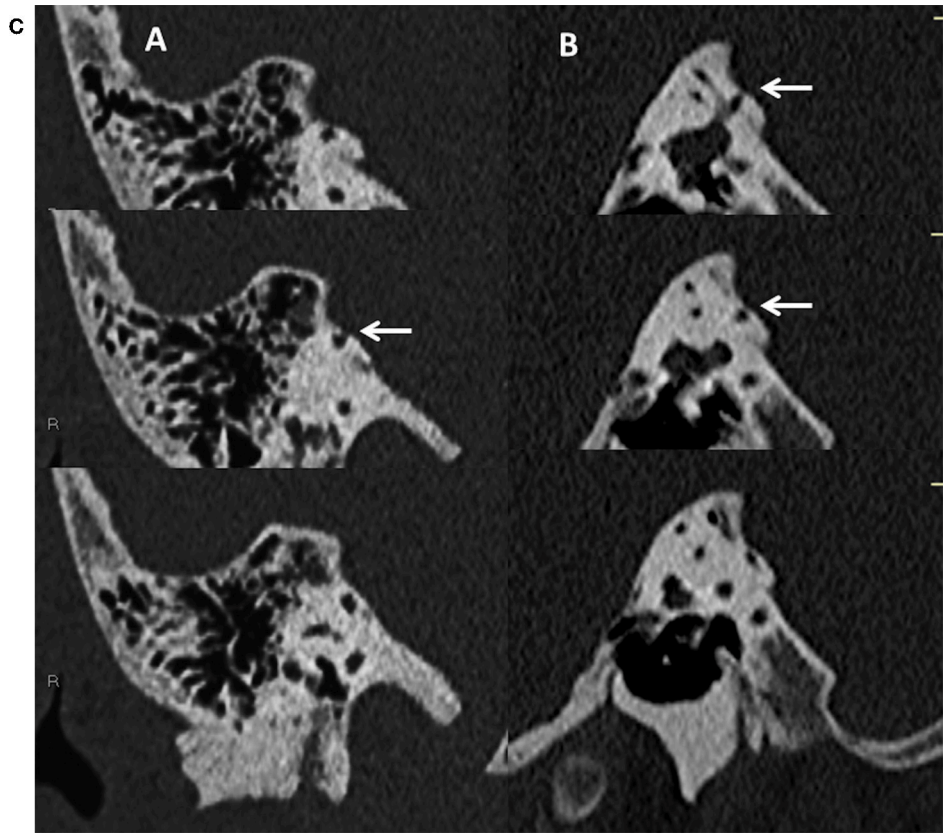

FIGURE 1 | (A) PTA in a child presenting with mixed hearing loss (child 1). **(B)** Video head impulse test in same child with at least 2 covert replicable saccades in the right posterior semicircular canal (arrow). **(C)** Coronal (A) and sagittal (B) reconstructions of a high resolution CT scan with consecutive slices demonstrating dehiscence of the right posterior semicircular canal (arrows).

DISCUSSION

Although well-researched in the adult population, evidence relating to semicircular canal dehiscence in children is limited especially regarding clinical presentation and functional and objective vestibular quantification. The largest series to this date is by Meiklejohn et al. (13) who in their series including 19 children from the age of 2 months until 7 years observed a zero percent prevalence of the condition at the age beyond 3 years which is the starting age range of the current study. The majority of this case series presented with hearing loss and included variable comorbidities and cochleo-vestibular dysplasias as well. The current study in its methodology excluded children under the age of 5 years and children with comorbidities due to 2 main reasons—firstly, the dehiscence may be part of normal development under the age of 5 years (6, 15) and secondly cochleovestibular comorbidities might be responsible for the presenting phenotype rather than the dehiscence.

The prevalence of semicircular canal dehiscence in children over the age of 5 years is not resolved as yet especially given the variable observations in the limited evidence; it ranges from 0 to 13% (11, 13). In the current series, this was observed to be 2.2% overall with 2.06% in the superior and 0.5% in the posterior semicircular canals. Saxby et al. (21) observed a prevalence of 1.7% SSCD and a 1.2% PSCD in their series. This study was investigating primarily SNHL in their cohort. The current study differs from other studies as it includes children with both audiological and vestibular phenotypes and is the largest series of its kind. It can be noted that available evidence in the majority pertains to a radiological diagnosis rather than diagnosis based on third window features.

In the current series it was observed that the right sided superior semicircular canal was the most common canal that showed dehiscence (66.6%). Sanverdi et al. (22) in their series of 560 children with SNHL and varying degrees of otic capsule incomplete ossification observed a 7.5% ossification asymmetry. Asymmetry is a frequent attribute in all body organs although the small size in the current sample may be responsible for this observation. Bilateral dehiscences were detected in 4 children (30.7%). This has been reported sporadically in the literature (11, 16) and number only 3 in published literature. This observation augments previous evidence that indeed otic capsule dehiscence may be developmental due to a deficit in ossification of the bony otic capsule.

Measured hearing loss was observed in the current series in 76.9% of children of varying degrees. This appears to be one

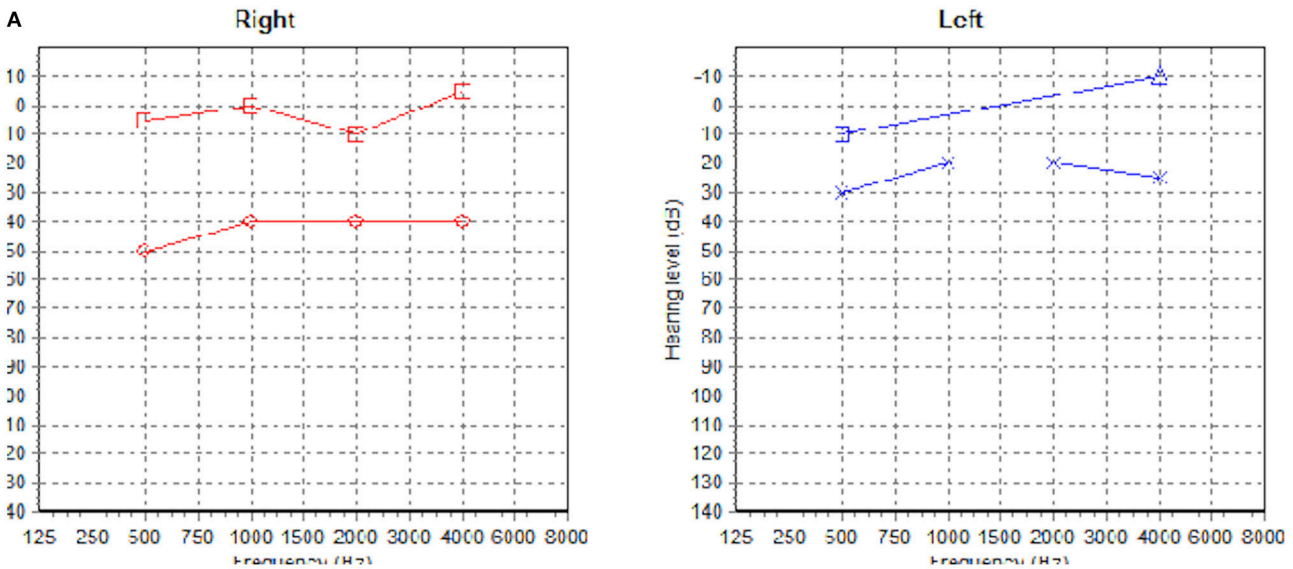

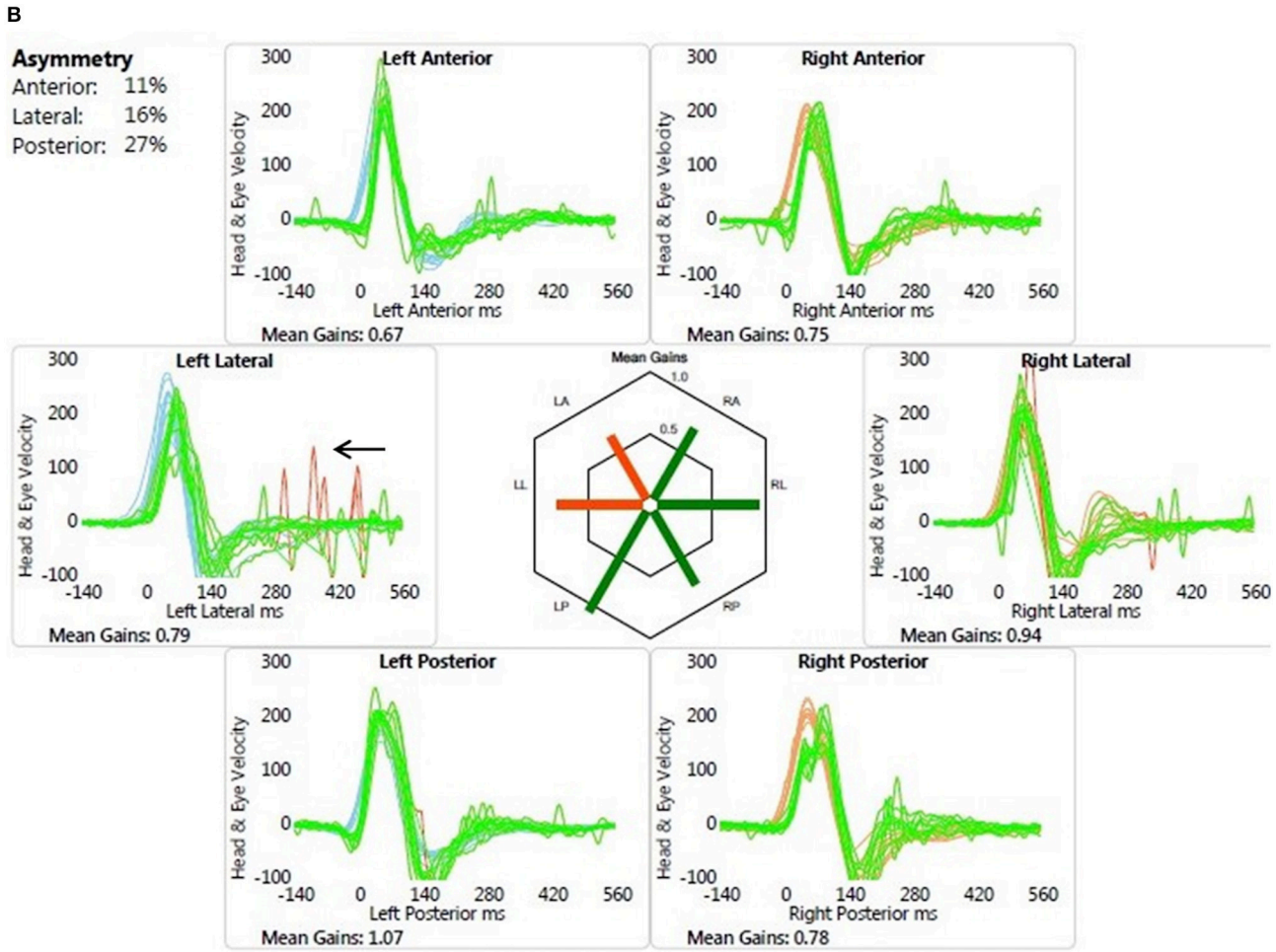

FIGURE 2 | Continued

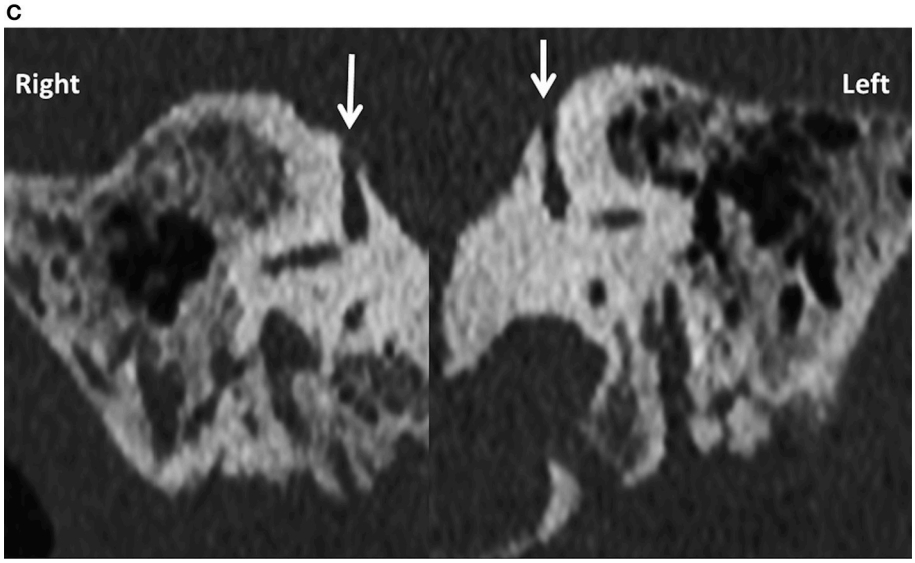

FIGURE 2 | (A) PTA in a child presenting with conductive hearing loss on both sides (child 6). **(B)** Video head impulse test in the same child with overt replicable saccades in the left lateral semicircular plane (arrow). **(C)** Coronal reconstruction of High resolution CT scan shows dehiscence of the superior semicircular canal on both sides (arrows).

of the most common presenting features of semicircular canal dehiscence in children and the findings in the current study agreed with other published evidence(3, 11–13, 16, 17, 23). There were 3 children who had normal hearing thresholds. This can be deemed as an important finding as this has been hardly reported except in the series by Lee et al. (12) and Wenzel et al. (17), where one child in each case had normal hearing thresholds. Variability in presentation is a frequent observation in semicircular canal dehiscences in all age groups that is well-known. It is interesting to note that in the studied case series, these three children presented with symptoms of third window.

The main type of hearing loss in the current series was a mixed or conductive hearing loss in 80% of the children with hearing losses. This observation replicates those found in other studies for example Zhou et al. (3), Chen et al. (11), and Lee et al. (12). The reason for a mixed or conductive loss can be explained by the third window effect. Sensorineural hearing loss is not unknown either (16, 17, 24, 25) and in this series it was observed in 2 children. These children did not show any balance symptoms and the reason they were requested for a high resolution CT was because their MRI was normal as suggested in the aetiological diagnosis algorithm. The large series by Meiklejohn et al. (13) observed SNHL in the majority, however, they included cochleo-vestibular dysplasias in their series which were likely responsible for the hearing loss. It was also observed in the current series that hearing loss did not essentially correlate with radiographic evidence of a dehiscence; i.e., a deficit in hearing might not show a dehiscence on that side or vice versa. The authors believe that since the condition can evolve, a HRCT might show a frank dehiscence in future in these cases.

The issue of negative bone conduction threshold as a criteria for diagnosing SSCD (5) deserves special mention. This functional subjective test establishes a pathological third window effect. In our case series, only 5 children demonstrated negative bone thresholds, out of which, 3 complained of conductive dysacusis. Merchant et al. (26) in their cohort of 20 children observed that whilst bone conduction thresholds may be negative in superior semicircular canal dehiscence, it might not be true for all subjects presenting with the condition. Instead, they pointed out that a measured air bone gap in the presence of normal middle ear function was a more consistent finding that we have also observed in the current series including the 2 with negative bone conduction thresholds not presenting with conductive dysacusis.

All the 13 children in our study case series with sensorineural or mixed hearing losses were extensively investigated with MRI scans, genetic and blood tests that were unremarkable. Therefore, by the process of elimination, it was more likely than not that their hearing losses can be explained by the demonstration of a radiological semicircular canal dehiscence. This of course cannot be proven by an observational retrospective descriptive study like the current one, however, neither can it be said that a radiological dehiscence in this group can be incidental only.

Only 30% in our series described classical third window symptoms that are crucial for a diagnosis in an adult but seldom available from children. These include gaze evoked tinnitus or audible eye movements, conductive dysacusis, autophony, Hennebert's phenomenon or Tullio's phenomenon and pulsatile tinnitus. Many of these symptoms cannot be described by younger children, however, these symptoms if present will lead to some predictable behavior that can be picked up by parents. This observation raises an interesting point as apparent from the current descriptive study that a radiological diagnosis of semicircular canal dehiscence might not lead to a fully blown

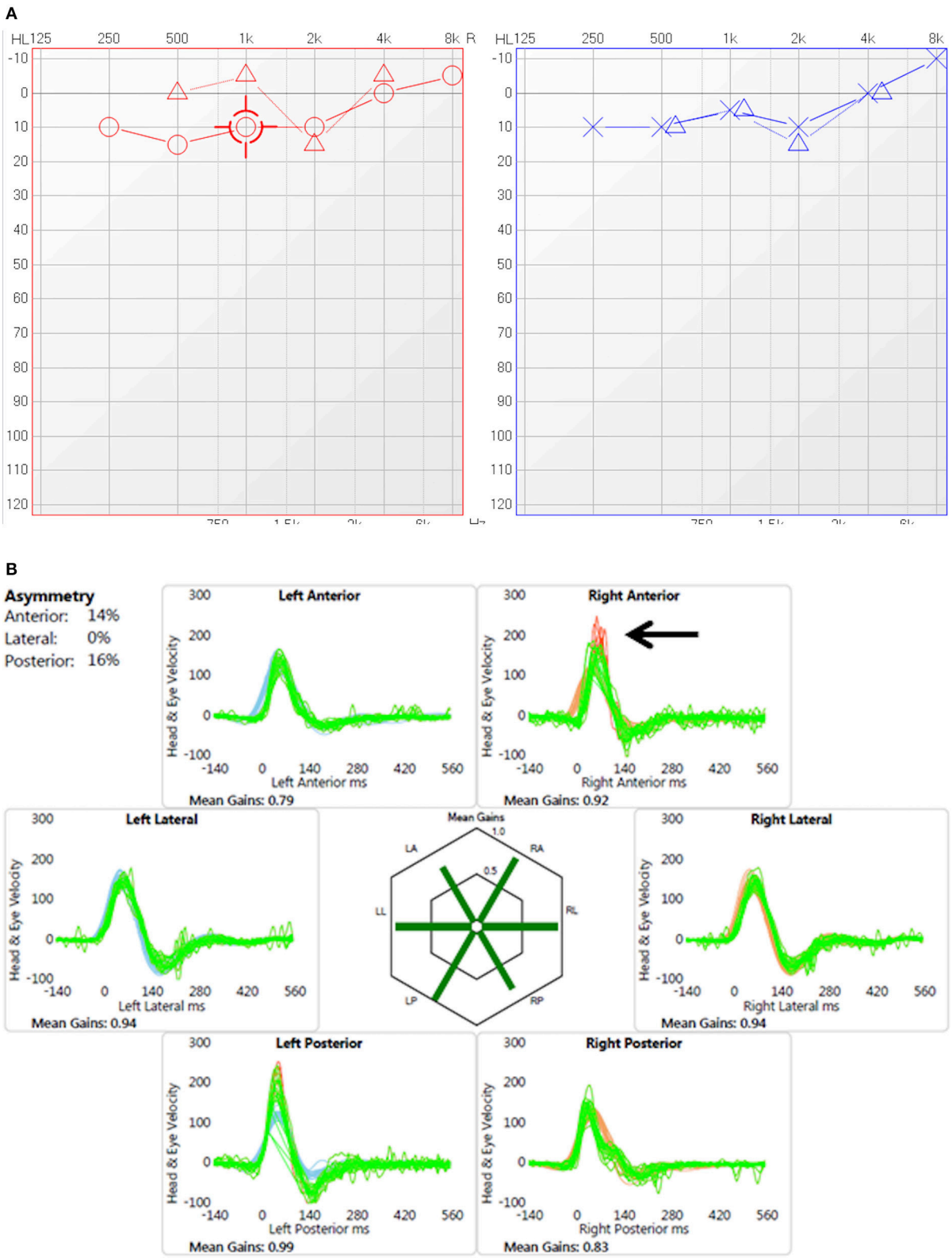

FIGURE 3 | Continued

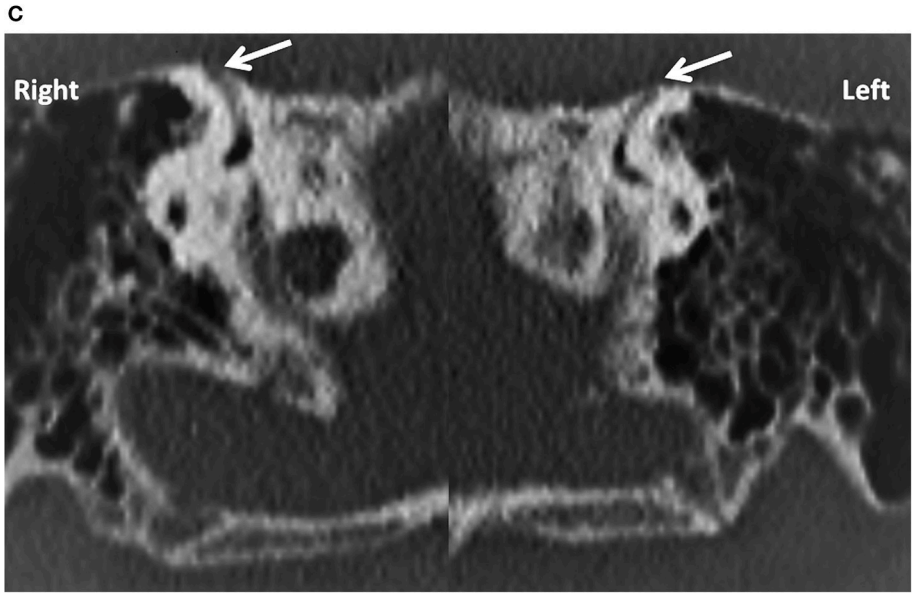

FIGURE 3 | (A) PTA in child presenting with conductive dysacusis (child 7). **(B)** Video head impulse test in a child with covert saccades in the right superior semicircular canal (arrow). **(C)** Coronal reconstruction of High resolution CT scan shows dehiscence of the superior semicircular canal on both sides (arrows).

semicircular canal dehiscence syndrome in children that has been well-defined in adults. As a result, the diagnosis of a semicircular canal dehiscence in children can be guided by a holistic picture rather by obtaining third window symptoms.

Tympanometry was normal in the majority of our children that virtually eliminated any middle ear disorder with normal otoscopy in our case series. The finer nuances of tympanometry in semicircular canal dehiscences were investigated in the adult population by Castelucci et al. (27) who measured interaural differences but overall, the peak compliance average was within normal limits. The majority of their subjects also demonstrated normal stapedial reflexes as this current series also observed. The only child who presented with flat tympanometry and reduced reflexes had middle ear disease in addition to a profound SNHL on one side.

The publication by Thabet (28) investigating the finer nuances of transient OAE in semicircular canal dehiscences indicated that by and large OAE tend to be preserved in semicircular canal dehiscences. The authors feel that objectively establishing normal middle ear and cochlear function is very important to suggest and make a case for an inner ear problem explaining a conductive and a mixed hearing loss as is frequently found in semicircular canal dehiscences. In frank cases of SNHL, the pathology itself can lead to cochlear dysfunction over riding the third window effect generating absent OAEs as found in 2 children in the current series. The child with the mixed loss and absent OAE very likely developed a cochlear element to his hearing loss due to the same reason. No other cause was detected to account for the hearing loss in these children after intense aetiological investigations as given earlier.

46.15% of children in the current case series presented with features of disequilibrium which is a hallmark in the adult population, but again it must be remembered that obtaining a proper history is often surrogate and dependent on observational behavior. In other series by Chen et al. (11), Lee et al. (12), and Kanaan et al. (16), this had been reported and the likely reason is that in children cerebral plasticity leads to good compensation precluding symptoms even in cases of vestibular deficit. Nevertheless, if there is a history of compromised balance, the possibility of a third window must be raised.

VNG examination with and without optic fixation, rotatory chair tests and vestibulo-spinal tests as well as mastoid vibration tests were normal in the majority of children in the current case series (76.9%) suggesting that gravitational sensor and static, low and mid frequency angular motion sensor vestibular function tend to be preserved in semicircular canal dehiscence in children. To our knowledge, the present study is the largest study to date to employ these tests in semicircular canal dehiscence in the pediatric population.

The video head impulse test since first described by MacDougal et al. (29) has revolutionized the diagnosis of high frequency semicircular canal vestibular function. Whilst extensive research in the adult population has been carried out and new observations are evolving, its use in the pediatric population has not been studied widely and in this respect its use in the diagnosis of semicircular canal dehiscence in children has not been studied at all except in one isolated case report by Wenzel (17). Similarly in the adult population, the evidence is extremely limited. The current series utilized this test routinely on the premise that semicircular canal dehiscence in children may lead to high frequency vestibular involvement as a result of aberrant endolymphatic fluid movement generated by the third window. Carey et al. (30) assessed passive head thrust

generated VOR gain with magnetic scleral coil search techniques in a group of patients with superior semicircular canal dehiscence in the preoperative and post-operative period. In the preoperative period, the VOR gain did not differ much from the normative data.

One important aspect to consider is the norms in the pediatric population due to the developing vestibular function. Wiener-Vacher and Wiener (31) published for the first time using the Synapsys system pediatric VOR gains in all 6 semicircular canals in the normal population and observed that although VOR gain increased as a function of age, their absolute numerical values are reasonably close to the adult population. However, a recent paper by Bachman et al. (19) suggested that whilst the VOR gain in the lateral semicircular canals match closely to those obtained in the adult population, the gain in the vertical canals can be distinctly lower in children. Bachman et al. (19) used the ICS Impulse system which is fundamentally different form the Synapsys system. This study utilized the ICS Impulse system and observed similar VOR gains as the Bachman study in a normal cohort (not a part of this audit). Saccades were considered as the most important indicator of vestibular dysfunction as Perez- Fernandez and Eva-Nunez (32) and Korsager et al. (18) had shown that saccades can be observed with normal VOR gain values during compensation that suggests persistent VOR deficits. Another important consideration is whether these saccades are artifactual or not which is a common problem to be encountered especially in the vertical canals (33). All the vHITs in the current study were analyzed and reviewed by the authors who are experienced clinicians and had performed over 800 vHITs in the pediatric population. They believe that just like an auditory brainstem response, vHITs need to be interpreted on an individual basis and correlated with the overall phenotype of the condition being investigated.

Replicable and repeatable saccades (consistently occurring multiple saccades up to 400 ms) were observed in 10 children (76.9%) whilst in 3 there were no discernible saccades. These saccades localized fairly accurately to the sides and the dehisced canals but with some exceptions. In 1 child with bilateral dehiscence, saccades localized to the lateral canal of one side only. In 1 child, they were observed in the left lateral semicircular canal for a left sided SSCD and in another child, in the right lateral semicircular canal for a right sided SSCD. Furthermore, in 2 children, they were observed in the right posterior semicircular canal for right SSCDs. In 1 child, the dehiscence was on the opposite side of an SNHL who had normal vHIT. Again, these outlying observations may suggest the variability of presentation of the condition. The saccades detected from vHIT in non-dehisced canals may be due to secondary effects generated by an aberrant endolymphatic fluid dynamics in response to the third window affecting the VOR. It is not known whether in the pediatric population, there could be a continuous damping effect of the VOR. Therefore, from this study, it appears that saccades may be important to assess high frequency vestibular function in semicircular canal dehiscences in children. This has not been reported before and indeed the authors feel that vHIT could be incorporated in the diagnostic process to take a decision whether to request HRCT for confirmation of diagnosis of a third window along with other clinical features.

The current series observed that measured hearing loss which is a functional measure and abnormalities in the video head impulse test which is an objective measure were present in a high percentage of children with semicircular canal dehiscences (76.9%). The majority of children with measured hearing losses complained of a functional deficit in hearing. However, only about 46.15% presented with functional deficits in balance in spite of an abnormal objective measurement. These observations suggest that semicircular dehiscences in children may tend to possess more functional hearing deficits than functional disequilibrium and the hearing loss may correlate to a measured objective balance deficit rather than a functional balance deficit.

The children in the current series did not undergo VEMPs to diagnose semicircular canal dehiscences as these tests were not available initially but were procured toward the end of the study period. It has been shown that otolith function may be enhanced in semicircular canal dehiscence (34) and measured by VEMPs. This remains an important tool for diagnosis of semicircular canal dehiscences to objectively confirm the third window effect in the adult population. However, in children, the evidence is still emerging. One of the difficulties in children is non-cooperation and achieving good muscle contraction for a robust response. As yet standardized norms derived from a sizeable population have not been published. It is likely that latencies and amplitudes will be less than in the adult population (35). Zhou et al. (36) studied VEMPS in children and observed that in inner ear structural abnormalities (for example enlarged vestibular aqueduct and semicircular canal dehiscences), VEMPs have lower thresholds and increased amplitude as one would expect in adults. However, it is not clear from this study as to what is defined by a structural inner ear abnormality. A structural inner ear abnormality is a vast entity and the authors did not mention as to how many of these actually had a third window.

VEMPs confirm the presence of a third window effect in the adult population that has been established (5). Ward et al. (5) in 2017 proposed the diagnostic criteria for third windows in adults that include high resolution CT confirmation and at least one third window feature enumerated previously and at least one of negative bone conduction thresholds in pure tone audiometry, enhanced VEMP responses and elevated summating potential to action potential ratio in electrocochleography in the absence of sensorineural hearing loss. Therefore, it can be noted that VEMPs in adults is one of the diagnostic criteria and not an obligatory one, although the paper mentioned that the authors believed that VEMPs are essential for diagnosis. In any case, VEMPs to demonstrate a third window effect in children may be required especially since children may not present with third window symptoms as discussed later.

Three children in the current case series presented with all 3 criteria—a negative bone conduction threshold, third window symptoms and a radiological evidence of semicircular

canal dehiscences. Two children with conductive hearing losses and radiological evidence of SSCD also demonstrated negative bone conduction thresholds. The majority of children with hearing losses do not fulfill the adult criteria nor do they present with third window symptoms, yet they demonstrate radiographic evidence of a dehiscence. As discussed earlier, a cochlear hearing loss can be a feature of semicircular dehiscences in children and this hearing loss can serve as a phenotype for the condition. The extensive study by Lagman et al. (37) analyzing data in existing literature pertaining to SSCD in children concluded that hearing loss was the commonest indication for performing a high resolution CT scan that showed SSCD; however, it must be noted that about 25% children in this analysis had other causes explaining the hearing loss. The current series is the first to exclude this comorbidity group by performing extensive investigation for hearing loss and also employed other features for example third window symptoms and disequilibrium and vestibular function tests as indicators for further imaging. These observations suggest that a radiologically demonstrated canal dehiscence may not result in a fully overt dehiscence syndrome in children.

The important difference between adults and children is the lack of third window symptoms that suggests that the pathophysiology of a semicircular canal dehiscence (not to be confused with a superior semicircular canal dehiscence syndrome) may differ from that in an adult. The reason for this could be attributed to the observation that endolymphatic movement in the child's ear and its response to the third window can be different as compared to an adult, a suggestion that can be gleaned from minor traumatic brain injuries in children (38). Therefore, the real effects of a third window in a pediatric population remain to be established. This in turn might influence VEMP findings in children with the condition.

As indicated earlier that high resolution CT may over diagnose the condition especially in children as normal otic capsule ossification follows a chronological pattern. Therefore, to decide whether a radiological diagnosis is indeed the cause for the clinical features that a child presents with is a matter of fine judgment and expertise. Thus, diagnosis of semicircular canal dehiscence in children must be guided by the whole clinical picture rather than by one investigation alone.

The results in this audit observed that a significant proportion of children with apparent radiological diagnosis of semicircular canal dehiscence may not fulfill all the diagnostic criteria for the condition as proposed in adults with the algorithm employed in the study. This is due to the absence of typical third window features. The CT scan findings can be incidental and not related to the phenotype. Hence it may be necessary to establish a third window effect if possible by objective means in children. This can be achieved by VEMPS and thus this audit leads to the recommendation that to investigate semicircular canal dehiscences in children further, other tests can add to the ones performed in the study to obtain a better idea about the condition in children. VEMPs in spite of its limitations in the pediatric population need to be explored to demonstrate this pathological third window effect in children who otherwise present without any third window features about which there is limited evidence. Furthermore, functional vestibular tests for example the functional head impulse test (39) and the gaze stabilization test (40) may be attempted to correlate a functional phenotype that is yet to be investigated in children. Demonstration of a third window effect has implications regarding operative intervention that is well-established in adults. In our experience, surgery is seldom required in children and they respond well to audiovestibular rehabilitation with amplification, customized vestibular rehabilitation and with cognitive behavioral therapy when needed.

There is a possibility that a dehiscence picked up in childhood may lead to frank third window features in the future, there is no way of predicting this in the absence of adequate evidence. Again, this could be due to bony remodeling. Consequently, these children and parents can be counseled to deal with emerging problems in the future. This underpins the holistic approach to pediatric medicine, it is not just invasive management or medical management but preparing the child from any eventuality in the wider sense. A robust transition plan will incorporate this information to inform adult services when the child graduates from pediatric to adult services.

The weaknesses of this study include a small sample size given the rarity of semicircular canal dehiscence in children and that this was a retrospective audit in the first instance. However, since the study group was assessed by the authors only, there was continuity of care thus eliminating one of the important biases of a retrospective study. There was consistency in the process and influence by confounding logistic variables were negligible as the analysis looked into a defined anatomical abnormality which is independent of any modification by these variables. This study did not pose any hypothetical research question and did not attempt to confirm statistically valid observations. This study presents a series of observations that became apparent on a retrospective case note review and draws conclusions that might lead to further research in diagnosing a rare pathology in children.

CONCLUSIONS

The pathological entity of semicircular canal dehsicences in children remains rare. High index of clinical suspicion to demonstrate the condition by dedicated imaging is suggested by good anamnesis, the presence of a conductive or a mixed hearing loss in the presence of normal middle ear and cochlear function and abnormal vestibular function tests. Sensorineural hearing loss may be a presenting feature. It observes that diagnosis of semicircular canal dehiscences in children depended on a number of functional and objective parameters. It does not suggest that any one test is best for diagnosis but rather provides an overview from a retrospective case note analysis that the phenotype in children is variable and diagnosis is a matter of clinical judgment. Furthermore, this study observes that an anatomical semicircular canal dehiscence might not present with

a frank semicircular canal dehiscence syndrome characterized by the constellation of symptoms well-described in adults.

DATA AVAILABILITY

All datasets generated for this study are included in the manuscript and/or the supplementary files.

AUTHOR CONTRIBUTIONS

SD and SR were the responsible clinicians for the children included in the case series. SD collated the data. SD and SR collaborated to write the manuscript and peer reviewed clinical findings and the manuscript drafts.

FUNDING

To be funded partly by department of Pediatric Audiology, Alder Hey Children's NHS Foundation Trust and partly by the contributing authors.

ACKNOWLEDGMENTS

We gratefully acknowledge the advice of Dr. Shivaram Avula, consultant pediatric head and neck radiologist, Alder Hey Children's NHS Foundation Trust; the audit department of Alder Hey NHS Foundations NHS Trust for registering this work and the assistance rendered to us by the department of Pediatric Audiology in the same hospital.

REFERENCES

1. Minor LB, Solomon D, Zinreich JS, Zee DS. Sound- and/or pressure-induced vertigo due to bone dehiscence of the superior semicircular canal. *Surgery*. (1998) 124:249–58.
2. Mau C, Kamal N, Badeti S, Reddy R, Ying YM, Jyung RW, et al. Superior semicircular canal dehiscence. Diagnosis and management. *J Clin Neurosci*. (2018) 48:58–65. doi: 10.1016/j.jocn.2017.11.019
3. Zhou G, Ohlms L, Liberman J, Amin M. Superior semicircular canal dehiscence in a young child: implication of developmental defect. *Int J Paediatr Otorhinolaryngol*. (2007) 71:1925–8. doi: 10.1016/j.ijporl.2007.08.009
4. Merchant SN, Rosowski JJ. Conductive hearing loss caused by third-window lesions of the inner ear. *Otol Neurotol*. (2008) 29:282–9. doi: 10.1097/MAO.0b013e318161ab24
5. Ward BK, Carey JP, Minor LB. Superior canal dehiscence syndrome: lessons from the first 20 years. *Front Neurol*. (2017) 8:177. doi: 10.3389/fneur.2017.00177
6. Jackson NM, Allen LM, Morell B, Carpenter CC, Givens VB, Kakade A, et al. The relationship of age and radiographic incidence of superior semicircular canal dehiscence in pediatric patients. *Otol Neurotol*. (2014) 36:99–105. doi: 10.1097/MAO.0000000000000660
7. Carey JP, Minor LB, Nager GT. Dehiscence or thinning of bone overlying the superior semicircular canal in a temporal bone survey. *Arch Otolaryngol Head Neck Surg*. (2000) 126:137–47. doi: 10.1001/archotol.126.2.137
8. Nadgir RN, Ozonoff A, Devaiah AK, Halderman AA, Sakai O. Superior semicircular canal dehiscence: congenital or acquired condition? *AJNR Am J Neuroradiol*. (2011) 32:947–9. doi: 10.3174/ajnr.A2437
9. Williamson RA, Vrabec JT, Coker NJ, Sandlin M. Coronal computed tomography prevalence of superior semicircular canal dehiscence. *Otolaryngol Head Neck Surg*. (2003) 129:481–9. doi: 10.1016/S0194-5998(03)01391-3
10. Zhou G, Gopen Q, Poe DS. Clinical and diagnostic characterisation of canal dehiscence syndrome: a great otologic mimicker. *Otol Neurotol*. (2007) 28:920–26. doi: 10.1097/MAO.0b013e31814b25f2
11. Chen EY, Paladin A, Phillips G, Raske M, Vega L, Peterson D, et al. Semicircular canal dehiscence in the paediatric population. *Int J Paediatr Otorhinolaryngol*. (2009) 73:321–7. doi: 10.1016/j.ijporl.2008.10.027
12. Lee GS, Zhou G, Poe D, Kenna M, Amin M, Ohlms L, et al. Clinical experience in diagnosis and management of superior semicircular canal dehiscence in children. *Laryngoscope*. (2011) 121:2256–61. doi: 10.1002/lary.22134
13. Meiklejohn DA, Corrales CE, Boldt BM, Sharon JD, Yeom KW, Carey JP, et al. Pediatric semicircular canal dehiscence: radiographic and histologic prevalence, with clinical correlation. *Otol Neurotol*. (2015) 36:1383–9. doi: 10.1097/MAO.0000000000000811
14. Sugihara EM, Babu SC, Kitsko DJ, Haupert MS, Thottam PJ. Incidence of paediatric superior semi-circular dehiscenceand inner ear anomalies: a large multicentre review. *Otol Neurotol*. (2016. 37:1370–5. doi: 10.1097/MAO.0000000000001194
15. Hagiwara M, Shaikh JA, Fang Y, Fatterpekar G, Roehm PC. Prevalence of radiographic semicircular canal dehiscence in very young children: an evaluation using high-resolution computed tomography of the temporal bones. *Pediatr Radiol*. (2012) 42:1456–64. doi: 10.1007/s00247-012-2489-9
16. Kanaan AA, Raad RA, Hourani RG, Zaytoun GM. Bilateral superior semicircular canal dehiscence in a child with sensorineural hearing loss and vestibular symptoms. *Int J Paediatr Otorhinolaryngol*. (2011) 75:877–9. doi: 10.1016/j.ijporl.2011.03.019
17. Wenzel A, Stuck BA, Servais JJ, Hörmann K, Hülse M, Hülse R. Superior canal dehiscence syndrome in children – A case report. *Int J Paediatr Otorhinolaryngol*. (2015) 79:1573–8. doi: 10.1016/j.ijporl.2015.05.022
18. Korsager LE, Faber CE, Schmidt JH, Wanscher JH. Refixation saccades with normal gain values: a diagnostic problem in the video head impulse test: a case report. *Front Neurol*. (2017) 8:81. doi 10.3389/fneur.2017.00081
19. Bachmann K, Sipos K, Lavender V, Hunter LL. Video head impulse testing in a pediatric population: normative findings. *J Am Acad Audiol*. (2018) 29:417–26. doi: 10.3766/jaaa.17076
20. The British Association of Audiovestibular, Physicians. *2015-2018. Guidelines and Clinical Standards*. (2019). Available online at: https://www.baap.org.uk/uploads/1/1/9/7/119752718/guideline_progressive_hl_final.pdf.
21. Saxby AJ, Gowdy C, Fandi-o M, Chadha NK, Kozak FK, Sargent MA, et al. Radiological prevalence of superior and posterior semi-circular canal dehiscence in children. *Int J Paediatr Otorhinolaryngol*. (2015) 79:411–8. doi: 10.1016/j.ijporl.2015.01.001
22. Sanverdi SE, Ozgen B, Dolgun A, Sarac S. Incomplete endochondral ossification of the otic capsule, a variation in children: evaluation of its prevalence and extent in children with and without sensorineural hearing loss. *AJNR Am J Neuroradiol*. (2015) 36:171–5. doi: 10.3174/ajnr.A4128
23. Gopen Q, Zhou G, Poe D, Kenna M, Jones D. Posterior semicircular canal dehiscence: first reported case series. *Otol Neurotol*. (2010) 31:339–44. doi: 10.1097/MAO.0b013e3181be65a4
24. Patel NS, Hunter JB, O'Connell BP, Bertrand NM, Wanna GB, Carlson ML. Risk of progressive hearing loss in untreated superior semicircular canal dehiscence. *Laryngoscope*. (2017) 127:1181–6. doi: 10.1002/lary.26322
25. Teixeira ED, Fonseca MT. Superior semicircular canal dehiscence without vestibular symptoms. *Int Arch Otorhinolaryngol*. (2014) 18:210–2. doi: 10.1055/s-0033-1351670
26. Merchant SN, Rosowski JJ, McKenna MJ. Superior semcircualr canal dehiscence mimicking otosclerotic hearing loss. *Adv Otorhinolaryngol*. (2007) 65:137–45. doi: 10.1159/000098790
27. Castellucci A, Brandolini C, Piras G, Modugno GC. Tympanometric findings in superior semicircular canal dehiscence syndrome. *Acta Otorhinolaryngol Ital*. (2013) 33:112–20.
28. Thabet EM. Transient evoked otoacoustic emissions in superior canal dehiscence syndrome. *Eur Arch Otorhinolaryngol*. (2011) 268:137–41. doi: 10.1007/s00405-010-1313-0

29. MacDougall HG, Weber KP, McGarvie LA, Halmagyi GM, Curthoys IS. The video head impulse test: diagnostic accuracy in peripheral vestibulopathy. *Neurology*. (2009) 73:1134–41. doi: 10.1212/WNL.0b013e3181bacf85
30. Carey JP, Migliaccio AA, Minor LB. Semicircular canal function before and after surgery for superior semicircular canal dehiscence. *Otol Neurotol*. (2007) 28:356–64. doi: 10.1097/01.mao.0000253284.40995.d8
31. Wiener-Vacher SR, Wiener SI. Video head impulse tests with a remote camera system: normative values of semicircular canal vestibulo-ocular reflex gain in infants and children. *Front Neurol*. (2017) 8:434. doi: 10.3389/fneur.2017.00434
32. Perez-Fernandez N, Eza-Nu-ez P. Normal gain of VOR with refixation saccades in patients with unilateral vestibulopathy. *J Int Adv Otol*. (2015) 11:133–7. doi: 10.5152/iao.2015.1087
33. Halmyagi GM, Chen L, MacDougall HG, Weber KP, McGarvie LA, Curthoys IS. The video head impulse test. *Front Neurol*. (2017) 8:258. doi: 10.3389/fneur.2017.00258
34. Manzari L, Burgess AM, MacDougall HG, Curthoys IS. Enhanced otolithic function in semicircular canal dehiscence. *Acta Oto Laryngol*. (2010) 131:107–12. doi: 10.3109/00016489.2010.507780
35. El-Danasoury I, El Sirafy G, Taha H, Hegazy S. Vestibular evoked myogenic potentials (VEMPS) in young children: test parameters and normative data. *Egypt J Ear Nose Throat Allied Sci*. (2015) 16:81–5. doi: 10.1016/j.ejenta.2014.09.002
36. Zhou G, Dargie J, Dornan B, Whittemore K. Clinical uses of cervical vestibular-evoked myogenic potential testing in pediatric patients. *Medicine*. (2014) 93:e37. doi: 10.1097/MD.0000000000000037
37. Lagman C, Ong V, Chung LK, Elhajjmoussa L, Fong C, Wang AC, et al. Paediatric superior semicircular canal dehiscence: illustrative case and systemic review. *J Neurosurg Paediatr*. (2017) 20:196–203. doi: 10.3171/2017.3.PEDS1734
38. Figaji AA. Anatomical and physiological differences between children and adults relevant to traumatic brain injury and the implications for clinical assessment and care. *Front Neurol*. (2017) 8:685. doi: 10.3389/fneur.2017.00685
39. Corallo G, Versino M, Mandalà M, Colnaghi S, Ramat S. The functional head impulse test: preliminary data. *J Neurol*. (2018) 265(Suppl. 1):35. doi: 10.1007/s00415-018-8910-z
40. Ward BK, Mohammed MT, Brach JS, Studenski SA, Whitney SL, Furman JM. Physical performance and a test of gaze stabilization in older adults. *Otol Neurotol*. (2010) 31:168–72. doi: 10.1097/MAO.0b013e3181c4c3e2

Conflict of Interest Statement: The authors declare that the research was conducted in the absence of any commercial or financial relationships that could be construed as a potential conflict of interest.

frontiers in Neurology

ORIGINAL RESEARCH
published: 09 April 2019
doi: 10.3389/fneur.2019.00321

Vestibulo-Ocular Responses and Dynamic Visual Acuity During Horizontal Rotation and Translation

Cecilia Ramaioli[1,2,3*†], *Luigi F. Cuturi*[4*†], *Stefano Ramat*[5], *Nadine Lehnen*[1,2,3] *and Paul R. MacNeilage*[6]

[1] German Center for Vertigo and Balance Disorders, University Hospital Munich, Munich, Germany, [2] Institute of Medical Technology, Brandenburg University of Technology Cottbus-Senftenberg, Senftenberg, Germany, [3] Department of Psychosomatic Medicine and Psychotherapy, Klinikum Rechts der Isar, Technical University of Munich, Munich, Germany, [4] Unit for Visually Impaired People, Italian Institute of Technology, Genoa, Italy, [5] Department of Electrical, Computer and Biomedical Engineering, University of Pavia, Pavia, Italy, [6] Department of Psychology, Cognitive and Brain Sciences, University of Nevada, Reno, NV, United States

Dynamic visual acuity (DVA) provides an overall functional measure of visual stabilization performance that depends on the vestibulo-ocular reflex (VOR), but also on other processes, including catch-up saccades and likely visual motion processing. Capturing the efficiency of gaze stabilization against head movement as a whole, it is potentially valuable in the clinical context where assessment of overall patient performance provides an important indication of factors impacting patient participation and quality of life. DVA during head rotation (rDVA) has been assessed previously, but to our knowledge, DVA during horizontal translation (tDVA) has not been measured. tDVA can provide a valuable measure of how otolith, rather than canal, function impacts visual acuity. In addition, comparison of DVA during rotation and translation can shed light on whether common factors are limiting DVA performance in both cases. We therefore measured and compared DVA during both passive head rotations (head impulse test) and translations in the same set of healthy subjects ($n = 7$). In addition to DVA, we computed average VOR gain and retinal slip within and across subjects. We observed that during translation, VOR gain was reduced (VOR during rotation, mean ± SD: position gain = 1.05 ± 0.04, velocity gain = 0.97 ± 0.07; VOR during translation, mean ± SD: position gain = 0.21 ± 0.08, velocity gain = 0.51 ± 0.16), retinal slip was increased, and tDVA was worse than during rotation (average rDVA = 0.32 ± 0.15 logMAR; average tDVA = 0.56 ± 0.09 logMAR, $p = 0.02$). This suggests that reduced VOR gain leads to worse tDVA, as expected. We conclude with speculation about non-oculomotor factors that could vary across individuals and affect performance similarly during both rotation and translation.

Keywords: vestibular system, vestibular ocular reflex, oculomotor, dynamic visual acuity (DVA), otoliths, semicircular canal, retinal slip, eye movements

OPEN ACCESS

Edited by:
Joel Alan Goebel, Washington University in St. Louis, United States

Reviewed by:
Bryan Kevin Ward, Johns Hopkins University, United States
Christopher Bockisch, University of Zurich, Switzerland

***Correspondence:**
Cecilia Ramaioli
cecilia.ramaioli@lrz.uni-muenchen.de
Luigi F. Cuturi
Luigi.cuturi@iit.it

†These authors have contributed equally to this work

Specialty section:
This article was submitted to Neuro-Otology, a section of the journal Frontiers in Neurology

Received: *31 October 2018*
Accepted: *14 March 2019*
Published: *09 April 2019*

Citation:
Ramaioli C, Cuturi LF, Ramat S, Lehnen N and MacNeilage PR (2019) Vestibulo-Ocular Responses and Dynamic Visual Acuity During Horizontal Rotation and Translation. Front. Neurol. 10:321. doi: 10.3389/fneur.2019.00321

INTRODUCTION

During natural movements, head perturbations have both translational and rotational components. In order to compensate for such movements and to maintain a stable image on the retina, the central nervous system (CNS) generates compensatory movements, most notably driven by the vestibulo-ocular reflex (VOR). Depending on the type of head movement, two kinds

of VOR are distinguished: the rotational VOR– in response to angular motion sensed by the semicircular canals (SCCs)—and the translational VOR– in response to linear motion sensed by otoliths.

The rotational VOR (rVOR) has been extensively studied. Performance is typically quantified by applying passive rotational head movements [as in the head-impulse test—HIT (1)], measuring eye and head velocity and computing the ratio of the two, which is referred to as the gain. The need for a precise and reliable measure of the oculomotor responses led to the use of video-oculography through head mounted cameras to record eye movements during the HIT (2, 3). Typical movement profiles have a frequency content in the order of 5–7 Hz, characterized by small amplitudes (10°-20°) and peak accelerations of 2,000–7,000°/s^2 (2, 4). Gain is most often computed during the first 100 ms following movement onset to ensure that responses are driven by vestibular input only. Visually-driven eye movements have a latency of more than ∼100 ms, while vestibularly-driven ones have a latency of <10 ms (1, 5). Gains near one are expected in normal subjects; the threshold for clinical diagnosis of pathological VOR response is gain <0.79 (3, 5, 6).

The translational VOR (tVOR) has been much less studied, in part because it can be difficult to administer well-controlled and repeatable passive translation stimuli. Past research has investigated tVOR in response to both horizontal (7–9), and vertical (10–12) translations. Typical movement profiles contain frequencies in the order of 1.5–2 Hz, with peak velocities and accelerations of 25–40 cm/s and 0.7–1 g. As with rVOR, gain is most often computed during the first 100 ms following movement onset to ensure that responses are driven by vestibular input only. Unlike the rVOR, viewing geometry dictates that larger eye movements are needed to stabilize near compared to far images during translational movement, implying that only images lying at the same viewing distance can be stabilized with a single eye movement. Compensation for linear head motion is incomplete, with reported gains between 0.1 and 0.63 with near viewing distances (8, 13). The reason why compensation is incomplete is still a matter of debate. Although linear movements pose less of a threat to stabilization for viewing distances above about 1 m, because of the mentioned inverse relationship with movement amplitude required for stabilization, published results have shown that the gain remains under-compensatory and roughly constant with different viewing distances, hinting that the compensated amount represents a choice of the CNS (7, 8), and not a limitation of the tVOR. In fact, one possible explanation for this finding is that the goal of the tVOR might not be that of stabilizing a single target of interest, but to minimize retinal image motion between objects lying in different depth planes in order to optimize motion parallax information (11, 12).

In addition to quantifying VOR gain, functional visual stabilization performance can be assessed by other techniques, such as measuring dynamic visual acuity (DVA), i.e., the ability to discern fine details of the visual image (14) during both active (15, 16) and passive (17, 18) head motion and different types of visual stimuli (18, 19). Passive head motion is however more informative in the detection of a vestibular dysfunction, as predictive strategies are not available (20, 21). Two further techniques have been proposed for such functional vestibular testing over the last 10 years: the gaze stabilization test (GST) (22, 23) and the functional head impulse test (fHIT) (24–26). All three are based on requiring the patient to identify an optotype displayed on a computer screen during head rotations, yet they differ in terms of visual stimulus triggering criteria and outcome measure: a change in visual acuity measure (logMAR) for the DVA test, the maximum head velocity that does not reduce visual acuity for the GST, the percentage of correctly identified optotypes during head rotations within a range of head angular accelerations for the fHIT. In contrast with VOR gain, functional testing provides a measure of the overall effectiveness of stabilization performance, including not only VOR but also catch-up saccades and other visually-driven responses. Thus, functional testing approaches can provide a clinically valuable measure of overall functional impairment (24, 25, 27–29).

Recent studies have assessed and compared VOR gain and HITD-FT (or functional head impulse test, fHIT) in response to head rotations (30, 31). Administration of opioids led to a decrease in VOR gain and also a decrease in the percentage of correctly identified targets (%CA) during HITD-FT, such that response gain and %CA were significantly correlated (30), yet no correlation was found in a group of patients with vestibular neuritis both on the affected and on the healthy side (29). It was also observed that catch-up saccades performed while the visual target was still present likely led to better reading performance (30, 31) and to better DVA (32).

To our knowledge, no prior study has examined both VOR and DVA in response to pure linear, passive horizontal head movement. The current study therefore aimed to address this gap by measuring both VOR and DVA in response to linear horizontal head movement and comparing these with measures of VOR and DVA during angular head movement in a single group of subjects. We expected to replicate prior findings that VOR gain is reduced during translation compared to rotation, and we expected that reduced gain should lead to DVA that is worse during translation compared to rotation. We also aimed to test the hypothesis that linear and angular measures of VOR and DVA are correlated with one another, which would suggest that performance in response to both linear and angular movements are affected by common factors or mechanisms that are not necessarily vestibular in origin (e.g., visual or perceptual mechanisms).

MATERIALS AND METHODS

Subjects

Seven healthy subjects (4 males), aged 27–41 years (median 33 years) participated in the study. They reported no history of neurological, neuro-otological, or neuro-ophthalmological disorders. Six subjects had normal vision, one subject had vision corrected to normal via glasses. In case subjects normally wore glasses, they performed the task without them because of set-up constraints both for the DVA and the static visual acuity, the latter measured prior to the test (see further in this section). The experimental procedure was approved by the Ethics Committee of the Medical Faculty of the Ludwig-Maximilians-University

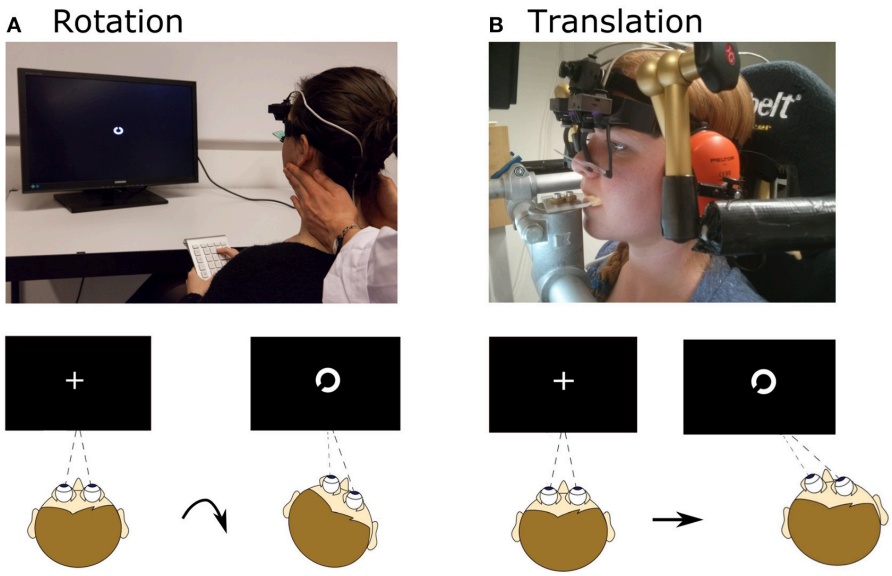

FIGURE 1 | Setup for rotational and translational VOR and DVA assessment. **(A)** Head rotation was induced by a trained experimenter manually rotating the head, as during a clinical head-impulse test. Subjects fixated a fixation point, which changed to a Landolt ring ∼72 ms after movement onset and displayed for ∼68 ms. After the movement subjects judged the orientation of the ring. **(B)** Translational movements were applied using a six-degree-of-freedom motion platform. The head was fixated with respect to the platform via bite bar and stabilizing braces over the ears. As for rotation, a Landolt ring appeared ∼75 ms after movement onset and was displayed for ∼49 ms; subjects judged its orientation. Written informed consent was obtained from the individual for the publication of the image represented in the figure.

and in accordance with the Declaration of Helsinki. All gave their informed consent prior to participation and were free to withdraw from the experiment at any time.

Experimental Procedure: Rotational VOR and DVA

First, the static visual acuity (SVA) was assessed. To this end, subjects were asked to identify 20 fixed sequential visual stimuli displayed on a monitor (size 60 × 53 cm, resolution 1,280 × 800 pixels, refresh rate 75 Hz) connected to the measuring laptop and situated 2 m in front of them, without moving their head. This procedure provided a baseline measure of subjects' visual acuity. The visual stimulus consisted of a Landolt ring with eight possible gap positions at 45° increments. As described in Colagiorgio et al. (33), subjects had to identify the position of the gap and provide answers using an external computer keypad consisting of buttons for each gap position and a special button if they had low confidence in their answer in order to further reduce the possibility of random correct answers. The size of the stimulus was adjusted depending on the subject's error rate, according to the QUEST algorithm (34) performed with the head still, starting from a value of 1 logMAR and estimating subject's acuity threshold in 20 trials, in analogy to the test performed in Colagiorgio et al. (33) to assess SVA.

Rotational VOR (rVOR) and DVA were then assessed (**Figure 1A**). An experienced examiner standing behind the subject performed at least 40 passive, rapid (6.4 ± 1.5 Hz), high-acceleration (3,300–4,000°/s^2 peak), and small amplitude (14°-24°) head rotations to the left and to the right (**Figure 2**, top) in the plane of the horizontal semicircular canals [standard clinical head-impulses (1)]. The impulses, at least 20 to the right, and at least 20 to the left, were delivered with random timing and direction, to prevent anticipatory compensatory movements. Display of the visual stimulus was triggered when head angular acceleration (as measured by the gyroscope integrated in the eye tracker) exceeded 300°/s^2, otherwise the trial was repeated. The actual timing of the visual stimulus was documented with a photodiode taped to the monitor (33). A fixation cross appeared prior to every rotation in the center of the screen. The visual stimulus was programmed to last 80 ms and it appeared on the screen on average 72 ± 2 ms (mean ± SD) after head movement start (defined as head velocity reaching 20°/s) as recorded with the photodiode. The visual stimulus remained on for 68 ± 3 ms (mean ± SD).

During all testing procedures, eye and head movements were recorded by monocular video-oculography on the left eye and integrated six-degrees-of-freedom inertial sensors [EyeSeeCam system, (2)]. Prior to each testing, calibration of the system was performed following its standard procedure using a laser-projected target grid at 1.5 m viewing distance (6). Sampling rate was 220 Hz.

Experimental Procedure: Translational VOR and DVA

Translational movements were applied using a six-degree-of-freedom motion platform (Moog© 6DOF2000E). Subjects were seated in a padded racing seat mounted on the platform. In order to guarantee only linear translations in the horizontal

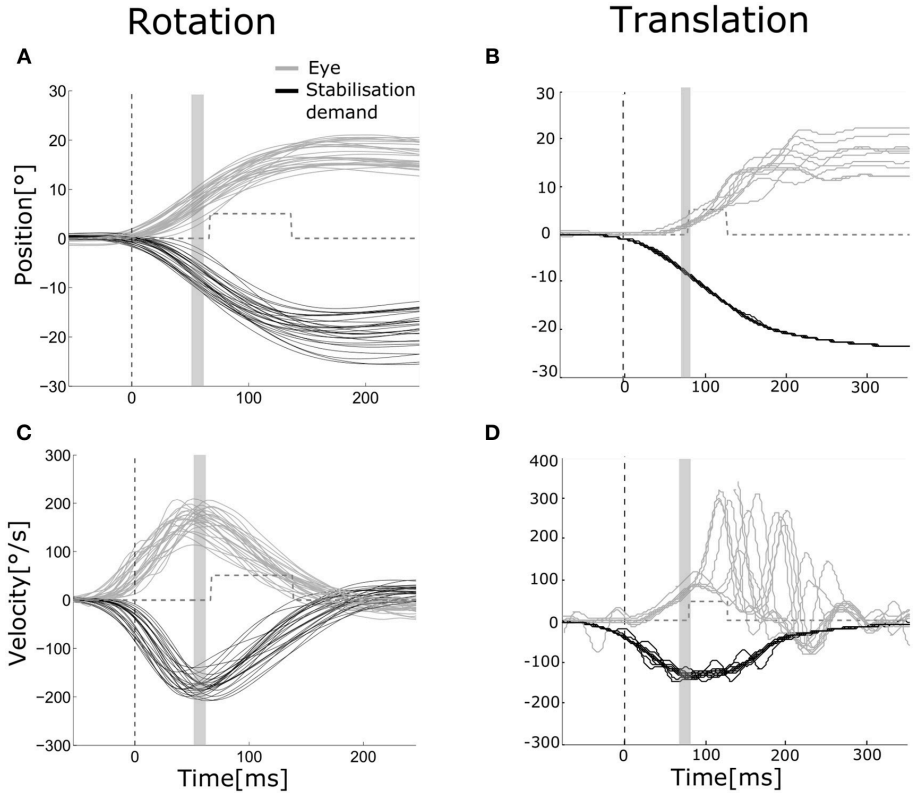

FIGURE 2 | Eye and head movements during rotation and translation Eye movement (gray) plotted vs. stabilization demand (black) for a representative subject during rotation [**(A,C)** head and eye movements to the left and to the right pooled, left eye] and translation [**(B,D)** movements to the right, right eye]. Position **(A,B)** and velocity **(C,D)** traces are aligned to stimulus presentation beginning. The dashed vertical line indicates the mean head movement start. The gray area indicates the time interval over which position and velocity gains of the VOR were computed (55–65 ms after movement onset). The gray dashed line shows the mean time interval when the visual stimulus was turned on to assess dynamic visual acuity.

plane during the assessment of the DVA, the subject's head was stabilized by means of a bite bar and passive noise canceling headphones connected through mechanical arms to metal poles fixed onto the motion platform (**Figure 1B**).

Subjects first performed calibration of the system and SVA assessment as previously described. Visual stimuli were projected on a screen (size 45 × 35 cm, resolution 1,400 × 1,500 pixels, refresh rate 75 Hz) located 15 cm in front of subjects' eyes. The screen was mounted to the platform, but the projector (Acer P5403) was mounted to the wall and therefore rendered an earth-fixed visual stimulus. Distance from projector to screen was 73 cm.

After the SVA was completed the translational protocol was performed. Each horizontal linear translation lasted 0.5 s and followed a Gaussian speed profile characterized by a displacement of 8 cm, peak velocity of 0.7 m/s and peak acceleration of 1.3 g (**Figure 2**, bottom). The delivery of translations, at least 20 toward the left (L) and at least 20 toward the right (R), was computerized with pseudorandom timing and direction, to prevent anticipatory compensatory movements. Onset of the visual stimulus was delayed by a fixed duration relative to the command to move the platform. The actual onset of the visual stimulus was documented with a photodiode taped to the screen as previously described. Onset was 75 ± 5 ms (mean ± SD) after platform movement start (defined as platform displacement of 3 mm from its starting position). A fixation cross appeared prior to every translation, to help subjects maintain the correct vergence angle. In the translation experiment, differently from the rotation experiment, and due to setup constraints, the visual target was projected on a screen (screen size 45 × 35 cm). The projector (Acer P5403, resolution 1,400 × 1,500 pixels, refresh rate 75 Hz) was mounted to the wall and connected to the measuring laptop. As in the rotational experiment, during translations the visual stimulus was programmed to last 80 ms and lasted on average 49 ± 2 ms, likely because of differences in the setup between the two experiments (e.g., the image was presented on a projection screen while in the rotation experiment was presented on a monitor). The difference of stimulus duration between rotations and translations is significantly different (paired *t*-test, $p < 0.001$). Eye and head movements were recorded by binocular video-oculography and integrated six-degrees-of-freedom inertial sensors [EyeSeeCam system, (2)]. Sampling rate was 220 Hz. Platform and head position was also recorded by an optical tracking system at 117 Hz (Optitrack S250e cameras and Motive software).

Data Analysis

For the rotation experiment, head angular velocity was derived from the sensors mounted on the EyeSeeCam system (2). Eye and head velocity (**Figure 2**, top) were processed as in Ramaioli et al. (30): eye velocity was filtered with a third order low-pass digital Butterworth filter with a cut-off frequency of 40 Hz, while head velocity was filtered by a second order zero-phase low-pass digital Butterworth filter with 30 Hz cut-off frequency. Eye and head position were computed from velocities. Head impulse start and end were automatically detected when head velocity first reached 20°/s and when it crossed zero again. Impulses with peak velocity slower than 80°/s were discarded. In addition, traces deemed noisy based on visual inspection were also discarded (manual correction). On average, 18 ± 3 head impulses were included in the rVOR analysis for each side. Position gain of the rVOR was computed by taking the median of eye and head positions in a window between 55 and 65 ms after head impulse start, and then taking the ratio of these median values. Velocity gain was computed using the same procedure applied to the velocity traces.

For the translation experiment, trial onset was defined as the moment when the motion platform had moved 3 mm away from its starting position, according to the optical tracking data. Stabilization demand for each trial (**Figure 2**, bottom) was computed based on viewing distance (v), inter-pupillary distance (ipd), and platform displacement (d) as *atan((–d± ipd/2)/v)* and was used to compute the gain of the tVOR as recorded/ideal eye movement (9). This calculation assumes that the platform displacement corresponds to head displacement, i.e., that the head was fixed with respect to the platform. The validity of this assumption was verified by measuring and comparing both head and platform movement. This analysis showed that measures taken to stabilize the head (bite bar and ear cups) were effective, resulting in only small rotations (∼2°) of the head relative to the platform. Eye position was filtered with a second order low-pass digital Butterworth filter with a cut-off frequency of 20 Hz. Eye position and stabilization demand were set to zero at the beginning of each trial, with possibility for manually discarding trials showing artifacts or re-fixation saccades in the first 90 ms after movement onset, as they could affect gain calculation. For each eye and direction of movement, 12 ± 3 trials were then considered. Velocities were derived from position traces. Position and velocity gain were computed as described above using data in a time window between 55 and 65 ms after movement onset. Gains were computed separately for the right and the left eye.

During translations, tVOR gain was often low and often catch-up or re-fixation saccades were triggered. Eye movements with an acceleration higher than 2,000°/s^2 were considered to be re-fixation saccades: saccade onset was defined when acceleration reached 2,000°/s^2, while saccade offset was defined with acceleration threshold of −2,000°/s^2. The primary measure of interest was the latency of the first re-fixation saccade after movement onset, because shorter latencies had been suggested to result in better functional performance when VOR gain is reduced (30, 35, 36).

TABLE 1 | SVA, rDVA, and tDVA data.

Subject ID	SVA (rotation)	SVA (translation)	rDVA right	rDVA left	tDVA right	tDVA left
s01	0.00	0.00	0.46	0.49	0.22	0.72
s02	0.00	0.00	0.56	0.46	0.59	0.55
s03	0.06	0.00	0.3	0.36	0.33	0.77
s04	0.00	0.00	0.22	0.36	0.34	0.69
s05	0.00	0.00	0.41	0.29	0.65	0.40
s06	0.63	0.00	0.17	0.09	0.59	0.91
s07	0.03	0.00	0	0.26	0.55	0.59

Rotation SVA and rDVA were taken with a monitor 2 m away from the subject. Translation SVA and tDVA were taken with a projection screen 15 cm away from the subject. Subject s06 is nearsighted and usually wears glasses as shown by the different SVA values for rotation and translation; however, they did not wear glasses during both SVA and DVA assessment.

Visual acuity in static (SVA) and dynamic (DVA) condition is tested requiring the subject to identify the orientation of a sequence of 20 Landolt rings. The size of the ring (and its gap) is scaled in accordance to the size and resolution of the screen, and to the subject's viewing distance to correspond to a Sloan eye chart. During testing the optotype size is reduced depending on the subject rate of incorrect answers using the QUEST adaptive algorithm, implemented in the Psychtoolbox. The algorithm starts with a value of 1 logMAR and estimates the subject's visual acuity threshold expressed in units of in logMAR in 20 trials. DVA was calculated as the difference between the threshold value given by the adaptive procedure and the SVA value and was computed separately for rotations to the right and to the left, and for translations to the right and to the left (see **Table 1**).

In addition, to examine how VOR gain could impact DVA, we also computed maximum gaze (i.e., head + eye) position and velocity during presentation of the visual stimulus. If this position and velocity are close to zero, the target should be near the fovea and relatively still on the retina, resulting in better acuity. If the target is far from the fovea and moving on the retina, even only a few degrees per seconds, DVA should be impaired and vision deteriorates (37, 38).

All analyses were performed offline using custom MATLAB software (MathWorks, Natick, MA).

Statistical Analysis

Differences in position and velocity gains during rotations to the right and left were assessed using a *t*-test with significance level of 0.05 (normal distribution verified by Shapiro-Wilk Test). The same procedure was applied to assess differences between gains of the right and left eye during translations to the left and to the right as well as differences in DVA depending on movement direction. As there were no significant differences, data were pooled across eyes and movement directions for all measures and test conditions.

Correlation analysis was performed across both rotational and translational measurements between DVA and all gain and slip measures.

RESULTS

Examples of eye movements in response to both rotation and translation are shown in **Figure 2**. The healthy rVOR (**Figure 2**, left) drives the eye to compensate almost perfectly for the imposed head rotation. Position and velocity gain computed during the time window ∼70 ms after movement onset (shown by the gray bar) are very near unity (position gain 1.07 ± 0.07, velocity gain 0.95 ± 0.09). Thanks to this compensation, the subject could correctly identify the visual stimulus when it was present (gray dashed line), achieving an rDVA of 0.29 logMAR (left rotations 0.36, right rotations 0.22), compared to an SVA of 0 logMAR. Data for all subjects regarding rDVA and tDVA as well as SVA are reported in **Table 1**.

In contrast, eye positions and velocities during translations were insufficient to compensate for head movement. For the example subject shown in **Figure 2** (right), position gain pooled across eyes and movement directions was 0.23 ± 0.07 and velocity gain was 0.42 ± 0.12. This decreased gain was associated with reduced tDVA during translation of 0.47 logMAR (0.22 to the right, 0.72 to the left) compared to an SVA of 0 logMAR.

Similar behavior and performance was observed in all seven subjects. Both position gain (**Figure 3A**) and velocity gain (**Figure 3B**) were significantly greater during rotation than during translation (paired *t*-test, $p < 0.001$). Mean position gain was 1.05 ± 0.04 during rotation and 0.21 ± 0.08 during translation. Mean velocity gain was 0.97 ± 0.07 during rotation and 0.51 ± 0.16 during translation. The insufficiency of ocular responses during translation is captured by the shortfall relative to a gain of 1 (i.e., 1 minus gain) which is plotted in the inset of **Figures 3A,B**.

Reduced VOR gains indicate incomplete compensation for head motion and this should be associated with increased retinal slip and worse DVA scores. To examine this relationship more closely, we computed maximum gaze position (i.e., target position relative to the fovea) and velocity (i.e., target velocity on the retina) as the sum of head and eye position and, respectively, head and eye velocity during acuity target presentation. Position error (**Figure 3D**) and slip velocity (**Figure 3E**) differed significantly between rotation and translation (position error, $p = 0.001$; slip velocity $p = 0.03$). They were close to zero during rotation but deviated substantially during translation, with negative values indicating slip due to insufficient ocular compensation. To capture this insufficiency, we plot shortfall in slip compensation (slip times minus 1) in the insets of **Figures 3D,E**. Measures of slip and gain during rotation and translation were not significantly correlated.

These differences in gain and slip were accompanied by differences in DVA (**Figure 3C**). The minimum angle of resolution was significantly higher during translation (0.56 ± 0.09 logMAR) than during rotation (0.32 ± 0.15 logMAR) ($p = 0.02$), indicating that the ability to recognize the orientation of the optotype was worse during translations in comparison to rotations. Measures of DVA during rotation and translation

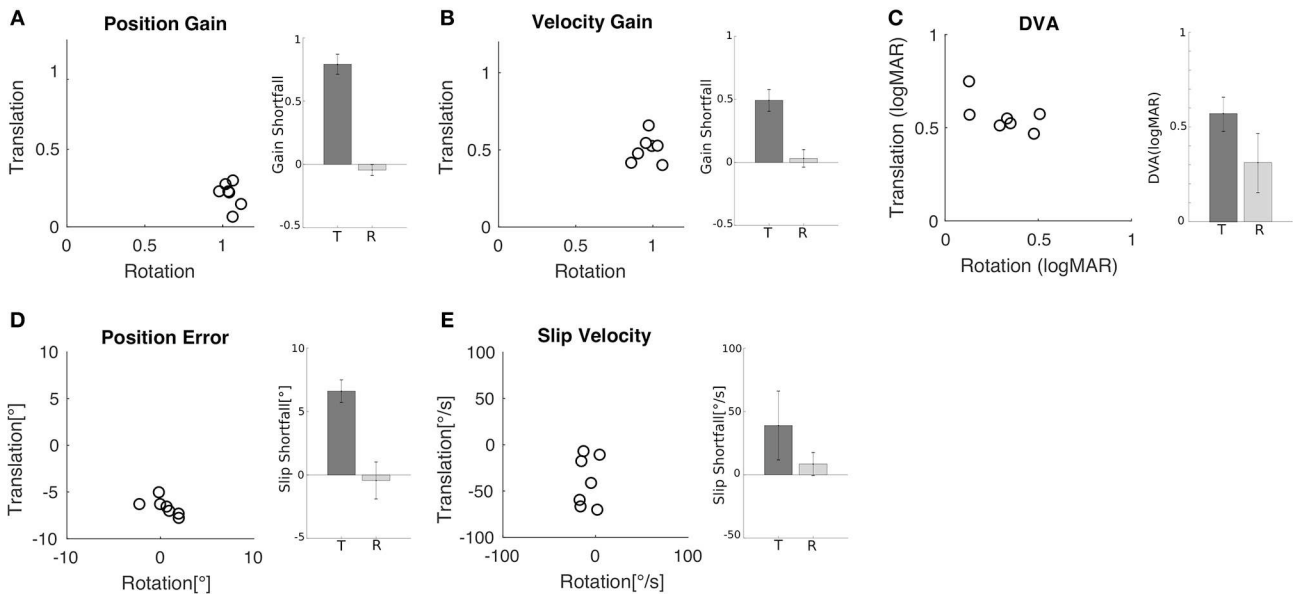

FIGURE 3 | Comparison of rotational and translational VOR gain, slip, and DVA. **(A)** Position error for translation vs. rotation for all subjects. Inset shows the mean (±SD) shortfall in gain relative to gain of one across subjects for translation (0.79 ± 0.08) and rotation (−0.05 ± 0.04). **(B)** Velocity gain for translation vs. rotation for all subjects. Inset shows the mean (±SD) shortfall across subjects for translation (0.49 ± 0.09) and rotation (0.07 ± 0.03). **(C)** DVA for translation vs. rotation for all subjects; larger values indicate worse acuity. Inset shows the mean (±SD) across subjects for translation (0.56 ± 0.09 logMAR) and rotation (0.32 ± 0.15 logMAR). **(D)** Retinal error during translation and rotation for all subjects. Negative values indicate under compensation. Inset shows the mean (±SD) shortfall relative to zero error across subjects for translation (6.61° ± 0.89°) and rotation (−0.44° ± 1.46°). **(E)** Retinal slip velocity during translation and rotation for all subjects. Inset shows the mean (±SD) shortfall across subjects for translation (39 ± 27.2°/s) and rotation (8.57 ± 9.05°/s).

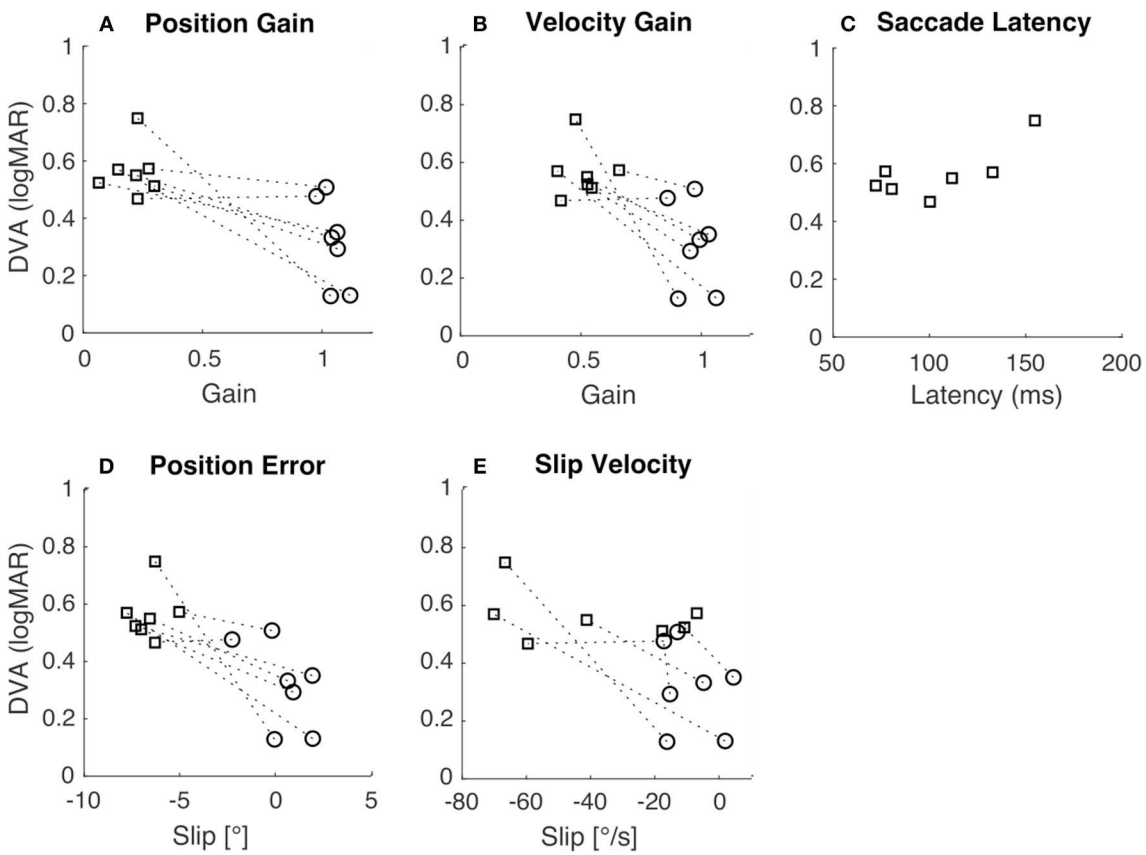

FIGURE 4 | Relation of DVA to gain, slip, and saccade latency. In all panels, squares indicate translation, circles indicate rotation, and the dashed lines connect the two data points from each subject. **(A)** DVA plotted vs. position gain ($R = -0.75$, $p < 0.01$). **(B)** DVA plotted vs. velocity gain ($R = -0.73$, $p < 0.01$). **(C)** DVA plotted vs. saccade latency during translation only ($R = 0.72$, $p = 0.07$). **(D)** DVA plotted vs. position error ($R = -0.77$, $p < 0.01$). **(E)** DVA plotted vs. slip velocity ($R = -0.59$, $p = 0.03$).

for an individual subject were not significantly correlated (**Figure 3C**; $R = 0.62$, $p = 0.14$).

To examine how gross differences in gain and slip between rotation and translation contribute to differences in DVA across movement types we tested for correlations between DVA and gain and slip measures. Pooled DVA across movement types was significantly correlated with velocity gain (**Figure 4B**; $R = -0.73$, $p < 0.01$), position error (**Figure 4D**; $R = -0.77$, $p < 0.01$), position gain (**Figure 4A**, $R = -0.75$, $p < 0.01$) and slip velocity (**Figure 4E**; $R = -0.59$, $p = 0.03$). When correlations were tested using only either rotational or translational data, no significance was observed (**Table 2**). This suggests that individual differences in either gain or slip do not necessarily allow accurate prediction of DVA performance; other factors are likely to influence DVA performance. We examined one such factor, namely the latency of catch-up or re-fixation saccades. Because gain was low during translation, subjects were often required to make saccades to maintain fixation. Latency of the first such saccade was not correlated with DVA during translation (**Figure 4C**; $R = 0.72$, $p = 0.07$), despite prior reports that catch-up saccades can play an important role in DVA (30, 31).

TABLE 2 | Statistical testing of correlations between DVA and positional gain, velocity gain, position error, and velocity slip.

Movement type	Measure	*R*-value	*p*-value
Rotation	Positional gain	−0.71	0.07
Rotation	Velocity gain	−0.30	0.51
Rotation	Position error	−0.53	0.22
Rotation	Velocity slip	−0.25	0.58
Translation	Positional gain	0.07	0.89
Translation	Velocity gain	0.02	0.97
Translation	Position error	0.18	0.7
Translation	Velocity slip	−0.36	0.43

DVA during rotational and translational movements was not significantly correlated with gain and slip measures.

DISCUSSION

Testing of visual acuity during head movement is important because it provides a functional measure of visual stabilization

performance. Historically, the first measures of DVA were performed with a combination of linear and angular vertical head movements [i.e., in the pitch axis (27, 38)]. Several further studies have investigated DVA by focusing on rotational horizontal active movements (15) and also by implementing passive movement techniques to allow unpredictable head rotations (16–18, 28). DVA during translational movements has been most often studied using earth-vertical translations, i.e., movement parallel to gravity, with subjects either upright, such that stimulation was along the vertical axis (10, 39), or on their side, such that stimulation was along the inter-aural axis (40). Here we report, for the first time, a measure of DVA during passive inter-aural translation (tDVA) in the earth horizontal plane. We found that horizontal plane tDVA is worse than rDVA in all subjects, which is in agreement with previous findings of a lower tVOR than rVOR gain (8, 9, 13).

Here, we are particularly interested in measuring and comparing tDVA and rDVA because this comparison allows us to test to what extent acuity is limited by similar factors or mechanisms during translation vs. rotation. Even though ocular responses during rotation and translation are driven by different vestibular organs, the canals and otoliths, respectively, we hypothesized that rDVA and tDVA may be similarly limited by common processes. For example, rVOR and tVOR share the same final common pathway circuitry (i.e., neural integrator, ocular motor plant). In addition, both rDVA and tDVA depend on common visual processes to maintain attention and acuity despite image motion. Several statistical results reported above failed to reach significance, perhaps due to the small number of subjects and lack of statistical power, but we nevertheless offer some speculations below based on these results that may be worthy of further investigation.

The Impact of VOR Gain and Retinal Slip on DVA

Following conventions in the literature, we computed both positional and velocity gain as the ratio of eye movement to head movement for rotations and the ratio of eye movement to ideal eye movement for translations, in the time window between 55 and 65 ms after movement onset. This ensures that responses are vestibularly-driven because visually-driven responses begin only after 100 ms (1, 5). Observed values for both positional and velocity gain were lower during translation than during rotation (**Figures 3A,B**), in line with previous reports (3, 7–9, 28). For example, we observed position gains of ∼1 for rotational movements whereas translational movements led to positional gains of ∼0.20.

We also computed the maximum gaze position error and retinal slip velocity as the sum of the corresponding eye and head quantities. We took the median value during target presentation, which was on average 75 ms after movement onset. Gaze position error during this time interval provides a rough indication of where the target was projected on the retina relative to the fovea. Lower gaze position error values indicate that the target was nearer the fovea, which should result in better acuity. Slip velocity, instead, provides a measure of how the target was moving on the retina during its presentation. Less movement should lead to reduced motion blur, and therefore better visual acuity. We observed greater position error and slip velocity during translation than rotation (**Figures 3D,E**), as expected based on the reduced gain during translation. These observations are also in line with previous reports (41).

To examine how gain and slip impact DVA, we analyzed the correlation between each of these factors and DVA. We expected that slip, not gain, would be the best predictor of DVA performance because slip provides an absolute measure of position and velocity of the target on the retina, whereas gain is a relative measure. However, we did not observe any significant correlations between DVA and these measures for rotation or translation (**Table 2**). Nonetheless, a previous study observed a significant correlation between rVOR gain and dynamic reading, but this study considered the functional head impulse testing paradigm instead of the DVA (30).

When similar correlational analyses were performed across pooled rotational and translational measures (**Figures 4A,B,D,E**) they reached significance. These correlations appear to be driven by gross differences between rotational and translational measures of gain, slip, and DVA. There was considerable variation in DVA measures across individuals, which did not seem to depend on gain or slip. Those subjects with higher rDVA also tended to have higher tDVA, regardless of gain or slip (see dashed lines in **Figure 4**). The analysis of correlation between rDVA and tDVA (**Figure 4C**) did not yield a significant result, perhaps due to the limited number of subjects. A significant correlation, which might be observed with greater numbers of subjects in future studies, would indicate that individual differences in factors other than VOR gain and resulting retinal slip contribute to limiting DVA across movement types. Moreover, it should be considered that visual acuity degrades when retinal slip reaches a velocity of ∼3°/s (42–44) thus decreasing the potential correlation between retinal slip and DVA.

The Role of Catch-Up Saccades

When VOR gain is reduced, observers often compensate by making catch-up saccades in order to foveate the target. During our DVA protocol, the target appeared on average after about 72 ms during rotation and after about 78 ms during translation, and then remained on for a period of about 68 ms for rotation and 49 ms for translation. This difference in the stimulus duration can be ascribed to the differences in the set-up used in the two experiments. Clearly, this difference could also have had an influence on our tDVA results both by reducing the time allowed for perception of the optotype and by decreasing the probability that the optotype was on screen at the end of the catch-up saccade. Nonetheless, catch-up saccades executed early enough following movement onset would have resulted in the target landing on or near the fovea before it was extinguished, and this may have allowed for better DVA performance.

We did not typically observe catch-up saccades during rotational movement, probably because VOR gains were close to unity so that these saccades were not necessary. However, during translational movements all subjects exhibited such saccades; examples are shown in **Figures 2B,D**. To examine the relationship between these saccades and DVA, we computed the average latency of the catch-up saccades for each subject and tested the correlation between this latency and DVA performance (**Figure 4C**). The correlation was not significant, but we nevertheless observed a trend suggesting that those subjects that executed catch-up saccades with short enough latency were able to partially compensate for the low tVOR gain by moving the target onto the fovea with a saccade before the target was extinguished. This could have allowed these subjects to achieve better DVA despite the low gain and high slip measures. This correlation could also arise (a) because the saccade generally helps with the task, or (b) because those subjects who make early saccades also happen to have better acuity. However, these results are in line with previous studies that observed associations between higher amplitude compensatory saccades with shorter latency and low VOR gain (45, 46) as well as with better HITD-FT performance (31).

The Possible Role of Non-oculomotor Stabilization Mechanisms

While catch-up saccades can possibly explain improved DVA performance during translation, they do not explain performance during rotation because catch-up saccades were seldom made. Nevertheless, DVA measures during rotation and translation could be related (**Figure 3C**). In other words, there may be individual differences in DVA performance that persist across movement types. Such an association could arise from non-oculomotor factors limiting DVA performance. For example, one possibility is attention. Subjects who paid greater attention may have performed better in both tDVA and rDVA tasks.

Alternatively, there may be non-oculomotor, visual mechanisms involved in visual stabilization and DVA. Acuity is compromised when (a) the image of the target lands outside the fovea, or (b) the image of the target moves on the retina, resulting in motion blur. However, retinal image motion is not always detrimental to visual acuity. Research on retinal image motion caused by fixational eye movements, including ocular drift and microsaccades, has been extensively studied indicating that visual acuity for high frequency is affected by the absence of fixational eye movements (47). Recent studies show that retinal image motion may actually lead to improved visual acuity compared to the condition in which the retinal image is artificially stabilized using a scanning laser ophthalmoscope (48). This improved acuity is thought to depend on processes that accumulate image information across both space and time to increase the signal-to-noise ratio (49).

If such accumulation processes exist for fixational eye movements, similar processes may operate on a larger spatial scale to augment DVA during the VOR. Indeed, there is evidence of motion deblurring during compensatory eye movements (50). If these mechanisms operate similarly during rotational and translation movement, and there are individual differences in the efficiency of these mechanisms, this could explain an association between tDVA and rDVA that is not accounted for by oculomotor behavior.

To conclude, our study provides a first investigation on how otoliths' function impacts on DVA and found the DVA is consistently lower during translations than during rotations. A more extensive study, involving more subjects and more trials for each subject could clarify the relationship between corrective saccades and functional head stabilization abilities. We suggest that further research on our test accompanied by other specific otolith tests (e.g., oVEMP) and visual acuity assessment procedures might provide a comprehensive picture of the visuo-vestibular interaction underlying translational VOR.

AUTHOR CONTRIBUTIONS

CR, LC, PM, and NL conceived the study. CR, LC, PM, and SR designed the experiments and analyzed the data. CR and LC developed the set-up and carried out the experiments. CR, LC, PM, NL and SR wrote and reviewed the manuscript.

FUNDING

This project was funded by the German Federal Ministry of Education and Research under grant code 01 EO 1401. This project was also supported by NIH P20GM103650.

ACKNOWLEDGMENTS

We thank Hans Hintermaier for the technical support and Marlene Spangenberg for the help in collecting data.

REFERENCES

1. Halmagyi GM, Curthoys IS. A clinical sign of canal paresis. *Arch Neurol.* (1988) 45:737–739. doi: 10.1001/archneur.1988.00520310043015
2. Bartl K, Lehnen N, Kohlbecher S, Schneider E. Head impulse testing using video-oculography. *Ann N Y Acad Sci.* (2009) 331–3. doi: 10.1111/j.1749-6632.2009.03850.x
3. MacDougall HG, Weber KP, McGarvie LA, Halmagyi GM, Curthoys IS. The video head impulse test: diagnostic accuracy in peripheral vestibulopathy. *Neurology*. (2009) 73:1134–1141. doi: 10.1212/WNL.0b013e3181bacf85
4. Macdougall HG, McGarvie LA, Halmagyi GM, Curthoys IS, Weber KP. Application of the video head impulse test to detect vertical semicircular canal dysfunction. *Otol Neurotol.* (2013) 34:974–9. doi: 10.1097/MAO.0b013e31828d676d
5. Halmagyi GM, Chen L, MacDougall HG, Weber KP, McGarvie LA, Curthoys IS. The video head impulse test. *Front Neurol.* (2017) 8:258. doi: 10.3389/fneur.2017.00258

6. Mossman B, Mossman S, Purdie G, Schneider E. Age dependent normal horizontal VOR gain of head impulse test as measured with video-oculography. *J Otolaryngol Head Neck Surg*. (2015) 44:29. doi: 10.1186/s40463-015-0081-7
7. Ramat S, Straumann D, Zee DS. Interaural translational VOR: suppression, enhancement, and cognitive control. *J Neurophysiol*. (2005) 94:2391–402. doi: 10.1152/jn.01328.2004
8. Ramat S, Zee DS. Ocular motor responses to abrupt interaural head translation in normal humans. *J Neurophysiol*. (2003) 90:887–902. doi: 10.1152/jn.01121.2002
9. Ramat S, Zee DS, Minor LB. Translational vestibulo-ocular reflex evoked by a "head heave" stimulus. *Ann N Y Acad Sci*. (2001) 942:95–113. doi: 10.1111/j.1749-6632.2001.tb03738.x
10. Cheng RC, Walker MF. Vertical head translation impairs dynamic visual acuity during near viewing. *J Vestib Res Equilib Orientat*. (2017) 26:417–23. doi: 10.3233/VES-160596
11. Liao K, Walker MF, Joshi A, Reschke M, Leigh RJ. Vestibulo-ocular responses to vertical translation in normal human subjects. *Exp Brain Res*. (2008) 185:553–62. doi: 10.1007/s00221-007-1181-z
12. Liao K, Walker MF, Joshi AC, Reschke M, Strupp M, Wagner J, et al. The linear vestibulo-ocular reflex, locomotion and falls in neurological disorders. *Restor Neurol Neurosci*. (2010) 28:91–103. doi: 10.3233/RNN-2010-0507
13. Crane BT, Tian J, Wiest G, Demer JL. Initiation of the human heave linear vestibulo-ocular reflex. *Exp Brain Res*. (2003) 148:247–55. doi: 10.1007/s00221-002-1301-8
14. Miller JW, Ludvigh E. The effect of relative motion on visual acuity. *Surv Ophthalmol*. (1962) 7:83–116.
15. Herdman SJ, Tusa RJ, Blatt P, Suzuki A, Venuto PJ, Roberts D. Computerized dynamic visual acuity test in the assessment of vestibular deficits. *Am J Otol*. (1998) 19:790–6.
16. Tian J, Shubayev I, Demer JL. Dynamic visual acuity during transient and sinusoidal yaw rotation in normal and unilaterally vestibulopathic humans. *Exp Brain Res*. (2001) 137:12–25. doi: 10.1007/s002210000640
17. Tian JR, Shubayev I, Demer JL. Dynamic visual acuity during passive and self-generated transient head rotation in normal and unilaterally vestibulopathic humans. *Exp Brain Res*. (2002) 142:486–95. doi: 10.1007/s00221-001-0959-7
18. Schubert MC, Migliaccio AA, Della Santina CC. Dynamic visual acuity during passive head thrusts in canal planes. *J Assoc Res Otolaryngol*. (2006) 7:329–38. doi: 10.1007/s10162-006-0047-6
19. Longridge NS, Mallinson AI. The dynamic illegible e-test: a technique for assessing the vestibulo-ocular reflex. *Acta Otolaryngol*. (1987) 103:273–9. doi: 10.3109/00016488709107283
20. Herdman SJ, Schubert MC, Tusa RJ. Role of central preprogramming in dynamic visual acuity with vestibular loss. *Arch Otolaryngol Head Neck Surg*. (2001) 127:1205–10. doi: 10.1001/archotol.127.10.1205
21. Della Santina CC, Cremer PD, Carey JP, Minor LB. Comparison ot head thrust test with head autorotation test reveals that the vestibulo-ocular reflex is enhanced during voluntary head movements. *Arch Otolaryngol Head Neck Surg*. (2002) 128:1044–54. doi: 10.1001/archotol.128.9.1044
22. Goebel JA, Tungsiripat N, Sinks B, Carmody J. Gaze stabilization test: a new clinical test of unilateral vestibular dysfunction. *Otol Neurotol*. (2007) 28:68–73. doi: 10.1097/01.mao.0000244351.42201.a7
23. Pritcher MR, Whitney SL, Marchetti GF, Furman JM. The influence of age and vestibular disorders on gaze stabilization: a pilot study. *Otol Neurotol*. (2008) 29:982–8. doi: 10.1097/MAO.0b013e31818457fb
24. Böhler A, Mandalá M, Ramat S. A software program for the head impulse testing device (HITD). *Conf Proc IEEE Eng Med Biol Soc*. (2010) 2010:6615–8. doi: 10.1109/IEMBS.2010.5627138
25. Ramat S, Colnaghi S, Boehler A, Astore S, Falco P, Mandalà M, et al. A device for the functional evaluation of the VOR in clinical settings. *Front Neurol*. (2012) 3:39. doi: 10.3389/fneur.2012.00039
26. Versino M, Colagiorgio P, Sacco S, Colnaghi S, Quaglieri S, Manfrin M, et al. Reading while moving: the functional assessment of VOR. *J Vestib Res*. (2014) 24:459–64. doi: 10.3233/VES-140531
27. Demer JL, Honrubia V, Baloh RW. Dynamic visual acuity: a test for oscillopsia and vestibulo-ocular reflex function. *Am J Otol*. (1994) 15:340–7.
28. Vital D, Hegemann SCA, Straumann D, Bergamin O, Bockisch CJ, Angehrn D, et al. A new dynamic visual acuity test to assess peripheral vestibular function. *Arch Otolaryngol Neck Surg*. (2010) 136:686. doi: 10.1001/archoto.2010.99
29. Corallo G, Versino M, Mandalà M, Colnaghi S, Ramat S. The functional head impulse test: preliminary data. *J Neurol*. (2018) 265(Suppl. 1):35–9. doi: 10.1007/s00415-018-8910-z
30. Ramaioli C, Colagiorgio P, Sağlam M, Heuser F, Schneider E, Ramat S, et al. The effect of vestibulo-ocular reflex deficits and covert saccades on dynamic vision in opioid-induced vestibular dysfunction. *PLoS ONE*. (2014) 9:e110322. doi: 10.1371/journal.pone.0110322
31. Lehnen N, Kellerer S, Knorr AG, Schlick C, Jahn K, Schneider E, et al. Head-movement-emphasized rehabilitation in bilateral vestibulopathy. *Front Neurol*. (2018) 9:562. doi: 10.3389/fneur.2018.00562
32. Wettstein VG, Weber KP, Bockisch CJ, Hegemann SC. Compensatory saccades in head impulse testing influence the dynamic visual acuity of patients with unilateral peripheral vestibulopathy. *J Vestib Res*. (2016) 26:395–02. doi: 10.3233/VES-160591
33. Colagiorgio P, Colnaghi S, Versino M, Ramat S. A new tool for investigating the functional testing of the VOR. *Front Neurol*. (2013) 4:165. doi: 10.3389/fneur.2013.00165
34. Watson AB, Pelli DG. Quest: a Bayesian adaptive psychometric method. *Percept Psychophys*. (1983) 33:113–20. doi: 10.3758/BF03202828
35. Weber KP, Aw ST, Todd MJ, McGarvie LA, Curthoys IS, Halmagyi GM. Head impulse test in unilateral vestibular loss: Vestibulo-ocular reflex and catch-up saccades. *Neurology*. (2008) 70:454–63. doi: 10.1212/01.wnl.0000299117.48935.2e
36. Lehnen N, Glasauer S, Jahn K, Weber KP. Head impulses in complete bilateral vestibular loss: Catch-up saccades require visual input. *Neurology*. (2013) 81:688–90. doi: 10.1212/WNL.0b013e3182a08d36
37. Leigh RJ, Averbuch-Heller L, Tomsak RL, Remler BF, Yaniglos SS, Dell'Osso LF. Treatment of abnormal eye movements that impair vision: Strategies based on current concepts of physiology and pharmacology. *Ann Neurol*. (1994) 36:129–41. doi: 10.1002/ana.410360204
38. Demer JL, Amjadi F. Dynamic visual acuity of normal subjects during vertical optotype and head motion. *Investig Ophthalmol Vis Sci*. (1993) 34:1894–906.
39. Schmäl F, Kunz R, Ortmann C, Stoll W, Nieschalk M, Fechner G. Effect of ethanol on dynamic visual acuity during vertical body oscillation in healthy volunteers. *Eur Arch Oto Rhino Laryngol*. (2000) 257:485–9. doi: 10.1007/s004050000260
40. Schmal F, Kunz R, Stoll W. Dynamic visual acuity during linear acceleration along the inter-aural axis. *Eur Arch Oto Rhino Laryngol*. (2000) 257:193–8. doi: 10.1007/s004050050221
41. MacDougall HG, Curthoys IS. Plasticity during vestibular compensation: the role of saccades. *Front Neurol*. (2012) 3:21. doi: 10.3389/fneur.2012.00021
42. Westheimer G, McKee SP. Visual acuity in the presence of retinal-image motion. *J Opt Soc Am*. (1975) 65:847–50. doi: 10.1364/JOSA.65.000847
43. Morgan MJ, Watt RJ, McKee SP. Exposure duration affects the sensitivity of vernier acuity to target motion. *Vision Res*. (1983) 23:541–6. doi: 10.1016/0042-6989(83)90129-3
44. Carney T, Amnon Silverstein D, Klein SA. Vernier acuity during image rotation and translation: visual performance limits. *Vision Res*. (1995) 35:1951–64. doi: 10.1016/0042-6989(94)00288-W
45. Anson ER, Bigelow RT, Carey JP, Xue QL, Studenski S, Schubert MC, et al. VOR gain is related to compensatory saccades in healthy older adults. *Front Aging Neurosci*. (2016) 8:150. doi: 10.3389/fnagi.2016.00150
46. Colagiorgio P, Versino M, Colnaghi S, Quaglieri S, Manfrin M, Zamaro E, et al. New insights into vestibular-saccade interaction based on covert corrective

saccades in patients with unilateral vestibular deficits. *J Neurophysiol.* (2017) 117:jn.00864.2016. doi: 10.1152/jn.00864.2016
47. Rucci M, Iovin R, Poletti M, Santini F. Miniature eye movements enhance fine spatial detail. *Nature*. (2007) 447:852–5. doi: 10.1038/nature05866
48. Ratnam K, Domdei N, Harmening WM, Roorda A. Benefits of retinal image motion at the limits of spatial vision. *J Vis.* (2017) 17:30. doi: 10.1167/17.1.30
49. Anderson AG, Olshausen BA, Ratnam K, Roorda A. A neural model of high-acuity vision in the presence of fixational eye movements. In: *2016 50th Asilomar Conference on Signals, Systems and Computers.* Pacific Grove, CA (2016) p. 588–92.
50. Tong J, Patel SS, Bedell HE. The attenuation of perceived motion smear during combined eye and head movements. *Vision Res.* (2006) 46:4387–97. doi: 10.1016/j.visres.2006.08.034

Conflict of Interest Statement: CR was an employee of EyeSeeTec GmbH. NL is a shareholder and paid consultant to EyeSeeTec GmbH.

The remaining authors declare that the research was conducted in the absence of any commercial or financial relationships that could be construed as a potential conflict of interest.

frontiers in Neurology

ORIGINAL RESEARCH
published: 16 April 2019
doi: 10.3389/fneur.2019.00365

The Functional Head Impulse Test to Assess Oscillopsia in Bilateral Vestibulopathy

T. S. van Dooren[1], F. M. P. Lucieer[1], S. Duijn[2], A. M. L. Janssen[3,4], N. Guinand[1,5], A. Pérez Fornos[5], V. Van Rompaey[6,7], H. Kingma[1,8], S. Ramat[9] and R. van de Berg[1,8]*

[1] Division of Balance Disorders, Department of Otorhinolaryngology and Head and Neck Surgery, Maastricht University Medical Centre, Maastricht, Netherlands, [2] Faculty of Health, Medicine and Life Sciences, University of Maastricht, Maastricht, Netherlands, [3] Department of ENT/Audiology, School for Mental Health and Neuroscience (MHENS), Maastricht University Medical Centre, Maastricht, Netherlands, [4] Department of Methodology and Statistics, Care and Public Health Research Institute (CAPHRI), Maastricht University, Maastricht, Netherlands, [5] Service of Otorhinolaryngology Head and Neck Surgery, Department of Clinical Neurosciences, Geneva University Hospitals, Geneva, Switzerland, [6] Faculty of Medicine and Health Sciences, University of Antwerp, Antwerp, Belgium, [7] Department of Otorhinolaryngology and Head and Neck Surgery, Antwerp University Hospital, Edegem, Belgium, [8] Faculty of Physics, Tomsk State Research University, Tomsk, Russia, [9] Department of Computer, Electric and Biomedical Engineering, University of Pavia, Pavia, Italy

OPEN ACCESS

Edited by:
Barry M. Seemungal, Imperial College London, United Kingdom

Reviewed by:
Klaus Jahn, Schön Klinik, Germany
Thomas Haslwanter, University of Applied Sciences Upper Austria, Austria

***Correspondence:**
Tessa van Dooren
tessa.van.dooren@mumc.nl

Specialty section:
This article was submitted to Neuro-Otology, a section of the journal Frontiers in Neurology

Received: *10 November 2018*
Accepted: *25 March 2019*
Published: *16 April 2019*

Citation:
van Dooren TS, Lucieer FMP, Duijn S, Janssen AML, Guinand N, Pérez Fornos A, Van Rompaey V, Kingma H, Ramat S and van de Berg R (2019) The Functional Head Impulse Test to Assess Oscillopsia in Bilateral Vestibulopathy. Front. Neurol. 10:365. doi: 10.3389/fneur.2019.00365

Introduction: Bilateral vestibulopathy (BV) is a chronic condition in which vestibular function is severely impaired or absent on both ears. Oscillopsia is one of the main symptoms of BV. Oscillopsia can be quantified objectively by functional vestibular tests, and subjectively by questionnaires. Recently, a new technique for testing functionally effective gaze stabilization was developed: the functional Head Impulse Test (fHIT). This study compared the fHIT with the Dynamic Visual Acuity assessed on a treadmill ($DVA_{treadmill}$) and Oscillopsia Severity Questionnaire (OSQ) in the context of objectifying the experience of oscillopsia in patients with BV.

Methods: Inclusion criteria comprised: (1) summated slow phase velocity of nystagmus of $<20°$/s during bithermal caloric tests, (2) torsion swing tests gain of $<30\%$ and/or phase $<168°$, and (3) complaints of oscillopsia and/or imbalance. During the fHIT (Beon Solutions srl, Italy) patients were seated in front of a computer screen. During a passive horizontal head impulse a Landolt C optotype was shortly displayed. Patients reported the seen optotype by pressing the corresponding button on a keyboard. The percentage correct answers was registered for leftwards and rightwards head impulses separately. During $DVA_{treadmill}$ patients were positioned on a treadmill in front of a computer screen that showed Sloan optotypes. Patients were tested in static condition and in dynamic conditions (while walking on the treadmill at 2, 4, and 6 km/h). The decline in LogMAR between static and dynamic conditions was registered for each speed. Every patient completed the Oscillopsia Severity Questionnaire (OSQ).

Results: In total 23 patients were included. This study showed a moderate correlation between OSQ outcomes and the fHIT [rightwards head rotations ($r_s = -0.559$; $p = 0.006$) leftwards head rotations ($r_s = -0.396$; $p = 0.061$)]. No correlation was found between OSQ outcomes and $DVA_{treadmill}$, or between $DVA_{treadmill}$ and fHIT. All patients completed the fHIT, 52% of the patients completed the $DVA_{treadmill}$ on all speeds.

Conclusion: The fHIT seems to be a feasible test to quantify oscillopsia in BV since, unlike $DVA_{treadmill}$, it correlates with the experienced oscillopsia measured by the OSQ, and more BV patients are able to complete the fHIT than $DVA_{treadmill}$.

Keywords: functional head impulse test (fHIT), dynamic visual acuity (DVA), Oscillopsia, oscillopsia severity questionnaire, functional vestibular testing, bilateral vestibulopathy (BV)

INTRODUCTION

Gaze stabilization is one of the many functions of the vestibular system. The vestibulo-ocular reflex (VOR) enables gaze stabilization during high-frequency head movements by moving the eyes directly in opposite direction of the head movement. A decreased VOR therefore impairs gaze stabilization, which leads to head or body movement-induced blurred vision (oscillopsia). Oscillopsia is one of the main symptoms of bilateral vestibulopathy (BV) (1).

BV is a heterogeneous chronic condition in which vestibular function is severely impaired or absent on both ears (2). BV patients have a variety of symptoms and report a significant reduction in quality of life. Therapeutic options are often limited to balance training, but studies are now focusing on restoring vestibular function with a vestibular implant (3–6).

To treat patients with BV, the condition must be first recognized by clinicians. The diagnosis of BV is often under- or misdiagnosed. Therefore, sufficient inclusion criteria and validated patient-reported outcome measures are needed for patients with BV. One of the components is to quantify the experience of oscillopsia in BV patients (2, 7).

Oscillopsia can be quantified subjectively by questionnaires, such as the Oscillopsia Severity Questionnaire (OSQ) (8). These questionnaires are designed to classify the disease burden experienced by patients in daily life. Additionally, oscillopsia can be quantified objectively by functional vestibular tests that assess dynamic visual acuity (DVA) (9, 10). Various clinical testing paradigms have been proposed to assess DVA, like walking on a treadmill or passively shaking the head, while reading an optotype chart (8, 11). A new technique was recently suggested: the functional head impulse test (fHIT). The fHIT provides information about the functional performance of the rotational VOR by testing its gaze stabilization ability during passive head impulses in a range of peak head accelerations from 3,000 to 6,000 deg/s^2 (12–15).

The aim of this study was to compare the fHIT with the DVA on a treadmill ($DVA_{treadmill}$) and OSQ outcomes in the context of quantifying oscillopsia in BV patients. Preliminary data from our laboratory showed inter- and intrasubject discrepancies between fHIT and $DVA_{treadmill}$ results in patients with BV. This might be the result of the different stimuli applied during these tests: fHIT selectively stimulates the horizontal semicircular canals with passive head movements, while $DVA_{treadmill}$ stimulates the whole vestibular system with active whole-body movements. Based on these experiences, it was hypothesized that: (1) fHIT and $DVA_{treadmill}$ differ with respect to quantifying oscillopsia since different stimuli are given, and (2) therefore one of them might correlate better to the OSQ.

METHODS

Study Population

This study comprised patients diagnosed with BV at the Division of Balance Disorders at Maastricht University Hospital. Inclusion criteria were: (1) summated slow phase velocity of nystagmus of $<20^\circ$/s during biothermal caloric tests (30 and 44°C, 300 mL in 30 s), (2) torsion swing tests gain of <30% and/or phase $<168^\circ$ (peak velocity of 60°/s; sinusoidal rotation 0.11Hz), and (3) complaints of oscillopsia and/or imbalance. The inclusion criteria differed on some aspects from the diagnostic criteria of BV from the Bárány Society, since inclusion of this study started before these criteria were published (1). Based on normative data in our laboratory, the lower limit of a normal caloric test on one side is a sum of bithermal slow phase velocities of nystagmus of 25°/s (15°/s warm, 10°/s cold). BV patients included in this study had a maximum sum of bithermal slow phase velocities of nystagmus on one side of 15°/s. In this study, some patients will not perfectly fit the BV criteria from the Bárány Society, nonetheless they definitely have a bilateral vestibular dysfunction (see **Supplementary Material**).

Exclusion criteria comprised peripheral neuropathy, being unable to stop vestibular suppressants for one week (cinnarizine and all psychiatric medication), or the inability to walk independently.

Testing

Every patient underwent fHIT and $DVA_{treadmill}$ on one day in the same order, and with a break in between. Both tests were performed by one trained examiner (FL) under standardized conditions, in the same room with controlled illumination. Patients were tested binocularly and corrective spectacles or contact lenses were worn during fHIT, and removed during $DVA_{treadmill}$.

Functional Head Impulse Test (fHIT) (12–14)

The fHIT was performed using the fHIT system (Beon Solutions srl, Zero Branco (TV), Italy). Patients were seated in a static chair in front of a computer screen at a distance of 1.5 meter with a keyboard in their hand. During a passive head impulse, when head acceleration reached its peak value, an optotype (Landolt C ring) was displayed on the screen for 80 ms. The size of the optotype was adjusted for every subject separately, and remained constant during testing. Before the start of the fHIT, the static visual acuity threshold was acquired by the fHIT system in 20 trials. Optotype size started from 1.0 LogMAR (log of the Minimum Angle of Resolution) and decreased depending on the subjects' rates of errors. The used optotype size was equal to this threshold, increased by 0.6 LogMAR (13). During fHIT,

patients had to choose the right optotype out of eight different options by pressing the corresponding button on the keyboard. No direct feedback was given. Head impulses comprised fast (peak velocity >150°/s) (16, 17), outwards, passive, horizontal rotational head movements with a low amplitude (±20°), unpredictable in timing and direction. At least 10 impulses were given to both sides. The absolute outcome was the percentage of correct answers (%CA) for each side, as calculated by the fHIT system. A %CA of <80 was considered abnormal. This cut-off was a conservative approximation of the criterion adopted by the fHIT system, which considers the level where the standardized normal deviate of the patient falls outside the 99% of the two-tailed Z distribution of a population of age-matched controls (14).

$DVA_{treadmill}$

DVA was assessed on a treadmill (1210 model, SportsArt, Inc., Tainan, Taiwan, China) with a computer screen placed at a distance of 2.8 meters from the subject. Sloan letter optotypes were used. Testing started with optotypes presented at a LogMAR of 1.0. When four out of five optotypes were recognized correctly, the corresponding LogMAR was considered achieved and the size was decreased by steps of 0.1 LogMAR. When three or less optotypes were recognized correctly, the corresponding LogMAR was considered unachieved. The best (i.e., lowest) achieved LogMAR was recorded. Patients were tested in static condition (while standing still) and in dynamic conditions (while walking on the treadmill at 2, 4, and 6 km/h). Every condition was tested once. In case the patient was not able to walk independently at a certain speed, the test was stopped and registered as impossible for that speed. Absolute outcome for every speed was the visual acuity difference (VA difference), calculated as the decline in LogMAR between static and dynamic conditions. $DVA_{treadmill}$ was considered abnormal when a VA difference of >0.2 was recorded at 2 and 4 km/h or >0.3 at 6 km/h (8, 18, 19).

Oscillopsia Severity Questionnaire (OSQ)

Every patient completed the oscillopsia severity questionnaire (OSQ) developed by the Division of Balance Disorders in Maastricht. The OSQ consists of nine questions about the patients' experience of oscillopsia in daily life, as shown in **Table 1**. Every question can be answered by one of the following five options Always (= 5), Often (= 4), Sometimes (= 3), Seldom (=2), or Never (=1). The outcome of every separate question was registered and the mean value for every patient was calculated. A mean value of three or more was considered as moderate to extreme oscillopsia severity (8, 20).

TABLE 1 | The oscillopsia severity questionnaire (OSQ).

OSCILLOPSIA SEVERITY QUESTIONNAIRE	
1.	Do you have the sensation that the visual environment is moving when it's not?
2.	By dim light, do you have the sensation that the visual environment is not stable?
3.	Is it difficult for you to recognize known faces when you are walking?
4.	When you are reading, do you have the sensation that the text is not stable?
5.	When you are watching television, do you have the sensation that the image is not stable?
6.	When you are driving your car, do you have the sensation that the visual environment is not stable?
7.	As a car passenger, do you have the sensation that the visual environment is not stable?
8.	When you are riding a bicycle, do you have the sensation that the visual environment is not stable?
9.	When you are walking on uneven ground, do you have the sensation that the visual environment is not stable?

Questions can be answered with Always = 5, Often = 4, Sometimes = 3, Seldom = 2, or Never =1. A mean value of 3 or more was considered as moderate to extreme oscillopsia severity.

Statistical Analysis

Data were analyzed using SPSS Statistics 24 for Windows. Significance was set on $p < 0.05$. Bonferroni correction was used in case of multiple comparisons. The Shapiro-Wilk test, and visual inspection of the histogram and normal Q-Q plot of the outcome distributions were used to determine whether the data were normally distributed. In case there was no normal distribution of data, non-parametric tests (Wilcoxon Sign-Rank test, McNemar, Mann-Whitney U or Spearman's Rank Correlation test) were used.

The correlation was calculated between fHIT and $DVA_{treadmill}$, between $DVA_{treadmill}$ (VA difference) at 2, 4, and 6 km/h and OSQ score, and between fHIT (%CA) and OSQ score. Duration of illness was compared between $DVA_{treadmill}$ outcome and OSQ score, and between fHIT outcome and OSQ score.

During further analyses 3 groups were differentiated: (1) fHIT abnormal vs. normal for rightwards and leftwards head rotations. In case fHIT was abnormal to at least one side, the outcome was considered abnormal during this analysis. (2) $DVA_{treadmill}$ impossible vs. possible. The impossible subgroup consists of patients that were not able to walk independently at 2, 4, and/or 6 km/h. (3) $DVA_{treadmill}$ abnormal vs. normal. During this analysis patients with an impossible $DVA_{treadmill}$ at any speed were considered missing data. Within these groups, OSQ outcomes were compared between the subgroups.

Ethical Considerations

This study was in accordance with the Declaration of Helsinki (amended version 2013). Approval was obtained from the ethical committees of Maastricht University Medical Center (NL52768.068.15/METC151027). All participants provided written informed consent prior to the study.

RESULTS

In this study 23 patients with BV were included, 13 male and 10 female. Mean age was 57.6 (SD 11.04). Duration of illness varied between 18 months and 33 years. Etiologies comprised: ototoxicity due to gentamicin treatment (3) or chemotherapy (1), post-infectious due to Lyme disease (1) or meningitis (1),

DFNA-9 gene mutation (3), bilateral Ménière's disease (2), autoimmune disease (1). In 10 patients, no cause could be found (idiopathic).

fHIT

All 23 patients (100%) completed the fHIT. Outcomes for rightwards and leftwards head rotations did not significantly differ. Eighteen patients (78%) showed an abnormal fHIT to both sides, and four patients (17%) had normal fHIT outcomes. One patient (4%) had a unilateral abnormal fHIT: 45%CA on the right side and 90%CA on the left side. No significant difference was found in OSQ score between patients with a normal and abnormal fHIT. A moderate correlation was found between %CA on the fHIT and OSQ score for rightwards ($r_s = -0.559$, $p = 0.006$) and leftwards ($r_s = -0.396$, $p = 0.061$) head impulses (**Figure 1**).

$DVA_{treadmill}$

In total 12 BV patients (52%) completed the DVA on all three speeds. With increasing speed, the number of patients that could not walk independently (and not complete the test) increased: two patients at 2 km/h and 11 patients at 6 km/h. VA difference between 2, 4, and 6 km/h did not differ statistically significant. DVA, at any speed, was only abnormal in four patients (17%). All four patients showed abnormal DVA at 4 km/h, and one even at 2 km/h. Of these four patients, neither completed a walking speed of 6 km/h. (**Table 2**) Mean OSQ outcome and duration of illness did not differ significantly between patients with a normal or abnormal DVA or between patients with a possible or impossible DVA. No correlation was found between OSQ outcome and the amount of VA difference at any speed.

fHIT vs. $DVA_{treadmill}$

fHIT showed more abnormal outcomes than $DVA_{treadmill}$ at all speeds: 78% vs. 17%. Next to this, fHIT was possible in all 23 patients, while $DVA_{treadmill}$ could not be completed in 11 of them. All four patients with abnormal $DVA_{treadmill}$ outcomes, showed abnormal bilateral fHIT outcomes as well. No correlation between fHIT and $DVA_{treadmill}$ was found at any tested speed (2, 4, 6 km/h), for both rightwards and leftwards head rotations.

DISCUSSION

This study compared the fHIT with DVA assessed on a treadmill, and OSQ outcomes in the context of quantifying oscillopsia in patients with BV. fHIT outcomes showed a moderate correlation with the experienced oscillopsia in daily life, as assessed by the OSQ. $DVA_{treadmill}$ outcomes, at any of the tested speeds, did not correlate to the severity of oscillopsia, as measured by OSQ. This is in agreement with previous studies with a large study population of BV patients (8). There is no gold standard for measuring oscillopsia, this study used the oscillopsia severity questionnaire (OSQ) to capture the subjective complaints of BV

TABLE 2 | $DVA_{treadmill}$ outcomes.

	DVA 2 km/h	DVA 4 km/h	DVA 6 km/h	DVA all speeds*
Normal	20 (87%)	16 (70%)	12 (52%)	8 (35%)
Abnormal	1 (4%)	4 (17%)	0 (0%)	4 (17%)
Not possible	2 (9%)	3 (13%)	11 (48%)	11 (48%)

*$DVA_{treadmill}$ was considered abnormal when a VA difference of >0.2 was recorded at 2 and 4 km/h or >0.3 at 6 km/h. In case a patient could not walk a certain speed independently, this speed was classified as "not possible." *DVA at all speeds was classified as "not possible" or "abnormal" when a patient did not complete the $DVA_{treadmill}$ protocol at all speeds or had an abnormal outcome at one or more speeds.*

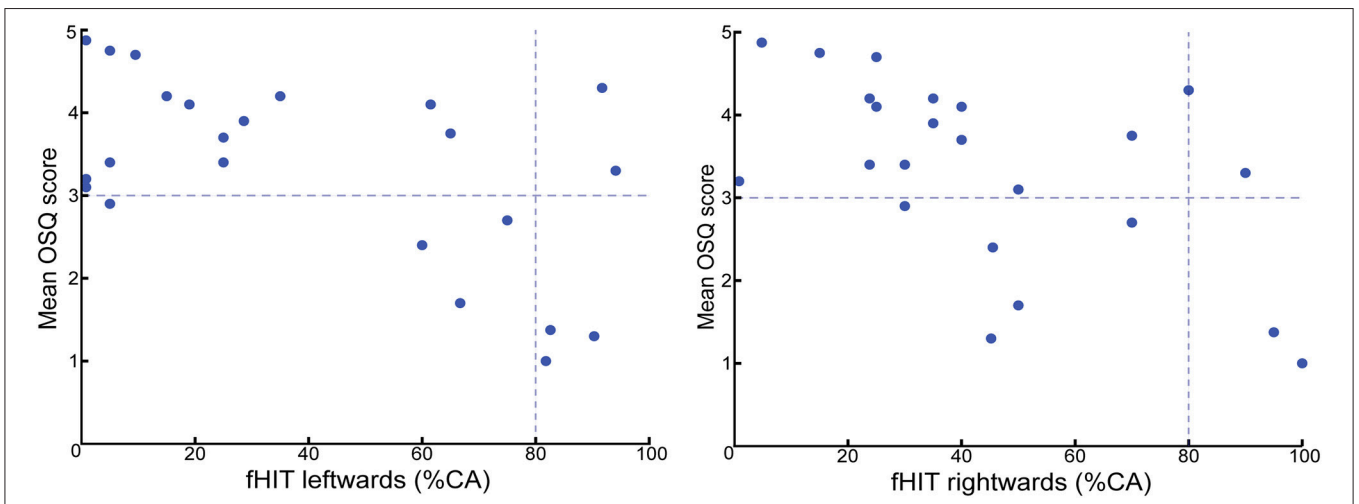

FIGURE 1 | fHIT outcome (percentage of correct answers, %CA) vs. mean OSQ score. The horizontal interceptive line represents the cut-off value of the OSQ; a value of three or more is considered as moderate to extreme oscillopsia severity. The vertical interceptive line represents the cut-off value of the fHIT; a %CA-value of <80 was considered abnormal. This study showed a moderate correlation between the severity of oscillopsia tested by the OSQ, and percentage of correct answers on the fHIT for both rightwards ($r_s = -0.559$; $p = 0.006$) and leftwards ($r_s = -0.396$; $p = 0.061$) head impulses.

patients. (8) Specific questions from this questionnaire—those with highest correlation with fHIT—could possibly be of value in establishing a validated patient reported outcome measures for BV (7).

fHIT showed more abnormal outcomes than $DVA_{treadmill}$ at all speeds (78 vs. 17%). This is probably due to multiple factors (9). First, the ability to compensate or adapt is less during fHIT than during $DVA_{treadmill}$. During walking on a treadmill, patients are able to use compensation mechanisms to improve gait or gaze stabilization (e.g., by trying to minimize the overall head movement). Secondly, an active movement is made during $DVA_{treadmill}$, in contrast to the passive movement during fHIT. Passive movements have been shown to be most useful in discriminating between healthy subjects and patients with bilateral vestibular loss (16, 21). Indeed, during walking an efference copy of the command producing the walking movement is available, thereby allowing patients to predict the retinal slippage as a consequence on the resulting head movement (22). Thirdly, the nature of the stimulus differs between the two tests. The fHIT selectively stimulates the plane of one semi-circular canal during passive head movements in high frequencies ($>150^{\circ}$/s), while $DVA_{treadmill}$ comprises an active movement which stimulates all semi-circular canals and otoliths at the same time (14). The frequency of the stimulus depends on the walking speed. When walking at a speed of 6 km/h, angular velocities are $\sim 178^{\circ}$/s, and lateral and horizontal head translations occur at 1 Hz and 2 Hz, respectively (23).

BV criteria, and the inclusion criteria of this study, comprise low or absent function of the horizontal semi-circular canal. In case the patient had residual function of other sensory parts of the vestibular system (i.e., the otoliths), it could be possible that this residual function was used during $DVA_{treadmill}$. This possible selection bias could lead to false negative $DVA_{treadmill}$ outcomes. These mechanisms might also (partially) explain why the fHIT has a stronger correlation to oscillopsia experience than $DVA_{treadmill}$.

Comparing the ability of subjects to complete a test, fHIT could be performed in more patients than $DVA_{treadmill}$. After all, in this study population 100% of the patients was able to complete the fHIT, while 87% of the patients completed the DVA-protocol at 4 km/h and only 52% at 6 km/h. The inability to walk faster than 5 km/h on a treadmill in BV patients was described in previous studies (11, 24).

A possible limitation of this study is the fact that $DVA_{treadmill}$ was tested without wearing any corrective spectacles. It is unlikely this has influenced the outcomes, since $DVA_{treadmill}$ outcome (VA difference) was calculated as the decline in LogMAR in a patient between static and dynamic conditions, both tested without corrective spectacles. Furthermore, different $DVA_{treadmill}$ cut-off values are reported in literature (1, 8, 18, 19). In this study, cut-off values were based on walking-speed-specific normative values from the vestibular laboratory of the Maastricht University Medical Center. Despite the fact this study showed a moderate correlation between fHIT and OSQ, the correlation between objective and subjective tests to quantify oscillopsia is not (yet) optimal. It is possible that the used questionnaire (OSQ) captures more complaints than only oscillopsia and can be influenced by a patients' coping of BV. Lastly, in this article fHIT and $DVA_{treadmill}$ are compared. Both tests give different stimuli to the vestibular system, as described above, and are therefore never fully comparable.

To summarize, the fHIT seems feasible for quantifying oscillopsia in patients with BV. In the future, it possibly could also be used to measure functional outcome in patients implanted with a Vestibular Implant.

CONCLUSION

The functional Head Impulse Test (fHIT) is a recently proposed technique to assess functionally effective gaze stabilization. The fHIT seems to be a feasible test to objectify oscillopsia in BV since, unlike DVA assessed on a treadmill, it correlates with the experienced oscillopsia measured by the OSQ, and more BV patients are able to complete the fHIT than DVA assessed on a treadmill.

ETHICS STATEMENT

This study was in accordance with the Declaration of Helsinki (amended version 2013). Approval was obtained from the ethical committees of Maastricht University Medical Center (NL52768.068.15/METC151027). All participants provided written informed consent prior to the study.

AUTHOR CONTRIBUTIONS

HK, SR, and RvdB: design of the work; FL: acquisition; TvD, SD, and AJ: analysis; TvD, FL, NG, AP, VV, HK, SR, and RvdB: interpretation; TvD, FL, SD, AJ, NG, AP, VV, HK, SR, and RvdB: revising the work, final approval of the version to be published, and agreement to be accountable for all aspects of the work in ensuring that questions related to the accuracy or integrity of any part of the work are appropriately investigated and resolved.

FUNDING

HK and RvdB are supported by the Russian Science Foundation (project No. 17-15-01249).

SUPPLEMENTARY MATERIAL

The Supplementary Material for this article can be found online at: https://www.frontiersin.org/articles/10.3389/fneur.2019.00365/full#supplementary-material

REFERENCES

1. Strupp M, Kim JS, Murofushi T, Straumann D, Jen JC, Rosengren SM, et al. Bilateral vestibulopathy: diagnostic criteria consensus document of the classification committee of the Barany society. *J Vestib Res.* (2017) 27:177–89. doi: 10.3233/VES-170619
2. Lucieer F, Vonk P, Guinand N, Stokroos R, Kingma H, van de Berg R. Bilateral vestibular hypofunction: insights in etiologies, clinical subtypes, and diagnostics. *Front Neurol.* (2016) 7:26. doi: 10.3389/fneur.2016.00026
3. van de Berg R, Guinand N, Ranieri M, Cavuscens S, Khoa Nguyen TA, Guyot JP, et al. The vestibular implant input interacts with residual natural function. *Front Neurol.* (2017) 8:644. doi: 10.3389/fneur.2017.00644
4. van de Berg R, Guinand N, Nguyen TA, Ranieri M, Cavuscens S, Guyot JP, et al. The vestibular implant: frequency-dependency of the electrically evoked vestibulo-ocular reflex in humans. *Front Syst Neurosci.* (2014) 8:255. doi: 10.3389/fnsys.2014.00255
5. van de Berg R, Guinand N, Stokroos RJ, Guyot JP, Kingma H. The vestibular implant: quo vadis? *Front Neurol.* (2011) 2:47. doi: 10.3389/fneur.2011.00047
6. Guinand N, Van de Berg R, Cavuscens S, Stokroos R, Ranieri M, Pelizzone M, et al. Restoring visual acuity in dynamic conditions with a vestibular implant. *Front Neurosci.* (2016) 10:577. doi: 10.3389/fnins.2016.00577
7. Lucieer F, Duijn S, Van Rompaey V, Pérez Fornos A, Guinand N, Guyot JP, et al. Full spectrum of reported symptoms of bilateral vestibulopathy needs further investigation-a systematic review. *Front Neurol.* (2018) 9:352. doi: 10.3389/fneur.2018.00352
8. Guinand N, Pijnenburg M, Janssen M, Kingma H. Visual acuity while walking and oscillopsia severity in healthy subjects and patients with unilateral and bilateral vestibular function loss. *Arch Otolaryngol Head Neck Surg.* (2012) 138:301–6. doi: 10.1001/archoto.2012.4.
9. van de Berg R, van Tilburg M, Kingma H. Bilateral vestibular hypofunction: challenges in establishing the diagnosis in adults. *ORL J Otorhinolaryngol Relat Spec.* (2015) 77:197–218. doi: 10.1159/000433549
10. Anson ER, Gimmon Y, Kiemel T, Jeka JJ, Carey JP. A tool to quantify the functional impact of oscillopsia. *Front Neurol.* (2018) 9:142. doi: 10.3389/fneur.2018.00142
11. Herdman SJ, Tusa RJ, Blatt P, Suzuki A, Venuto PJ, Roberts D. Computerized dynamic visual acuity test in the assessment of vestibular deficits. *Am J Otol.* (1998) 19:790–6.
12. Bohler A, Mandala M, Ramat S. A software program for the head impulse testing device (HITD). *Conf Proc IEEE Eng Med Biol Soc.* (2010) 2010:6615–8. doi: 10.1109/IEMBS.2010.5627138
13. Colagiorgio P, Colnaghi S, Versino M, Ramat S. A new tool for investigating the functional testing of the VOR. *Front Neurol.* (2013) 4:165. doi: 10.3389/fneur.2013.00165
14. Ramat S, Colnaghi S, Boehler A, Astore S, Falco P, Mandalà M, et al. A device for the functional evaluation of the VOR in clinical settings. *Front Neurol.* (2012) 3:39. doi: 10.3389/fneur.2012.00039
15. Corallo G, Versino M, Mandalà M, Colnaghi S, Ramat S. The functional head impulse test: preliminary data. *J Neurol.* (2018) 265 (Suppl. 1):35–9. doi: 10.1007/s00415-018-8910-z
16. Vital D, Hegemann SC, Straumann D, Bergamin O, Bockisch CJ, Angehrn D, et al. A new dynamic visual acuity test to assess peripheral vestibular function. *Arch Otolaryngol Head Neck Surg.* (2010) 136:686–91. doi: 10.1001/archoto.2010.99
17. MacDougall HG, Weber KP, McGarvie LA, Halmagyi GM, Curthoys IS. The video head impulse test: diagnostic accuracy in peripheral vestibulopathy. *Neurology*. (2009) 73:1134–41. doi: 10.1212/WNL.0b013e3181bacf85
18. Fife TD, Tusa RJ, Furman JM, Zee DS, Frohman E, Baloh RW, et al. Assessment: vestibular testing techniques in adults and children: report of the therapeutics and technology assessment subcommittee of the American academy of neurology. *Neurology.* (2000) 55:1431–41. doi: 10.1212/WNL.55.10.1431
19. Hain TC, Cherchi M, Yacovino DA. Bilateral vestibular loss. *Semin Neurol.* (2013) 33:195–203. doi: 10.1055/s-0033-1354597
20. Guinand N, Boselie F, Guyot JP, Kingma H. Quality of life of patients with bilateral vestibulopathy. *Ann Otol Rhinol Laryngol.* (2012) 121:471–7. doi: 10.1177/000348941212100708
21. Tian JR, Shubayev I, Demer JL. Dynamic visual acuity during passive and self-generated transient head rotation in normal and unilaterally vestibulopathic humans. *Exp Brain Res.* (2002) 142:486–95. doi: 10.1007/s00221-001-0959-7
22. Bhansali SA, Stockwell CW, Bojrab DI. Oscillopsia in patients with loss of vestibular function. *Otolaryngol Head Neck Surg.* (1993) 109:120–5.
23. Moore ST, Hirasaki E, Raphan T, Cohen B. The human vestibulo-ocular reflex during linear locomotion. *Ann N Y Acad Sci.* (2001) 942:139–47.
24. Lambert S, Sigrist A, Delaspre O, Pelizzone M, Guyot JP. Measurement of dynamic visual acuity in patients with vestibular areflexia. *Acta Otolaryngol.* (2010) 130:820–3. doi: 10.3109/00016480903426592

Conflict of Interest Statement: SR is the author of a Patent Deposit Application regarding the technique used in the functional head impulse test and is a shareholder of the company producing of the fHIT system used in this study [Beon Solutions srl, Zero Branco (TV), Italy].

The remaining authors declare that the research was conducted in the absence of any commercial or financial relationships that could be construed as a potential conflict of interest.

frontiers in Neurology

ORIGINAL RESEARCH
published: 30 April 2019
doi: 10.3389/fneur.2019.00387

Functional Head Impulse Test in Professional Athletes: Sport-Specific Normative Values and Implication for Sport-Related Concussion

Fausto Romano[1,2,3†], *Giovanni Bertolini*[1,2,3*†], *Daniel Agostino*[3], *Dominik Straumann*[1,2,3], *Stefano Ramat*[4] *and Nina Feddermann-Demont*[1,2,3]

[1] Department of Neurology, University of Zurich, Zurich, Switzerland, [2] Clinical Neuroscience Center, University Hospital of Zürich, Zurich, Switzerland, [3] Swiss Concussion Center, Zurich, Switzerland, [4] Department of Computer, Electric and Biomedical Engineering, University of Pavia, Pavia, Italy

OPEN ACCESS

Edited by:
Daniele Nuti,
University of Siena, Italy

Reviewed by:
Jorge Kattah,
University of Illinois at Chicago, United States
Hans VanDerSteen,
Erasmus University Rotterdam, Netherlands

***Correspondence:**
Giovanni Bertolini
giovanni.bertolini@swissconcussion.com

[†]These authors have contributed equally to this work

Specialty section:
This article was submitted to Neuro-Otology, a section of the journal Frontiers in Neurology

Received: 08 January 2019
Accepted: 29 March 2019
Published: 30 April 2019

Citation:
Romano F, Bertolini G, Agostino D, Straumann D, Ramat S and Feddermann-Demont N (2019) Functional Head Impulse Test in Professional Athletes: Sport-Specific Normative Values and Implication for Sport-Related Concussion. Front. Neurol. 10:387. doi: 10.3389/fneur.2019.00387

Dizziness, slow visual tracking, or blurred vision following active head (or body) movements are among the most common symptoms reported following sport-related concussion, often related to concurrent dysfunctions of the vestibular system. In some cases, symptoms persist even if bedside and auxiliary standard vestibular tests are unremarkable. New functional tests have been developed in recent years to objectify neurological alterations that are not captured by standard tests. The functional head impulse test (fHIT) requires the patient to recognize an optotype that is briefly flashed during head rotations with various angular accelerations (2,001–6,000 deg/s^2) and assesses the proportion if correct answers (*pca*). 268 active professional athletes (23.70 ± 5.32y) from six different sports were tested using fHIT. *Pca* were analyzed both pooling head acceleration in the range of 2,001–6,000 deg/s^2 and computing a single *pca* value for each 1,000 deg/s^2 bin in the range 2,001–8,000 deg/s^2. No significant difference ($p = 0.159$) was found between responses to head impulses in the plane of horizontal (*pca*: 0.977) and vertical semicircular canals (*pca*: 0.97). The sport practiced had a major effect on the outcome of the fHIT. Handball players achieved a better performance ($p < 0.001$) than the whole athlete group, irrespective of the direction of head impulses. The *pca* achieved by athletes practicing snowboard, bob and skeleton were instead significantly below those of the whole athlete group ($p < 0.001$) but only when vertical head impulses were tested. Overall, *pca* declined with increasing head acceleration. The decline was particularly evident in the range not included in the standard fHIT exam, i.e., 6,001–8,000 deg/s^2 for horizontal and 5,001–8,000 deg/s^2 for vertical head impulses. When vertical head impulses were tested, athletes practicing snowboard, bob and skeleton (non-ball sports) showed, beside the lower overall *pca*, also a steeper decline as a function of vertical head acceleration. The findings suggest that: (1) functional VOR testing can help understanding sport-specific VOR requirements; (2) the fHIT is able to detect and objectify subtle, sport-specific changes of functional VOR performance; (3) if sport-specific normative values are used, the fHIT test procedure needs to be optimized, starting from the highest acceleration to minimize the number of head impulses.

Keywords: functional head impulse test, VOR (Vestibulo-Ocular Reflex), sport related concussion, visual acuity (VA), professional athletes, acceleration, normative data, vestibulogram

INTRODUCTION

Sport-related concussion (SRC, syn; mild traumatic brain injury), the most frequent form of traumatic brain injury, is a clinical diagnosis (1, 2) frequently based on the results of symptom scales and neurological, neuropsychological and balance examinations. Accurate assessment following a head impact is challenging. Since different domains may be affected, no clinical test, or biomarker can currently make the diagnosis in isolation (1). Furthermore, although concussion typically results in the rapid onset of short-lived functional impairments that resolve spontaneously, clinical recovery might be prolonged and unpredictable in selected cases (2, 3). Symptoms may remain, change or newly evolve during the following days, months, or years (2, 4) and continue even after alterations of clinically observable parameters have normalized. Consequently, if examinations are performed several days after the impact, the reported symptoms might not match with the picture emerging from the results of objective clinical tests (5). The latter situation, unfortunately, is not uncommon in professional athletes, where a short period of rest followed by rapid return to routine training and match play is often attempted and referral to specialized centers occurs only when symptoms fail to subside spontaneously.

These considerations call for the implementation of functional tests that, integrating the currently valid clinical tests, allow objective assessment of the functional impairment causing the symptoms occurring in real life conditions and, when considering athletes, during professional sport activities.

Dizziness has a prominent role among the symptoms reported following concussion with an incidence between 35 and 80% in athletes [it is the second most common symptom following headache in SRC (1, 6)] and up to 80% in the general population of concussed patients (7). Even more important, the presence of dizziness immediately after the impact is the single greatest risk factor for longer symptoms remission time and delayed recovery (8–10), with 18–20% of the patients still symptomatic after 2–5 years (11, 12). The high occurrence of dizziness following a head impact clearly suggests that impairments along the pathways processing visual and/or vestibular signals are common in concussed patients (13, 14). The most frequent peripheral cause of dizziness and vertigo after concussion is benign paroxysmal positional vertigo (BPPV). It is caused by the mechanical effect of the impact, dislodging calcium carbonate concrements from the otolith organs. The concrements, once loose, may enter the semicircular canals and, as a result, perturb the normal flow of endolymph required to sense head motion (15–17). Dizziness following concussion, however, may also be consequence of other peripheral, i.e., labyrinthine damage (18), or central, i.e., brainstem and cerebellar lesions (17, 19), vestibular impairment. Extensive assessment of the vestibular function is therefore critical to identify the cause of dizziness following concussion (5).

The rotational vestibulo-ocular reflex (VOR) aims at stabilizing vision by generating eye movements precisely compensating for head rotation. Testing the VOR is an excellent method to test the functioning of the vestibular organs, since a direct, rapid three-neurons pathway connects the semicircular canals with the eye muscles (20). The head impulse test (and its video-oculography based adaptation, the video head impulse test—vHIT) (21–23) quantifies the VOR responses to head accelerations at frequencies (1–5 Hz) (24) in the upper range of natural head movements (25). It consists in asking the patient to keep fixation on a stationary target while the examiner imposes a small, abrupt rotation of his/her head along the plane of a single canal pair. Randomly alternating impulses in both directions, the test assesses the functioning of each single canal. Since each pair of semicircular canals works in in a push-pull mechanism, a head impulse in one direction inhibits the afferents from one canal and excites those from the other. Accordingly, if the impulse exceeds a velocity threshold (around 200 deg/s) (26), the afferents of the inhibited side reach inhibitory cut off (i.e., zero firing rate) and the response to the amount of head velocity above threshold is accounted for by the excited canal only. The test outcome (denoted as "VOR gain") is the ratio of a measure of eye movement to the corresponding head movement (e.g., eye velocity/head velocity) averaged within a time window. The VOR gain objectively quantifies the percentage of head movement compensated by the ocular motor response. From a clinical perspective, the assessment of VOR gain with vHIT is therefore of primary importance to exclude that dizziness in a concussed patient derives from an impairment of the semicircular canals.

On the other hand, while VOR gain tells us whether the compensatory eye movements indicate a normal functioning of the semicircular canals, it does not directly assess the functional effectiveness of such movement, i.e., if gaze stabilization was sufficient to permit clear vision. It is indeed not uncommon that athletes who suffered a SRC report blurred vision or fogginess during fast head movements, even in presence of a normal VOR gain (27). This may originate from different impairments ranging from suboptimal visual processing (slower visual processing speed or reduced retinal slip tolerance) (28, 29), to an insufficiently long period of optimal visual stability during the head impulse. In fact, visual stabilization is achieved by a complex combinations of eye movements consisting of an optimal tradeoff between head position and head velocity compensation (30) at any instant of the head movement. Testing the functional effectiveness of VOR for head impulses is therefore complementary, not identical, to the vHIT.

Currently, two tests have been developed to assess the functional performance of the VOR during passive head impulses: the dynamic visual acuity test (DVA) (31–33) and the functional head impulse test (fHIT) (34–36). They both assess VOR function by requiring the patient to identify an optotype briefly presented during the passive head impulses. Their outcome, however, is profoundly different. The DVA first determines the minimum size optotype that can be recognized while keeping the head still (static visual acuity, measured in term of the visual angle it subtends—logMAR) and then quantify the decrease in visual acuity occurring during head impulses (called dynamic visual acuity) keeping the range of head angular accelerations and speeds as consistent as possible (37, 38). The fHIT, after assessing the static visual acuity, quantifies the percentage of correctly recognized optotypes using a relatively large, fixed-size optotype (0.6 logMAR larger than the static

visual acuity) during head impulses scanning a wide range of head angular accelerations (2,001–6,000 deg/s^2). The two systems provide therefore two different assessments. The DVA, by measuring the decrease of a functional parameter, quantifies how much head movements with high acceleration and high frequency degrade visual acuity, but it does not evaluate if and how this degradation leads to a practical impairment in daily activities. The fHIT, by measuring performance in a task that should be flawlessly executed by healthy individuals [the 0.6 logMAR increase was selected to minimize error in healthy individuals in the range 1,001–4,000 deg/s^2 (39)], identifies how much the actual stabilization ability is impaired as head acceleration increases, but does not provide a measure of the actual degradation of visual acuity (40). In short, the DVA quantifies the amount of lost visual acuity during head motion while the fHIT the residual performance in a standardized, simple visual task.

The current paper focuses on the fHIT, since it directly assesses VOR functional performance across different head accelerations. We hypothesize that the fHIT may indeed capture the specific performance level required for the professional activity of athletes and help therefore to objectify the impairment underlying dizziness and blurred vision occurring on the field. Accordingly, since diagnosis with functional vestibular tests is based on the comparison of the patients' behavior with that of healthy individuals, we speculate that group-specific references are necessary for professional athletes.

The aim of the current study was therefore to evaluate the outcomes of the fHIT in a large population of healthy professional athletes, investigate differences among sports with high risks of concussion and quantify the effect of different head accelerations. To our knowledge, since no previous study investigated how the fHIT (or even DVA) outcomes vary as a function of the head acceleration, this study is also the first to address this question on the functional testing of the vestibular system.

MATERIALS AND METHODS

Two hundred and sixty nine active athletes (23.70 ± 5.32 [15, 39] y.o.; average ± sd [min, max]) were included (named *whole athlete group*). They were considered professional in six different sports considered at risk of concussion [four contact and ball-based sports (American football, football, handball, ice hockey) and two non-contact winter sports (bob and skeleton, snowboard) (41)—see **Table 1** and **Figures 1A,C** for additional details]. The athletes' ages were adequately distributed across the range tested, counting at least 5 athletes per year (**Figure 1B**).

As control, 26 healthy individuals (27.26 ± 6.19 [20, 40] y.o.) not practicing any sport activities at professional level were included (named *control group*). Data were extracted from the normative population provided by the company commercializing the fHIT device that was used in this study (Beon Solution, Zero Branco (TV), Italy), discarding the subjects above 40 y.o..

The study protocol was approved by the local ethics committee (cantonal ethics commission Zürich, KEK-ZH-2018-01168) and was in accordance with the ethical standards laid down in the 2013 Declaration of Helsinki for research involving human subjects. Written informed consent was obtained from each participant. For the participants under the age of 18, written informed consent was obtained from the parents or guardians of participants.

Experimental Setup and Procedure

The experimental setup and the testing procedure replicated the one first introduced by (35), validated on patients with vestibular deficits (40, 42), and now commercially distributed as fHIT (Beon Solutions, Italy).

In brief, all recordings were obtained with the athlete seated on a chair placed at 150 cm distance from a computer screen connected with the fHIT device. The athletes using mean of static visual acuity correction (e.g., contact lenses), were requested to wear them during the test. A trained operator performed subsequent head impulses, consisting of brief, small rotatory movements impressed with both hands to the head of the athlete in the plane of each semicircular canals pair. An optotype, the Landolt ring, was displayed for 80 ms on the computer screen (60 Hz) when the imposed head angular acceleration and velocity exceeded pre-defined thresholds. The athlete was requested to recognize the ring orientation reporting it on a keypad showing all possible ring orientations. The Landolt ring allows 8 different orientations reducing the probability of random correct answers respect to the Sneller E optotype, which typically is presented only in 4 orientations (43). The ring size was adjusted according to a preliminary test of static visual acuity, increasing the smallest line seen by 0.6 LogMAR (39). No time limit was set to provide the answer after each impulse. To test the vertical semicircular canals, the chair was rotated 45 degrees (to the left for the left-anterior-right-posterior semicircular canal plane and to the right for the right-anterior-left-posterior plane). The athlete was asked to counterrotate the head to look straight at the screen and impulses were performed in the sagittal plane of the athlete's body. This procedure allows testing the recognition of the optotype during impulses with the eye starting from the primary position (i.e., the visual axis is aligned with head straight ahead axis), reducing the risk that occlusions from the eyelids or the constraints of the oculomotor system (e.g., Listing law) affect the test outcome. The software of the fHIT device guided the initial positioning of the head to ensure that the impulses are performed in the planes of each pair of vertical canals.

The operator performed a minimum of 10 head impulses in each direction for each semicircular canal plane (Left horizontal [11, 36] [min, max]; Right horizontal [12, 35]; Left Anterior [11, 32]; Right Posterior [11, 31]; Right Anterior [11, 29]; Left Posterior [10, 33]) attempting to achieve accelerations covering all the 1,000 deg/s^2 bins from 3,000 deg/s^2 to 8,000 deg/s^2 according to the classification of the fHIT software (e.g., the 3,000 deg/s^2 bin includes the acceleration range between 2,001 and 3,000 deg/s^2).

TABLE 1 | Sport and age distributions of athletes.

Sport type		Number of subjects	Gender distribution		Age (mean ± std y.o.)
			M	F	
Ball sports	American Football (AF)	13	13	0	21.8 ± 3.7
	Football (FB)	40	40	0	17.5 ± 1.2
	Handball (HB)	43	43	0	25.1 ± 4.0
	Ice Hockey (IH)	118	118	0	26.2 ± 5.3
Non-ball sports	Bob and Skeleton (BS)	31	21	10	23.5 ± 4.2
	Snowboard (SB)	24	13	11	20.8 ± 3.1

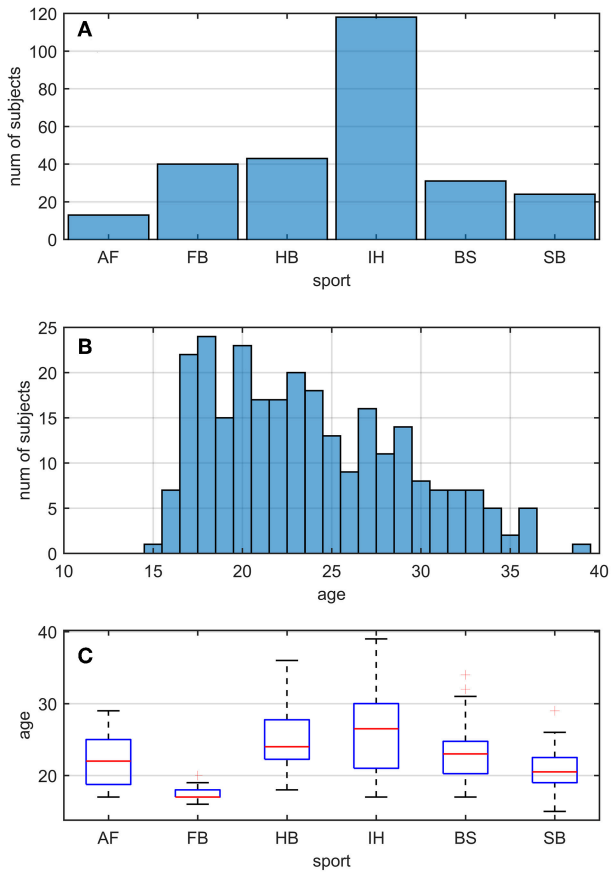

FIGURE 1 | Sport and age distributions of athletes. AF, American Football; FB, Football; HB, Handball; IH, Ice Hockey; BS, Bob and Skeleton; SB, Snowboard. **(A)** Number of athletes divided by sport. **(B)** Age distribution in the athletes. As visible, for each bin of one y.o. (expect for 15, 35, and 39), our data counted at least five athletes. **(C)** Boxplots of age distribution per sports. Despite sport groups did not cover overlapping age ranges, no relationship between and test performance was found (see Pooled Bin Approach: Between Sports Analysis in Results).

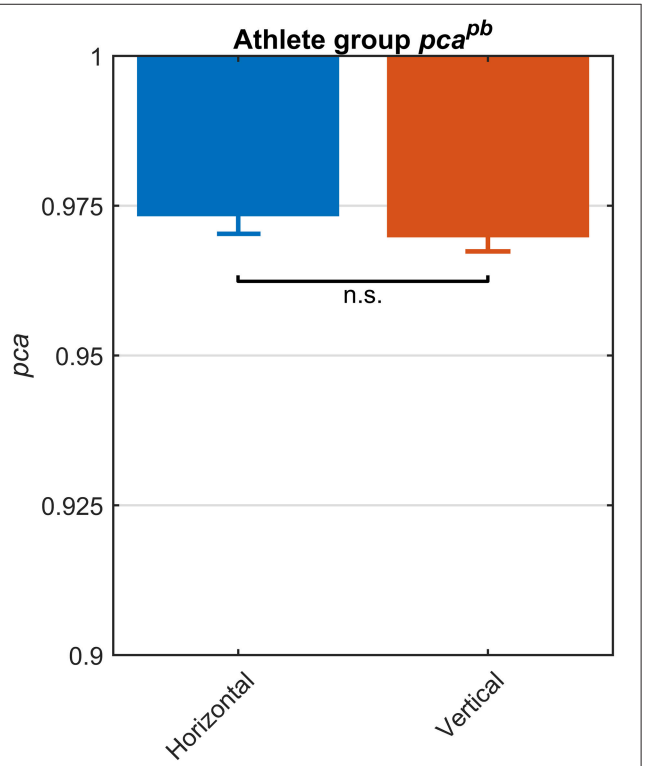

FIGURE 2 | Proportions of correct answers (*pca*) for each vestibular canal in the *whole athlete group*. *Pca* of impulses performed in the horizontal (blue) and vertical canals (red) were computed using the pooled approach (Equation 1) considering only head movements in the range of 2,001–6,000 deg/s^2. Zeta distribution was used to estimate the lower bound of 95% confidence interval for *pca,* as the number of trials (i.e., performed head movements) was large enough (>>200). As visible, the fHIT performance was not significant influenced by canals (n.s.).

Data Analysis

The fHIT software automatically separated the trials (i.e., head impulses) according to the acceleration bins defined above and the semicircular canal stimulated. For each bin of acceleration a, two variables were used for the data analysis, the number of trials t_a performed by the tester and the number of correct answers c_a (e.g., for a = 5,000 deg/s^2, t_{5000} and c_{5000} were used). Data were imported in MATLAB Version R2016b (The Mathworks, Natick, MA, USA) and further data analysis was performed using custom-written programs.

Data from different semicircular canal planes were grouped, creating two "virtual" semicircular canals, a horizontal and a vertical canal. Specifically, for the "virtual" horizontal canal, the t_a and c_a of left and right horizontal semicircular canals were

grouped together, while left and right semicircular canals of the anterior and posterior canals were grouped into the t_a and c_a of the "virtual" vertical canal. Such approach was considered since it is not in the scope of the current study to investigate natural asymmetries between and within the left and right vestibular organs and it is reasonable to assume that the overall population of the tested athletes has negligible systematic asymmetries.

Pooled Bin Approach

fHIT Procedure

As established by the fHIT procedure, the test performance was assessed estimating the proportion of correct answer (*pca*). The *pca* was computed using the procedure proposed by (35), called pooled bin approach *(pb)*. Specifically, the data in the acceleration bins ranging from 3,000 to 6,000 deg/s^2 were pooled together and the *pca* was computed as follow:

$$pca^{pb} = \frac{\sum_{s=1}^{n_{subjs}} \sum_{a=1}^{n_{bins}} c_{sa}}{\sum_{s=1}^{n_{subjs}} \sum_{a=1}^{n_{bins}} t_{sa}} \quad (1)$$

with $n_{bins} = 4$ (i.e., the number of acceleration bins) and n_{subjs} = the number of athletes considered for the *pca* estimation. It is worth noting that the *pb* approach does not consider between-subject variability, creating an *pca* estimation of the whole group (Equation 1). The 7,000 and 8,000 deg/s^2 bins were excluded in the *pb* approach, according to the procedure used by the fHIT software when comparing a single patient to the reference population. To compare the estimated *pca* between different groups, the Zeta-test for two proportions was used, keeping in line with the procedure used by the fHIT software.

Comparisons Between PCA of the PB approach

The *pb* approach was used to perform three analyses: between-canals, between-sports, and *whole athlete group* vs. *control group*.

Between-canals analysis: The analysis aimed at assessing potential differences between the athletes' performances during horizontal and vertical head movements. The pca^{pb}_{hor} and the pca^{pb}_{vert}, obtained using Equation 1 on the data of the virtual horizontal and semicircular canals, respectively, were compared.

Between-sports analysis: The analysis aimed to compare the performance of each subgroup of athletes pooled by sport to the *whole athlete group*. Six comparisons were performed, one per sport, testing whether the pca^{pb}_{sport} of the athletes from one sport (e.g., pca^{pb}_{HB} for handball, see **Table 1** for sport coding) was different to the pca^{pb}_{ath} of the *whole athlete group*. In this series of comparisons, the α used for the Zeta test was corrected using Bonferroni procedure to reduce the type-1 error due to multiple comparisons ($\alpha_{bonf} = \frac{\alpha}{n_{comparison}} = \frac{0.05}{6} = 0.0083$; with $n_{comparison} = n_{sports} = 6$). The analysis procedure was performed separately for the horizontal and vertical canal.

Whole athlete group vs. control group analysis: The analysis aimed at assessing whether the fHIT discriminates between *whole athlete group's* and *control group's* performances, comparing the pca^{pb}_{ath} of athlete *group* to the one of *control group* (pca^{pb}_{ctr}). Such procedure was performed only for the horizontal canal, as no normative data of anterior and posterior canals was available.

Single Bin Approach

To test whether a relationship between the proportion of correct answers and head accelerations exists in the *whole athlete group*, a single bin *(sb)* procedure was used. Compared to the *pb* approach (Equation 1), where trails with different head accelerations (up to 6,000 deg/s^2) were pooled, here the proportion of correct answers was computed separately for each bin of acceleration (*a*) as follows:

$$pca^{sb}_{a} = \frac{\sum_{s=1}^{n_{subjs}} c_{sa}}{\sum_{s=1}^{n_{subjs}} t_{sa}} \quad (2)$$

with n_{subjs} = the number of athletes considered for the *pca* estimation.

Relationship Between PCA and Head Acceleration

To avoid postulating any assumption on the relationship between the *pca* and the head acceleration, all 15 possible pairs of the six pca^{sb}_{a} (one per acceleration bins between 3,000 deg/s^2 and 8,000 deg/s^2), were compared using the Zeta-test for proportions (i.e., 15 zeta-tests). According to the Bonferroni correction, a *p*-value lower than 0.003 was considered statistically significant ($\alpha_{bonf} = \frac{\alpha}{n_{comparison}} = 0.05/15$). Analyses were performed separately for horizontal and vertical canals.

Relationship Between PCA and Head Acceleration Within Sports

The same approach was used to evaluate the effects of acceleration within each sport. To limit the number of statistical comparisons and the associate *p*-value corrections, two subgroups of athletes were defined using one characteristic of sports, namely if a ball is used or not. The two groups were named the ball and non-ball group, respectively. The ball group included American football, soccer, handball and ice-hockey athletes, while the non-ball group included snowboard, bob and skeleton athletes. As described for the *whole athlete group*, six pca^{sb}_{a} were estimated (one for each acceleration bin) and compared each pair of accelerations (15 comparisons). Additionally, comparison between ball and non-ball groups was performed for each bin of acceleration (e.g., $pca^{sb\ -Ball}_{a=3000\ \mathrm{deg}/s^2}$ *vs* $pca^{sb-\ nonBall}_{a=3000\ \mathrm{deg}/s^2}$), adding 6 more comparisons. Bonferroni procedure was used to correct the significance level of z-tests ($\alpha_{bonf} = \frac{\alpha}{n_{comparison}} = 0.05/21 = 0.0024$).

RESULTS

Pooled Bin Approach

Horizontal vs. Vertical Canals

The fHIT test outcome computed over the *whole athlete group* according to the standard procedure of the fHIT software (i.e., pooling the acceleration bins in the range 3,000–6,000 deg/s^2) evidenced no differences between head impulses in the plane of the horizontal and of the vertical canals (**Figure 2**). The *pca* of vertical canals ($pca^{pb}_{vert} = 0.970$) was only ∼0.3% less than the

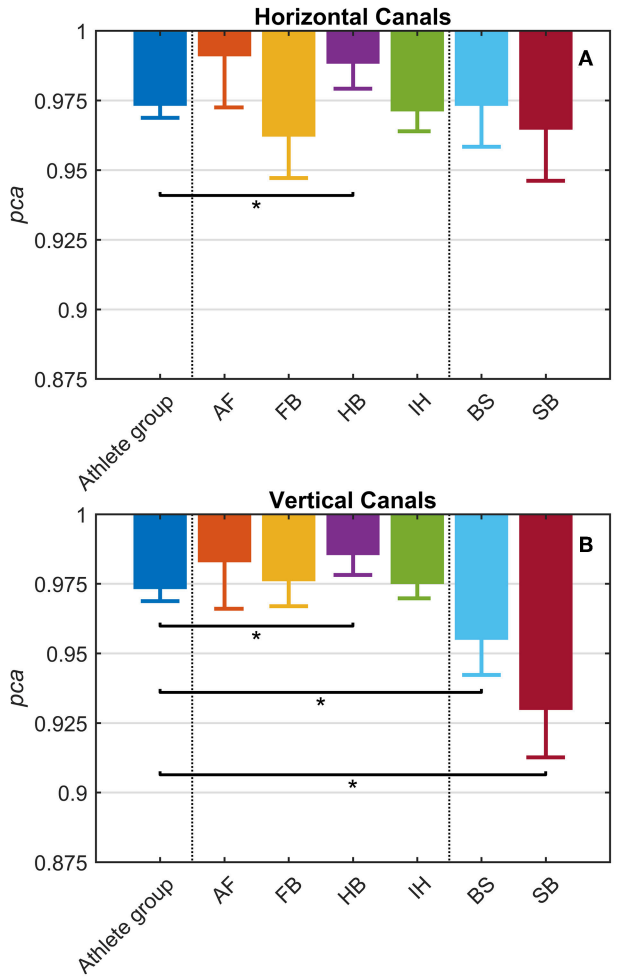

FIGURE 3 | Proportion of correct answers (*pca*) in the *whole athlete group* and single sport. AF, American Football; FB, Football; HB, Handball; IH, Ice Hockey; BS, Bob and Skeleton; SB, Snowboard. For ease of visualization, the dashed vertical lines separate the *whole athlete group* from the ball sports (first vertical line) and the non-ball sport (second vertical line). All *pca* were computed using the pooled approach (Equation 1) considering only head movements in the range of 2,001–6,000 deg/s^2. Zeta distribution was used to estimate the lower bound of 95% confidence interval (*c.i.*) for *pca,* as the number of trials (i.e., head movements) was large enough (>>200). The asterisk (*) represents the statistically significant comparisons (*p*-value < α_{bonf} = 0.0083). **(A)** *Horizontal canals.* HB players (violet bar) showed a significant higher fHIT performance (*pca* >0.975) respect to the *whole athlete group* (dark blue bar). **(B)** *Vertical canals.* The fHIT performance in vertical canal was clearly lower *pca* in the non-ball sport players (i.e., BS and SB, respectively the light blue and dark red bar) respect to the *whole athlete group*. HB player, instead, confirmed the same finding for the horizontal canals, achieving a higher *pca* for impulses performed in the vertical canals as well.

pca of the horizontal canals (pca^{pb}_{hor} = 0.972); accordingly, the Zeta-test did not show a significant difference (p = 0.159).

Between Sports Analysis

Each sport showed distinctive fHIT performance levels for head impulses in the plane of the horizontal and vertical canals, suggesting that the specific sports practiced by an athlete has a relation with his/her *pca* (**Figure 3**). Such observation is also confirmed by the multiple comparisons (see **Table 2**). Despite a non-significant difference was found between head impulses in the plane of the horizontal and vertical canals in the *whole athlete group*, between-sport analysis revealed that a canal–sport interaction was present. The sport-specific pca^{pb}_{sport} estimated on the tested athletes are presented in **Table 2**.

Only handball players (HB) showed significantly higher performance than the *whole athlete group* irrespective of the tested canal (horizontal canals: p = 0.002; vertical canals: $p < 0.001$). The *pca* of HB players was ∼1.5% higher than the *pca* of the *whole athlete group* for both the horizontal canals (pca^{pb}_{HB} = 0.989 vs. pca^{pb}_{ath} =0.973) and the vertical canals (pca^{pb}_{HB} = 0.986 vs. pca^{pb}_{ath} = 0.970).

Two out of three winter sports, snowboard (SB) and bob and skeleton (BS), showed a *pca* lower than the *pca* of the *whole athlete group*, but limited to head impulses stimulating the vertical canals (BS: p = 0.002; SB: $p < 0.001$—light blue and dark red bars of **Figure 3B**). Despite the *pca* of the SB athletes appears to be lower than the one of the *whole athlete group* also for impulses in the plane of the horizontal canals (**Figure 3A** and **Table 2A**), the difference was not significant. The non-uniform distribution of age and gender among sports (**Figure 1** and **Table 1**) poses the question of whether these factors rather than the sport may influence the fHIT outcome.

Using Equation 1, a *pca* was estimated grouping the athletes by age, using one-year-old bins. No significant association between age and *pca* was found (**Figure 4**) both for head impulses in the

TABLE 2A | Single sport vs. *whole athlete group*—horizontal canals.

Compared sport		pca^{pb}_{sport}	$pca^{pb}_{athletes}$	*P*-value
Ball sports	AF	0.991	0.973	0.043
	FB	0.962	0.973	0.045
	HB	0.989	0.973	0.002
	IH	0.971	0.973	0.595
Non-ball sports	BS	0.973	0.973	0.991
	SB	0.965	0.973	0.187

PCA was estimated using the pooled bin approach (Equation 1). Using the Bonferroni correction, only p < 0.0083 (highlighted in gray) were consider statistically significant.

TABLE 2B | Single sport vs. *whole athlete group*—vertical canals.

Compared sport		pca^{pb}_{sport}	$pca^{pb}_{athletes}$	*P*-value
Ball sports	AF	0.983	0.970	0.077
	FB	0.976	0.970	0.127
	HB	0.986	0.970	< 0.001
	IH	0.975	0.970	0.052
Non-ball sports	BS	0.955	0.970	0.002
	SB	0.930	0.970	< 0.001

PCA was estimated using the pooled bin approach (Equation 1). Using the Bonferroni correction, only p < 0.0083 (highlighted in gray) were consider statistically significant.

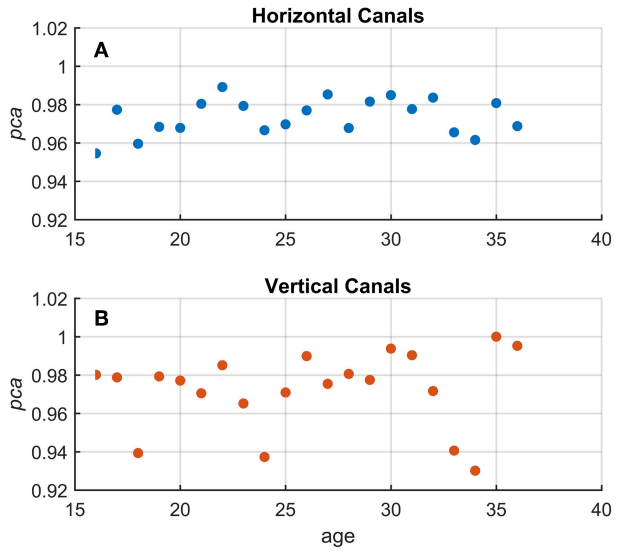

FIGURE 4 | Relationship between age and proportion of correct answers (*pca*) in the *whole athlete group*. Each point in the scatter plot represents a *pca* estimated in subgroups of athletes pooled by age (1-year-old bin). All *pca* were computed using the pooled approach (Equation 1) considering only head movements in the range of 2,001–6,000 deg/s^2. As evident in the two scatter plots for fHIT performed in the horizontal (**A** and blue points) and vertical (**B** and red points), the point dispersal did not argument any potential correlation and/or interaction between the age and *pca* (i.e., test performance). The values of *pca* appear, indeed, randomly distributed regardless of age in a range between 1–0.95 and 1–0.92 for the horizontal and vertical canals, respectively.

plane of the horizontal (Kendal's τ coefficient = 0.13; $p = 0.420$) and vertical canals (Kendal's τ coefficient = 0.143; $p = 0.386$).

The potential gender effect was tested comparing the *pca* estimated for the female and male athletes. No significant difference ($p = 0.14$) was found in fHIT performance for head impulses in the plane of the horizontal canals ($pca^{pb}_{female} = 0.965$ vs. $pca^{pb}_{male} = 0.974$). The results of the head impulses in the plane of the vertical canals evidenced that male athletes had a significantly higher *pca* ($p < 0.001$) than female ones ($pca^{pb}_{female} = 0.945$ vs. $pca^{pb}_{male} = 0.973$, see **Figure 5A**). The sample of female athletes, however, was composed entirely by athletes of the two sports with the lowest performance for head impulses in the plane of the vertical canals (i.e., BS and SB, **Table 2B**). The comparison of the *pca* of the male and female athletes subgroups within these two sports (**Figures 5B,C**), showed no significant difference between female and male athletes both in BS ($pca^{pb}_{female} = 0.944$ vs. $pca^{pb}_{male} = 0.961$, $p = 0.104$), and in SB ($pca^{pb}_{female} = 0.941$ vs. $pca^{pb}_{male} = 0.919$, $p = 0.133$). Furthermore, since even the non-significant differences between genders have opposite signs in the two sports (i.e., female are better in SB and worse in BS), it is therefore evident that the finding of an overall gender difference is due to the non-uniform distribution of genders between sports (**Table 1**—i.e., all female athletes in the sample are from sports with lower fHIT outcomes).

Athlete Group vs. Control Group

To investigate whether sport activity at professional level affects athletes' performance in fHIT, their *pca* was compared to the one of the *control group*, extracted by the normative dataset of the fHIT.

Despite the two groups were not age-matched ($p = 0.001$), their age ranges were comparable and, as confirmed in **Figure 4**, no relationship between age and *pca* was found in the range 16−39 y.o.

The *athletes group* and the *control group* showed comparable pca^{pb} (**Figure 6**) and a clear overlap between the lower limits of 95% confidence intervals. Such tendency was confirmed by Zeta-test. Accordingly, the test did not show a significant difference ($p = 0.089$) between the *pca* of *whole athlete group* ($pca^{pb}_{ath} = 0.973$) and *control group* ($pca^{pb}_{ctr} = 0.977$).

Since the *pca* of the HB players was significantly higher than the *one* of the *whole athlete group* (**Table 2A**), it was worth it to compare HB subgroup to *control group*. The *pca* of HB players revealed ($pca^{pb}_{HB} = 0.989$) a significantly higher performance ($p = 0.034$) than *control group* ($pca^{pb}_{ctr} = 0.977$).

Single Bin Approach

Relationship Between Head Acceleration and PCA in the Athlete Group

The influence of head acceleration on the fHIT outcome is visible in **Figure 7**, where the athletes' *pca* clearly decreases for the highest head accelerations tested. The effect distinctively emerges by the series of comparisons between the pca of all possible pairs of acceleration bins (**Tables 3A**,**B**).

For impulses in the plane of the horizontal canals, a significant worsening of fHIT performance was shown for the range of acceleration 6,001–8,000 deg/s^2 compared to the one between 2,001 and 5,000 deg/s^2 (see **Table 3A** for *p*-values). Specifically, the *pca* of the 7,000 deg/s^2 bin ($pca^{7000\,deg/s^2}_{athletes} = 0.941$) was significantly higher than the pca of the 3000 ($pca^{3000\,deg/s^2}_{athletes} = 0.982$, $p < 0.001$), 4000 ($pca^{4000\,deg/s^2}_{athletes} = 0.975$, $p < 0.001$) and 5,000 deg/s^2 ($pca^{5000\,deg/s^2}_{athletes} = 0.971$, $p < 0.001$) bins, showing a decrease of ∼4.1, ∼3.5, and ∼3%, respectively. As expected, such decreases remain significant (**Table 3A**) for higher acceleration as well (i.e., 8,000 deg/s^2 bin, $pca^{8000\,deg/s^2}_{athletes} = 0.909$).

An earlier decline of performance with increasing head acceleration is observed for impulses in the planes of the vertical canals (**Figure 7**, red curve). The worsening of fHIT outcome was indeed already significant for accelerations 1,000 deg/s^2 lower than for impulses in the plane of the horizontal canals. Specifically, the Zeta tests revealed a significant decrease ($p < 0.001$) of *pca* in the range 4,001–8,000 deg/s^2 compared to the range 2,001–4,000 deg/ s^2 (**Table 3B**). This worsening is particularly evident in the two bins not considered in the pooled bin approach (7,000 and 8,000 deg/s^2), where the performance decreases exceed 5% ($pca^{7000\,deg/s^2}_{athletes} = 0.929$, $pca^{8000\,deg/s^2}_{athletes} = 0.910$) of the *pca* achieved in the lowest accelerations bins (i.e., $pca^{2000\,deg/s^2}_{athletes} = 0.983$, $pca^{3000\,deg/s^2}_{athletes} = 0.977$).

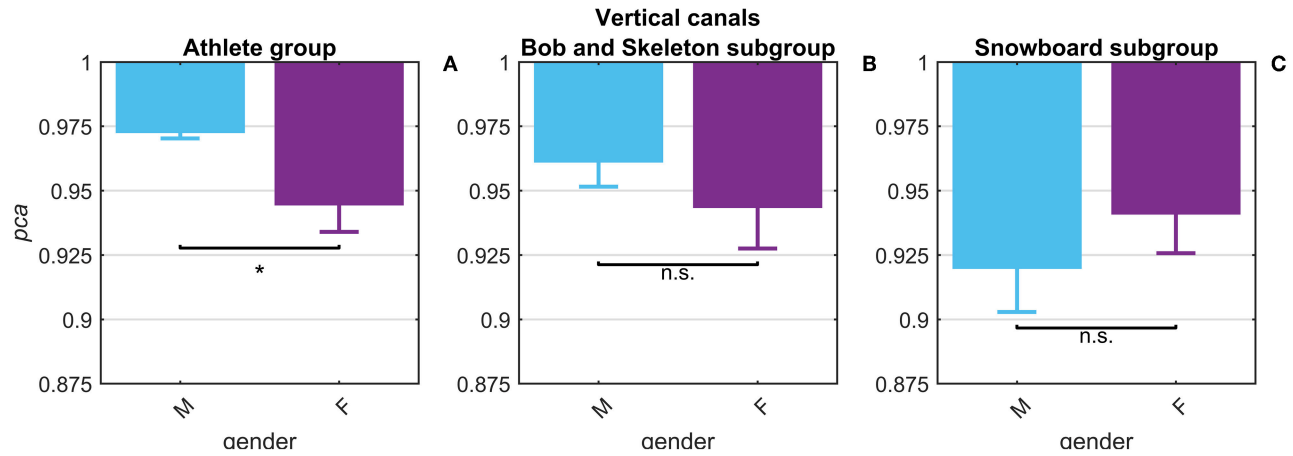

FIGURE 5 | Gender effect on proportion of correct answers (*pca*) for impulses in the plane of the vertical canals. Each bar represents the complement of *pca (*i.e.*, 1-pca)* estimated in subgroups of athletes pooled by gender (female: violet bars; male: light blue bar). All *pca* were computed using the pooled approach (Equation 1) considering only head movements in the range of 2,001–6,000 deg/s^2. Confidence intervals for *pca* were estimated as in **Figure 3**. The asterisk (*) represents the statistically significant comparisons (*p*-value $<$ $\alpha = 0.05$). Using the *athlete group* **(A)**, the *pca* estimated in the subgroups of female athlete was significant lower than the *pca* of male athlete. The effect of gender on fHIT performance, however, was not present considering also the sport factor **(B,C)**. The significant difference between genders, indeed, was induced by a non-uniform distribution of female athletes that were recruited only in the two sports (BS and SB) with the lowest *pca* for impulses performed in the vertical canals (see **Table 2A**).

Relationship Between Head Acceleration and PCA in the Ball and Non-ball Subgroups

A further analysis of the relationship between head acceleration and *pca* was performed on two subgroups of athletes, separating the sports where no balls are used (BS and SB) from those where the athletes needs to focus their attention on a ball-like object (AF, FB, HB, IH). The performance for head impulses in the plane of the horizontal canals did not differ between the two groups, as evidenced by the two overlapping curves in **Figure 8A**. The zeta tests did not show significant differences when comparing the *pca* of ball and non-ball groups within each bin of acceleration tested ($p > 0.36$, for individual *p*-values see **Table 4A**).

A different finding emerged from the analysis of the head impulses in the plane of the vertical canals (**Figure 8B**). The *pca* of the group of athletes from ball sports was significantly greater than the one of non-ball sports, regardless of the head accelerations ($p < 0.006$, for the single p-values see **Table 4B**). Pooling together all bins (from 3,000 up to 8,000 deg/s^2), the non-ball group showed a ∼5% lower *pca* than the ball group ($pca^{3000-8000\,\mathrm{deg}/s^2}_{non-ball} = 0.929$, $pca^{3000-8000\,\mathrm{deg}/s^2}_{ball} = 0.978$).

Despite the difference in the fHIT outcome emerges at all head accelerations, the two curves in **Figure 8B** evidence that the two subgroups present two different relationships between head acceleration and *pca*. In the non-ball group, the *pca* of the 3,000 and 4,000 deg/s^2 bins was significantly higher than that of the last three bins (6,000, 7,000, and 8,000 deg/s^2 - *p*-values in **Table 5B**). Furthermore, the *pca* decrease did not "slowdown" at higher accelerations. The *pca* in 5,000 deg/s^2 bin ($pca^{5000\,\mathrm{deg}/s^2}_{non-ball} = 0.939$) was still significantly higher than the ones in the 7,000 and 8,000 deg/s^2 bins ($pca^{7000\,\mathrm{deg}/s^2}_{non-ball} = 0.843$, $pca^{8000\,\mathrm{deg}/s^2}_{non-ball} = 0.807$), and the *pca* in 6,000 deg/s^2 bins was also significantly higher than the one in the 8,000 deg/s^2 bin ($pca^{6000\,\mathrm{deg}/s^2}_{non-ball} = 0.906$).

In the ball group, only the comparisons involving the two lowest acceleration bins (3,000 and 4,000 deg/s^2, *p*-values in **Table 5A**) were significant. Specifically, the *pca* in the 3,000 deg/s^2 bin ($pca^{3000\,\mathrm{deg}/s^2}_{non-ball} = 0.987$) was significantly higher only than the *pca* in the 5,000 and 6,000 deg/s^2 bins ($pca^{5000\,\mathrm{deg}/s^2}_{non-ball} = 0.974$, $p = 0.002$; $pca^{6000\,\mathrm{deg}/s^2}_{non-ball} = 0.969$, $p < 0.001$), while more surprisingly only in the 6,000 deg/s^2 bin the ball group showed a significant reduction ($p < 0.001$) of the *pca* compared to the 4,000 deg/s^2 ($pca^{4000\,\mathrm{deg}/s^2}_{non-ball} = 0.974$). These isolated differences suggest that the decrease of reading performance with increasing acceleration in the ball group, if any, is relatively weak and is masked by the increase of measure variability observed at higher accelerations.

DISCUSSION

According to the fHIT outcome, functional performance of the vestibular ocular reflex (VOR) was close to perfection in the professional athletes tested, granting them a clear vision during head motion. The reading performance, quantified by an overall proportion of correct answer >97% for head accelerations ranging 2,001–6,000 deg/s^2, was independent of the semicircular canals tested (i.e., horizontal or vertical). Head acceleration, on the other hand, affected reading performance. The effect, which is prominent for accelerations exceeding 6,000 deg/s^2 (>5% difference to the 3,000 deg/s^2 bin), differed between horizontal and vertical head impulses, with the latter showing a significant decline already within the range of accelerations used in the standard fHIT outcome measure (i.e., 2,001–6,000 deg/s^2).

Within the overall high level of performance, sport specific differences were also observed (**Table 2**). Handball players performed better in the fHIT than the overall population of

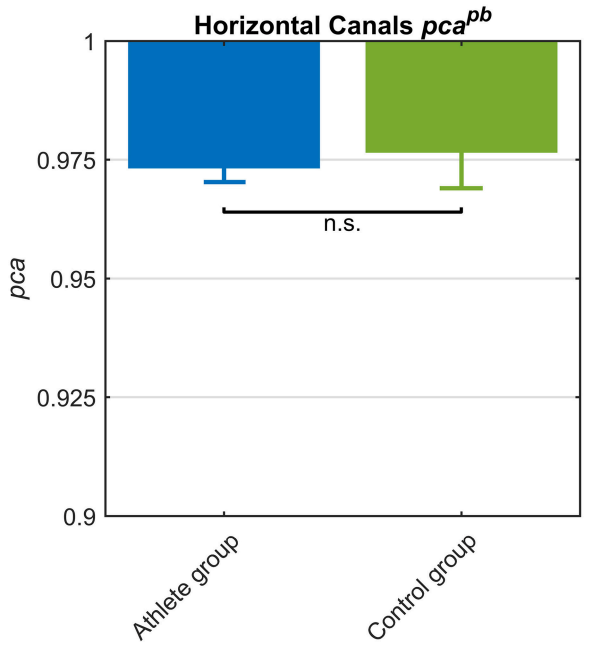

FIGURE 6 | Proportion of correct answers (*pca*) in *whole athlete group* (blue) and *control group* (green). The two *pca* for the impulses performed in the plane of the horizontal canals were computed using the pooled approach (Equation 1) considering only head movements in the range of 2,001–6,000 deg/s^2. Confidence intervals for *pca* were estimated as in **Figure 3**. The *whole athlete group* and *control group* showed a comparable performance for impulses performed in the horizontal canals, as showed by the overlapping *c.i.*. Accordingly, the *pca* were revealed no significant (n.s.) different by Zeta test (see section Results).

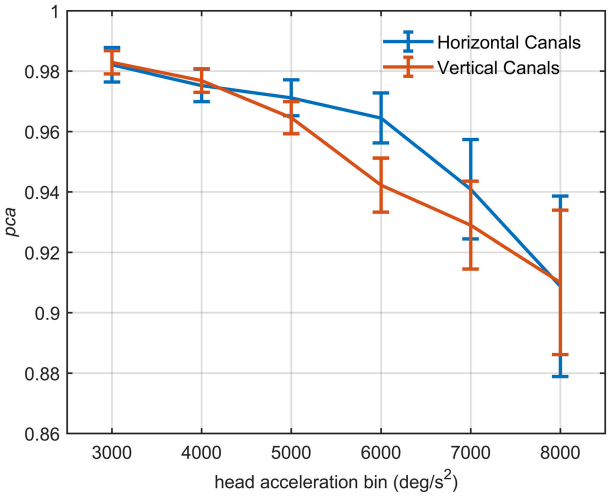

FIGURE 7 | Proportion of correct answers (*pca*) of the *whole athlete group* at different head acceleration bins. The error bars represent the *pca* and 95% confidence intervals estimated for bin of acceleration (3,000–8,000 deg/s^2). *Pca* were computed using the single approach (Equation 1) for impulses performed in the plane of the horizontal (blue line) and vertical (red line) canals. Confidence intervals for *pca* were estimated as in **Figure 3**. The relationship between head acceleration and test performance appeared different between the two tested vestibular canals. The vertical canals showed, indeed, a significant decrease of the *pca* already from the 5,000 deg/s^2 bin, while for the horizontal canal, the worsening in performance occur only after the 6,000 deg/s^2 bin (**Table 3**).

athletes tested (*whole athlete group*), irrespectively of the plane of head rotations (i.e., both for vertical and horizontal canals stimulations). Athletes practicing bob, skeleton and snowboard performed worse for head impulses in the vertical planes than the overall population of athletes tested (i.e., for vertical canals only). Although age and gender distributions differed between the groups, the absence of any overall correlation between age and the fHIT outcome, and the absence of a gender effect within the sports where both males and females were tested, suggest that age and gender inhomogeneity played no role in the observed sport-specific differences.

At first sight, sport-related differences as small as few percentage points may appear of little importance in relation to the almost perfect response rate of the *whole athlete group*. These values as well as the effect of head acceleration, however, have considerable relevance for three different aspects: (1) to understand the sport-specific requirement for functional VOR performance; (2) to improve the interpretation of the fHIT and clarify its relevance when testing athletes; (3) to adjust the testing procedure of the fHIT with respect to testing athletes.

Sport-Specific Requirement for Functional VOR Performance

The sport-specific differences may allow to gain insight in the VOR demand posed by different sports and, consequently, in the importance of accurate vestibular assessment for the athletes in the process of return to sport following sport related concussion (SRC). The results evidence that athletes taking part in ball sports (i.e., American football, football, handball and ice hockey) have higher reading performance during vertical head impulses than those from non-ball sports (i.e., bob, skeleton, and snowboard). Such a clear separation between sport types allows speculation on how the different VOR demands occur. Possibly, athletes of ball sports continuously need to rapidly, though precisely, focus on single objects (e.g., the ball/puck or the movement of other players body parts to foresee their action) while repetitively and rapidly moving the head to explore the field or see the ball. For bob, skeleton and snowboard athletes achieving (or recovering after a concussion) a VOR-based gaze stabilization exceeding the requirement for everyday life may not be necessary, since, although they move rapidly, they do not need to focus small visual cues.

The higher functional performance of the horizontal VOR observed in handball players respect to the *whole athlete group*, including football and ice hockey players, is instead more difficult to interpret. Higher visual acuity in dynamic conditions (i.e., recognized in moving target) has been observed in basketball, water polo, volleyball and baseball players (44–47). It is possible to speculate that, for ball-based games with rapid gameplay (e.g., basketball, handball, ice-hockey), the demand to the VOR-based gaze stabilization relates inversely to the size of the field (in small fields targets as ball or other players are closer, thus requiring larger, and thus faster, head motions). Handball, having a rapid gameplay and a smaller field than soccer and hockey may therefore require a higher VOR functional performance.

TABLE 3A | *Whole athlete group*: *p*-values of the multiple comparisons of *pca* between head acceleration bin—horizontal canals.

Acceleration bin	*pca*	3000 deg/s^2	4000 deg/s^2	5000 deg/s^2	6000 deg/s^2	7000 deg/s^2	8000 deg/s^2
		0.982	0.975	0.971	0.965	0.941	0.909
3000 deg/s^2	0.982	-	0.206	0.048	0.005	<0.001	<0.001
4000 deg/s^2	0.975	0.206	-	0.454	0.076	<0.001	<0.001
5000 deg/s^2	0.971	0.048	0.454	-	0.314	0.001	<0.001
6000 deg/s^2	0.965	0.005	0.076	0.314	-	0.028	<0.001
7000 deg/s^2	0.941	<0.001	<0.001	0.001	0.028	-	0.129
8000 deg/s^2	0.909	<0.001	<0.001	<0.001	<0.001	0.129	-

PCA was estimated using the single bin approach (Equation 2). Using the Bonferroni correction, only p < 0.0042 (highlighted in gray) were consider statistically significant.

TABLE 3B | *Whole athlete group*: *p*-values of the multiple comparisons of *pca* between head acceleration bin—vertical canals.

Acceleration bin	*pca*	3000 deg/s^2	4000 deg/s^2	5000 deg/s^2	6000 deg/s^2	7000 deg/s^2	8000 deg/s^2
		0.983	0.977	0.965	0.942	0.929	0.910
3000 deg/s^2	0.983	-	0.090	<0.001	<0.001	<0.001	<0.001
4000 deg/s^2	0.977	0.090	-	0.023	<0.001	<0.001	<0.001
5000 deg/s^2	0.965	<0.001	0.023	-	<0.001	<0.001	<0.001
6000 deg/s^2	0.942	<0.001	<0.001	<0.001	-	0.216	0.024
7000 deg/s^2	0.929	<0.001	<0.001	<0.001	0.216	-	0.295
8000 deg/s^2	0.910	<0.001	<0.001	<0.001	0.024	0.295	-

PCA was estimated using the single bin approach (Equation 2). Using the Bonferroni correction, only p < 0.0042 (highlighted in gray) were consider statistically significant.

Handball and American football are also the only ball sports tested where the ball is played evenly above and below eye level (but handball has also a smaller field and a faster gameplay), possibly requiring higher performance in the vertical VOR. Such speculation, however, would need confirmation from analysis of head kinematics during the activities of the different sports. The underlying assumption of these speculations is that the hypothesized higher VOR demand of some sports is associated with observing fHIT results higher than normal in the athletes practicing such sport. Accordingly, handball players performed better than the *control group* (data available only for head impulses in the horizontal plane). No difference, however, was observed between the *whole athlete group* and *control group*. This suggests that the level of functional performance of the VOR (as assessed by the fHIT) does not solely dependent from the athletic level of the tested person, but it may be higher in athletes of specific sports.

Interpretation of the fHIT Results and Its Relevance in Professional Athletes

Standard fHIT Outcome (Proportion of Correct Answers for Head Accelerations 2,001–6,000 deg/s^2)

The fHIT outcome did not differ between the *whole athlete group* and the *control group* (note that data from only 26 controls in a comparable age range were available). This finding may question the clinical relevance of the observed sport-related differences and the suitability of the fHIT in the evaluation of subtle functional VOR impairments that may affect the professional activity of athletes following sport related concussion.

The absence of differences between a wide group of professional athletes (a*thlete group*) and the *control group* is not surprising. The fHIT settings (39) (e.g., size of the presented optotype, duration of the stimulus, etc.) were specifically optimized to null the number of errors committed by normal healthy individuals during head impulses in the accelerations range 1,001–4,000 deg/s^2. Accordingly, a typical healthy individual is expected to perform very close to 100% correct answers in standard fHIT test (the standard fHIT outcome pools head impulses with accelerations in the range 2,001–6,000 deg/s^2). While this strategy maximizes specificity (i.e., proportion of healthy individual that are correctly identified by fHIT) with respect to vestibular impairments (35, 40), it pushes the scores of all healthy individuals close to the 100%, reducing the differences between subgroups. The high significance of the observed sport-specific differences suggests however that, when sport-specific performances are present, the fHIT is able to distinguish them (e.g., handball). This makes the fHIT a valid candidate for an objective assessment of the subtle impairments affecting athlete's return to play (2, 48).

Comparing the *whole athlete group* with a small *control group* of undefined healthy non-athletes is not informative, as the compared subgroups are not sufficiently characterized to grant that any difference is actually present. It cannot be excluded that few individuals of the *control group* have unexpected characteristics [e.g., amateur players of sport requiring elevated eye-head coordination such as table tennis (49)] that pose a demand to the VOR similar or even superior to that of some professional sport activities. As discussed above, the level of VOR

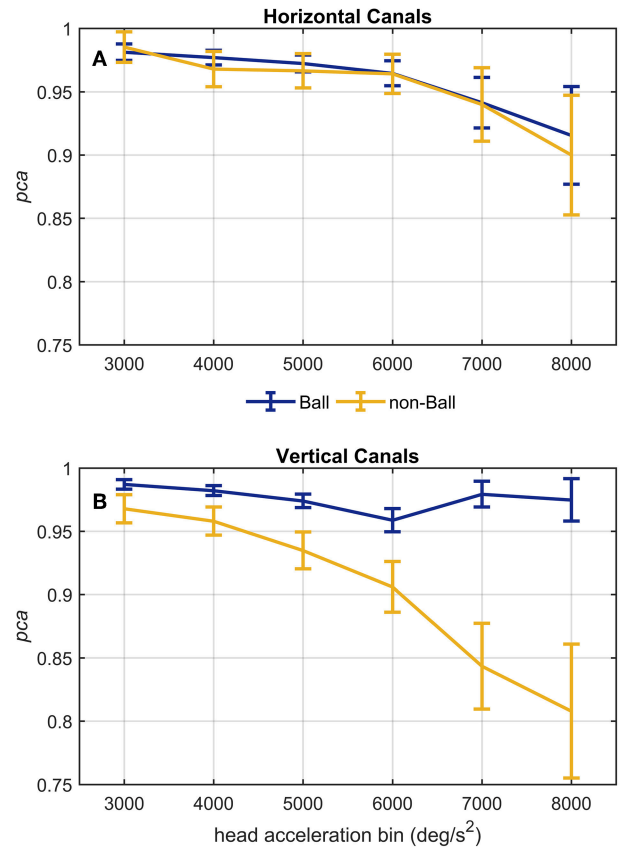

FIGURE 8 | Proportion of correct answers (*pca*) of ball and non-ball groups at different head acceleration bins. The error bars represent the *pca* and 95% confidence intervals estimated for bin of acceleration (3,000–8,000 deg/s^2). *Pca* were computed using the single approach (Equation 1) for impulses performed in the plane ot the horizontal **(A)** and vertical **(B)** canals. Confidence intervals for *pca* were estimated as in **Figure 3**. Dark blue and yellow lines represent the *pca* estimated for the ball and non-ball groups, respectively. **(A)** The relationship between head acceleration and test performance appeared comparable between the two subgroups of athletes (ball and non-balls) for the impulses collected in the plane of the horizontal canals. No significant difference was, indeed, found for every acceleration bin (**Table 4A**). **(B)** As visible, the two ball and non-ball subgroups showed two peculiar relationships of head acceleration and *pca*. The comparisons between the subgroups showed a significant higher *pca* of the ball group than the non-ball group, irrespective of head acceleration bins (**Table 4B**).

functional performance does not solely depend on the athletic level of the tested person. Athletes do not necessarily have a superior functional VOR performance, since not every sport, even if it requires rapid movements, is associated with an elevated functional VOR demand.

To better interpret the fHIT results it is important to understand the origin of the observed errors. The sport-specific differences suggest that, if the number of head impulse is high enough, even small numbers of errors cannot be considered lapses, but actual VOR errors (lapses rate is unlikely to generate such an elegant picture of sport-specific differences). The occurrence of errors during head accelerations ranging 2,001–6,000 deg/s^2 suggests that failure of visual stabilization, although rare, occurs in healthy individuals. This is not surprising. With the video head impulse test (vHIT) VOR gains as low as 0.8 are not considered pathological as they are found in healthy individuals that do not report functional impairments in everyday life [vHIT is often performed up to a 3,000–4,000 deg/s^2 (24, 50), while acceleration up to 10,000 deg/s^2 normally occurs during natural locomotion (25)]. An elegant study (30) calculating point-by-point VOR errors (both in position and in velocity) during the whole course of head impulses demonstrated that healthy individuals show errors as big as 10–20% of the desired compensation of the head movement with head accelerations below 10,000 deg/s^2. During such head impulses, however, only occasional, small corrective saccades are present (30). The absence of relevant corrections suggests that the VOR errors do not systematically affect visual function in real life (no compensatory mechanism had evolved to correct them). The high proportion of correct answers interleaved by occasional errors not attributable to lapses that are found in the fHIT results of the *control group* implies that the VOR errors only occasionally affect the fHIT task. This suggests that the fHIT task is correctly tuned to be a proxy to a VOR challenge comparable to everyday life. In this context, the ability of the fHIT to differentiate significantly higher performances in specific sports further confirms that using the sport specific values, the fHIT can capture the extra functional tuning aimed at minimizing the effect of VOR errors on sport activities requiring elevated visual stability.

In summary, it is possible to speculate that a test outcome below the proportion of correct answers of the normal population (or of the *whole athlete group*) would be related to a functional VOR deficit that may be relevant in everyday life. An outcome lower than a sport-specific normative value only, would instead be related to a functional VOR impairments that affect the specific activities of that sport. According to this interpretation, for sports where no difference with the performance of *control group* is observed, the time course of VOR functional recovery for return to sport activity and return to everyday life should match. A final confirmation of this interpretation, however, requires evidence from testing patients during their return to activity.

fHIT Vestibulogram (Proportion of Correct Answers as Function of Head Acceleration)

Differently from the vHIT and DVA test, where head velocities must be consistent between head impulses, the fHIT openly requires the examiner to test various head accelerations. This procedure generates a functional vestibulogram, presenting the proportion of correct answers as function of the peak acceleration in the head impulses, divided in 1,000 deg/s^2 wide bins up to 7,000 deg/s^2. This unique feature is not yet exploited by the standard outcome metric, which pools the results from all impulses in the range 2,001–6,000 deg/s^2. Accordingly, no specific restriction on the minimum number of impulses per bin is specified and the functional vestibulogram is provided for visual evaluation only.

The proportion of correct answers of the *whole athlete group* decreased non-linearly as the head acceleration increased

TABLE 4A | Ball vs. non-ball sports: comparisons of *pca* at different head acceleration bin—horizontal canals.

	Head acceleration bin					
Sport type	**3000 deg/s^2**	**4000 deg/s^2**	**5000 deg/s^2**	**6000 deg/s^2**	**7000 deg/s^2**	**8000 deg/s^2**
Ball	0.981	0.977	0.972	0.9645	0.941	0.915
Non-ball	0.985	0.968	0.967	0.964	0.940	0.900
p-value	0.851	0.358	0.608	0.900	0.902	0.839

PCA was estimated using the single bin approach (Equation 2). Using the Bonferroni correction, only $p < 0.0027$ (highlighted in gray) were consider statistically significant.

TABLE 4B | Ball vs. non-ball sports: comparisons of *pca* at different head acceleration bin—vertical canals.

	Head acceleration bin					
Sport type	**3000 deg/s^2**	**4000 deg/s^2**	**5000 deg/s^2**	**6000 deg/s^2**	**7000 deg/s^2**	**8000 deg/s^2**
Ball	0.987	0.982	0.974	0.959	0.979	0.975
Non-Ball	0.968	0.958	0.935	0.906	0.843	0.808
p-value	0.001	<0.001	<0.001	<0.001	<0.001	<0.001

PCA was estimated using the single bin approach (Equation 2). Using the Bonferroni correction, only $p < 0.0027$ (highlighted in gray) were consider statistically significant.

TABLE 5A | Ball sports: *p*-values of the multiple comparisons of *pca* between head acceleration bin—vertical canals.

Acceleration bin	***pca***	**3000 deg/s^2**	**4000 deg/s^2**	**5000 deg/s^2**	**6000 deg/s^2**	**7000 deg/s^2**	**8000 deg/s^2**
		0.987	0.982	0.974	0.959	0.979	0.975
3000 deg/s^2	0.987	-	0.183	0.002	<0.001	0.250	0.214
4000 deg/s^2	0.982	0.183	-	0.047	<0.001	0.783	0.571
5000 deg/s^2	0.974	0.002	0.047	-	0.015	0.577	0.887
6000 deg/s^2	0.959	<0.001	<0.001	0.015	-	0.043	0.321
7000 deg/s^2	0.979	0.250	0.783	0.577	0.043	-	0.896
8000 deg/s^2	0.975	0.214	0.571	0.887	0.321	0.896	-

PCA was estimated using the single bin approach (Equation 2). Using the Bonferroni correction, only $p < 0.0027$ (highlighted in gray) were consider statistically significant.

TABLE 5B | Non-ball sports: *p*-values of the multiple comparisons of *pca* between head acceleration bin—vertical canals.

Acceleration bin	***pca***	**3000 deg/s^2**	**4000 deg/s^2**	**5000 deg/s^2**	**6000 deg/s^2**	**7000 deg/s^2**	**8000 deg/s^2**
		0.968	0.958	0.935	0.906	0.843	0.808
3000 deg/s^2	0.968	-	0.3816	0.006	<0.001	<0.001	<0.001
4000 deg/s^2	0.958	0.3816	-	0.0454	<0.001	<0.001	<0.001
5000 deg/s^2	0.935	0.006	0.0454	-	0.0630	<0.001	<0.001
6000 deg/s^2	0.906	<0.001	<0.001	0.0630	-	0.0075	0.0012
7000 deg/s^2	0.843	<0.001	<0.001	<0.001	0.0075	-	0.410
8000 deg/s^2	0.808	<0.001	<0.001	<0.001	0.0012	0.410	-

pca were estimated using the single bin approach (Equation 2). Using the Bonferroni correction, only $p < 0.0027$ (highlighted in gray) were consider statistically significant.

(the evaluation was extended to include head impulses up to 8,000 deg/s^2 to further confirm the trend). For the head impulses in the plane of the horizontal canals this decrease became statistically significant for the 7,000 deg/s^2 and 8,000 deg/s^2 bins with respect to the bins $\leq$ 5,000 deg/s^2 and $\leq$ 6,000 deg/s^2, respectively. This suggests that around 6,000 deg/s^2 there is a "critical" acceleration above which the reading performance declines with a slope causing significant difference every 2,000 deg/s^2. For the vertical canals the decline occurs with head accelerations at least 1,000 deg/s^2 lower (between 4,001 deg/s^2 and 5,000 deg/s^2). The slope in the functional vestibulogram, however, also depends on the sport. When vertical

semicircular canals are tested, the athletes of non-ball sports had not only an overall lower level of proportion of correct answers (as already evident from the standard fHIT outcome—**Table 2B** and **Figure 3B**), but also a faster decline with increasing acceleration (**Figure 8B**).

Although VOR gain was shown to decline with the velocity of head impulses (51), to our knowledge, this is the first work providing a detailed description of the decline of functional VOR performance with head acceleration, demonstrating that it differs between the planes of head impulses and between different subgroups of healthy individuals. A previous work observed that DVA loss was lower for impulses faster than 100 deg/s head velocity than if only head velocities higher than 150 deg/s were considered (32). A study using the gaze stabilization test (GST—recognition of an optotype repeatedly presented with a fixed size during active head motion) showed a general increase of the visual acuity loss with head velocity testing the range 60–220 deg/s in step of 40 deg/s (52). GST, however, is based on active head movements tested with progressively increasing velocity. Since it is well-known that DVA testing leads to lower visual acuity loss if performed with active than with passive head motion (32), the decline observed with GST may also depends on the additional functions involved with the active testing (e.g., anticipation).

Altogether, the results of the current study provide evidence that the functional vestibulogram has both theoretical and clinical relevance. The decline of VOR functional performance observed with the fHIT test at acceleration within the range of normal head movements suggest that, even in healthy individuals, occasional blurring can occur when the VOR is challenged with intense activities like those required by professional sports. Whether the differences observed among different sports is a consequence of training (i.e., it can also be rehabilitated) or if it is a natural feature differentiating athletes who succeed within one specific sport from those who don't, cannot be inferred based on the current data. The practical implication of the observed trend, however, is that, when assessing professional athletes, testing higher accelerations may be significantly more informative and may shorten the test duration significantly.

Sport-Specific Normative Values and Testing Procedure for the fHIT

The sport-specific proportion of correct answer identified in the current study allows defining normative values for each sport (**Table 6**). Although the differences may appear negligible, they may have relevance for the assessment of athletes reporting

TABLE 6A | Sport specific lower boundary of *pca* and minimum number of head impulses to identify a deficit—horizontal canals.

	Head acceleration bin						
	3000-6000 deg/s^2	8000 deg/s^2	7000 deg/s^2	6000 deg/s^2	5000 deg/s^2	4000 deg/s^2	3000 deg/s^2
Group	5% c.i. pca	5% c.i. pca	5% c.i. pca	5% c.i. pca	5% c.i. pca	5% c.i. pca	5% c.i. pca
	# impulses	# impulses	# impulses	# impulses	# impulses	# impulses	# impulses
athlete group	0.969	0.861	0.915	0.951	0.962	0.967	0.973
	33	8	12	21	27	31	38
AF	0.972	N/A	0.677	0.940	0.940	0.964	0.906
	36	N/A	4	17	17	28	11
FB	0.947	0.681	0.811	0.891	0.949	0.924	0.944
	19	4	6	10	20	14	18
HB	0.979	0.853	0.940	0.972	0.963	0.975	0.950
	48	7	17	36	28	40	20
IH	0.964	0.802	0.884	0.935	0.948	0.961	0.968
	28	6	9	16	20	26	32
BS	0.958	0.853	0.870	0.937	0.934	0.935	0.960
	24	7	8	16	16	16	25
SB	0.946	0.701	0.854	0.906	0.928	0.927	0.926
	19	4	7	11	14	14	14

Pca^{pb} were estimated using the pooled bin approach (Equation 1). Pca^{sb} were estimated using the single bin approach (Equation 2). The coefficient intervals were estimated using the Fisher–Snedecor distribution (53), although conservative, a higher reliability of estimate was ensured when in a bin < 200 number of impulses were collected.

TABLE 6B | Sport specific lower boundary of *pca* and minimum number of head impulses to identify a deficit—vertical canals.

	Head acceleration bin						
	3000-6000 deg/s^2	8000 deg/s^2	7000 deg/s^2	6000 deg/s^2	5000 deg/s^2	4000 deg/s^2	3000 deg/s^2
Group	5% c.i. pca	5% c.i. pca	5% c.i. pca	5% c.i. pca	5% c.i. pca	5% c.i. pca	5% c.i. pca
	# impulses	# impulses	# impulses	# impulses	# impulses	# impulses	# impulses
athlete group	0.966	0.873	0.907	0.929	0.956	0.971	0.977
	30	8	11	15	23	35	44
AF	0.966	0.782	0.838	0.816	0.958	0.951	0.961
	30	5	7	6	24	21	26
FB	0.967	0.868	0.927	0.931	0.945	0.963	0.975
	31	8	14	15	19	28	40
HB	0.978	0.931	0.939	0.931	0.971	0.976	0.975
	46	15	17	15	35	42	40
IH	0.970	0.912	0.949	0.935	0.957	0.971	0.974
	34	12	20	16	24	35	39
BS	0.942	0.745	0.777	0.886	0.917	0.947	0.973
	18	4	5	9	13	19	38
SB	0.913	0.610	0.759	0.815	0.879	0.915	0.919
	12	3	5	6	9	12	13

Pca^{pb} were estimated using the pooled bin approach (Equation 1). Pca^{sb} were estimated using the single bin approach (Equation 2). The coefficient intervals were estimated using the Fisher–Snedecor distribution (53), although conservative, a higher reliability of estimate was ensured when in a bin < 200 number of impulses were collected.

difficulties in returning to the professional activity. In line with the consideration of the previous paragraph, handball players may require to focus on the ball hundreds of times during the rapid actions occurring during the game and a difference of 1% may impact more than a few of the most critical actions (e.g., scoring) in a single game.

If sport-specific normative values were considered, sport-specific testing procedures needs to be defined accordingly. The minimum number of head impulses required to verify whether an athlete achieves its sport-specific level (e.g., to assess sport-specific recovery or sport-specific functional impairment) depends on the distance between the sport-specific proportion of correct answer and 100%. As all the proportions of correct answers are close to 100%, the sport-specific minimum number of required head impulses varies significantly. For example, for the horizontal semicircular canals, handball players (lower bound of correct answer = 97.9%) should be tested with at least 48 impulses. For soccer players (lower bound = 94.7%) the required minimum is only 19 impulses. **Table 6** lists the sport-specific, minimum numbers of head impulses required to discriminate the sport-specific lower bound of correct answer. Considering the number of impulses needed for testing the athletes of sports reaching the highest performance, the fHIT may become unpractical (to test all six semicircular canals, 280 head impulses would be the minimum required for a handball player). The observed decline of reading performance with increasing head acceleration, however, may be used to simplify testing. Recalling that during head impulses in the plain of one canal pair, the higher is the acceleration the lower is the contribution of the inhibited semicircular canal (only the excited semicircular canals account for the part of acceleration exceeding the inhibitory cut of the inhibited semicircular canal), a deficit in reading performance observable during head impulses at the lowest accelerations should be more evident during testing at the highest accelerations. Accordingly, an optimal testing strategy would be to start testing the highest acceleration bin and, only if a deficit is present, progressively decrease the acceleration to identify where the pathological behavior stops. With such strategy, a handball player would require a minimum of 17 head impulses at 7,000 deg/s^2 (the maximum acceleration currently displayed on the fHIT interface) per semicircular canal to be identified as healthy, i.e., comparable to the number of impulses used in a valid head impulse test (51, 54, 55).

In conclusion, the results of the current study suggest that fHIT can be used to characterize the functional vestibular performance of athletes and establish sport-specific reference values. For the sports associated with higher scores, the sport specific-reference values can possibly help to differentiate between a functional VOR performance sufficient for ordinary activities of daily living and one for sport-related activities at

professional level only. Furthermore, as the *whole athlete group* showed a sport-specific decrease of VOR functional performance, the results suggest performing the fHIT starting with head impulses at higher accelerations (6,000–8,000 deg/s^2). This strategy reduces the number of impulse necessary to identify a deficit. All together the fHIT demonstrated a sport-specific sensitivity that supports further extensive tests, focusing on athletes who suffered SRC, to verify sensitivity and specificity for this patients' population. Direct evidence from patients during their return to sport will also be required to confirm that the fHIT can help to identify subtle functional impairments that may become relevant in the athletes when challenged by their professional activity.

ETHICS STATEMENT

The study protocol was approved by the local ethics committee (cantonal ethics commission Zürich, KEK-ZH-2018-01168) and was in accordance with the ethical standards laid down in the 2013 Declaration of Helsinki for research involving human subjects. Informed consent was obtained from each subject.

AUTHOR CONTRIBUTIONS

FR supported the implementation of the research study, supported the data acquisition, analyzed the data, interpreted the results, and wrote the manuscript. GB supported the conceivement and the implementation of the research study, acquired the data, interpreted the results and wrote the manuscript. DA supported the management of the research study, acquired the data, participated in the interpretation of the results and critically revised the manuscript. DS participated in the interpretation of the results and critically revised the manuscript. SR supported the data analysis, participated in the interpretation of the results and critically revised the manuscript. NF-D conceived and implemented the research study, managed the research study and the data acquisition, participated in the interpretation of the results and critically revised the manuscript.

FUNDING

This work was supported by the Schulthess Foundation (Zürich, Switzerland).

REFERENCES

1. Feddermann-Demont N, Echemendia RJ, Schneider KJ, Solomon GS, Hayden KA, Turner M, et al. What domains of clinical function should be assessed after sport-related concussion? A systematic review. *Br J Sports Med.* (2017) 51:903–18. doi: 10.1136/bjsports-2016-097403
2. McCrory P, Meeuwisse W, Dvořák J, Aubry M, Bailes J, Broglio S, et al. Consensus statement on concussion in sport—the 5th international conference on concussion in sport held in Berlin, October 2016. *Br J Sports Med.* (2017) 51:838–47. doi: 10.1136/bjsports-2017-097699
3. Ventura RE, Balcer LJ, Galetta SL. The neuro-ophthalmology of head trauma. *Lancet Neurol.* (2014) 13:1006–16. doi: 10.1016/S1474-4422(14)70111-5
4. De Beaumont L, Henry LC, Gosselin N. Long-term functional alterations in sports concussion. *Neurosurg Focus.* (2012) 33:E8. doi: 10.3171/2012.9.FOCUS12278
5. Arshad Q, Roberts RE, Ahmad H, Lobo R, Patel M, Ham T, et al. Patients with chronic dizziness following traumatic head injury typically have multiple diagnoses involving combined peripheral and central vestibular dysfunction. *Clin Neurol Neurosurg.* (2017) 155:17–9. doi: 10.1016/j.clineuro.2017.01.021
6. Kontos AP, Elbin RJ, Schatz P, Covassin T, Henry L, Pardini J, et al. A revised factor structure for the post-concussion symptom scale: baseline and postconcussion factors. *Am J Sports Med.* (2012) 40:2375–84. doi: 10.1177/0363546512455400
7. Sharp DJ, Jenkins PO. Concussion is confusing us all. *Pract Neurol.* (2015) 15:172–86. doi: 10.1136/practneurol-2015-001087
8. Cancelliere C, Hincapié CA, Keightley M, Godbolt AK, Côté P, Kristman VL, et al. Systematic review of prognosis and return to play after sport concussion: results of the International Collaboration on Mild Traumatic Brain Injury Prognosis. *Arch Phys Med Rehabil.* (2014) 95(3 Suppl):S210–29. doi: 10.1016/j.apmr.2013.06.035
9. Iverson GL, Gardner AJ, Terry DP, Ponsford JL, Sills AK, Broshek DK, et al. Predictors of clinical recovery from concussion: A systematic review. *Br J Sports Med.* (2017) 51:941–8. doi: 10.1136/bjsports-2017-097729
10. Suh M, Kolster R, Sarkar R, McCandliss B, Ghajar J. Cognitive and Neurobiological Research Consortium (2006). Deficits in predictive smooth pursuit after mild traumatic brain injury. *Neurosci Lett.* 401, 108–113. doi: 10.1016/j.neulet.2006.02.074
11. Berman JM, Fredrickson JM. Vertigo after head injury–a five year follow-up. *J Otolaryngol.* (1978) 7:237–45.
12. Cartlidge NEF. Post-concussional syndrome. *Scott Med J.* (1978) 23:103 doi: 10.1177/003693307802300146
13. Capó-Aponte JE, Urosevich TG, Temme LA, Tarbett AK, Sanghera NK. Visual dysfunctions and symptoms during the subacute stage of blast-induced mild traumatic brain injury. *Mil Med.* (2012) 177:804–13. doi: 10.7205/MILMED-D-12-00061
14. Chamelian L, Feinstein A. Outcome after mild to moderate traumatic brain injury: The role of dizziness. *Arch Phys Med Rehabil.* (2004) 85:1662–6. doi: 10.1016/j.apmr.2004.02.012
15. Ahn SK, Jeon SY, Kim JP, Park JJ, Hur DG, Kim DW, et al. Clinical characteristics and treatment of benign paroxysmal positional vertigo after traumatic brain injury. *J Trauma Inj Infect Crit Care.* (2011) 70:442–6. doi: 10.1097/TA.0b013e3181d0c3d9
16. Brandt T. *Vertigo: Its Multisensory Syndromes.* London: Springer (2003).
17. Shepard N. (2013). Balance and dizziness. In: Zasler N, Katz D, Zafonte R, editors. *Brain Injury Medicine: Principles And Practice.* New York, NY: Demos Medical Publishing. p. 779–793.
18. Davies RA, Luxon LM. Dizziness following head injury: A neuro-otological study. *J Neurol.* (1995) 242:222–30. doi: 10.1007/BF00919595
19. Kushner, D. (1998). Mild traumatic brain injury: toward understanding manifestations and treatment. *Arch Intern Med.* 158:1617–24. doi: 10.1001/archinte.158.15.1617
20. de NÓ RL. (1933). Vestibulo-Ocular Reflex Arc. *Arch Neurol Psychiatry.* 30:245–91. doi: 10.1001/archneurpsyc.1933.02240140009001
21. Halmagyi GM, Curthoys IS. A clinical sign of canal paresis. *Arch Neurol.* (1988) 45:737–9.
22. MacDougall HG, Weber KP, McGarvie LA, Halmagyi GM, Curthoys IS. The video head impulse test: diagnostic accuracy in peripheral vestibulopathy. *Neurology.* (2009) 73:1134–41. doi: 10.1212/WNL.0b013e3181bacf85
23. Weber KP, MacDougall HG, Halmagyi GM, Curthoys IS. Impulsive testing of semicircular-canal function using video-oculography. *Ann N Y Acad Sci.* (2009) 1164:486–91. doi: 10.1111/j.1749-6632.2008.03730.x
24. Halmagyi GM, Curthoys IS, Cremer PD, Henderson CJ, Todd MJ, Staples MJ, et al. The human horizontal vestibulo-ocular reflex in response to high-acceleration stimulation before and after unilateral vestibular neurectomy. *Exp brain Res.* (1990) 81:479–90. doi: 10.1007/BF02423496

25. Grossman GE, Leigh RJ, Abel LA, Lanska DJ, Thurston SE. Frequency and velocity of rotational head perturbations during locomotion. *Exp brain Res.* (1988) 70:470–6. doi: 10.1007/BF00247595
26. Fernandez C, Goldberg JM. Physiology of peripheral neurons innervating semicircular canals of the squirrel monkey. II Response to sinusoidal stimulation and dynamics of peripheral vestibular system *J Neurophysiol.* (1971) 34:661–75. doi: 10.1152/jn.1971.34.4.661
27. Wallace B, Lifshitz J. Traumatic brain injury and vestibulo-ocular function: current challenges and future prospects. *Eye Brain Vol.* (2016) 8:153–64. doi: 10.2147/EB.S82670
28. Brosseau-Lachaine O, Gagnon I, Forget R, Faubert J. Mild traumatic brain injury induces prolonged visual processing deficits in children. *Brain Inj.* (2008) 22:657–68. doi: 10.1080/026990508022 03353
29. Covassin T, Stearne D, Elbin R. Concussion history and postconcussion neurocognitive performance and symptoms in collegiate athletes. *J Athl Train.* (2008) 43:119–24. doi: 10.4085/1062-6050-43.2.119
30. Peng GCY, Zee DS, Minor LB. Phase-plane analysis of gaze stabilization to high acceleration head thrusts: a continuum across normal subjects and patients with loss of vestibular function. *J Neurophysiol.* (2004) 91:1763–81. doi: 10.1152/jn.00611.2002
31. Herdman SJ, Tusa RJ, Blatt P, Suzuki A, Venuto PJ, Roberts D. Computerized dynamic visual acuity test in the assessment of vestibular deficits. *Am J Otol.* (1998) 19:790–6.
32. Vital D, Hegemann SCA, Straumann D, Bergamin O, Bockisch CJ, Angehrn D, et al. A new dynamic visual acuity test to assess peripheral vestibular function. *Arch Otolaryngol - Head Neck Surg.* (2010) 136:686–91. doi: 10.1001/archoto.2010.99
33. Wettstein VG, Weber KP, Bockisch CJ, Hegemann SC. Compensatory saccades in head impulse testing influence the dynamic visual acuity of patients with unilateral peripheral vestibulopathy. *J Vestib Res.* (2016) 26:395–402.doi: 10.3233/VES-160591
34. Böhler A, Mandalá M, Ramat S. A software program for the head impulse testing device (HITD). In: *2010 Annual International Conference of the IEEE Engineering in Medicine and Biology Society, EMBC'10* (IEEE), 6615–6618 (2010).
35. Ramat S, Colnaghi S, Boehler A, Astore S, Falco P, Mandalà M, et al. A device for the functional evaluation of the VOR in clinical settings. *Front. Neurol.* (2012) 3:39. doi: 10.3389/fneur.2012.00039
36. Versino M, Colagiorgio P, Sacco S, Colnaghi S, Ramat S. Artifact avoidance for head impulse testing. *Clin Neurophysiol.* (2014) 125:1071–3. doi: 10.1016/j.clinph.2013.09.024
37. Demer JL, Honrubia V, Baloh RW. Dynamic visual acuity: a test for oscillopsia and vestibulo-ocular reflex function. *Am J Otol.* (1994) 15:340–7
38. Schubert MC, Migliaccio AA, Della Santina CC. Dynamic visual acuity during passive head thrusts in canal planes. *JARO J Assoc Res Otolaryngol.* (2006) 7:329–38. doi: 10.1007/s10162-006-0047-6
39. Colagiorgio P, Colnaghi S, Versino M, Ramat S. A new tool for investigating the functional testing of the VOR. *Front Neurol.* (2013) 4:165. doi: 10.3389/fneur.2013.00165
40. Versino M, Colagiorgio P, Sacco S, Colnaghi S, Quaglieri S, Manfrin M, et al. Reading while moving: the functional assessment of VOR. *J Vestib Res.* (2014) 24:459–64. doi: 10.3233/VES-140531
41. Daneshvar DH, Nowinski CJ, Mckee AC, Cantu RC. The epidemiology of sport-related concussion. *Clin Sports Med.* (2011) 30:1–17. doi: 10.1016/j.csm.2010.08.006
42. Corallo G, Versino M, Mandalà M, Colnaghi S, Ramat S. The functional head impulse test: preliminary data. *J Neurol.* (2018) 265:35–39. doi: 10.1007/s00415-018-8910-z
43. Goebel JA, Tungsiripat N, Sinks B, Carmody J. Gaze stabilization test: A new clinical test of unilateral vestibular dysfunction. *Otol Neurotol.* (2007) 28:68–73. doi: 10.1097/01.mao.0000244351.42201.a7
44. Beals RP, Mayyasi AM, Templeton AE, Johnston WL. The relationship between basketball shooting performance and certain visual attributes. *Optom Vis Sci.* (1971) 48:585–90. doi: 10.1097/00006324-197107000-00007
45. Don Morris GS, Kreighbaum E. Dynamic visual acuity of varsity women volleyball and basketball players. *Res Q Am Alliance Heal Phys Educ Recreat.* (1977) 48:480–3. doi: 10.1080/10671315.1977.10615449
46. Quevedo-Junyent L, Aznar-Casanova JA, Merindano-Encina D, Cardona G, Solé-Fortó J. Comparison of dynamic visual acuity between water polo players and sedentary students. *Res Q Exerc Sport.* (2018) 82:644–651. doi: 10.1080/02701367.2011.10599801
47. Uchida Y, Kudoh D, Murakami A, Honda M, Kitazawa S. Origins of superior dynamic visual acuity in baseball players: superior eye movements or superior image processing. *PLoS ONE.* (2012) 7:e31530. doi: 10.1371/journal.pone.0031530
48. Wallace J, Covassin T, Lafevor M. Use of the stepwise progression return-to-play protocol following concussion among practicing athletic trainers. *J Sport Heal Sci.* (2018) 7:204–9. doi: 10.1016/j.jshs.2016.11.002
49. Rodrigues ST, Vickers JN, Williams AM. Head, eye and arm coordination in table tennis. *J Sports Sci.* (2002) 20:187–200. doi: 10.1080/026404102317284754
50. Schmid-Priscoveanu A, Straumann D, Böhmer A, Obzina H. Vestibulo-ocular responses during static head roll and three-dimensional head impulses after vestibular neuritis. *Acta Otolaryngol.* (1999)119:750–7.
51. McGarvie LA, MacDougall HG, Halmagyi GM, Burgess AM, Weber KP, Curthoys IS. The video head impulse test (vHIT) of semicircular canal function - age-dependent normative values of VOR gain in healthy subjects. *Front Neurol.* (2015) 6:154. doi: 10.3389/fneur.2015.00154
52. Mohammad MT, Furman JM, Sparto PJ, Marchetti GF, Whitney SL. The effect of optotype size and velocity parameters on the performance of healthy young adult subjects on the gaze stabilization test. *Otol Neurotol.* (2013) 34:1090–5. doi: 10.1097/MAO.0b013e31827f192e
53. Zar JH. *Biostatistical Analysis.* 4th ed. Upper Saddle River, NJ: Prentice Hall (1999).
54. Agrawal Y, Schubert MC, Migliaccio AA, Zee DS, Schneider E, Lehnen N, et al. Evaluation of quantitative head impulse testing using search coils versus video-oculography in older individuals. *Otol Neurotol.* (2014) 35:283–8. doi: 10.1097/MAO.0b013e3182995227
55. Curthoys IS, Manzari L. Clinical application of the head impulse test of semicircular canal function. *Hear Balanc Commun.* (2017) 15:113–26. doi: 10.1080/21695717.2017.1353774

Conflict of Interest Statement: SR is the author of a Patent Deposit Application regarding the technique used in the functional head impulse test and is a shareholder of a company producing of the fHIT system used in this study (Beon Solutions srl, Zero Branco (TV), Italy).

The remaining authors declare that the research was conducted in the absence of any commercial or financial relationships that could be construed as a potential conflict of interest.

frontiers in Neurology

ORIGINAL RESEARCH
published: 28 May 2019
doi: 10.3389/fneur.2019.00550

Functional Testing of Vestibulo-Spinal Contributions to Balance Control: Insights From Tracking Improvement Following Acute Bilateral Peripheral Vestibular Loss

John H. J. Allum[1]*, *Heiko Mario Rust*[2,3] and *Flurin Honegger*[1]

[1] Division of Audiology and Neurootology, Department of Otorhinolaryngology (ORL), University Hospital Basel, Basel, Switzerland, [2] Department of Neurology, University of Basel Hospital, Basel, Switzerland, [3] Division of Brain Sciences, Academic Department of Neuro-Otology, Charing Cross Hospital, Imperial College, London, United Kingdom

Background: A battery of stance and gait tasks can be used to quantify functional deficits and track improvement in balance control following peripheral vestibular loss. An improvement could be due to at least 3 processes: partial peripheral recovery of sensory responses eliciting canal or otolith driven vestibular reflexes; central compensation of vestibular reflex gains, including substitution of intact otolith responses for pathological canal responses; or sensory substitution of visual and proprioceptive inputs for vestibular contributions to balance control.

Results: We describe the presumed action of all 3 processes observed for a case of sudden incapacitating acute bilateral peripheral loss probably due to vestibular neuritis. Otolith responses were largely unaffected. However, pathological decreases in all canal-driven vestibular ocular reflex (VOR) gains were observed. After 3 months of vestibular rehabilitation, balance control was normal but VOR gains remained low.

Conclusions: This case illustrates the difficulty in predicting balance control improvements from tests of the 10 vestibular end organs and emphasizes the need to test balance control function directly in order to determine if balance control has improved and is normal again despite remaining vestibular sensory deficits. This case also illustrates that the presence of residual otolithic function may be crucial for balance control improvement in cases of bilateral vestibular hypofunction.

Keywords: bilateral vestibular loss, posturography, vestibulo-spinal reflexes, vestibular evoked, vemps, vestibulo-ocular reflexes, video head impulse test

OPEN ACCESS

Edited by:
Herman Kingma,
Maastricht University, Netherlands

Reviewed by:
Eric Anson,
University of Rochester, United States
Eugen Constant Ionescu,
Hospices Civils de Lyon, France
Kristen Leigh Janky,
Boys Town, United States

***Correspondence:**
John H. J. Allum
john.allum@usb.ch

Specialty section:
This article was submitted to Neuro-Otology, a section of the journal Frontiers in Neurology

Received: *13 November 2018*
Accepted: *07 May 2019*
Published: *28 May 2019*

Citation:
Allum JHJ, Rust HM and Honegger F (2019) Functional Testing of Vestibulo-Spinal Contributions to Balance Control: Insights From Tracking Improvement Following Acute Bilateral Peripheral Vestibular Loss. Front. Neurol. 10:550. doi: 10.3389/fneur.2019.00550

INTRODUCTION

It is an open question whether any improvement in balance control following an acute bilateral peripheral vestibular loss (BVL) uses the same neural processes to improve function as when the acute peripheral vestibular loss is unilateral (UVL). An acute UVL resulting from presumed vestibular neuritis (VN) causes a characteristic deficit in the vestibular ocular reflex (VOR) function

easily observed with a head impulse test of the deficit side VOR by the presence of catch-up saccades and a gain <0.74 (1). Acutely, no or little change in VOR function is observed with a video head impulse test (vHIT) for head rotations to the normal side (gain equal to 1). A gain reduction to 0.5 on average occurs for rotations to the deficit side (2). Insights into the neural processes underlying central compensation for the UVL deficit side gain can be obtained by examining a group of acute UVL patients who have a large, almost complete, lateral canal loss as determined with caloric testing [that is, a 90% and greater canal paresis (CP)], and also no CP recovery over the following 3 months. Despite no CP recovery, that is, no recovery of the peripheral sensory function, the vHIT deficit side gains improve on average in this group from 0.45 in the acute state to 0.64 over the following 3 months. It is assumed that this improvement is due to central compensation, specifically, that the crossed intact side input contributing to the VOR for head rotations to the deficit side is enhanced (3–5). The question thus arises when there is no recovery of peripheral vestibular function *bilaterally*, as indicated by absent caloric responses, and abnormally low canal-elicited vHIT responses at acute onset, that is a gain below 0.6 bilaterally, [see Strupp et al. for a consensus definition of BVL (6)] whether there can be any improvement in VOR gains and balance control. In this situation, there is no normal side response to aid central compensation.

Long-term (<3 months) differences in peripheral vestibular recovery, which may be observed as differences in vHIT gains following an acute UVL, do not lead to long-term differences in balance control during stance and gait tests (5, 7). For example, for the stance test most sensitive to an acute UVL, standing eyes closed on foam (8), there is no significant difference in trunk sway for those with and without peripheral vestibular recovery after 3 months (5). Sway for both groups is, on average, normal. This is not the case for patients with chronic bilateral vestibular loss (BVL) (9). These patients still have sway velocities and angles greater than normal (9). For the gait test most sensitive to an acute UVL, walking eyes closed (8, 10), differences do emerge, trunk roll angle and pitch velocity is larger and greater than normal for the non-recovery group (5). There are several possible reasons for these differences in functional deficits which could have application to cases with an acute BVL. Firstly, there is a difference in recovery times for stance and gait tasks, with stance tasks recovering more rapidly after an acute UVL (11), possibly because VOR recovery is more rapid for the slow vs. the high head accelerations which occur with stance and gait, respectively (11, 12). Secondly, central compensation increasing the use of visual contributions to balance control could restrict the tests with differences to normal values to those performed with eyes closed. Nonetheless, even with eyes closed, the effect of central compensation increasing the use of somatosensory inputs could help improve balance stability.

There are other more fundamental problems involved with predicting balance capabilities from VOR responses in canal planes. Given the generally weak correlations between vHIT results and balance measures (7), except for roll during gait (13), the question arises how to determine the relationship between weakened canal VOR responses and vestibulo-spinal contributions to roll and pitch balance control during stance and gait. As spared function of the otoliths could be used by the CNS to generate angular velocity based sensory inputs no longer provided by canal reflexes (14, 15), it would be important to include tests of otolith function in the determination of these relationships.

Otolith function is usually measured using vestibular evoked myogenic potentials (VEMPs) elicited by sound-induced movements of the otoliths from the sternocleidomastoid (SCM) and inferior oblique (Inf Obl) muscles (16, 17). It is difficult to translate VEMP responses, if pathological, into deficits in balance control for three reasons: firstly, because it is difficult to elicit VEMPs from muscles such as soleus, tibialis anterior, and paraspinals (18) that are involved in balance control; secondly, because the amplitude polarity of vestibulo-spinal contributions of muscle responses elicited by perturbations to stance of these muscles differ across the body (19, 20) as does the amplitude polarity of VEMP responses to tone bursts in different muscles (16): thirdly, because the VEMP waveforms are often regarded as present or absent, except in the case of vertical canal dehiscence (21), the strength of the response does not necessarily translate into a strength or degree of function or dysfunction. Thus, although SCM and Inf Obl VEMPs provide an insight into the status of otolith sensory inputs to vestibular spinal control, these are unlikely to replace functional tests of the influence of vestibule-spinal signals on balance control.

In the current report, we emphasize the importance of recording VEMPs as these may provide insights into otolith-based balance improvements, in addition to insights into canal-based improvements revealed by the amount of recovery in vHIT examinations. While testing for the status of sensory contributions to balance control is important, we consider it crucial to ascertain the status of balance control with appropriate stance and gait tests. In this reported case of a sudden acute BVL we were impressed with the remarkable recovery in balance control despite the weak improvement in all canal VOR responses. In stark contrast, sacculus c-VEMP responses were normal, and utriculus o-VEMP responses were only weaker than normal on the right side. This report differs from a previous report of an acute BVL patient with only modest improvement in patient symptoms (22) in 3 aspects. Firstly, in our patient the loss involved all canal VOR responses and not just those served by the superior vestibular nerve (lateral and anterior canals). Secondly, our patient had remaining otolith function for all 4 otoliths. Thirdly, by tracking balance control we were able to document its remarkable improvement, matching improvement in patient symptoms.

METHODS

The current case concerns a male, 49 years old high rise crane driver who was suddenly incapacitated with vertigo (both tilting and turning) and nausea in his crane cockpit and had to be rescued with another crane. Initially, he could not walk without assistance. The patient and his general practitioner reported no prior deficit of balance control and no medical history consistent

with a previous vestibular sensory deficit. Previous periodic testing of hearing by the Swiss Accident Insurance also revealed no deficits. Such testing is mandatory in Switzerland for high-rise crane drivers. The lateral canal vHIT gains measured on entry to our hospital's emergency ward were 0.27 right and 0.43 left. Hearing was normal. A neurological examination on the same day revealed no other abnormalities. Specifically, a 3 Tesla MRI on the day of admission and 7 months later showed no signs of an ischemic attack. Based on the test results consistent with vestibular neuritis, the patient was treated intravenously with methylprednisolone (125 mg Solumedrol^{TM} per day) and then on discharge 6 days after entry with the oral medication. The patient received sessions of balance-oriented physical therapy daily while an in-patient and twice weekly with muscle conditioning for 9 months on discharge. Tests of optokinetic nystagmus, smooth pursuit tracking, and saccades performed 8 days after initial onset of the symptoms were normal except for a bias in the optokinetic nystagmus tests approximately equal to the level of spontaneous nystagmus (4 deg/s).

Scientific use of the data collected for this study was approved (approval 2014–16) by the local ethics committee responsible for the University Hospital Basel [Ethics Committee Northwest and Central Switzerland (EKNZ)]. Written informed consent was obtained from the acute BVL patient for the publication of his data from routine clinical examinations to be presented in this report.

VOR Measures

Canal paresis measures could not be determined using a bithermal (44 and 30°C) caloric test due to the very low responses (see **Figure 1**). Instead, only the average eye slow phase velocity (SPV) over the culmination phases of nystagmus was computed for the left and right ear irrigations at 44°C (see **Figure 1**)[1]. To measure VOR function in response to high angular accelerations (above 2,000°/s^2) a video head impulse test (vHIT) system was used (ICS system from GN Otometrics) according to the protocol described by MacDougall et al. (24) with head angular velocities reaching 80–250°/s by 100 ms. At least 20 head lateral rotations to each side and in the planes of each vertical semi-circular canals were performed. During the head movements, the patient was seated and fixed gaze on a small target 3 m away. Sections of the data with covert saccades and artifacts were removed from the recordings prior to gain calculations by the vHIT manufacturer's software. Gains were calculated based on the quotient of the areas under the eye and head velocity impulse responses. The interval used started 100 ms prior to peak head velocity and ended when head velocity first crossed zero after the peak. In the emergency ward, the patient's first vHITs were measured with an ESC system (Interacoustics). Gain values are computed differently with this system compared to the ICS system we used for all subsequent vHITs. For this reason, the gain ESC gain values were converted to equivalent ICS gains using the technique described in Cleworth et al. (25).

Balance Control Measures

Balance control was assessed by measuring trunk sway during a sequence of 14 stance and gait tasks. All stance and gait tasks were performed in the same order and executed without shoes. The tasks used were chosen based on our previous studies comparing balance for the 14 stance and gait balance tasks between different patient groups and healthy controls (10, 26). The same protocol is also used for routine clinical balance control examinations in our clinic. Trunk sway during the tasks was measured with a SwayStar^{TM} device (Balance International Innovations GmbH, Switzerland) which uses two gyroscopes to measure pitch (anterior-posterior) and roll (lateral) angular velocities of the lower trunk at a sample rate of 100 Hz. Angles were determined on-line by trapezoid integration of the velocity signals. The device is worn in the middle of the lower back of the patient to be tested (at the level of lumbar vertebrae L3–L5) near the body's center of mass (10). The SwayStar^{TM} device has been validated by a number of clinical studies, specifically on patient groups affected by vestibular loss (8, 10, 11), and allows comparison with a normal reference data set (26).

Four 2-legged balance tests were performed with the feet spaced shoulder width apart. Two were performed with eyes open, on a normal surface and on a foam surface (height 10 cm, density 25 kg/m^3), and 2 with eyes closed (abbreviated s2eo/s2ec/s2eof/s2ecf). Three 1-legged stance tasks were performed eyes open, two on a normal surface (eyes open and eyes closed) and one, eyes open, on the foam surface (s1eo/s1ec/s1eof). For the 1-legged tasks, the patient was asked to stand on their preferred leg. The stance tasks were performed on foam to reduce the contribution of lower-leg proprioceptive inputs to balance control. Stance tasks were performed for 20 s or until the patient lost balance. The patient performed 2 tandem gait tasks: walking 8 tandem steps on a normal and foam surface (w8tan/w8tanf), and 3 walking tasks: walking 3 m while pitching the head up and down with eyes open (w3mhp); while rotating the head left and right with eyes open (w3mhr) and walking 3 m, eyes closed (w3mec). Tasks were performed with eyes closed to eliminate visual inputs to balance control. For gait tasks, the patient was asked to walk at their comfortable pace. Finally, the patient was asked to walk up and down a set of 3 stairs (constructed similar to a podium), and walk over 4 low (24 cm) barriers spaced 1 m apart. For gait tasks, the task duration was the time it took to complete the task or until the patient lost balance and needed to be assisted by a spotter. To standardize the start of each gait task, the patient was asked to stand comfortably with feet hip-width apart.

Vestibular-Evoked Myogenic Potentials (VEMPs)

VEMPs were elicited from the sternocleidomastoid (SCM) and inferior oblique (Inf Obl) muscles using 5 ms duration air-conducted 500 Hz tone bursts (rise and fall times 2 ms) and delivered at a rate of 5.1 Hz. Normally the test amplitude was 85 dB normal hearing level. This level was increased or decreased

[1]Due to the unpleasant patient reactions we do not use ice water calorics. Instead we use rotating chair tests, with accelerations of 20 and 40 deg/s^2, to determine if there is a remaining peripheral function. In the current case, this test revealed, 4 days after BVL onset, amplitudes of 4.9 and 0.7 deg/s for right and left slow phase eye velocity, respectively, compared to the lower limit of normal responses 20 deg/s (mean-2sds) for20 deg/s^2 accelerations.

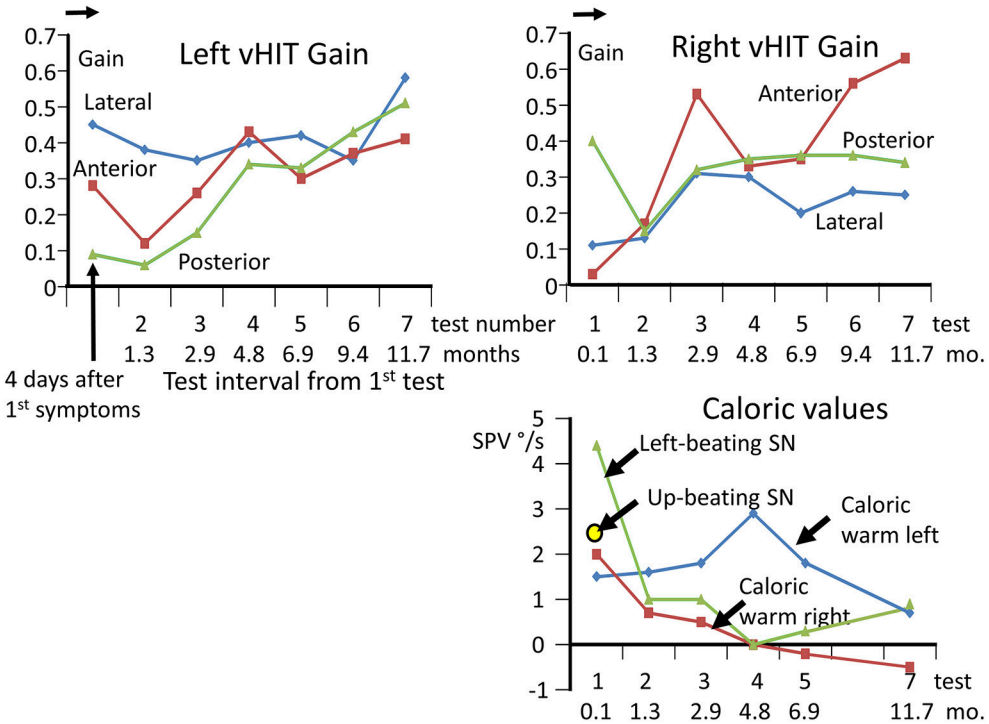

FIGURE 1 | Upper panels: changes in vHIT gains in each canal direction, from 4 days after onset of acute symptoms until 11.7 months later. A total of 7 tests were performed. Note the gradual improvement in the vHIT gains except for the left lateral and right posterior gain. All gains are lower than normal as marked by the arrow on the gain ordinate, indicating the lower 95% limit of healthy controls (23). Lower right panel: caloric measurement values over time and levels of spontaneous nystagmus. The values for the nystagmus slow phase velocity (SPV) elicited during the culmination phase 60–80 s from the start of a 60 s irrigation of 44°C are listed after subtraction of the SPV of the left-beating spontaneous nystagmus recorded over 20 s prior to the irrigation. Because of the small values, the canal paresis was not calculated. For the examination at 4 days only, an up-beating vertical spontaneous nystagmus was also observed.

depending on whether a response was observed at 85 dB. All muscles were tonically active during the experiments to ensure a VEMP response was elicited. The SCM was activated by having the patient voluntarily maintain a yaw head rotation 60° to the left for right ear stimulation, and vice-versa for the left ear. The Inf Obl was activated by having the patient look upwards. Averages to 500 stimuli were computed after high and low pass filtering at 10 and 1,500 Hz, respectively. From these averages peak-to-peak p13 to n23 amplitudes for c-VEMPs and n1 to p1 for o-VEMPs were compared with the lower 95% amplitude of normal responses (27). For further details, see the legend to **Figure 4**.

Data Processing and Statistical Analysis

The outcome measurements of each balance control trial were the peak-to-peak ranges for roll angle (ra), pitch angle (pa), roll angular velocity (rv), pitch velocity (pv), and the task duration (dur). We concentrated on 2 primary measures, a global balance control index with (BCI) and without stairs test (BCIns) to track improvements in balance control of the acute BVL patient over time. This index combines results from several different tasks into one index (see details below). As secondary measures, we examined trunk sway for those eyes closed tasks which comprise this index. The BCI is an additive composite score based on measures from several tests: From the test standing on 2 legs on foam with eyes closed (2 × pv), for walking 8 tandem steps (1 × ra), for walking 3 m eyes closed (1.5 × pv + 20 × dur), walking 3 m while pitching the head up and down (1.5× pv) and stairs (12× ra). That is BCI = $2 \times s2ecf_{pv} + tan8_{ra} + 1.5 \times w3ec_{pv} + 20 \times w3ec_{dur} + 1.5 \times w3hp_{pv} + 12 \times stairs_{ra}$ (28). For the first examination, the acute BVL patient could not complete the stairs task so we also used the same index without this task (BCIns). The step-wise discriminant analysis used to select the above task measures entering the BCI is described in Allum and Adkin (8). This combination of the selected balance outcome measures has been shown previously to have a high accuracy in detecting patients with impaired balance (8). The upper 95% limit of the BCI, BCIns, and secondary sway measures of 54 healthy persons of the same mean age (±5 years) as the patient were used to determine if the patient had pathological balance control (see also arrows on ordinates of **Figures 2**, **3**, **5**). We also compared the balance measures of the acute BVL patient with those of 8 chronic (over 10 years) male BVL patients of mean age 44 years whose data had been recorded in previous studies (29, 30). All BVL patients had bilateral absent responses or response <3 deg/s slow phase eye velocity (SPV) during caloric culmination periods. There was no difference between the rotating chair response amplitudes to 20 deg/s^2 accelerations of the acute BVL patient

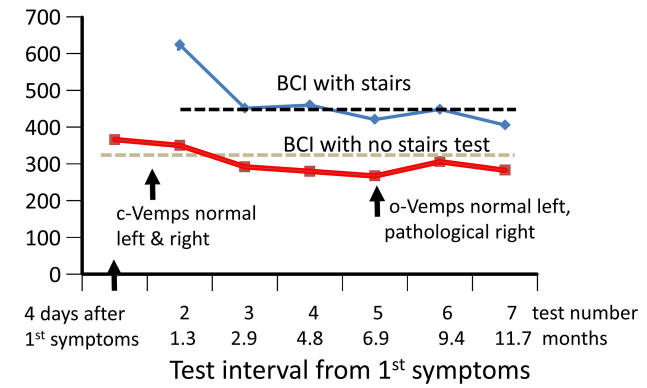

FIGURE 2 | Changes in Balance Control Index (BCI) over 12 months from onset of acute symptoms. The values of the BCI with and without the stairs test included are shown. The stairs test could not be performed for the first test due to the instability of the patient. The upper 95% limit of BCI values (lower values more normal) for the 54 healthy subjects whose ages were within ± 5 years of that of the patient (49 years) are shown by the dashed black and gray lines. The times the c- and o-VEMPs were measured are also indicated.

(mean SPV 3.9 and −2.6 deg/s) compared to the chronic BVL group (mean SPV 3.2 and −3.2 deg/s).

To compare the difference between the repeated acute BVL and chronic BVL patient population balance measures, and differences in acute BVL vHIT measures over time, both paired *t*-tests and non-parametric paired analyses (Wilcoxon signed rank tests) were used. Significance level was set at $p < 0.05$, and significance was accepted if both tests were significant. We also examined whether individual test values of the acute BVL differed from those of the chronic BVL population using the techniques described by Crawford et al. (31), yielding trends in differences ($0.1 < p < 0.05$) where significance was observed with paired *t*-tests.

RESULTS

At Acute Onset

The lateral plane vHIT responses gains on emergency inpatient admission were less than normal, 0.43 and 0.27 for left and right head impulses, respectively. There was also a spontaneous nystagmus beating to the left. These gains did not differ, significantly, from vHIT gains (0.45 left, 0.11 right) recorded for lateral canal planes 4 days later (see **Figure 1**). Covert and overt catch-up saccades were still present in the vHITs after 4 days. The left beating spontaneous nystagmus was still present having a SPV of 4.4 deg/s. In addition, an upbeat nystagmus with a SPV of 2 deg/s was observed. The initial diagnosis of an acute peripheral BVL could be confirmed by the absent responses to caloric irrigation of 44°C of each ear. After subtraction of the spontaneous nystagmus level, the average SPV over the culmination phase was only 1–2 deg/s (see **Figure 1**), making computation of the canal paresis of limited use. On admission, a 2-dimensional FLAIR magnetic resonance imaging (MRI) did not show a perfusion deficit or any other abnormality in the brainstem or the cerebellum. A follow-up 2-dimensional CISS MRI, 7 months later, also did not show any signs of a preceding stroke explaining the deficit in this patient. Despite the obvious peripheral loss, functional balance testing revealed results with values indicating better stability than we had expected. The balance control index (BCI), a combined index from several balance tests (8) was slightly larger than normal (see **Figure 2**) when the stairs test, which the patient could not complete, was excluded. The primary reasons for the lower (more normal) than expected BCI were firstly the almost normal pitch trunk sway velocity when standing eyes closed on a firm and foam surface (see **Figure 3**). Based on values from the group of chronic BVL subjects we had expected larger trunk sway amplitudes (see **Figure 3**, upper panels). Secondly, for the walking trials over 3 m, with head rotating left and right, pitching up and down or walking with eyes closed (see **Figure 5**), normal trunk sway amplitudes were observed. Nonetheless, the durations of these gait trials were longer than normal. [Typically for acute UVL patients both trunk velocity and task duration are greater than normal (8) as they attempt to improve stability by walking slowly (32)]. These results indicated together with the greater than normal dependence on visual inputs during stance (see lower panel **Figure 3**), a more rapid compensation than has been observed with acute UVL patients having an almost total unilateral peripheral loss (5).

Tests of c-VEMP indicated that sacculus-driven vestibular spinal reflexes were normal (see **Figure 4**, left panels). Tests of o-VEMPs carried out at 6 months were normal for the left with lower peak-to-peak amplitudes for the right stimulation side.

Improvement Over Time

The caloric responses did not improve over time but the horizontal spontaneous nystagmus decreased (see **Figure 1**) and the vertical nystagmus was no longer present. With the exception of the left lateral and right posterior VORs, vHIT response gains increased (see **Figure 1**) significantly over the 12 months follow-up ($p = 0.002$). However, covert and overt catch-up saccades were still present in the vHITs at 12 months. vHIT gain was below 0.6 bilaterally over the first 9 months [fitting the consensus definition of BVL (6)] and with the exception anterior right (0.63) remained below 0.6 at 12 months (see **Figure 1**). Balance control as summarized by the BCI value remained on the borderline of normal but was <95% limit of normal control subjects after 3 months (see **Figure 2**). This was partially due to sway during stance eyes closed on foam decreasing over time, remaining significantly less ($p < 0.03$) than the sway of chronic BVL subjects (see **Figure 3**). There was also a gradual decrease in the visual and increase in the somatosensory contribution to stance determined from pitch sway velocities during stance tasks (see **Figure 3**). However, at 9 months visual and somatosensory contributions were within normal bounds and at 12 months vestibular contributions were normal too (see **Figure 3**). Another reason for the reduction of the BCI was the increase in gait speed with trunk roll sway angles and velocities

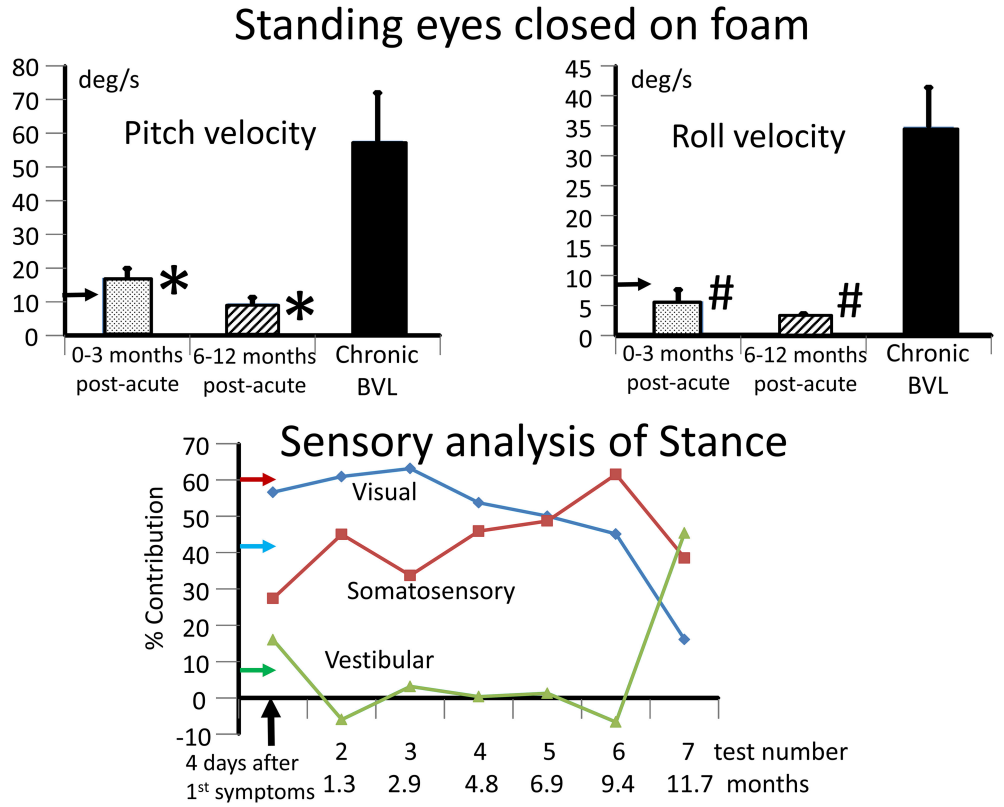

FIGURE 3 | Upper panels: mean values and standard error of mean (sem) of BVL subjects for the range of trunk pitch and roll velocity while standing eyes closed on a foam surface. The leftmost column in each panel depicts the mean of 3 tests in the 3 months post-acute onset. The middle column in each panel depicts the mean of 3 tests in the 6–12 months period post-acute onset. The right column represents the mean values of the population of 8 chronic BVL subjects (mean age 44 years), all of whom had velocity values >95% upper limit of 54 normals of mean age 49. This limit, 11 deg/s for pitch and 8.4 deg/s for roll velocity, is shown by the horizontal arrows on the plot ordinates. The bars on the columns represent the sems. *$p < 0.03$ for the comparison of acute to chronic BVL pitch velocity means. #$p < 0.003$ for the comparison of roll velocity means. Lower panel: sensory analysis of stance profile over the 12 months follow-up of the acute BVL subject. The estimated contribution of each sensory input to pitch sway was computed using the technique of Horlings et al. (9). For example, for the 4 2-legged stance test conditions normal floor eyes open and closed (s2eo, s2ec) and foam support eyes open and closed (s2eof, s2ecf) the visual contribution is estimated to be:
((s2ecf-s2eof)+(s2ec-s2eo))/(s2ecf+s2eof+s2ec+s2eo)*100%.
The somatosensory contribution is estimated to be:
((s2ecf-s2ec)+(s2eof-s2eo))/(s2ecf+s2eof+s2ec+s2eo)*100%.
The vestibular contribution is estimated to be 100% minus the visual and somatosensory contributions. The 95% upper limit for visual and somatosensory contribution estimates with respect to healthy controls are shown by the horizontal arrows on the ordinate (larger values pathological), likewise the lower normal 5% limit (smaller values pathological) for the vestibular contribution. Thus, the visual and somatosensory contributions were pathologically greater than normal from 1.3 to 11.7 months and therefore the vestibular contribution less than normal over this period.

remaining normal. For example, as illustrated in **Figure 5**, task duration for the eyes closed gait task was significantly reduced ($p < 0.002$), with respect to chronic BVL subjects, over the last 6 months of the 12 months follow-up period, as was the roll angle amplitude.

These results match the symptoms reported by the patient and the improvement in balance control reported by his physiotherapist. Oscillopsia reported by the patient was first reduced at examination 5 (at 6.8 months) and absent at examination 6 at 9.4 months. Vertigo and imbalance with fast head movements reported by the patient were also absent at 9.4 months. Persistent problems still noted by the patient were walking in the dark and at dusk. Furthermore, a loss of orientation occurred when swimming under water.

DISCUSSION

This case study raises questions about examination strategies for balance control deficits for patients with suspected vestibular loss. The most important questions are firstly how extensive should testing for sensory deficits be, and secondly at which time points should functional testing of vestibulo-spinal influences on balance control occur. This case emphasizes the viewpoint that VEMP tests of otolith function are crucial for assessing remaining vestibular function in BVL patients (22). We assume that functional balance testing will be required regularly as changes in balance control following a vestibular deficit cannot be predicted, with the possible exception of roll instability during gait (13), by the sensory vestibular loss observed in canal-based responses (7, 11).

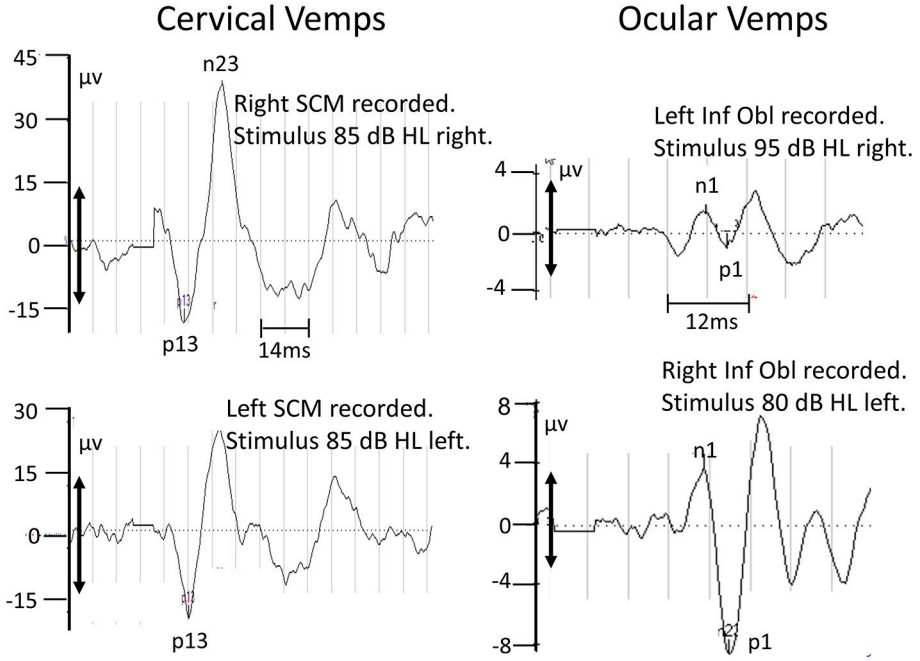

FIGURE 4 | Recordings of c-VEMPs (left panels) and o-VEMPs (right panel) taken 1 and 6.9 months after acute onset of symptoms, respectively. The upper 2 sets of traces are for right ear stimulation, the lower 2 sets for left ear stimulation. The air-conducted (500 Hz) stimulation level was increased to 95 dB to elicit right o-VEMPs. The double-headed arrows on the ordinates indicate the minimum VEMP amplitude (28.6 μV for c-VEMPs, 5.2 μV for o-VEMPs) necessary to define a normal response (above the lower 5% limit of normal control subjects; (27)]. Based on these criteria the right o-VEMPs are not normal.

This case study indicates that it is crucial in cases of BVL to measure ocular and cervical vestibular evoked myogenic potentials (o- and c-VEMPs) in order to determine if utricular and saccular driven vestibule-spinal reflexes are functioning normally. In our acute BVL patient, VEMPs showed little abnormalities (see **Figure 4**) despite absent caloric, and lower than normal vHIT VOR canal gains. Remarkably, with apparent preservation of otolith function, the patient was able to stand, without falling, eyes closed on foam for the test time of 20 s within 1 month of acute symptoms, having, except at acute onset, none of the typical stance instability as indicated by higher trunk angular velocities shown on foam surfaces by our group of chronic BVL patients (9). Also, the acute BVL patient was able to walk quicker and more securely after 3 months with eyes closed than chronic BVL patients. These 2 tests together with other stance and gait tests form the basis of functional balance tests identifying patients with vestibular loss (10). As visual compensating inputs are not available during these eyes-closed tests, the most parsimonious explanation for the normal stance and gait performance 3 months after acute BVL onset is that the otolith inputs had been "reprogrammed" to partially replace canal-based vestibular sensory contributions to balance control. It is therefore of interest to consider the basis of the current neurophysiological differences underlying the central adjustments to deficits in semicircular canal responses.

O- and c-VEMPs have been studied before in BVL patients (27, 33). Brantberg and Löfqvist (33) reported preserved c-VEMPs in 5 patients with bilateral vestibular areflexia, in 3 of them there was no significant caloric response, no per-rotatory nystagmus and clinical head-impulse-tests showed corrective saccades following horizontal and vertical head-movements (in two patients head-impulse-tests were not performed). Brain-MRIs of these patients were unremarkable. The recent findings of Agrawal et al. (27) on BVL patients suggest preservation of sacculus and utriculus function relative to semicircular canal function in approximately 40% of BVL patients with decreased function due to aminoglycoside ototoxicity or bilateral Ménière's disease (27). In other BVL cases not described by Agrawal et al. (27), those with vestibular neuritis causing sudden, severe and long-lasting vertigo, the lesion is presumed to be located in the vestibular nerve with a preference for sparing of the inferior nerve due to anatomical considerations (34–36). A bilateral neuritis of the superior vestibular nerve which spared sacculus function (22) can therefore be explained by such anatomical considerations. In our case with bilaterally intact c- and almost intact o-VEMPs alternative explanations must be sought.

An interesting aspect of our observations of this case is the presence of a left beating spontaneous nystagmus (SN), consistent with the slightly greater response to warm caloric irrigation on the left, and the greater lateral canal vHIT gain on the left (see **Figure 1**). Kattah (37) reported that for subacute and chronic BVL gaze evoked SN is generally not present. We assume that if the degree of loss is unequal between the left and right lateral canal nerves, then a left beating SN would result. Four days after 1st symptoms a weak up beating vertical SN (2.5 deg/s) was also observed. In the following weeks no vertical SN was observed

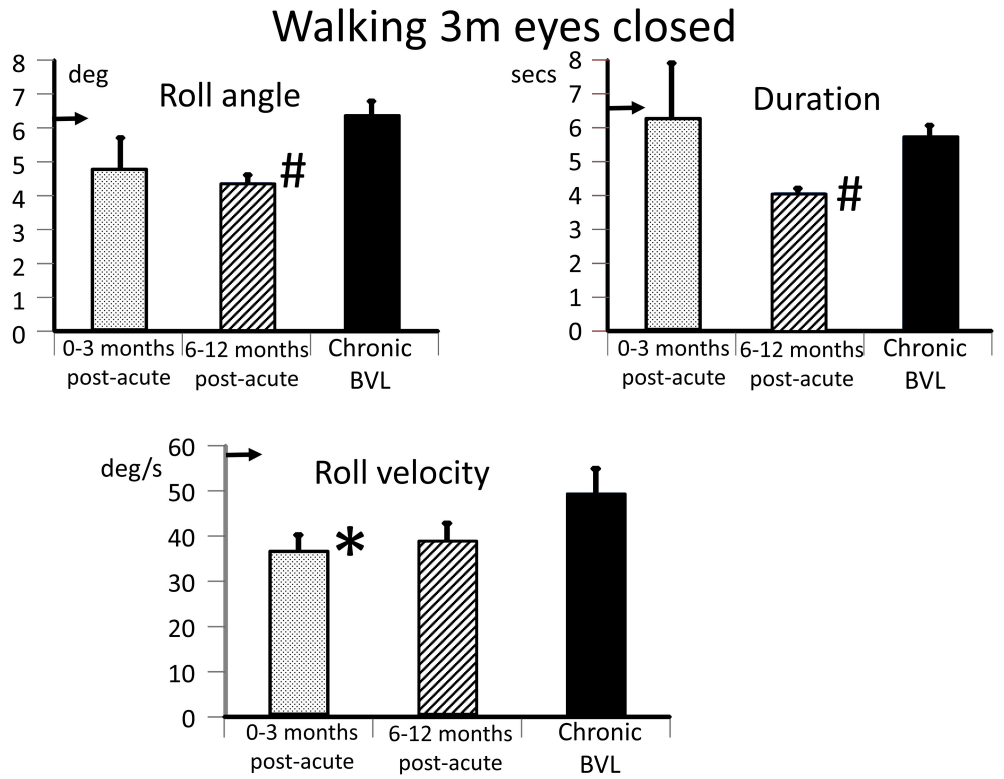

FIGURE 5 | Measures of trunk balance control for the task, walking 3 m eyes closed. The layout of the figure is identical to that of **Figure 3** (upper panels). The mean values of the acute BVL subject are compared to a population of 8 chronic BVL subjects and 54 normal control subjects (horizontal arrows on the ordinates). #$p \leq 0.002$ and *$p = 0.05$.

in our recordings. We assume that this vertical SN is probably the result of bilaterally differing vertical canal VOR gains. Initially, the anterior canal vHIT gain was lower on right side compared to left, and the posterior canal gain was lower on the left side compared to the right (see **Figure 1**), indicating a greater effect of the underlying disease on the right superior nerve and the left inferior nerve. However, the presence o-VEMPs on the right side would tend to exclude a case of pure right superior nerve neuritis. Yacovino et al. (22) reported an upbeating SN with fixation removed in their case of bilateral superior nerve loss suggesting a difference between the peripheral vestibular losses left and right. However, in their case, which they assumed the SN resulted from vestibular neuritis, o-VEMPs were initially absent bilaterally. Likewise, in our case the presence of c-VEMPs bilaterally would tend to exclude a left inferior nerve neuritis. While we assume that differences in peripheral loss bilaterally underlies the left and up beating SN we observed in our BVL case, we cannot exclude that changes in central processing partially underlie the presence of the observed SN. In short, if we assume that our results are consistent with a concomitant vestibular neuritis, we would have to assume that otolith nerves were spared. Confirmatory evidence for this mechanism needs to be acquired from several patients. Here our patho-physiological observations are limited to one patient and do not include 3-dimensional MRI procedures to visualize affected nerves.

Recent advances in 3-dimensional MRI procedures (38, 39) have suggested that it may be possible to visualize which nerves are affected by vestibular neuritis. To date these techniques have been limited to showing that the duration of SN is longer when a higher signal intensity was present on the deficit side (39). In future, use of such MRI signal enhancement techniques in combination with physiological recordings (spontaneous nystagmus, vHIT, VEMPs, and functional balance control examinations as reported here) could provide information on which vestibular nerves were affected following acute BVL or UVL and thereby provide new insights into the etiology of patients' balance deficits and bases for rehabilitative treatment.

The average increase in vHIT gains over 12 months for all 3 test axes for both ears was 0.23 with most of the gain change occurring over the first 7 months (see **Figure 1**). This value is similar to the increase in lateral vHIT gain, 0.19, observed after 3 months for acute UVL patients who had no caloric recovery from a lateral canal paresis of >90% (5). For the lateral canals, the unchanged CP values indicated that this improvement must be due to central compensation. For the vertical canals, there is no known way to establish whether any peripheral recovery occurred. It is assumed that central compensation with a unilateral loss occurs through a reweighting of the normal contralateral input to the deficit side (3, 4). In the case of bilateral loss, this mode of compensation would appear to be limited.

An alternative mode of compensation would be to increase the gain of cervico-ocular reflexes which are known to be increased following BVL (40). Nonetheless, the central compensation of canal VOR responses appears to be modest in our acute BVL patient in comparison to the spared otolith function.

The overall response characteristics we observed are similar to those observed with canal plugging in animals. This preparation inactivates the semicircular canals but not the otoliths. Subsequent testing of the animals indicated that postural stability mainly requires otoliths inputs (14, 15), as we found in our patient.

One theory of central compensation that has been proposed (41) is based on otolith responses being processed by a different portion of the vestibular nuclei (caudally) than canal responses (rostrally). According to this theory, the caudal vestibular nuclei have a greater capacity for sensory substitution. A further possibility is that the caudal vestibular nuclei are more capable of enhancing remaining otolith input than the rostral nuclei are for the modest improvement in canal sensory inputs leading, as illustrated in **Figure 1**, to only a modest improvement in VOR gains.

One drawback of the current study is that the follow-up period of 1 year may have been too short to determine the long-term result of acute BVL due, as we assume, to vestibular neuritis. Most studies including our own (29, 30) investigated patients with chronic BVL lasting over 10 years. Thus, the differences we observed between the acute and chronic BVL patients may have been due to this short follow-up interval. It is important to note, however, that in this acute BVL case otolith responses were preserved as these were in 40% of BVL patients with other etiologies (27). Another problem with comparing chronic (over 10 years) and recently acute BVL patients is that changes in test procedures occur over time making comparisons difficult, for example, for more recently introduced procedures such as vHIT and VEMPs.

The role of prior training in the use of otolith inputs, due to being the crane cockpit and receiving off-axis rotation may have positively influenced the rapid recovery of the patient. For example, both figure skaters and gymnasts have superior interpretation of otolith signals when no canal signal is present (42, 43). With the preserved otolith responses we observed, the patient could have benefitted from a prior learning to recognize head rotation using otolith signals. This learned strategy may have been reinforced by the intensive physiotherapy the patient received.

Testing for the presence of VEMPs would seem to be crucial in aiding the patient's vestibular rehabilitation in physiotherapy. Further periodic testing of balance control while the patient is receiving physiotherapy provides important information for physiotherapists and physicians needing to base the decision to allow the patient to work again on functional balance control tests. In this report, we have emphasized testing for deficient vestibular contributions to balance control using body-mounted sensors recording trunk sway during functional stance and gait tasks. Other techniques such as dynamic posturography combined with electro-myographic recordings can also be employed (44), but are generally more complex.

ETHICS STATEMENT

Scientific use of the data collected for this study was approved (Approval 2014-16) by the local ethics committee responsible for the University Hospital Basel [Ethics Committee Northwest and Central Switzerland (EKNZ)].

AUTHOR CONTRIBUTIONS

JA and FH analysed the data. JA wrote the first draft of the manuscript. FH and HR revised the manuscript. All three authors contributed to the selection and planning of patient tests.

ACKNOWLEDGMENTS

We thank Ms Barbara Wenger for editorial assistance.

REFERENCES

1. Halmagyi GM, Chen L, MacDougall HG, Weber KP, McGarvie LA, Curthoys IS. The video head impulse test. *Front Neurol.* (2017) 8:258. doi: 10.3389/fneur.2017.00258
2. Allum JH, Cleworth T, Honegger F. Recovery of vestibulo-ocular reflex symmetry after an acute unilateral peripheral vestibular deficit: time course and correlation with canal paresis. *Otol Neurotol.* (2016) 37:772–80. doi: 10.1097/MAO.0000000000001054
3. Sadeghi S, Goldberg J, Minor L, Cullen K. Effects of canal plugging on the vestibuloocular reflex and vestibular nerve discharge during passive and active head rotations. *J Neurophysiol.* (2009) 102:2693–703. doi: 10.1152/jn.00710.2009
4. Sadeghi S, Minor L, Cullen K. Response of vestibular-nerve afferents to active and passive rotations under normal conditions and after unilateral labyrinthectomy. *J Neurophysiol.* (2007) 97:1503–14. doi: 10.1152/jn.00829.2006
5. Allum JHJ, Scheltinga A, Honegger F. The effect of peripheral vestibular recovery on improvements in vestibulo-ocular reflexes and balance control after acute unilateral vestibular loss. *Otol Neurotol.* (2017) 38:e531–8. doi: 10.1097/MAO.0000000000001477
6. Strupp M, Kim J-S, Murofushi T, Straumann D, Jen J, Rosengren S, et al. Bilateral vestibulopathy: diagnostic criteria consensus document of the classification committee of the bárány society. *J Vestib Res.* (2017) 27:177–89. doi: 10.3233/VES-170619
7. Allum JHJ, Honegger F. Relation between head impulse tests, rotating chair tests, and stance and gait posturography after an acute unilateral peripheral vestibular deficit. *Otol Neurotol.* (2013) 34:980–9. doi: 10.1097/MAO.0b013e31829ce5ec
8. Allum JH, Adkin AL. Improvements in trunk sway observed for stance and gait tasks during recovery from an acute unilateral peripheral vestibular deficit. *Audiol Neurootol.* (2003) 8:286–302. doi: 10.1159/000071999
9. Horlings CG, Kung UM, Bloem BR, Honegger F, Van Alfen N, Van Engelen BG, et al. Identifying deficits in balance control following vestibular or proprioceptive loss using posturographic analysis of stance tasks. *Clin Neurophysiol.* (2008) 119:2338–46. doi: 10.1016/j.clinph.2008.07.221
10. Allum JH, Carpenter MG. A speedy solution for balance and gait analysis: angular velocity measured at the centre of body mass. *Curr Opin Neurol.* (2005) 18:15–21. doi: 10.1097/00019052-200502000-00005

11. Allum JHJ, Honegger F. Recovery times of stance and gait balance control after an acute unilateral peripheral vestibular deficit. *J Vestib Res*. (2016) 25:219–31. doi: 10.3233/VES-150561
12. Allum JH. Recovery of vestibular ocular reflex function and balance control after a unilateral peripheral vestibular deficit. *Front Neurol*. (2012) 3:83. doi: 10.3389/fneur.2012.00083
13. Allum JH, Honegger F. Correlations between multi-plane vHIT and balance control after onset of an acute unilateral vestibular deficit. *Otol Neurotol*. (in press).
14. Money KE, Scott JW. Functions of separate sensory receptors of nonauditory labyrinth of the cat. *Am J Physiol*. (1962) 202:1211–20. doi: 10.1152/ajplegacy.1962.202.6.1211
15. Schor RH, Miller AD. Vestibular reflexes in neck and forelimb muscles evoked by roll tilt. *J Neurophysiol*. (1981) 46:167–78. doi: 10.1152/jn.1981.46.1.167
16. Rosengren SM, Welgampola MS, Colebatch JG. Vestibular evoked myogenic potentials: past, present and future. *Clin Neurophysiol*. (2010) 121:636–51. doi: 10.1016/j.clinph.2009.10.016
17. Sandhu J, George S, Rea P. The effect of electrode positioning on the ocular vestibular evoked myogenic potential to air-conducted sound. *Clin Neurophysiol*. (2013) 124:1232–6. doi: 10.1016/j.clinph.2012.11.019
18. Naranjo EN, Cleworth TW, Allum JHJ, Inglis JT, Lea J, Westerberg BD, et al. Vestibulo-spinal and vestibulo-ocular reflexes are modulated when standing with increased postural threat. *J Neurophysiol*. (2016) 115:833–42. doi: 10.1152/jn.00626.2015
19. Allum JH, Honegger F, Acuña H. Differential control of leg and trunk muscle activity by vestibulo-spinal and proprioceptive signals during human balance corrections. *Acta Otolaryngol*. (1995) 115:124–9. doi: 10.3109/00016489509139273
20. Allum JHJ, Honegger F. Interactions between vestibular and proprioceptive inputs triggering and modulating human balance-correcting responses differ across muscles. *Exp Brain Res*. (1998) 121:478–94. doi: 10.1007/s002210050484
21. Govender S, Fernando T, Dennis D, Welgampola M, Colebatch J. Properties of 500 Hz air- and bone-conducted vestibular evoked myogenic potentials (VEMPs) in superior canal dehiscence. *Clin Neurophysiol*. (2016) 127:2522–31. doi: 10.1016/j.clinph.2016.02.019
22. Yacovino DA, Finlay JB, Urbina Jaimes VN, Verdecchia DH, Schubert MC. Acute bilateral superior branch vestibular neuropathy. *Front Neurol*. (2018) 9:353. doi: 10.3389/fneur.2018.00353
23. McGarvie LA, MacDougall HG, Halmagyi GM, Burgess AM, Weber KP, Curthoys IS. The Video Head Impulse Test (vHIT) of semicircular canal function—age-dependent normative values of vor gain in healthy subjects. *Front Neurol*. (2015) 6:154. doi: 10.3389/fneur.2015.00154
24. MacDougall HG, Weber KP, McGarvie LA, Halmagyi GM, Curthoys IS. The video head impulse test: diagnostic accuracy in peripheral vestibulopathy. *Neurology*. (2009) 73:1134–41. doi: 10.1212/WNL.0b013e3181bacf85
25. Cleworth T, Carpenter MG, Allum JHJ. Differences in head impulse test results due to analysis techniques. *J Vestib Res*. (2017) 26:163–72. doi: 10.3233/VES-170614
26. Gill J, Allum JH, Carpenter MG, Held-Ziolkowska M, Adkin AL, Honegger F, et al. Trunk sway measures of postural stability during clinical balance tests: effects of age. *J Gerontol A Biol Sci Med Sci*. (2001) 56:M438–47. doi: 10.1093/gerona/56.7.M438
27. Agrawal Y, Bremova T, Kremmyda O, Strupp M. Semicircular canal, saccular and utricular function in patients with bilateral vestibulopathy: analysis based on etiology. *J Neurol*. (2013) 260:876–83. doi: 10.1007/s00415-012-6724-y
28. Hegeman J, Shapkova EY, Honegger F, Allum JHJ. Effect of age and height on trunk sway during stance and gait. *J Vestib Res*. (2007) 17:75–87.
29. Honegger F, Hillebrandt IMA, van den Elzen NGA, Tang K-S, Allum JHJ. The effect of prosthetic feedback on the strategies and synergies used by vestibular loss subjects to control stance. *J Neuroeng Rehabil*. (2013) 10:115. doi: 10.1186/1743-0003-10-115
30. Allum JH, Oude Nijhuis LB, Carpenter MG. Differences in coding provided by proprioceptive and vestibular sensory signals may contribute to lateral instability in vestibular loss subjects. *Exp Brain Res*. (2008) 184:391–410. doi: 10.1007/s00221-007-1112-z
31. Crawford J, Garthwaite P, Howell D, Gray C. Inferential methods for comparing a single case with a control sample: modified *t*-tests versus mycroft et al.'s (2002) modified anova. *Cogn Neuropsychol*. (2004) 21:750–5. doi: 10.1080/02643290342000276
32. Goutier KMT, Jansen SL, Horlings CGC, Küng UM, Allum JHJ. The influence of walking speed and gender on trunk sway for the healthy young and older adults. *Age Ageing*. (2010) 39:647–50. doi: 10.1093/ageing/afq066
33. Brantberg K, Löfqvist L. Preserved vestibular evoked myogenic potentials (VEMP) in some patients with walking-induced oscillopsia due to bilateral vestibulopathy. *J Vestib Res*. (2007) 17:33–8.
34. Goebel JA, O'Mara W, Gianoli G. Anatomic considerations in vestibular neuritis. *Otol Neurotol*. (2001) 22:512–8. doi: 10.1097/00129492-200107000-00018
35. Himmelein S, Lindemann A, Sinicina I, Horn AKE, Brandt T, Strupp M, et al. Differential involvement during latent herpes simplex virus 1 infection of the superior and inferior divisions of the vestibular ganglia: implications for vestibular neuritis. *J Virol*. (2017) 91:e00331–17. doi: 10.1128/JVI.00331-17
36. Schuknecht HF, Witt RL. Acute bilateral sequential vestibular neuritis. *Am J Otolaryngol*. (1985) 6:255–7. doi: 10.1016/S0196-0709(85)80051-X
37. Kattah JC. Clinical characteristics and etiology of bilateral vestibular loss in a cohort from central illinois. *Front Neurol*. (2018) 9:46. doi: 10.3389/fneur.2018.00046
38. Park KM, Shin KJ, Ha SY, Park JS, Kim SE. A case of acute vestibular neuritis visualized by three-dimensional FLAIR-VISTA magnetic resonance imaging. *Neuro-Ophthalmology*. (2014) 38:60–1. doi: 10.3109/01658107.2013.874454
39. Byun H, Chung J, Lee S, Park C, Park D, Kim T. Clinical value of 4-hour delayed gadolinium-enhanced 3D FLAIR MR images in acute vestibular neuritis. *Laryngoscope*. (2018) 128:1946–51. doi: 10.1002/lary.27084
40. Bronstein AM, Morland AB, Ruddock KH, Gresty MA. Recovery from bilateral vestibular failure: implications for visual and cervico-ocular function. *Acta Otolaryngol Suppl*. (1995) 520(Pt 2):405–7. doi: 10.3109/00016489509125283
41. McCall AA, Yates BJ. Compensation following bilateral vestibular damage. *Front Neurol*. (2011) 2:88. doi: 10.3389/fneur.2011.00088
42. Hartmann M, Haller K, Moser I, Hossner E-J, Mast F. Direction detection thresholds of passive self-motion in artistic gymnasts. *Exp Brain Res*. (2014) 232:1249–58. doi: 10.1007/s00221-014-3841-0
43. Tanguy S, Quarck G, Etard O, Gauthier A, Denise P. Are otolithic inputs interpreted better in figure skaters? *Neuroreport*. (2008) 19:565–8. doi: 10.1097/WNR.0b013e3282f9427e
44. Allum JH, Bloem BR, Carpenter MG, Honegger F. Differential diagnosis of proprioceptive and vestibular deficits using dynamic support-surface posturography. *Gait Posture*. (2001) 14:217–26. doi: 10.1016/S0966-6362(01)00142-4

Conflict of Interest Statement: JA and FH worked as consultants for the company manufacturing the balance measuring equipment used in this study. HR has received travel support from Bayer Healthcare, Teva, and Genzyme.

frontiers in Neurology

ORIGINAL RESEARCH
published: 20 February 2020
doi: 10.3389/fneur.2020.00079

Improvement After Vestibular Rehabilitation Not Explained by Improved Passive VOR Gain

Jennifer L. Millar[1,2], *Yoav Gimmon*[2,3], *Dale Roberts*[4] *and Michael C. Schubert*[1,2]*

[1] Department of Physical Medicine and Rehabilitation, Johns Hopkins University School of Medicine, Baltimore, MD, United States, [2] Laboratory of Vestibular NeuroAdaptation, Department of Otolaryngology - Head and Neck Surgery, Baltimore, MD, United States, [3] Department of Physical Therapy, Faculty of Health Sciences, Ben-Gurion University of the Negev, Beer-Sheva, Israel, [4] Department of Neurology, Johns Hopkins University School of Medicine, Baltimore, MD, United States

Gaze stability exercises are a critical component of vestibular rehabilitation for individuals with vestibular hypofunction and many studies reveal the rehabilitation improves functional performance. However, few studies have examined the vestibular physiologic mechanisms (semicircular canal; otolith) responsible for such recovery after patients with vestibular hypofunction complete gaze and gait stability exercises. The purpose of this study was to compare behavioral outcome measures (i.e., visual acuity during head rotation) with physiological measures (i.e., gain of the vestibulo-ocular reflex) of gaze stability following a progressive vestibular rehabilitation program in patients following unilateral vestibular deafferentation surgery (UVD). We recruited $n = 43$ patients ($n = 18$ female, mean 52 ± 13 years, range 23–80 years) after unilateral deafferentation from vestibular schwannoma; $n = 38$ (25 female, mean 46.9 ± 15.9 years, range 22–77 years) age-matched healthy controls for dynamic visual acuity testing, and another $n = 28$ (14 female, age 45 ± 17, range 20–77 years) healthy controls for video head impulse testing. Data presented is from $n = 19$ patients (14 female, mean 48.9 ± 14.7 years) with UVD who completed a baseline assessment ~6 weeks after surgery, 5 weeks of vestibular physical therapy and a final measurement. As a group, subjective and fall risk measures improved with a meaningful clinical relevance. Dynamic visual acuity (DVA) during active head rotation improved [mean ipsilesional 38.57% ± 26.32 ($n = 15/19$)]; mean contralesional 39.96% ± 22.62 ($n = 12/19$), though not uniformly. However, as a group passive yaw VOR gain (mean ipsilesional pre 0.44 ± 0.18 vs. post 0.44 ± 0.15; mean contralesional pre 0.81 ± 0.19 vs. post 0.85 ± 0.09) did not show any change ($p \geq 0.4$) after rehabilitation. The velocity of the overt compensatory saccades during ipsilesional head impulses were reduced after rehabilitation; no other metric of oculomotor function changed ($p \geq 0.4$). Preserved utricular function was correlated with improved yaw DVA and preserved saccular function was correlated with improved pitch DVA. Our results suggest that 5 weeks of vestibular rehabilitation using gaze and gait stability exercises improves both subjective and behavioral performance despite absent change in VOR gain in a majority of patients, and that residual otolith function appears correlated with such change.

Keywords: vestibular rehabilitation, dynamic visual acuity, vestibulo-ocular reflex gain, compensatory saccades, otolith function

OPEN ACCESS

Edited by:
Joel Alan Goebel, Washington University School of Medicine in St. Louis, United States

Reviewed by:
Angelica Perez Fornos, Geneva University Hospitals (HUG), Switzerland
Christopher Bockisch, University of Zurich, Switzerland

***Correspondence:**
Michael C. Schubert
mschube1@jhmi.edu

Specialty section:
This article was submitted to Neuro-Otology, a section of the journal Frontiers in Neurology

Received: *15 November 2019*
Accepted: *22 January 2020*
Published: *20 February 2020*

Citation:
Millar JL, Gimmon Y, Roberts D and Schubert MC (2020) Improvement After Vestibular Rehabilitation Not Explained by Improved Passive VOR Gain. Front. Neurol. 11:79. doi: 10.3389/fneur.2020.00079

INTRODUCTION

Gaze stability refers to the eyes maintaining a stable position in space (and the head in this context) relative to a head movement, which is essential for providing stable visual acuity during walking and other activities of daily living. While walking, healthy controls experience gait velocity ranging from 0.6 to 2.5 m/s while the head translates in frequencies ranging from 1.4 to 2.5 Hz (1, 2). When running, the frequency of head rotation in pitch is twice that of yaw (pitch median = 3.2 Hz, yaw median <2 Hz) and can reach peaks from 15 to 20 Hz (2). Given the high range of velocity and frequency of head motion encountered during such typical life, healthy vestibular function is essential to ensure gaze stability (3). When lesioned, the vestibulo-ocular reflex (VOR) is unable to stabilize the eyes during head motion and visual acuity degrades (4–6).

Gaze stability exercises are considered a critical component of vestibular rehabilitation for individuals with vestibular hypofunction (7). Prior studies have shown gaze stability exercises are effective at improving visual acuity during active head rotation (dynamic visual acuity) as well as postural stability in patients with unilateral vestibular hypofunction (UVH) (8, 9) and following vestibular schwannoma resection (10). Interestingly, patient's self-report of oscillopsia post intervention does not correlate with improved dynamic visual acuity (DVA), nor does age, time from onset, initial DVA score, duration or type of exercise (8, 11).

There is evidence that the lesioned VOR gain (eye/head velocity) to slow velocity passive head rotation can be improved. Enticott et al. (5), reported patients who performed gaze stabilization exercises following vestibular schwannoma tumor resection did reduce their asymmetry of VOR gain, as measured during slow velocity (60°/s) rotatory chair testing. Additionally, those patients reported reduced dizziness compared to control subjects. More recently, Sadeghi et al. have used passive ipsilesional whole-body rotation to reduce VOR asymmetry (12). There is some evidence the VOR gain can improve to faster, active (self-generated) head velocity rotation as well. Measuring the eye and active head velocity (scleral search coil) before and after a 5 weeks of vestibular rehabilitation in patients with unilateral vestibular hypofunction due to presumed vestibular neuritis, Schubert et al. (9) described a 35% improvement in ipsilesional VOR gain during the active DVA testing [mean gain 0.7 ± 0.2 to 0.9 ± 0.2 ($p < 0.05$)]. Additionally, the patient subjects recruited a larger number of compensatory saccades (saccades in the direction of the deficient VOR) to assist with gaze stability that was dependent on magnitude of the VOR gain (9, 13). Others have shown a similar inverse relationship with the presence of compensatory saccades and magnitude of VOR gain change after vestibular rehabilitation (14).

To our knowledge, no study has assessed the effect of active head rotation gaze stability exercises on functional and physiological outcome measures of vestibular function. The purpose of this study was to compare behavioral (i.e., DVA) and functional (i.e., fall risk) outcome measures with vestibular physiological measures including semicircular canal (i.e., VOR gain) and otolith (saccule and utricule) function following a progressive 5 week vestibular rehabilitation program in patients following unilateral vestibular deafferentation (UVD) surgery.

METHODS

Subjects

We recruited $n = 43$ patients ($n = 18$ female, mean 52 ± 13 years, range 23–80 years) post UVD surgery due to vestibular schwannoma tumor resection; 19 of those patients completed the study (14 female, mean 48.9 ± 14.7 years). We also recruited and collected data in $n = 38$ ($n = 25$ female, mean 46.9 ± 15.9 years, range 22–77 years) aged matched healthy controls for DVA testing, and another $n = 28$ (14 female, age 45 ± 17, range 20–77 years) healthy controls for video head impulse testing. Patients were excluded for traumatic brain injury, cerebrovascular accident, or multiple sclerosis. The study was approved by the Johns Hopkins University Institutional Review Board and written informed consent was obtained from each individual.

Data presented below is from the $n = 19$ patients with UVD who completed an initial measurement, 5 weeks of vestibular physical therapy (VPT), and a final measurement. Sixteen patients were lost to follow up given they resided out of state; the final eight patients were excluded from the data analysis due to extended time between surgery and initial testing or extended time between pre and post VPT testing.

Overview

The pre VPT measure was collected ∼6 weeks post vestibular schwannoma tumor resection in an outpatient clinic setting (39 ± 31 days). The post VPT measure was collected mean 56 ± 25 days from the pre VPT measure. Outcome measures were collected from the physiologic (i.e., VOR gain), performance (i.e., computerized DVA), and subjective (i.e., dizziness handicap inventory) domains. Data collection and intervention was performed by one of two research physical therapists (JLM, YG). VPT included 5 weeks of gaze stability exercises as well as static and dynamic postural stability tasks (8). Each patient was given a home exercise program and followed up weekly with in-clinic outpatient visits. Each patient received 5 weeks of treatment. All data was stored into a customized online cloud database (REDCap Vanderbilt University) for offline analysis.

Physiologic Measures

The Video Head Impulse Test (vHIT)

The vHIT (ICS Otometrics, Natus Medical Incorporated, Denmark) measured VOR gain (eye velocity/head velocity) as well as metrics of the compensatory saccades [latency, frequency, velocity, and the overall PR score (measure of variability in latency, termed as gathered or scattered)]. Compensatory saccades are defined as those saccades occurring within 350 ms of the onset head rotation, in the direction of the deficient VOR. Covert saccades occur during the head rotation, overt saccades occur after the head rotation ends. VOR gain values within 0.8–1.2 with standard deviation <0.12 were considered normal (15, 16).

Patients were seated 1 meter from a stationary visual target, in room light. Right eye velocity and head velocity were sampled at 220 Hz in response to passive right and left head rotations. Care was taken to avoid the examiner's hands making contact with the head strap to avoid goggle slip. At least 12 passive head rotations were performed in three planes: yaw, right anterior/left posterior (RALP) and left anterior/right posterior (LARP). vHIT traces were deleted if the eye velocity trace preceded head velocity, or if the passive head rotation trace did not match the acceleration profile suggested by the manufacturer.

Vestibular Evoked Myogenic Potential Test (VEMP)

Both ocular and cervical VEMP was measured using the Otometrics VEMP Chartr EP 200 System (Natus Medical Incorporated, Denmark). A burst tone stimulus [loud clicks, typically 95–105 decibels above normal hearing level (dB nHL), in 200 ms intervals] was applied during both ocular and cervical (O and C VEMP) paradigms. VEMP testing was considered abnormal for reduced sound threshold (dB) and/or latency of the positive and negative response being greater than the mean and 2SD above age matched controls (17). Percent asymmetry ratio was calculated for the ocular and cervical VEMP tone burst stimulus:

$$\text{Asymmetry ratio (AR)} = 100\% \frac{\text{X(Left amplitude} - \text{Right amplitude)}}{\text{(Left amplitude} + \text{Right amplitude)}}$$

Subjective Measures

Dizziness Handicap Inventory (DHI)

Patients reported their perceived level of disability via the DHI. The DHI is a 25-item subjective measure that collects data on how disabling the patients perceive their dizziness is affecting them. Clinically relevant change scores were defined as a decrease in the DHI of either 18 points or 42% from the pre-treatment level (18, 19).

Activities-Specific Balance Confidence Scale (ABC)

The ABC evaluates a subject's level of perceived balance confidence by asking them to rate confidence performing various daily activities from 0 (no confidence) to 100% (complete confidence). Total scores >80% are interpreted as having a high level of balance confidence and scores below 67% predict a person is at risk for falls (20). The ABC has excellent test-retest reliability ($r = 0.92$) (21, 22).

Performance Measures

Dynamic Visual Acuity (DVA)

We developed a custom, portable computerized DVA test using a Samsung Galaxy Pro tablet (Seoul, South Korea) with a single inertia measurement unit (XSENS Technologies, Enschede, Netherlands) mounted on a headband. Visual acuity was first measured during head still and then during active horizontal and vertical sinusoidal head rotation (right, left, up, down) while the subject sat 200 cm from the tablet. A minimum of >120°/s of active head rotation was required to generate the random optotype presentation, with no maximum head velocity limitation. Ten individual optotypes (capital letters C D H K N O S R V Z) were presented and scores were tabulated in the logarithm of the minimal angle resolution (LogMAR). Possible LogMAR scores ranged from −0.3 to 1.7 (Snellen equivalent of 20/10 to 20/800). Details of the DVA paradigm, as well as normative values can be found at Li et al. (23).

Dynamic Gait Index (DGI)

The DGI is an 8-item functional outcome measure that asks subjects to perform various dynamic gait tasks (i.e., walk and then turn 180°, walk and step over an obstacle). The DGI measures fall risk with scores <19/24 points reflecting a 2.58 times greater likelihood to have fallen in the previous 6 months (24). The DGI has excellent inter-rater ($r = 0.96$) and intra-rater ($r = 0.98$) reliability in older adults (25). A change score of > 3 is considered clinically significant (26).

Timed Up and Go (TUG)

The TUG measures the duration to stand, walk 3 m, and turn 180° before returning to sit. The TUG indicates fall risk when scores are >13.5 s in older adults with vestibular disorders (27). The TUG has excellent inter and intra-rater reliability (28).

Gait Speed and Endurance

The Ten Meter Walk Test (10MWT) tasks subjects to walk 10M during which their preferred gait speed is determined. The 2 min walk test (2MWT) tasks subjects to walk for 2 min while distance (endurance) is measured. The minimally clinical important difference (MCID) for gait speed is dependent on patient population, and not explicitly known for patients with vestibular disorders. We selected a substantial meaningful change at 0.1 m/s (29, 30). The 2MWT has excellent reliability ($r = 0.95$) (30, 31) and the minimal detectable change (MDC) is 12.2 m (31).

Exercise Group Categorization

Patients were placed in an exercise category (A, B, or C) to ensure high intensity, yet safe training to achieve maximum benefits of the VPT program. This categorization served a second purpose of limiting variability of the exercises prescribed. Placement into one of the three groups was based on the combined results of an individual's gait speed and scores on the DHI, ABC, TUG, and DGI (**Table 1**). Scores were tallied with patients being placed into either A, B, or C categories. In the case of an equivalent score between individual sub-scores (i.e., a patients' ABC score met the criteria for the B subcategorization, yet the same patients' DGI criteria placed them in C categorization), exercises from the more challenging group (group C in this example) were prescribed.

Vestibular Rehabilitation Program

Each exercise group (A, B, C) completed 6 exercises including 2 active gaze stability, 2 static balance, and 2 dynamic balance exercises (please see **Data Sheet 1**). Patients were asked to perform each exercise for 3 repetitions of 1.5 min duration each for a total of 27 min, 7 days per week for 5 weeks (7). Additionally, patients were instructed to complete a daily walk. Gaze stability exercises included active sinusoidal head rotations at fast head velocities with the understanding that the visual target should appear stable

TABLE 1 | ABC treatment categorization.

VPT difficulty	DHI*	ABC[&]	TUG^	DGI[#]	Gait [%] <age 70	Gait [%] >age 70
A	>60	≤30	>14	<15	0.8	0.7
B	31–60	31–65	11–14	15–18	1.1	1.0
C	≤30	>65	<11	≥19	1.4m/s	1.3m/s

*A, Least Challenge; B, Moderate Challenge; C, Most challenge; VPT, vestibular physical therapy; DHI, Dizziness Handicap Inventory; TUG, Timed Up and Go, DGI, Dynamic Gait Index. *Jacobson and Newman (18) and Whitney et al. (32); [&]Lajoire and Gallagher (20) and Whitney et al. (33); ^Whitney et al. (24); [#]Whitney et al. (24); [%]Bohannon (34), and Bohannon and Glenney (35); [%]Perera et al. (29); [%]van Loo et al. (36).*

and clear. Each week, a progressively more difficult set of gaze stability, static, and dynamic balance exercises were provided (i.e., gaze stability exercise done against a busy visual background), and provided to the patient that included detailed verbal, written, and illustrated instructions. The study team monitored the patients' ability to perform the exercises appropriately in a clinic setting, when possible, and also monitored the patient compliance based on the subjects' self-completed exercise flow sheets. Some patients opted to participate with outpatient VPT close to their home (in addition to our exercise program). Those patients ($n = 3$) who additionally participated in an outpatient VPT program agreed to complete only the research study-prescribed home exercise program.

Statistical Analysis

Statistical analysis was performed using SPSS (version 26, Chicago, IL, USA) software. All variables were normally distributed, thus parametric analysis was performed. A paired *t*-test was performed to compare variables between pre and post VPT. The level of statistical significance was set at alpha ≤0.05. As sample size permitted, simple correlations were determined in Excel using the Correl function (MS office, Redmond WA, USA). In addition to statistical significance, a change score of 10% in the compensatory saccade physiologic metrics and dynamic visual acuity was considered improved. For VOR gain, a change in magnitude > 0.06 was considered significant (37).

RESULTS

Vestibular Physiological Outcomes

vHIT

As expected, all patients had reduced VOR gain during passive ipsilesional yaw head impulse testing (**Table 2**). The average passive head velocity during vHIT for yaw rotations was 177.47 ± 55.7°/s. Although three subjects showed improved (>0.06) ipsilesional VOR gain to passive head impulse testing (mean 59 ± 14.6%), as a group yaw VOR gain (vHIT) did not show significant change after VPT (**Table 2**). Velocity of the overt compensatory saccades (CS) during ipsilesional head impulses were significantly reduced after VPT (mean 18 ± 6.6%), but no other metric of the CS showed any group changes ($p \geq 0.4$, **Table 2**). Nine subjects did show reduction (>10%) in latency variability of the CS (PR score, mean 45 ± 19%), though this was not statistically significant (**Figure 1**).

TABLE 2 | Physiologic measures of change in vHIT gain and compensatory saccades (mean + 1 SD).

Oculomotor function	Pre	Post	*p*-value (2-tailed)
Control left yaw	0.93 ± 0.05		
Control right yaw	0.99 ± 0.05		
Contralesional yaw	0.81 ± 0.19	0.85 ± 0.09	0.412
Ipsilesional yaw	0.44 ± 0.18	0.44 ± 0.15	0.984
Yaw % asymmetry	50.16 ± 19.76	50.95 ± 15.01	0.813
Contralesional anterior canal	0.68 ± 0.19	0.68 ± 0.18	0.989
Ipsilesional anterior canal	0.43 ± 0.26	0.39 ± 0.21	0.331
Contralesional posterior canal	0.81 ± 0.21	0.86 ± 0.22	0.229
Ipsilesional posterior canal	0.45 ± 0.14	0.50 ± 0.28	0.505
Variability of latency of saccades (PR ipsilesional score)	58.69 ± 30.12	48.94 ± 23.31	0.280
Ipsi covert saccade latency (ms)	124.57 ± 28.2	115.79 ± 39.4	0.485
Ipsi covert saccade velocity (°/s)	217.79 ± 71.2	220.64 ± 54.2	0.895
Ipsi overt saccade latency (ms)	211.06 ± 39.4	211.00 ± 31.5	0.996
Ipsi overt saccade velocity (°/s)	217.75 ± 63.7	200.81 ± 57.5	**0.042***

*vHIT, video head impulse test; ms, milliseconds; ipsi, direction of head rotation toward the lesioned side; covert, compensatory saccade during head rotation; overt, compensatory saccades after head rotation; PR, range of variability in the latency of compensatory saccades. A low PR score reflects maximum gathered responses vs. a high PR score reflects maximum scattered responses. *Denotes significance at $p < 0.05$.*

VEMP

Six of our 19 subjects did not have complete VEMP data collection due to equipment failure or the external auditory meatus being sewn closed ($n = 1$). Four of the remaining 13 subjects had absent and/or >2SD of mean cVEMP asymmetry ratios (mean 88 ± 16%). Five of the 13 subjects had absent and/or > 2SD oVEMP asymmetry ratios (mean 93 ± 9%). The rest of the subjects had measurable ocular (mean 26 ± 18%) or cervical (mean 35 ± 14%) VEMP responses within two SD of healthy controls (17).

Subjective Measures

As a group, the dizziness handicap inventory (DHI) total score as well as each subscale significantly improved (**Table 3**). The ABC scale also showed significant improvement after VPT. Neither age nor exercise compliance were correlated with the change in the DHI or the ABC.

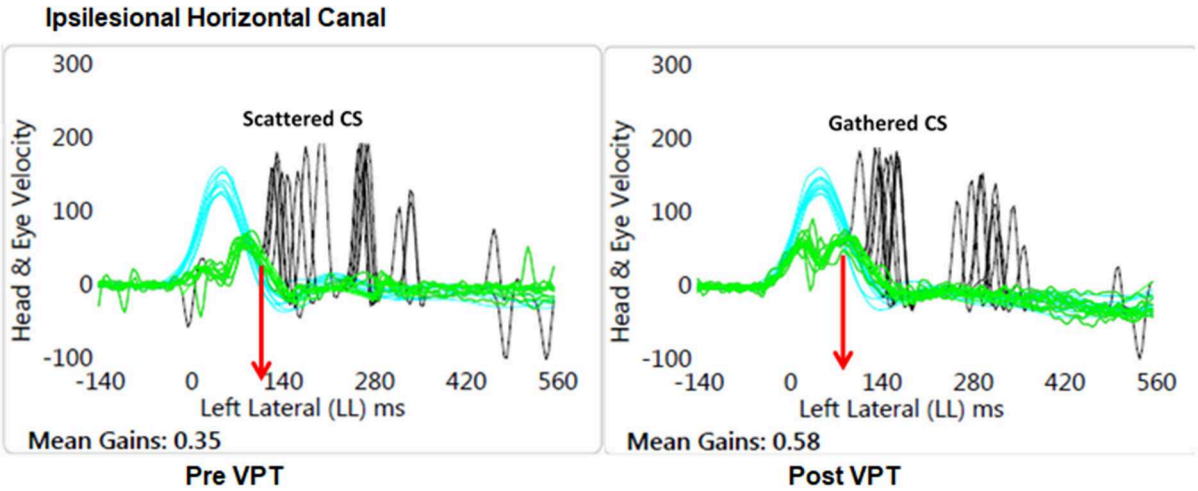

FIGURE 1 | Graphical plot of the improved VOR gain and reduced variability of the latency of the compensatory saccades (CS). Also, note the CS latency (red arrow) has reduced at the Post VPT plot. Blue, head velocity; Green, eye velocity; Black, compensatory saccades; VPT, vestibular physical therapy.

TABLE 3 | Change in subjective and performance outcome measures.

	ABC (%)	DHI-P	DHI –F	DHI -E	DHI -total	DGI	TUG (sec)	10MWT (m/s)	2MWT (m)
Pre	67.3 ± 21.0	15.2 ± 6.8	12.7 ± 9.6	20.8 ± 9.7	48.7 ± 23	20.7 ± 4.3	8.5 ± 1.8	1.3 ± 0.3	160.3 ± 27.6
Post	87.1 ± 12.7	10.4 ± 7.7	8.0 ± 8.6	10.2 ± 11	26.9 ± 25	23.2 ± 1.7	7.5 ± 1.0	1.4 ± 0.2	164.1 ± 46.1
% Change	29%* $P = 0.002$	32%* $P = 0.002$	37%* $p = 0.00$	51%* $p = 0.000$	45%** $p = 0.000$	12%** $p = 0.016$	12%* $p = 0.002$	8%** $p = 0.009$	2%

*ABC, Activities Balance Confidence Scale; DHI, Dizziness Handicap Inventory; P, Physical DHI; F, Functional DHI; E, Emotional DHI; DGI, Dynamic Gait Index; TUG, Timed Up and Go test; 10MWT, gait velocity: 2MWT, gait endurance. **Minimal Clinically Important Difference; *Statistically significant.*

Performance Measures

The DGI, TUG, and gait speed all improved after VPT (**Table 3**). Additionally, improvement in DGI was negatively correlated with tumor size ($r = -0.4$). There was no correlation between age and exercise compliance and the change score for the ABC, DGI, TUG, or gait speed.

Dynamic Visual Acuity

DVA scores for the healthy controls were similar ($p = 0.64$) in yaw for left (mean 0.21 ± 0.11 LogMAR) and right (0.20 ± 0.9 LogMAR) active head rotation and thus were combined and compared against the patients with UVD. DVA for the patients with UVD was worse than the healthy controls for yaw [ipsilesional ($p < 0.001$); contralesional ($p < 0.001$)] and pitch [up ($p = 0.006$); down ($p = 0.003$)] active head rotation (**Figure 2**).

As a group, DVA did not improve ($p \geq 0.13$) for any head direction (**Table 4**). However, 79% of our subjects ($n = 15/19$) did show improved DVA by at least 10%. A within-subject sub-analysis was performed on those patients who showed a minimum 10% improvement vs. those that did not. Ten percent was chosen as this represents the difference in LogMAR between lines of visual acuity (i.e., LogMAR 0.0 vs. 0.1). Within the positive responders, the mean improvement in DVA during ipsilesional head rotation was significant at 38.57% ± 26.32 ($n = 15/19$), and 39.96% ± 22.62 ($n = 12/19$) for contralesional yaw head rotation ($p < 0.001$). The magnitude of improved DVA score was negatively correlated ($r = -0.37$) with the magnitude of residual ocular VEMP function. The cervical VEMP response was not correlated with any change in yaw DVA ($r = 0.1$). For pitch down, DVA improved 59.23 ± 47.47% ($n = 14/19$, $p < 0.01$), which was correlated with the residual magnitude of both oVEMP ($r = -0.53$) and cVEMP ($r = -0.33$) asymmetry ratios. For pitch up, DVA improved 34.29 ± 112.76% ($n = 3/19$, $p = 0.03$; **Figure 3**). Correlations were not done between VEMP response and DVA up due to limited sample.

Of the negative responders, the mean reduction in % DVA change for ipsilesional head rotation was −122.76 ± 11.55 ($n = 4/19$ patients did not improve) and −70.38 ± 62.19 ($n = 7/19$ patients did not improve) during contralesional head rotation. Vertical DVA worsened by −60.89 ± 76.41% ($n = 3/19$ patients did not improve) for down DVA and −140.97 ± 232.24 ($n = 3/19$ patients did not improve) for the up direction. Correlations were not done due to limited sample.

DISCUSSION

Our data suggest that improvements in patient reported subjective measures of dizziness and confidence, as well as fall risk are not explained by changes in the gain of the

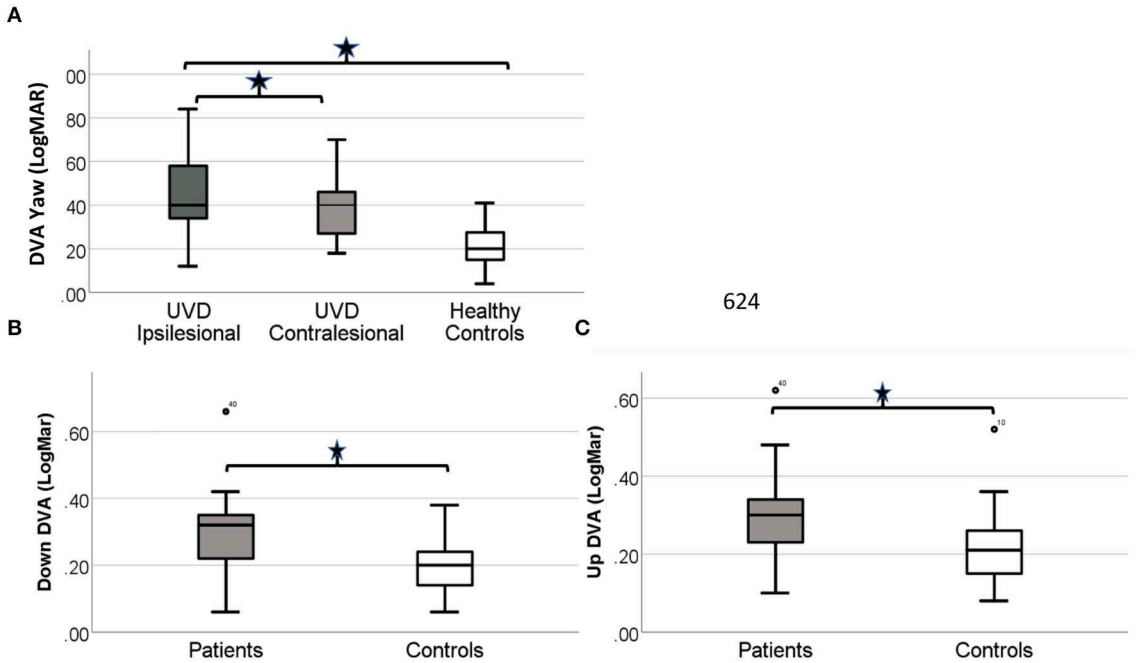

FIGURE 2 | Simple boxplot of the DVA scores for healthy controls and patients with UVD before VPT. **(A)** DVA scores for the patients with UVD are significantly worse for both ispi and contra-lesional active head rotation ($p < 0.0001$). DVA scores for the patients with UVD are significantly worse ($p < 0.01$) for up **(B)** and down **(C)** active head rotation. The thick line in the middle is the median. The top and bottom box lines show the first and third quartiles. The whiskers show the maximum and minimum values. Outliers are noted by the circles.

TABLE 4 | Dynamic visual acuity scores for active head rotation in yaw and pitch.

UVD $n = 19$	**Static**	**Ipsi**	**Contra**	**Up**	**Down**
Pre	0.01 ± 0.18	0.45 ± 0.22	0.38 ± 0.21	0.31 ± 0.21	0.31 ± 0.19
Post	0.02 ± 0.29	0.40 ± 0.38	0.33 ± 0.26	0.27 ± 0.3	0.28 ± 0.27
	Static	**Left**	**Right**	**Up**	**Down**
Healthy controls $n = 38$	−0.06 ± 0.19	0.15 ± 0.22	0.15 ± 0.23	0.13 ± 0.23	0.15 ± 0.22

UVD, unilateral vestibular deafferentation; LogMAR, logarithm of the minimal angle of resolution. ipsi, direction of head rotation toward the lesioned side; contra, direction of head rotation toward the contralesional side. A LogMAR score of 0 equates with 20/20 visual acuity on the Snellen acuity scale. A lower LogMAR scores reflect better visual acuity.

passively measured VOR. Furthermore, the improvements we report supersede the established MCID for the DHI, DGI, and gait speed (18, 26, 35). Recently, it has been reported that the VOR gain to passive head impulses improved 246% after completing a unique form of vestibular rehabilitation involving active ipsilesional head impulse rotation only (14). Lacour et al. also reveal limited change in the gain of the VOR in those patient groups that delayed their rehabilitation. One likely difference for the discrepancy between our data and that of Lacour et al. is the patient population. We studied a more complete lesion (deafferentation) relative to those of the Lacour study whom all had vestibular neuritis. Another explanation relates to the context of the gaze stability training. In our study, subjects performed gaze stability exercises using a sinusoid and lower frequency head rotation (<2 Hz) in yaw (and pitch). In contrast, the vHIT measures VOR gain during impulsive head rotation that includes higher frequency content of motion. We have recently shown that motor learning in the VOR is frequency specific, with evidence that VOR gain adaptation in the higher frequencies does not occur after lower frequency training (38). Thus, our results of VOR gain not changing after sinusoid gaze stability exercise implies that higher-frequency head movements are required during training if the goal is to change the VOR gain to higher frequencies. It remains possible that the absence of VOR gain change after our VPT program was related to the difference in training (active head rotation) vs. testing (passive head rotation). This is unlikely however, given recent evidence that VOR gain training using active impulses is adequate at improving the passive VOR (39).

In contrast to VOR gain, we did show the velocity of the overt compensatory saccades (CS) did reduce during ipsilesional head impulses after 5 weeks of VPT (albeit other CS metrics did

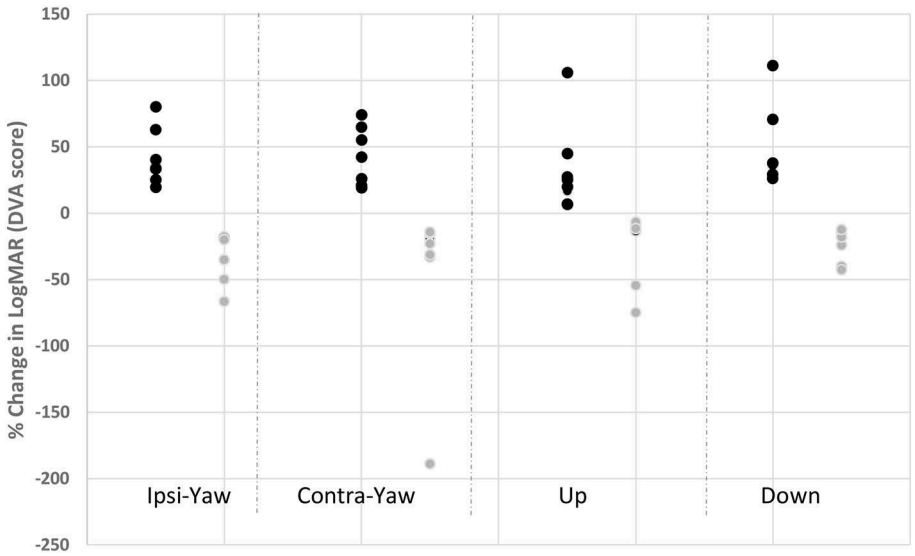

FIGURE 3 | Change in individual DVA scores for head rotation in responders and non-responders. Dark circles represent those subjects with improved DVA score after vestibular rehabilitation (responders); gray circles represent those subjects with worse DVA score after vestibular rehabilitation. Ipsi yaw, ipsilesional head rotation in yaw; Contra yaw, contralesional head rotation in yaw; Up, upward head rotation; Down, downward head rotation.

not). Prior studies have shown that the frequency and velocity of CS do change over time with VPT (13, 14, 40–42). Together, these data suggest that the current standard of care prescribing gaze stability exercises for VPT (sinusoidal head rotation) may not be restoring slow phase (i.e., vestibular) eye velocity during passive head rotation, but instead lead to an altered CS velocity putatively to improve gaze stability. Recent case study evidence suggests that improving the gain of the VOR to passive rapid head rotation using active bilateral impulse training is not only possible in vestibular hypofunction but also leads to improved gait and dynamic visual acuity (43, 44).

Change in DVA With VPT

Although 79% of our patients did show improved DVA after VPT, a few of our patients with UVD did not show a significant change ($n = 4/19$ patients did not improve their ipsilesional DVA). This is in contrast to prior studies and one possible explanation for this discrepancy may be related to the different methods used to measure DVA (8, 10, 40). Our method of DVA testing tasked patients to identify 10 optotype choices, which should be more difficult to complete (23). Additionally, our version of the DVA test does not limit a maximum head velocity threshold. Prior versions of the computerized DVA test limit the optotype presentations to four (letter E oriented in up/down/left/right) and have set the upper head velocity threshold to 180 d/s. A second reason is that all of our patients had a more complete lesion given surgical excision of the vestibular schwannoma, where other studies examined unilateral vestibular hypofunction for broader reasons (i.e., neuritis). The fact that our group results were not significant is also in-part related to the large variability in LogMAR scores, with some individuals doing much worse on their post testing measure. We investigated the surgical record of the four subjects in our study who did not show improvement in DVA. In summary, three of the four patients had facial paralysis and indication of central brainstem or cerebellar changes as evidence by statements including "small acute/subacute infarction postero-inferiorly in the right cerebellar hemisphere, not directly at the site of recent surgery"; "stable degree of mass effect on the left brachium pontis"; and "patchy edema within the dorsal and dorsolateral aspects of the right cerebellar hemisphere." Therefore, it remains possible that the absent change in DVA from these three patients is related to their central pathology. We cannot explain why the fourth subject showed no change in DVA. Finally, it remains possible that patients improve their DVA via strategies different from the mechanisms we measured. For example, the unique roles of sensory re-weighting or cervical proprioception may also explain the change in DVA with vestibular rehabilitation.

The Role of Otolith Function on Compensation From Vestibular Rehabilitation

Our data is the first behavioral evidence to show correlations between improved DVA (putative semicircular canal function) and preserved otolith function (smaller magnitude asymmetry ratio) as measured by ocular and cervical VEMP. It has recently been shown that labyrinthectomized mice also missing otolith function (otopetrin 1), are unable to adapt their angular VOR gain as well as healthy mice (45). Our data support the murine evidence that otolith function does appear to have a critical role in compensation to semicircular canal damage. Additional and recent evidence also suggests that the otolith pathways as measured via the head tilt and head/trunk tilt tests improve

more quickly than the semicircular canal pathways in patients recovering from vestibular schwannoma resection (46, 47).

Limitations

We lost a significant number of subjects to follow up based on being a tertiary care facility that draws patients from distances inconvenient for return visits. Additionally, given we did not include a patient control group, we are unable to know for sure whether rehabilitation was the reason why people subjectively and objectively improve as we report. Furthermore, we are unable to determine if our intervention may have led to changes in vestibular physiological measures were the patients examined closer to their surgical onset—although we did select "chronic patients" to avoid a possible confound of natural recovery. The exercise categories we developed in attempt to standardize the rehabilitation provided have not been validated, though do represent the current standard of care given rehabilitation providers commonly choose exercise difficulty based on clinical presentation. Finally, a greater sample size is needed to establish the unique roles that residual semicircular and otolith function have on improving impairments in patients with vestibular hypofunction.

CONCLUSION

After 5 weeks of vestibular rehabilitation, subjective and performance outcomes were clinically and statistically improved despite absent change in VOR gain. Some individuals did have evidence for physiologic change. Dynamic visual acuity improved in 79% of our subjects, and was correlated with otolith, not semicircular canal function.

DATA AVAILABILITY STATEMENT

The datasets generated for this study are available on request to the corresponding author.

ETHICS STATEMENT

The studies involving human participants were reviewed and approved by Johns Hopkins Internal Review Board. The patients/participants provided their written informed consent to participate in this study.

AUTHOR CONTRIBUTIONS

MS, JM, and YG: concept and data analysis. JM and YG: data collection. DR and MS: software development. JM, MS, YG, and DR: manuscript preparation.

FUNDING

MS was funded from the Department of Defense under the Neurosensory and Rehabilitation Research Award Program (Grant award # W81XWH-15-1-0442).

SUPPLEMENTARY MATERIAL

The Supplementary Material for this article can be found online at: https://www.frontiersin.org/articles/10.3389/fneur.2020.00079/full#supplementary-material

Data Sheet 1 | Johns Hopkins University Vestibular Rehabilitation Exercise and Compliance Log.

REFERENCES

1. Hirasaki E, Moore ST, Raphan T, Cohen B. Effects of walking velocity on vertical head and body movements during locomotion. *Exp Brain Res*. (1999) 127:117–30. doi: 10.1007/s002210050781
2. Grossman GE, Leigh RJ, Abel LA, Lanska DJ, Thurston SE. Frequency and velocity of rotational head perturbations during locomotion. *Exp Brain Res*. (1988) 70:470–6.
3. Huterer M, Cullen K. Vestibuloocular reflex dynamics during high-frequency and high-acceleration rotations of the head on body in rhesus monkey. *J Neurophysiol*. (2002) 88:13–28. doi: 10.1152/jn.2002.88.1.13
4. Cousins V, Li CW, Hooper R. Vestibulo-ocular compensation following unilateral vestibular de-afferentation. *Ann Otol Rhinol Laryngol*. (1992). 101:525–9. doi: 10.1177/000348949210100614
5. Enticott JC, O'Leary SJ, Briggs RJS. Effects of vestibulo-ocular reflex exercises on vestibular compensation after vestibular schwannoma surgery. *Otol Neurotol*. (2005) 6:265–9. doi: 10.1097/00129492-200503000-00024
6. Herdman SJ. Role of vestibular adaptation in vestibular rehabilitation. *Otolaryngol Head Neck Surg*. (1998) 119:49–54. doi: 10.1016/S0194-5998(98)70195-0
7. Hall CD, Herdman SJ, Whitney SL, Cass SP, Clendaniel RA, Fife TD, et al. Vestibular rehabilitation for peripheral vestibular hypofunction: an evidence-based clinical practice guideline. *JNPT*. (2016) 40:124–54. doi: 10.1097/NPT.0000000000000120
8. Herdman SJ, Schubert MC, Das VE, Tusa RJ. Recovery of dynamic visual acuity in unilateral vestibular hypofunction. *Arch Otolaryngol Head Neck Surg*. (2003) 129:819–24. doi: 10.1001/archotol.129.8.819
9. Schubert MC, Migliaccio AA, Clendaniel RA, Allak A, Carey JP. Mechanism of dynamic visual acuity recovery with vestibular rehabilitation. *Arch Phys Med Rehabil*. (2008) 89:500–7. doi: 10.1016/j.apmr.2007.11.010
10. Herdman SJ, Clendaniel RA, Mattox DE, Holliday MJ, Niparko JK. Vestibular adaptation exercises and recovery: acute stage after acoustic neuroma resection. *Otolaryngol Head Neck Surg*. (1995) 113:77–87. doi: 10.1016/S0194-5998(95)70148-6
11. Herdman SJ, Hall CD, Schubert MC, Das VE, Tusa RJ. Recovery of dynamic visual acuity in bilateral vestibular hypofunction. *Arch Otolaryngol Head Neck Surg*. (2007) 133:383–9. doi: 10.1001/archotol.133.4.383
12. Sadeghi NG, Sabetazad B, Rassaian N, Sadeghi SG. Rebalancing the vestibular system by unidirectional rotations in patients with chronic vestibular dysfunction. *Front Neurol*. 9:1196. doi: 10.3389/fneur.2018.01196
13. Schubert MC, Migliaccio AA, Della Santina CC. Modification of compensatory saccades after aVOR gain recovery. *J Vestib Res*. (2006) 16:285–91.
14. Lacour M, Tardivet L, Thiry A. Rehabilitation of dynamic visual acuity in patients with unilateral vestibular hypofunction: earlier is better. *Eur Arch Oto-Rhino-Laryngol*. (2019) 277:103–13. doi: 10.1007/s00405-019-05690-4
15. MacDougall HG, Weber KP, McGarvie LA, Halmagyi GM, Curthoys IS. The video head impulse test: diagnostic accuracy in peripheral vestibulopathy. *Neurology*. (2009) 73:1134–41. doi: 10.1212/WNL.0b013e3181bacf85
16. Halmagyi GM, Chen L, MacDougall HG, Weber KP, McGarvie LA, Curthoys IS. The video head impulse test. *Front Neurol*. (2017) 8:258. doi: 10.3389/fneur.2017.00258

17. Nguyen K, Welgampola M, Carey J. Test-retest reliability and age-related characteristics of the ocular and cervical vestibular evoked myogenic potential tests. *Otol Neurotol*. (2010) 31:793–802. doi: 10.1097/MAO.0b013e3181e3d60e
18. Jacobson GP1, Newman CW. The development of the dizziness handicap inventory. *Arch Otolaryngol Head Neck Surg*. (1990) 116:424–7. doi: 10.1001/archotol.1990.01870040046011
19. Clendaniel R, Goode A. Measurement properties of the dizziness handicap inventory. In: *APTA Combined Sections Meeting*. San Diego, CA (2013).
20. Lajoie Y, Gallagher SP. Predicting falls within the elderly community: comparison of postural sway, reaction time, the berg balance scale and the activities-specific balance confidence (ABC) scale for comparing fallers and non-fallers. *Arch Gerontol Geriatr*. (2004) 38:11–26. doi: 10.1016/S0167-4943(03)00082-7
21. Myers AM, Fletcher PC, Myers AH, Sherk W. Discriminative and evaluative properties of the activities-specific balance confidence (ABC) scale. *J Gerontol*. (1998) 53A:M287–94. doi: 10.1093/gerona/53A.4.M287
22. Powell LE, Myers AM. The Activities-specific Balance Confidence (ABC) Scale. *J Gerontol A l Sci Med Sci*. (1995) 50A:28–34. doi: 10.1037/t13026-000
23. Li C, Beaumont JL, Rine RM, Slotkin J, Schubert MC. Normative scores for the NIH Toolbox dynamic visual acuity test from 3 to 85 years. *Front Neurol*. (2014) 5:223. doi: 10.3389/fneur.2014.00223
24. Whitney SL, Marchetti GF, Schade A, Wrisley DM. The sensitivity and specificity of the Timed "Up & Go" and the dynamic gait index for self-reported falls in persons with vestibular disorders. *J Vestib Res*. (2004) 14:397–409.
25. Shumway-Cook A, Baldwin M, Polissar NL, Gruber W. Predicting the probability for falls in community-dwelling older adults. *Phys Ther*. (1997) 77:812–9. doi: 10.1093/ptj/77.8.812
26. Hall CD, Herdman SJ. Reliability of clinical measures used to assess patients with peripheral vestibular disorders. *J Neurol Phys Ther*. (2006) 30:74–81. doi: 10.1097/01.NPT.0000282571.55673.ed
27. Shumway-Cook A, Brauer S, Woollacott M. Predicting the probability for falls in community-dwelling older adults using the Timed Up & Go Test. *Phys Ther*. (2000) 80:896–903. doi: 10.1093/ptj/80.9.896
28. Podsiadlo D, Richardson S. The timed "Up & Go": a test of basic functional mobility for frail elderly persons. *J Am Geriatr Soc*. (1991) 39:142–8. doi: 10.1111/j.1532-5415.1991.tb01616.x
29. Perera S, Mody SH, Woodman RC, Studenski SA. Meaningful change and responsiveness in common physical performance measures in older adults. *J Am Geriatr Soc*. (2006) 54:743–9. doi: 10.1111/j.1532-5415.2006.00701.x
30. Bohannon RW, Wang YC, Gershon RC. Two-minute walk test performance by adults 18 to 85 years: normative values, reliability, and responsiveness. *Arch Phys Med Rehabil*. (2015) 96:472–7. doi: 10.1016/j.apmr.2014.10.006
31. Connelly DM, Thomas BK, Cliffe SJ, Perry WM, Smith RE. Clinical utility of the 2-minute walk test for older adults living in long-term care. *Physiother Can*. (2009) 61:78–87. doi: 10.3138/physio.61.2.78
32. Whitney SL, Wrisley DM, Brown KE, Furman JM. Is perception of handicap related to functional performance in persons with vestibular dysfunction? *Otol Neurotol*. (2004) 25:139–143. doi: 10.1097/00129492-200403000-00010
33. Whitney SL, Hudak MT, Marchetti GF. The activities-specific balance confidence scale and the dizziness handicap inventory: a comparison. *J Vestib Res*. (1999) 9:253–9.
34. Bohannon RW. Comfortable and maximum walking speed of adults aged 20-79 years: reference values and determinants. *Age Ageing*. (1997) 26:15–9. doi: 10.1093/ageing/26.1.15
35. Bohannon RW, Glenney SS. Minimal clinically important difference for change in comfortable gait speed of adults with pathology: a systematic review. *J Eval Clin Pract*. (2014) 20:295–300. doi: 10.1111/jep.12158
36. van Loo MA, Moseley AM, Bosman JM, de Bie RA, Hassett L. Test-retest reliability of walking speed, step length and step width measurement after traumatic brain injury: a pilot study. *Brain Inj*. (2004) 18:1041–8. doi: 10.1080/02699050410001672314
37. Chang TP, Schubert MC. Association of the video head impulse test with improvement of dynamic balance and fall risk in patients with dizziness. *JAMA Otolaryngol Head Neck Surg*. (2018) 144:696–703. doi: 10.1001/jamaoto.2018.0650
38. Rinaudo CN, Schubert MC, Figtree WVC, Todd CJ, Migliaccio AA. Human vestibulo-ocular reflex adaptation is frequency selective. *J Neurophysiol*. (2019) 122:984–93. doi: 10.1152/jn.00162.2019
39. Mahfuz MM, Schubert MC, Figtree WVC, Toddm CJ, Khan SI, Migliaccio AA. Optimal human passive vestibulo-ocular reflex adaptation does not rely on passive training. *J Assoc Res Otolaryngol*. (2018) 19:261–71. doi: 10.1007/s10162-018-0657-9
40. Schubert MC, Della Santina CC, Shelhamer M. Incremental angular vestibulo-ocular reflex adaptation to active head rotation. *Exp Brain Res*. (2008) 191:435–46. doi: 10.1007/s00221-008-1537-z
41. Trinidad-Ruiz G, Rey-Martinez J, Batuecas-Caletrio A, Matiño-Soler E, Perez-Fernandez N. Visual performance and perception as a target of saccadic strategies in patients with unilateral vestibular loss. *Ear Hear*. (2018) 39:1176–86. doi: 10.1097/AUD.0000000000000576
42. Sjögren J, Fransson PA, Karlberg M, Magnusson M, Tjernström F. Functional head impulse testing might be useful for assessing vestibular compensation after unilateral vestibular loss. *Front Neurol*. 9:979. doi: 10.3389/fneur.2018.00979
43. Gimmon Y, Migliaccio AA, Kim KJ, Schubert MC. VOR adaptation training and retention in a patient with profound bilateral vestibular hypofunction. *Laryngoscope*. (2019) 129:2568–73. doi: 10.1002/lary.27838
44. Rinaudo CN, Schubert MC, Cremer PD, Figtree WVC, Todd CJ, Migliaccio AA. Improved oculomotor physiology and behavior after unilateral incremental adaptation training in a person with chronic vestibular hypofunction: a case report. *Phys Ther*. (2019) 99:1326–33. doi: 10.1093/ptj/pzz083
45. Khan SI, Della Santina CC, Migliaccio AA. Angular vestibuloocular reflex responses in Otop1 mice. II Otolith sensor input improves compensation after unilateral labyrinthectomy. *J Neurophysiol*. (2019) 121:2300–7. doi: 10.1152/jn.00812.2018
46. Otero-Millan J, Treviño C, Winnick A, Zee DS, Carey JP, Kheradmand A. The video ocular counter-roll (vOCR): a clinical test to detect loss of otolith-ocular function. *Acta Otolaryngol*. (2017) 137:593–7. doi: 10.1080/00016489.2016.1269364
47. Sadeghpour S, Fornasari F, Otero-Millan, J, Zee DS, Carey JP. Kheradmand AVideo ocular counter-roll (vOCR): a new clinical test of otolith-ocular function. In: *Association for Research in Otolaryngology Meeting*. Baltimore, MD (2019).

Conflict of Interest: The authors declare that the research was conducted in the absence of any commercial or financial relationships that could be construed as a potential conflict of interest.

Advantages of publishing in Frontiers

OPEN ACCESS
Articles are free to read for greatest visibility and readership

FAST PUBLICATION
Around 90 days from submission to decision

HIGH QUALITY PEER-REVIEW
Rigorous, collaborative, and constructive peer-review

TRANSPARENT PEER-REVIEW
Editors and reviewers acknowledged by name on published articles

Frontiers
Avenue du Tribunal-Fédéral 34
1005 Lausanne | Switzerland

Visit us: www.frontiersin.org
Contact us: info@frontiersin.org | +41 21 510 17 00

REPRODUCIBILITY OF RESEARCH
Support open data and methods to enhance research reproducibility

DIGITAL PUBLISHING
Articles designed for optimal readership across devices

FOLLOW US
@frontiersin

IMPACT METRICS
Advanced article metrics track visibility across digital media

EXTENSIVE PROMOTION
Marketing and promotion of impactful research

LOOP RESEARCH NETWORK
Our network increases your article's readership